University of Alberta

Lipid Modified Polymers for Transfection of Human CRL Fibroblasts, and for siRNA Mediated MDR Reversal in Melanoma Cancer Therapy

by

Meysam Abbasi

A thesis submitted to the Faculty of Graduate Studies and Research in partial fulfillment of the requirements for the degree of

Doctor of Philosophy

in

Biomedical Sciences

Department of Biomedical Engineering

Edmonton, Alberta

Fall 2010

EXAMINING COMMITTEE

Supervisor: Dr. Hasan Uludag, Department of Chemical & Materials Engineering
University of Alberta

Committee Members: Dr. Michael Weinfeld, Department of Oncology

Dr. Luc Berthiaume, Department of Cell Biology

Dr. Robert Burrell, Department of Biomedical Engineering

Dr. Alan Willman, Department of Biomedical Engineering

Dr. Judith Hugh, Department of Laboratory Medicine & Pathology
University of Alberta

External Examiner: Dr. Suzie Pun, Department of Bioengineering

University of Washington

DEDICATION

This thesis is dedicated to:

My loving and caring wife, Shirin Emami, who stood by me and shared my joy and grief through this journey and made major sacrifices for my success.

My always loving and supporting parents, Dr. Mashallah Abbasi and Mrs. Parvin Ghadaksaz, and inlaws, Dr. Nasrollah Emami and Mrs. Maliheh Fakhrzad, who flourished my passion for science and encouraged me through every stage of my research.

My beloved brothers Mehdi and Mohammad, and my beloved brother in laws Shervin and Farzin, whose advice I carried throughout my studies and their faith in me gave me motivation and positive energy.

My supervisor Dr. Hasan Uludağ for his strong guidance and having the confidence in my abilities to allow me to pursue the scientific topics I chose.

ABSTRACT

Gene delivery for therapeutic purposes is quickly emerging as the best potential treatment option for inherited genetic diseases and cancer. Viral gene carriers have been the choice for this purpose due to their high efficiency, but harmful immunogenic and oncogenic host reactions have limited their in vivo use. Cationic polymers provide a safe alternative to viral carriers as they can be engineered to reduce immunogenic and toxic responses and serve therapeutic purposes in the body. Due to their strong positive charge, they are able to compact the negatively charged nucleotides to small nano-sized particles appropriate for cellular uptake. Additionally, they efficiently encapsulate the highly sensitive nucleotides, and protect them against degradation by the nucleases present at the physiological milieu. In this thesis work, I have used a novel approach for gene delivery by combining the critical properties of a cationic polymer (i.e., nucleotide condensing ability) with that of a fatty acid (i.e., lipid membrane compatibility). The resulting lipid modified polymer increased delivery of our gene of interest into target cells and resulted in increased siRNA delivery for gene therapy.

ACKNOWLEDGEMENTS

The studies in this thesis were financially supported by operating grants from the Canadian Institutes of Health Research (CIHR), and Natural Sciences and Engineering Research Council of Canada (NSERC).

I thank my supervisory committee Drs. Luc Berthiaume, Robert Burrell, Afsaneh Lavasanifar and Michael Weinfeld for their guidance and wise advices.

I thank my mentor Dr. Aziz Ghahary for his continued support throughout my studies.

I thank my collegue Dr. Vanessa Incani for the synthesis of the lipid-substituted polymers used in my studies. I also thank Ms. Xiaoyue Lin for her assistance in the cell culture experiments and Ms. Elaine Moasse for helping me with my *in vivo* studies.

TABLE OF CONTENTS

LIST OF TABLES

LIST OF FIGURES

LIST OF ABBREVIATIONS

1. AAV; Adeno-Associated Virus

2. ABC; ATP Binding Cassette

3. AF 546; Alexafuor 546

4. AFM; Atomic Force Microscopy

5. ASO; Antisense Oligonucleotides

6. BCRP; Breast Cancer Resistance Protein

7. β-gal; β-galactosidase

8. CA; Caprylic Acid

9. COL; Collagen

10. CyA; Cyclosporine A

11. DCC; Dicyclohexylurea

12. DMEM; Dublecco's Modified Eagle Medium

13. DMSO; Dimethyl Sulfoxide

14. DNA; Deoxyribonucleic Acid

15. DOX; Doxorubicin

16. Doxil; Liposomal Doxorubicin

17. DP; Dimethyldipropylenetriamine

18. DTT; Dithiothreitol

19. EDTA; Ethylenediaminetetraacetic Acid

20. FGF; Fibrolast Growth Factor

21. FITC; Fluorescein Isothiocyanate

22. GAPDH; Glyceraldehyde 3-Phosphate Dehydrogenase

23. GFP; Green Fluorescent Protein

24. h; Hour

25. IGF; Insulin Like Growth Factor

26. IL; Interleukine

27. KGF; Keratinocyte Growth Factor

28. LA; Linoleic Acid

29. LISW; Laser Induced Stress Waves

30. LRP; Lung Resistance-Related Protein

31. MA; Myristic Acid

32. miRNA; Micro RNA

33. MDR; Multidrug Resistance

34. mRNA; Messenger RNA

35. MRP; Multiple Resistant Protein

36. MS; Multiple Sclerosis

37. MuLV; Murine Leukemia Virus

38. MW; Molecular Weight

39. N:P; Nitrate:Phosphate

40. NMR; Nuclear Magnetic Resonance

41. OA; Oleic Acid

42. OTC; Ornithine Transcarbamylase

43. PA; Palmitic Acid

44. PCL; Poly Caprolactone

45. PDGF; Platelet Derrived Growth Factor

46. PDNA; Plasmid DNA

47. PEG; Polyethylene Glycol

48. pEGFP; plasmid Enhanced Green Fluorescent Protein

49. PEI; Polyethyleneimine

50. PEO; Polyethylene Oxide

51. P-gp; P-Glycoprotein

52. PLL; Poly(*L*-lyine)

53. PTX; Paclitaxel

54. RDEB; Dystrophilic Epidermyolisis Bullosa

55. RISC; RNA Induced Scilencing Complex

56. RNA; Ribonucleic Acid

57. ScAAV; Self Complementary AAV

58. SD; Standard Deviation

59. shRNA; Short Hairpin RNA

60. SID; Severe Immunodefficiency

61. siRNA; Small Interfering RNA

62. SP; Spermine

63. TNBS; Trinitrobenzosulfonic Acid

64. TP; Tetraethylenepentamine

65. VEGF; Vascular Endothelial Growth Factor

66. WT; Wild Type

67. XP; Xerodermapigmentosum

CHAPTER I

Scope of Dissertation

This thesis is composed of a total of eight chapters. Each chapter is an independent study and chapters II-VII are formatted in such ways that are suitable as a standalone manuscript for publication.

The scope of the dissertation is presented in **CHAPTER I** (the present chapter).

CHAPTER II of this thesis work consists of a survey of delivery systems used for epidermal gene therapy. The viral gene carriers (including adenovirus, adeno-associated virus, retrovirus and lentivirus), non-viral gene carriers (liposomes, Lipofectamine™ 2000, FuGene™ 6) and physical delivery methods (gene gun and electroporation) used for epidermal gene delivery are introduced in this Chapter and their advantages and limitations for gene delivery are discussed. Furthermore, a summary of *in vitro* and *in vivo* gene therapy approaches used for epidermal gene delivery for various therapeutic purposes has been provided.

In a novel approach for epidermal gene delivery, a lipid-modified polymeric carrier was used for delivery of a reporter gene, enhanced green fluorescent protein (EGFP), into human skin CRL fibroblasts. A palmitic acid-modified poly(*L*-lysine) (PLL-PA) was synthesized, and the transfection efficiency of this novel carrier was compared to transfection efficiencies of other carriers, including PLL, polyethyleneimine (PEI), an adenovirus, Lipofectamine™ 2000 and Fugene™ 6. The results of this study are provided in **CHAPTER III** of this thesis. Initially, PLL modification by PA was verified by NMR and the size of polymer-plasmid DNA complexes was assessed using atomic force microscopy (AFM). Later, the cellular uptake of carrier-plasmid DNA complexes was investigated by confocal microscopy and flow cytometry. Finally, transfection efficiency and toxicity of each complex was evaluated by flow cytometry and hemocytometer cell counts respectively. This study indicated that adenovirus and PEI lead to a

higher transfection of the human CRL fibroblasts compared to PLL-PA. But these carriers also introduced significant cytotoxicity, whereas the PLL-PA introduced no cytotoxicity and produced the highest numbers of transfected cells.

The success of PA modification of PLL, led us to investigate whether PLL modification with other endogenous fatty acids would be beneficial for gene delivery. In **CHAPTER IV** of this thesis, a library of modified PLL with 8-20 carbon endogenous fatty acids was synthesized and the characteristics of each polymer in plasmid DNA delivery were assessed. Gel electrophoresis was performed to detect formation of polymer-plasmid DNA complexes, dissociation of plasmid DNA from the complex, and protection of plasmid DNA by polymers against nucleases. A positive correlation was seen between the plasmid DNA dissociation from polymers and the hydrophobicity (i.e., degree of lipid substitution) of the polymers. Cellular uptake of plasmid DNA by the polymers was observed by flow cytometry, and recovery of internalized plasmid DNA into cells was detected by gel electrophoresis. A positive correlation was also observed between of cellular uptake of plasmid DNA and the hydrophobicity of polymers. Transfection efficiency of the polymer library was assessed by flow cytometry. Myristic acid PLL (PLL-MA) and stearic acid PLL (PLL-StA) were the most hydrophobic polymers and proved to be the most efficient carriers in plasmid DNA uptake and transfection efficiency. This led us to conclude that the increase in hydrophobicity and not the nature of the lipid was the main factor behind increased efficiency of lipid-modified polymers in plasmid delivery.

At this point of my thesis, I decided to utilize the lipid-modified polymers to pursue a therapeutic outcome, rather than focusing on reporter genes. One of the major applications of gene therapy is in the field of cancer. I concentrated my focus on reversing multidrug resistance

(MDR) in cancer, and used the most efficient lipid modified PLL (PLL-StA) for the delivery of small interfering RNA (siRNA) to down-regulate P-glycoprotein (P-gp) and increase the efficiency of chemotherapy. **CHAPTER V** is composed of an introduction on MDR, P-gp, and the mechanisms involved in P-gp inhibition and MDR reversal. Furthermore, the siRNA approach for gene down-regulation is introduced and its structure and function is discussed in the context of this thesis work. Finally, a literature review of siRNA delivery for P-gp down-regulation in various types of cancers is conducted, the different types of carriers used for siRNA delivery/expression are introduced, and the efficiency of each approach is evaluated.

The feasibility of siRNA delivery for the purpose of P-gp down-regulation and reversal of MDR is assessed in **CHAPTER VI**. As before, our polymeric delivery system was compared to commercially available gene carriers PEI and Lipofectamine^{TM} 2000. Formation of carrier-siRNA complexes, dissociation of siRNA from complexes, and protection of siRNA by the carriers against serum degradation was assessed by gel electrophoresis. Then, uptake of siRNA to the MDA435/LCC6 MDR1 melanoma tumor cells was investigated by the carriers using flow cytometry. For efficacy studies, a specific siRNA for P-gp down-regulation (ABCB1 siRNA) was used, and the extent of P-gp down-regulation was detected by using P-gp antibody staining and flow cytometry. Flow cytometry was also used to determine the extent of MDR reversal, by detecting the increase in chemotherapeutic drug doxorubicin (DOX) and paclitaxel (PTX) uptake of the ABCB1 siRNA treated cells compared to the scrambled siRNA treated cells. Additionally, the toxicity of these drugs on ABCB1 siRNA treated cells was compared to the scrambled siRNA treated cells using the MTT assay. As seen in this chapter, by using a low siRNA concentration (20 nM) for P-gp down-regulation we have been able to significantly increase chemotherapeutic drug accumulation and toxicity in the melanoma tumor cells.

Translation of the successful siRNA delivery results from *in vitro* to *in vivo* systems is vital for the future of siRNA therapy in cancer. Therefore, an *in vivo* siRNA delivery approach was explored for P-gp down-regulation in an animal model, and the results are summarized in **CHAPTER VII** of this thesis. To pursue this approach, some important questions had to be answered regarding the intracellular fate of siRNA after uptake and the in-situ siRNA half-life. These questions were (i) how long will it take for the complexes to enter the cells, (ii) how long will it take for the siRNA to disscociate from the polymers, and (iii) how long will siRNA survive in the cells. Confocal microscopy was used to determine the answer to these questions using *in vitro* cell culture. Then, to increase the efficiency of P-gp down-regulation, an *in vitro* approach was taken by using a combination of three ABCB1 siRNAs for P-gp down-regulation in the MDA435/LCC6 MDR1 cells by flow cytometry. To establish an *in vivo* model, MDA/435 LCC6 MDR1 cells were injected in to the right flank of SCID mice to form tumors. For the *in vivo* siRNA uptake studies, intratumoral injection of siRNA was performed and gel electrophoresis, flow cytometry, and microscopy were used to determine the amount of siRNA uptake in tumor cells. Intravenous (IV) injection of DOX was also performed to determine the amount of DOX that is localized in the tumor cells. Finally, ABCB1 siRNA was injected intratumorally in combination with IV injection of DOX to determine increase in DOX uptake after chemotherapy.

Overall this dissertation provides evidence-based information on the characteristics of some of the non-viral carriers used for DNA and siRNA. Additionally, barriers to successful gene delivery are addressed and studies have been undertaken to overcome these barriers in gene delivery. A novel therapeutic approach (*in vitro* and *in vivo*) for the down-regulation of P-gp and MDR reversal for cancer therapy has also been taken, leading to some significant conclusions

and future directions. **CHAPTER VIII** of this thesis consists of the conclusion of this thesis work and the future studies that could further develop the strategies used for improving DNA and siRNA delivery for gene therapy.

CHAPTER II

Introduction to Epidermal Gene Therapy

2.1 A Survey of Delivery Systems Used for Epidermal Gene Therapy

Gene therapy aims to reconstitute a missing or defective gene with a correct copy in a host [1]. This is possible when an effective gene carrier is used to deliver a gene of interest to target cells. A variety of diseases and deficiencies, such as multiple sclerosis (MS) [2], sustained immunodeficiency (SID) [3], and various types of cancers [4] may be potentially cured using this method with high specificity and limited side effects. Epidermal gene therapy may benefit a variety of inherited skin disorders and certain systemic diseases, and can also impact clinical skin regeneration and wound healing [5]. Prolonging gene expression in skin using gene delivery techniques could stimulate skin regeneration and wound healing, decrease infection, and potentially improve the success of tissue-engineered skin [6]. For efficient gene delivery, a biocompatible gene carrier must be used to transport the desired genes into target cells. The ideal carrier must be able to encapsulate, condense, and protect a functional gene-bearing DNA molecule against degrading enzymes, transfer it across the cellular membrane and facilitate endosomal escape and nuclear uptake of the internalized gene [7,8]. In this section of my thesis introduction, I will provide some of the advantages and limitations of viral and non-viral carriers used for epidermal gene therapy.

2.1.1 Viral DNA Delivery

Viral carriers have been the choice among clinicians for gene delivery since viruses evolved to introduce their DNA payload into mammalian cells and to facilitate intracellular trafficking of the DNA for a sustained gene expression. The common viral carriers include retroviruses, lentiviruses, adenoviruses, and adeno-associated viruses. Retroviruses contain

reverse transcriptase and are able to produce DNA from their RNA genome. This allows integration of their genome into the host genome. Two types of retroviral vectors have been developed for gene delivery: replication competent and replication defective [9,10]. Replication defective viruses are the preferred retroviruses used for gene delivery since they do not have the ability to replicate in the host independently and require an additional virus for replication [11]. Replication competent retroviruses have all the necessary genes for replication and will replicate after infection. However due to the fact that they contain a lot of endogenous gene, their cargo is smaller and therefore the length of the inserted viral gene is shorter [9]. Lentiviruses are a subclass of retroviruses. They can integrate their gene into the host genome of non-dividing cells [12]. Viral RNA is reverse transcribed and the resultant DNA is inserted into the host genome by viral integrase enzymes, passing the vector to the next generation of cells. With adenoviral vectors, the viral DNA does not integrate into the host genome and does not get replicated during cell division. This limits their use in gene therapy and only transient gene expression is feasible using this gene carrier. It is known that the adenoviruses can trigger rapid immune response and lead to potentially dangerous consequences, since we have been continuously exposed to adenoviruses in everyday life [13]. Adeno-associated viruses (AAV) have been developed to overcome some of the drawbacks of adenoviruses. They elicit very mild immune responses as they do not express any viral protein. AAVs can infect both dividing and non-dividing cells, and may incorporate their genome into host cells [14]. They are an attractive candidate for creating viral vectors for gene therapy.

The viral carriers are, however, associated with important drawbacks. They are difficult to produce and can carry limited amounts of DNA, and have the potential to give rise to uncontrolled proliferation of modified cells [15]. Adenoviruses can trigger inflammatory and/or

immunological reaction to the modified cells [16,17]. An immune response caused by adenoviral gene therapy of a patient with ornithine transcarbamylase (OTC) caused the patient's death in the year 2000 [13]. Retroviruses and lentiviruses can potentially produce oncogenes leading to cancer. Other drawbacks are also associated with retroviral carriers: (i) Cells have to be actively dividing for transduction, so cells that do not replicate (e.g. neurons) resist transduction (ii) there are concerns for mutational mutagenesis due to the integration of gene to the host genome. Insertional oncogenesis has caused leukemia in 4 SID patients treated by retroviral gene therapy [18]. These concerns have limited the application of gene therapy only to a select set of disorders, in particularly cancer, where the therapeutic benefit of viral gene therapy can be justified.

2.1.2 Non-Viral DNA Delivery

Synthetic materials capable of delivering an exogenous DNA molecule into mammalian cells has been pursued as a clinically safer alternative to viral carriers [19,20], but their low effectiveness has hampered their utility in a clinical setting [8]. Several types of lipid-based carriers have been used by research group for DNA encapsulation and delivery for skin regeneration and wound healing. Lipofectamine™ 2000, FuGene™ 6 and cationic liposomes are the lipid-based carriers used for epidermal gene therapy. Lipofectamine™ 2000 and FuGene™ 6 are commercially available products and are able to form lipocomplexes with DNA and perform gene delivery. Cationic liposomes are synthetic carriers that protect the DNA from nuclease-mediated degradation and improve transgene-cell interactions. The ease of synthesis and versatility of lipid-based carriers makes them an appropriate choice for DNA delivery and they

have shown high efficiency in some *in vitro* studies. However, their *in vivo* use has been questioned due to considerable side effects. Acute inflammatory reactions have been reported in animals treated with intravenous injection of lipoplexes [21]. Significant toxicity has also been associated with lipid mediated gene delivery [22,23]. Systemic gene delivery via the tail vein using lipids has also been shown to produce toxic effects in the lungs, liver, and spleen. One report has also associated tail vain delivery of lipids to induction of inflammatory cytokines and decrease in white cell counts [24]. In humans, various degrees of adverse inflammatory reactions, including flu like symptoms with fever and airway inflammation, were noted among subjects who received lipoplexes [22]. These early clinical data suggest that some lipoplex formulations are inadequate for use in humans.

Physical delivery methods have gained considerable attention for *in vivo* epidermal gene therapy. The leading methods used include gene gun delivery and electroporation. They use a physical force to penetrate the cell membrane and facilitate intracellular uptake. Gene gun DNA delivery is an *in vivo* approach for transfection of cells. In this method, DNA is coupled to a nanoparticle of an inert solid (usually gold) and shot directly into the target cell's nucleus using pressurized gas. The particle is able to penetrate a few millimeters into the tissue and release the DNA into the cell's path. Gene delivery using this method provides good efficiency in gene expression, especially in the tissues near the surface of the body. Studies are on going to improve the chemical coating of the gold surface to improve DNA coating [25]. A drawback of the gene gun delivery system is possible tissue damage caused by the pressurized release of the gold particle [26]. Electroporation is another *in vivo* transfection method which is used predominantly in skin and muscle tissues, but could be applied in other tissues as well [27]. In this method, an electrical field is used to increase the electrical conductivity and permeability of the plasma

membrane. DNA as large as 100 kb has been delivered *in vivo* using this method [28], and stable transfection for as long as 1 year after single electroporation has been seen [29]. Some studies have suggested that using intravenous DNA injection followed by electroporation of a selected site increases localized gene delivery in the selected site [30]. Some major limitations have been associated with electroporation. It has a limited range between the electrodes (~1 cm), which makes it difficult to transfect cells in a large area of tissues. Additionally, a surgical procedure is required to place the electrodes deep into the internal organs and finally, the high voltage applied to tissues can result in severe tissue damage [27]. However, some of these concerns may be resolved by optimizing the design of electrodes, the field strength, and the duration and frequency of electric pulses.

2.2 A Survey of Epidermal Gene Delivery

Below, I aim to provide a survey for the application of viral and non-viral methods of DNA delivery for epidermal gene delivery. Compilation of this survey is based on the type of gene delivered and the therapeutic target of gene therapy.

2.2.1 Delivery of Reporter Genes

Many research groups have explored the efficiency of viral gene carriers in *in vivo* and *in vitro* systems by using reporter genes. Hasson *et al.* explored using various viral delivery systems to determine an efficient delivery method for the delivery of the reporter gene beta-galactosidase (ß-gal) to micro organs prepared from spleen, lung, colon and skin. The viruses they compared in

this study were herpes simplex virus type 1, adenovirus, vaccinia virus, and murine leukemia virus (MuLV). They conclude that all viral vectors were able to transfect the target tissues with adenovirus yielding significantly higher transfection values [31]. Despite this, the viral vector that has been most consistently used for reporter gene carrier for epidermal gene delivery has been retrovirus. Del Rio *et al.* used retrovirus for enhanced green fluorescent protein (EGFP) transduction in a preclinical model for analyzing the genetically modified human skin in a mouse model and identified epidermal stem cell clones responsible for human skin regenerated in NOD/SCID recipients [32]. Lu *et al.* and Ghazizadeh *et al.* used retroviral vectors to transduce LacZ reporter gene in mouse epidermis for cutaneous gene therapy in two separate studies. They were able to gain transduction but reported loss of transgene expression by 3 weeks after transduction, concurrent with the onset of host immune responses to the transgene product. They suggest that long-term cutaneous gene therapy may require development of strategies to interfere with activation or function of T-cell populations [33,34]. Bickenbach *et al.* also used retrovirus to transfer LacZ to preselected human epidermal stem cells and reported that transduced cells showed persistent expression of ß-gal through 12 weeks [35]. Their study revealed the feasibility of using preselected stem cells for epidermal gene therapy. Escamez *et al.* established an *in vivo* tumor model and explored the efficiency of a retroviral vector in the delivery of EGFP and reported that their delivery system is a suitable tool for therapeutic applications of human skin wound healing [36]. A polyethylene glycol (PEG) polymer was used by Ohsawa *et al.* to enhance adenovirus mediated gene transfer of the Lac Z. They suggested that PEG modification of this virus is a simple, safe, and effective method for facilitating virus-mediated gene therapy in the skin [37].

Non-viral gene delivery by lipid based carriers has also been assessed for epidermal gene delivery using reporter genes. Birchall *et al.* used a complexation of cationic liposomes with a reporter plasmid DNA to form lipid:plasmid DNA (pDNA) vectors that protected the DNA from nuclease-mediated degradation and improved lipoplex-cell interactions. Their results indicated that cationic lipid:pDNA lipoplexes could mediate uptake and expression of reporter plasmid DNA 33-fold higher compared with control in viable epidermal tissue [38]. Hellgren *et al.* used cell-mediated gene transfer by using the lipid based carrier FuGene^{TM} 6 both *in vitro* and *in vivo*. They detected high efficiency in transfection of primary human and rabbit fibroblasts for future therapeutic non-viral gene delivery [39].

Physical delivery methods have also been shown to be efficient for epidermal reporter gene delivery. Ogura *et al.* used laser-induced stress waves (LISWs) to transfer EGFP gene in mice and detected highly efficient and site-specific gene transfer by applying a few pulses of nanosecond pulsed LISWs to rat skin *in vivo* [40]. Babiuk *et al.* used needle-free plasmid injection in combination with electroporation to transfer the luciferase gene to pigs and detected significant enhancement in gene expression. They suggest that possible improvement in cellular uptake of plasmid DNA maybe the reason behind increased gene expression of their delivery system [41].

2.2.2 Gene Delivery for Functional Wound Healing

One of the major applications of gene therapy is wound healing, where the skin is torn, cut or punctured. The source of wounds could be accidents, cuts, gunshots, traumas, hematomas, or diabetic ulcers. Many research groups have used a gene therapy approach to enhance wound

healing by transducing growth factors in mouse and rat models. A growth factor is a naturally occurring substance capable of stimulating cellular growth, proliferation and differentiation. Gene therapy approaches using growth factors for wound healing are intended to promote the growth and proliferation of epidermal cells (fibroblast and keratinocytes), leading to the growth and repair of the lost skin tissue. Retroviral vectors have been among the candidates used for this purpose. Breitbart *et al.* used retrovirus for platelet derived growth factor–B (PDGF-B) delivery for diabetic wound healing in a mouse model and demonstrated the promising potential for gene therapy in diabetic wound healing [42]. They further reported that experimentation with additional genes in combination with PDGF-B for additional, improved wound healing is required [43].

Adenoviral vectors have also been used for epidermal gene therapy for wound healing. Di Peppe *et al.* explored vascular endothelial growth factor (VEGF) gene transfer for wound healing in order to promote angiogenesis in CD1 diabetic mice using adenovirus. Their results suggested that VEGF gene transfer by adenovirus may be used as a therapeutic tool for the treatment of diabetic ulcers [44]. Luo *et al.* used an adenoviral vector for gene therapy aimed at restoring cutaneous nitric oxide bioavailability. Their studies were aimed at providing an effective means to enhance delayed diabetic wound healing and they were able to gain partial success [45]. Gu *et al.* used an adenovirus encoding human PDGF-B in a rabbit dermal wound model and showed that repeated doses of PDGF-B gene therapy using adenovirus led to robust, localized tissue repair [46]. Using AAV for wound healing gene therapy, Deodato *et al.* [47] and Galeano *et al.* [48] transduced VEGF-A (the most important member of the VEGF family) in mice and suggested that their method might represent a novel approach to treat wound healing disorders. Furthermore, Galeano *et al.* explored the efficiency of an AAV vector in the transduction of the

VEGF gene for wound healing after burn injuries. They detected increased epithelial proliferation, angiogenesis, and maturation of the extracellular matrix after transduction. Furthermore, their gene delivery system enhanced VEGF expression, and the wound content of the mature protein [49].

Non-viral delivery systems have also been used for wound healing. Jeschke *et al.* delivered insulin-like growth factor-I (IGF-I) gene using liposomal gene delivery. The liposomes that they used were formulated from 1:1 (M/M) DMRIE (1,2-dimyristyloxypropyl-3-dimethyl-hydroxyl ethyl ammonium bromide) and cholesterol suspended in water. They have been able to improve dermal and epidermal regeneration in rats using this lipid-based delivery system [50]. In a separate study, the same group used the same liposomes containing the Keratinocyte Growth Factor (KGF) and IGF-I at three different concentrations for *in vivo* skin regeneration and observed a dose-dependent response in the number of the transfected cells, and the degree of skin cell proliferation and angiogenesis [51]. Marti *et al.* used electroporative transfection with KGF-1 DNA to improve wound healing in a diabetic mouse model. Based on their results, injection of KGF plasmid DNA coupled with electroporation improved wound closure at the wound site [52].

Other groups have explored the use of viral gene therapy for constructing skin substitutes. Jung *et al.* used an adenovirus-mediated angiopoietin-1 (protein growth factor that promotes angiogenesis) gene therapy in a rat model and suggested that therapeutic angiogenesis in patients who undergo skin reconstructive procedures may be promoted using this delivery method [53].

2.2.3. Gene Delivery for Various Clinical Applications Involving Skin

Gene therapy has also been used to treat many other skin disorders in animal models. Among them is the erythropoietic protoporphyra, a disease associated with the lack of the ferrochelatinase enzyme. This results in deficiencies in heme biosynthesis and accumulation of ferrochelatase's substrate, protoporphyra, leading to painful photosensitivity. Symptoms include burning and itching sensation on the surface of the skin. Viral gene therapy approaches have been used to restore the ferrochelatinase enzyme and treat this genetic disease. Richard *et al.* used a lentiviral vector to transduce the human ferrochelatase gene for a mouse model and show improvement in the efficiency of gene transfer with lentiviruses [54]. Pawliuk *et al.* used a retrovirus expressing both human ferrochelatase and GFP to transduce pre-selected hematopoietic stem cells and detected long-term correction of skin photosensitivity in all transplanted mice [55].

Other groups have explored viral gene therapy approaches for the treatment of dystrophic epidermolysis bullosa (RDEB), an inherited blistering skin condition in which the filaments that anchor the epidermis to the underlying dermis are either absent or do not function. This is due to defects in the gene for type VII collagen, a fibrous protein that is the main component of the anchoring filaments. A number of research groups have made attempts to restore the type VII collagen in order to treat this disease. Woodley *et al.* used a self-inactivating lentiviral vector to deliver the COL7A1 gene which encodes for collagen type VII and showed efficient and long-term gene transfer *in vivo* in RDEB mice [56]. Chen *et al.* used a lentiviral vector to transduce human type VII collagen gene (COL7A1) in wound healing by promoting angiogenesis in CD1 diabetic mice. They demonstrated that restoring type VII collagen gene expression in RDEB skin *in vivo* is feasible using this gene therapy approach [57]. Gache *et al.* used a retroviral

vector to transduce collagen type VII and were successful in constructing skin equivalents in RDEB dogs and mice [58].

Viral gene therapy treatment of xeroderma pigmentosum (XP) has also been attempted. XP is a genetic disorder of DNA repair in which the ability to repair damage caused by UV light is deficient. This is especially significant in the case of tumor suppressor genes (e.g. p53) or the proto-oncogenes (e.g. RAS), where lack of DNA repair could result in cancer. Therefore patients with XP are at a high risk for developing skin cancers. Marchetto *et al.* used adenovirus for the delivery of human XP-A gene to skin cells to prevent cancer in XP mice. They conclude that efficient adenovirus gene delivery to the skin is a promising tool for reconstitution of specific DNA repair defects in XP patients [59].

Other groups have attempted to boost the immune system by increasing the expression of cytokines. Injection of plasmid DNA without carrier seems to be beneficial in some studies to boost the immune system. Tsuji-Yamada *et al.* explored the effect of the cytokine interleukin-12 (IL-12) encoding plasmid on tight-skin mouse for a therapeutic effect on systemic sclerosis, a systemic connective tissue disease. After one week of injection, the mice exhibited a marked decrease in the skin thickness compared to controls. The serum levels of antibodies were diminished in IL-12 treated mice, indicating that IL-12 administration into the mice had beneficial effects in preventing the collagen accumulation in the skin and suppressing the autoimmunity. Their study suggests that the IL-12 encoding plasmid administration might have a therapeutic effect on systemic sclerosis [60]. Chun *et al.* compared the delivery efficiency of vaccinia virus and herpes simplex virus to free plasmid DNA for IL-10 gene transfection. They detected that the viral vector system was better for obtaining short-term effects, whereas the free

plasmid DNA approach provided superior therapeutic effects due to the fact that it was longer lasting [61].

Viral vectors have also been used in this approach. Carretero *et al.* used adenoviruses to transduce human antimicrobial peptides HBD-2, HBD-3, and LL-37 and showed inhibition of bacterial growth in human keratinocytes [62]. Noel *et al.* used retrovirus for sustained systemic delivery of monoclonal antibodies by genetically modified skin fibroblasts and suggested that skin fibroblasts can potentially be used in antibody-based gene/cell therapy protocols without adverse immune response [63].

A non-viral approach is the study by Egashira *et al*. using a liposome containing the plasmid DNA encoding for anti-monocyte chemoattractant protein-1 to inhibit vascular remodeling in rats. They reported that their model may be useful for gene therapy against arteriosclerosis (thickening of arteries) [64].

Gene gun delivery has also been used in boosting the immune system. Oshikawa *et al.* used gene gun delivery for IL-12 gene transfer in a mouse tumor model and detected increased anti-metastatic activities of T-cells, NK-cells, interferon-α (IFN-α), and anti-angiogenesis [65]. Yang *et al.* used cytokine transgene delivery *in vivo* by gene gun and introduced this as a means for improving the efficiency of cytokine gene therapy and DNA vaccines in future clinical studies [66].

As reviewed in this report, viral carriers have been widely used for epidermal gene therapy *in vivo* and *in vitro*. They are highly efficient and usually lead to stable transfection of genes of interest in target cells/tissues. However as discussed earlier, major drawbacks are associated with viral carriers which limits their *in vivo* applications. The use of non-viral carriers for epidermal gene delivery has been limited to studies using lipid-based carriers and physical

delivery methods. To our knowledge, no group has investigated the efficiency of polymeric carriers of epidermal gene delivery. In this thesis work, I aim to investigate the efficiency of polymeric gene carriers for gene delivery to skin cells. Polymeric carriers provide a safe alternative to the potentially immunogenic and toxic viral and lipid-based carriers for gene delivery. They can be engineered to reduce immunogenic and toxic responses and serve therapeutic purposes in the body. I am especially exploring the efficiency of lipid substitution on poly(*L*-lysine) for gene encapsulation, protection against degrading enzymes, and delivery into the human CRL fibroblasts. This will be a novel approach for gene delivery in two aspects. Initially, to my knowledge, lipid substitution of PLL has not been previously applied by any research groups for gene delivery purposes. Secondly, polymeric carriers in general have not been previously used for epidermal gene delivery. I will initially explore the efficiency of lipid substituted PLL compared to other commercially available gene carriers such as adenovirus, polyethyleneimine (PEI), PLL, Lipofectamine™ 2000, and FuGene™ 6 for the delivery of the reporter gene EGFP. Ultimately, I will explore the efficiency of this delivery system for a therapeutic target.

REFERENCES

1. Anderson WF. Human gene therapy. Science. 1992, 256, 808-13.
2. Furlan R, Butti E, Pluchino S, Martino G. Gene therapy for autoimmune diseases. Curr Opin Mol Ther. 2004, 6, 525-36.
3. Cavazzana-Calvo M, Lagresle C, Hacein-Bey-Abina S, Fischer A. Gene Therapy for Severe Combined Immunodeficiency. An Rev of Med. 2005, 56, 585-602.
4. Kouraklis G. Review: Gene Therapy for Cancer. Dig Dis & Sciences. 2000, 45, 1045-52.
5. Branski LK, Pereira CT, Herndon DN, Jeschke MG. Gene therapy in wound healing: present status and future directions. Gene Ther. 2007, 14, 1-10.
6. Meilander-Lin NJ, Cheung PJ, Wilson DL, Bellamkonda RV. Sustained *in vivo* gene delivery from agarose hydrogel prolongs nonviral gene expression in skin. Tissue Eng. 2005, 11, 546-55.
7. Mintzer MA, Simanek EE. Nonviral vectors for gene delivery. Chem Rev. 2009, 109, 259–302.
8. Al-Dosari MS, Gao X. Nonviral gene delivery: principle, limitations, and recent progress. The AAPS J. 2009, 11, 671-81.
9. Logg CR, Tai CK, Logg A, Anderson WF, Kasahara N. A uniquely stable replication-competent retrovirus vector achieves efficient gene delivery *in vitro* and in solid tumors. Hum Gene Ther. 2001, 20, 921-32.
10. Flamant F, Samarut J. Virofection: A one-step procedure for using replication-defective retrovirus vectors. Virol. 1995, 211, 234-40.
11. Miller DG, Adam MA, Miller AD. Gene transfer by retrovirus vectors occurs only in cells that are actively replicating at the time of infection. Mol & Cell Biol. 1990, 10, 4239-42.

12. Federico M. Lentiviruses as gene delivery vectors. Curr Opin in Biotech. 1999, 10, 448-53.

13. Beardsley T. A tragic death clouds the future of an innovative treatment method. Sci Am. 2000, 282, 36-7.

14. McCarty DM, Samuel M, Young JR, Samulski J. Integration of adeno-associated virus (AAV) AND recombinant aav vector. Ann Rev of Genetics. 2004, 38, 819-845.

15. Kohn DB, Sadelain M, Glorioso JC. Occurrence of leukaemia following gene therapy of X-linked SCID. Nat Rev Cancer. 2003, 3, 477–488.

16. Zaiss AK, Vilaysane A, Cotter MJ, Clark SA, Meijndert SC, Colarusso P, Yates RM Petrilli V, Tschopp J, Muruve DA. Antiviral antibodies target adenovirus to phagolysosomes and amplify the innate immune response. J Immunol. 2009, 182, 7058-68.

17. Bessis N, GarciaCozar FJ, Boissier MC. Immune responses to gene therapy vectors: influence on vector function and effector mechanisms. Gene Ther. 2004, 11, 10-17.

18. Hacein-Bey-Abina S, Garrigue A, Wang GP, Soulier J, Lim A, Morillon E, Clappier E, Caccavelli L, Delabesse E, Beldjord K, Asnafi V, MacIntyre E, Cortivo LD, Radford I, Brousse N, Sigaux F, Moshous D, Hauer J, Borkhardt A, Belohradsky BH, Wintergerst U, Velez MC, Leiva L, Sorensen R, Wulffraat N, Blanche S, Bushman FD, Fischer A, Cavazzana-Calvo M. Insertional oncogenesis in 4 patients after retrovirus-mediated gene therapy of SCID-X1. The J of Clin Investigation. 2008, 118, 3132–42.

19. Wagner E. Strategies to improve DNA polyplexes for *in vivo* gene transfer: will “artificial viruses” be the answer? Pharm Res. 2004, 21, 8–14.

20. Putnam D. Drug delivery: the heart of the matter. Nat Mater. 2008, 7, 836-7.

21. Song YK, Liu F, Chu S, Liu D. Characterization of cationic liposome-mediated gene transfer *in vivo* by intravenous administration. Hum Gene Ther. 1997, 8, 1585-94.

22. Ruiz FE, Clancy JP, Perricone MA, Bebok Z, Hong JS, Cheng SH, Meeker DP, Young KR, Schoumacher RA, Weatherly MR, Wing L, Morris JE, Sindel L, Rosenberg M, van Ginkel FW, McGhee JR, Kelly D, Lyrene RK, Sorscher EJ. A clinical inflammatory syndrome attributable to aerosolized lipid-DNA administration in cystic fibrosis. Hum Gene Ther. 2001, 12, 751-61.
23. Scheule RK, St George JA, Bagley RG, Marshall J, Kaplan JM, Akita GY, Wang KX, Lee ER, Harris DJ, Jiang C, Yew NS, Smith AE, Cheng SH. Basis of pulmonary toxicity associated with cationic lipid-mediated gene transfer to the mammalian lung. Hum Gene Ther. 1997, 8, 689-707.
24. Yew NS, Scheule RK. Toxicity of cationic lipid-DNA complexes. Adv Genetics. 2005, 53, 189-214.
25. O'Brien J, Lummis SC. An improved method of preparing microcarriers for biolistic transfection. Brain Res Protoc. 2002, 10, 12-15.
26. Gao X, Kim K-S, Liu D. Nonviral gene delivery: what we know and what is next. AAPS. 2007, 9, 92-104.
27. Durieux AC, Bonnefoy R, Busso T, Freyssenet D. *In vivo* gene electrotransfer into skeletal muscle: effects of plasmid DNA on the occurrence and extent of muscle damage. J Gene Med. 2004, 6, 809-16.
28. Magin-Lachmann C, Kotzamanis G, D'Aiuto L, Cooke H, Huxley C, Wagner E. *In vitro* and *in vivo* delivery of intact BAC DNA-comparison of different methods. J Gene Med. 2004, 6, 195-209.
29. Molnar MJ, Gilbert R, Lu Y, Liu AB, Guo A, Larochelle N, Orlopp K, Lochmuller H, Petrof BJ, Nalbantoglu J, Karpati G. Factors influencing the efficacy, longevity, and safety of

electroporation-assisted plasmid-based gene transfer into mouse muscles. Mol Ther. 2004, 10, 447-55.

30. Sakai M, Nishikawa M, Thanaketpaisarn O, Yamashita F, Hashida M. Hepatocyte-targeted gene transfer by combination of vascularly delivered plasmid DNA and *in vivo* electroporation. Gene Ther. 2005, 12, 607-16.
31. Hasson E, Slovatizky Y, Shimoni Y, Falk H, Panet A, Mitrani E. Solid tissues can be manipulated ex vivo and used as vehicles for gene therapy. J Gene Med. 2005, 7, 926-35.
32. Del Rio M, Larcher F, Serrano F, Meana A, Muñoz M, Garcia M, Muñoz E, Martin C, Bernad A, Jorcano JL. A preclinical model for the analysis of genetically modified human skin *in vivo*. Hum Gene Ther. 2002, 13, 959-68.
33. Lu Z. Ghazizadeh S. Host immune responses in ex vivo approaches to cutaneous gene therapy targeted to keratinocytes. Derm. 2005, 14, 727-35.
34. Ghazizadeh S, Kalish RS, Taichman LB. Immune-mediated loss of transgene expression in skin: implications for cutaneous gene therapy. Mol Ther. 2003, 7, 296-303.
35. Bickenbach JR. Roop DR. Transduction of a preselected population of human epidermal stem cells: consequences for gene therapy. Proc of the Ass of Am Phys. 1999, 111, 184-9.
36. Escámez MJ, García M, Larcher F, Meana A, Muñoz E, Jorcano JL, Del Río M. An *in vivo* model of wound healing in genetically modified skin-humanized mice. J Invest Derm. 2004, 123, 1182-91.
37. Ohsawa T, Nakamura T, Mihara M, Sato K. Enhancement of adenovirus-medicated gene transfer into dermal fibroblasts *in vitro* and *in vivo* by polyethylene glycol 6000. J Derm. 2000, 27, 244-51.

38. Birchall JC, Marichal C, Campbell L, Alwan A, Hadgraft J, Gumbleton M. Gene expression in an intact ex-vivo skin tissue model following percutaneous delivery of cationic liposome-plasmid DNA complexes. Int J Pharm. 2000, 197, 233-8.

39. Hellgren I, Drvota V, Pieper R, Enoksson S, Blomberg P, Islam KB, Sylvén C. Highly efficient cell-mediated gene transfer using non-viral vectors and FuGene 6: *in vitro* and *in vivo* studies. Cel & Mol Life Sci. 2000, 57, 1326-33.

40. Ogura M, Sato S, Nakanishi K, Uenoyama M, Kiyozumi T, Saitoh D, Ikeda T, Ashida H, Obara M. *In vivo* targeted gene transfer in skin by the use of laser-induced stress waves. Lasers in Surg & Med. 2004, 34, 242-8.

41. Babiuk S, Baca-Estrada ME, Foldvari M, Baizer L, Stout R, Storms M, Rabussay D, Widera G, Babiuk L. Needle-free topical electroporation improves gene expression from plasmids administered in porcine skin. Mol Ther. 2003, 8, 992-8.

42. Breitbart AS, Mason JM, Urmacher C, Barcia M, Grant RT, Pergolizzi RG, Grande DA. Gene-enhanced tissue engineering: applications for wound healing using cultured dermal fibroblasts transduced retrovirally with the PDGF-B gene. Annal of Plastic Surg. 1999, 43, 632-9.

43. Breitbart AS, Laser J, Parrett B, Porti D, Grant RT, Grande DA, Mason JM. Accelerated diabetic wound healing using cultured dermal fibroblasts retrovirally transduced with the platelet-derived growth factor B gene. Annal of Plastic Surg. 2003, 51, 409-14.

44. Romano Di Peppe S, Mangoni A, Zambruno G, Spinetti G, Melillo G, Napolitano M, Capogrossi MC. Adenovirus-mediated VEGF (165) gene transfer enhances wound healing by promoting angiogenesis in CD1 diabetic mice. Gene Ther. 2002, 9, 1271-7.

45. Luo JD, Wang YY, Fu WL, Wu J, Chen AF. Gene therapy of endothelial nitric oxide synthase and manganese superoxide dismutase restores delayed wound healing in type 1 diabetic mice. Circulation. 2004, 110, 2484-93.

46. Gu DL, Nguyen T, Gonzalez AM, Printz MA, Pierce GF, Sosnowski BA, Phillips ML, Chandler LA. Adenovirus encoding human platelet-derived growth factor-B delivered in collagen exhibits safety, biodistribution, and immunogenicity profiles favorable for clinical use. Mol Ther. 2004, 9, 699-711.

47. Deodato B, Arsic N, Zentilin L, Galeano M, Santoro D, Torre V, Altavilla D, Valdembri D, Bussolino F, Squadrito F, Giacca M. Recombinant AAV vector encoding human VEGF165 enhances wound healing. Gene Ther. 2002, 9, 777-85.

48. Galeano M, Deodato B, Altavilla D, Cucinotta D, Arsic N, Marini H, Torre V, Giacca M, Squadrito F. Adeno-associated viral vector-mediated human vascular endothelial growth factor gene transfer stimulates angiogenesis and wound healing in the genetically diabetic mouse. Diabetologia. 2003, 46, 546-55.

49. Galeano M, Deodato B, Altavilla D, Squadrito G, Seminara P, Marini H, Stagno d'Alcontres F, Colonna M, Calò M, Lo Cascio P, Torre V, Giacca M, Venuti FS, Squadrito F. Effect of recombinant adeno-associated virus vector-mediated vascular endothelial growth factor gene transfer on wound healing after burn injury. Crit Care Med. 2003, 31, 1017-25.

50. Jeschke MG, Richter G, Höfstädter F, Herndon DN, Perez-Polo JR, Jauch KW. Non-viral liposomal keratinocyte growth factor (KGF) cDNA gene transfer improves dermal and epidermal regeneration through stimulation of epithelial and mesenchymal factors. Gene Ther. 2002, 9, 1065-74.

51. Jeschke MG, Richter G, Herndon DN, Geissler EK, Hartl M, Hofstätter F, Jauch KW, Perez-Polo JR. Therapeutic success and efficacy of nonviral liposomal cDNA gene transfer to the skin *in vivo* is dose dependent. Gene Ther. 2001, 8, 1777-84.

52. Marti G, Ferguson M, Wang J, Byrnes C, Dieb R, Qaiser R, Bonde P, Duncan MD, Harmon JW. Electroporative transfection with KGF-1 DNA improves wound healing in a diabetic mouse model. Gene Ther. 2004, 11, 1780-5.

53. Jung H, Gurunluoglu R, Scharpf J, Siemionow M. Adenovirus-mediated angiopoietin-1 gene therapy enhances skin flap survival. Microsurgery. 2003, 23, 374-80.

54. Richard E, Mendez M, Mazurier F, Morel C, Costet P, Xia P, Fontanellas A, Geronimi F, Cario-André M, Taine L, Ged C, Malik P, de Verneuil H, Moreau-Gaudry F. Gene therapy of a mouse model of protoporphyria with a self-inactivating erythroid-specific lentiviral vector without preselection. Mol Ther. 2001, 4, 331-8.

55. Pawliuk R, Bachelot T, Wise RJ, Mathews-Roth MM, Leboulch P. Long-term cure of the photosensitivity of murine erythropoietic protoporphyria by preselective gene therapy. Nature Medicine. 1999, 5, 768-73.

56. Woodley DT, Keene DR, Atha T, Huang Y, Ram R, Kasahara N, Chen M. Intradermal injection of lentiviral vectors corrects regenerated human dystrophic epidermolysis bullosa skin tissue *in vivo*. Mol Ther. 2004, 10, 318-26.

57. Chen M, Kasahara N, Keene DR, Chan L, Hoeffler WK, Finlay D, Barcova M, Cannon PM, Mazurek C, Woodley DT. Restoration of type VII collagen expression and function in dystrophic epidermolysis bullosa. Nat Gen. 2002, 32, 670-5.

58. Gache Y, Baldeschi C, Del Rio M, Gagnoux-Palacios L, Larcher F, Lacour JP, Meneguzzi G. Construction of skin equivalents for gene therapy of recessive dystrophic epidermolysis bullosa. Hum Gene Ther. 2004. 15, 921-33.

59. Marchetto MC, Muotri AR, Burns DK, Friedberg EC, Menck CF. Gene transduction in skin cells: preventing cancer in xeroderma pigmentosum mice. Proc Nat Acad Sci USA. 2004, 10, 17759-64.

60. Tsuji-Yamada J, Nakazawa M, Takahashi K, Iijima K, Hattori S, Okuda K, Minami M, Ikezawa Z, Sasaki T. Effect of IL-12 encoding plasmid administration on tight-skin mouse. Biochem & Biophys Res Com. 2001, 280, 707-12.

61. Chun S, Daheshia M, Lee S, Rouse BT. Immune modulation by IL-10 gene transfer via viral vector and plasmid DNA: implication for gene therapy. Cel Immun. 1999, 194, 194-204.

62. Carretero M, Del Río M, García M, Escámez MJ, Mirones I, Rivas L, Balague C, Jorcano JL, Larcher F. A cutaneous gene therapy approach to treat infection through keratinocyte-targeted overexpression of antimicrobial peptides. FASEB J. 2004, 18, 1931-3.

63. Noël D, Pelegrin M, Brockly F, Lund AH, Piechaczyk M. Sustained systemic delivery of monoclonal antibodies by genetically modified skin fibroblasts. J Invest Derm. 2000, 115, 740-5.

64. Egashira K, Koyanagi M, Kitamoto S, Ni W, Kataoka C, Morishita R, Kaneda Y, Akiyama C, Nishida KI, Sueishi K, Takeshita A. Anti-monocyte chemoattractant protein-1 gene therapy inhibits vascular remodeling in rats: blockade of MCP-1 activity after intramuscular transfer of a mutant gene inhibits vascular remodeling induced by chronic blockade of NO synthesis. FASEB J. 2000, 14, 1974-8.

65. Oshikawa K, Rakhmilevich AL, Shi F, Sondel PM, Yang N, Mahvi DM. Interleukin 12 gene transfer into skin distant from the tumor site elicits antimetastatic effects equivalent to local gene transfer. Hum Gene Ther. 2001, 12, 149-60.

66. Yang CH, Shen SC, Lee JC, Wu PC, Hsueh SF, Lu CY, Meng CT, Hong HS, Yang LC. Seeing the gene therapy: application of gene gun technique to transfect and decolour pigmented rat skin with human agouti signalling protein cDNA. Gene Ther. 2004, 11, 1033-9.

CHAPTER III

Palmitic Acid-Modified Poly-L-Lysine for Non-Viral Delivery of Plasmid DNA to Skin Fibroblasts

[1]The Contents of this chapter have been previously published in: Abbasi M, Uludağ H, Incani V, Olson C, Lin X, Clements BA, Rutkowski D, Ghahary A, Weinfeld M. Palmitic Acid-Modified Poly-L-Lysine for Non-Viral Delivery of Plasmid DNA to Skin Fibroblasts. Biomacromolecules. 2007, 8, 1059-1063.

INTRODUCTION

Gene therapy aims to reconstitute a missing or defective gene with a correct copy in a host genome [1]. This is possible when one utilizes biocompatible gene carriers to transport desired genes into target cells [2]. Viral carriers have been preferred by clinicians for this purpose since viruses have evolved to effectively transfect mammalian cells and to facilitate intracellular trafficking of the genetic material for a sustained gene expression. The viral carriers are, however, associated with important drawbacks. They have the potential to give rise to uncontrolled proliferation of modified cells [3], cause inflammation at the site of administration, and raise immunological reactions against the modified cells [4,5]. These concerns have limited the application of gene therapy only to a select set of disorders, cancers most notably, whose potential benefits of the therapy clearly justify the possible adverse effects associated with viral gene delivery. Synthetic biomaterials capable of delivering an exogenous DNA into mammalian cells have been pursued as a clinically safer alternative to viral carriers [6-8]. Polymeric biomaterials with cationic charges can effectively condense a DNA molecule into nano-size particles, which facilitates the intracellular uptake of DNA. The polymers are more compatible with physiological systems, since they cause minimal host reactions, but their low effectiveness has hampered their utility in a clinical setting. More effective carriers capable of transferring exogenous DNA into target cells will greatly facilitate application of gene therapy.

This study was conducted to engineer effective non-viral carriers for modification of clinically useful cells. The non-viral vectors were designed by combining a prototypical cationic polymer (poly-*L*-lysine, PLL), which display a strong DNA binding property, with an endogenous lipid, palmitic acid (PA; HOOC-$(CH_2)_{14}$-CH_3). PA is utilized by mammalian cells for intracellular protein trafficking; by introducing a hydrophobic moiety to hydrophilic (i.e.,

water-soluble) proteins during post-translational modification, protein transport is facilitated through lipid-based sub-cellular membranes on their way to the site of activity [9]. We reasoned that incorporating this natural lipid molecule into a cationic polymer should result in a 'biomimetic' mechanism for facilitated transport of exogenous DNA into cells. The feasibility of this approach was explored by using a model plasmid encoding enhanced green fluorescent protein (pEGFP-N2), and skin fibroblasts as a clinically-useful cell target. These cells are actively pursued in human gene therapy protocols [10], since they are readily harvested from patients, expanded *in vitro*, and grafted into a host without systemic immunosuppressants. Skin fibroblasts can be manipulated *ex vivo* to construct functional tissues for tissue replacement [11] or used for constitutive delivery of systemic gene products [12]. As with other cells, gene delivery into fibroblasts has been primarily achieved with viral vectors but, in this study, we show that palmitylated PLL (PLL-PA) is capable of delivering an effective dose of exogenous DNA into cells, is compatible with cellular growth in culture, and sustain transgene expression in a significant (10-50%) fraction of fibroblasts.

The PA was grafted to 25 kDa PLL (25 mg) by reacting the polymer with *N*-hydroxy-succinimide ester of PA (<10% amine equivalent) in 50:50 DMF:DMSO (2 mL) for 2 h (**Scheme 1**; see [13] for details of synthesis and characterization). Excess ethyl ether was added to precipitate the product, which was washed with ethyl ether and dried under vacuum at room temperature. The composition of the final product was determined by ^{1}H-NMR with D_2O as the solvent. The proton shifts specific for PA (δ~0.8 ppm; -C$\underline{H}_3$) and PLL (δ~4.3 ppm; –NH-C$\underline{H}$-CO) were integrated, and normalized for the Hs in each peak to obtain the extent of PA substitution. The PA substitution was effectively controlled by the amount of *N*-hydroxy-succinimide ester of PA in the reaction mixture [13]. The PLL-PA up to 16.2 PA/PLL (mol/mol)

was soluble in aqueous buffers, so that this polymer was chosen for further investigation in this study.

MATERIALS & METHODS

Materials. Branched PEI (25 and 1.8 kDa), PLL hydrobromide (4 and 25 kDa), *N*-hydroxysuccinimide ester of palmitic acid, 5% (w/v) 2,4,6-trinitrobenzosulfonic acid (TNBS), trypsin/EDTA, and Hanks' Balanced Salt Solution (HBSS) were obtained from SIGMA (St. Louis, MO). Dulbecco's Modified Eagle Medium (DMEM; high glucose with L-glutamine), Penicillin (10,000 U/mL), Streptomycin (10,000 μg/mL) and Lipofectamine^{TM} 2000 were from Invitrogen (Carlsbad, CA). FuGene^{TM} 6 was obtained from Roche Diagnostics (Montreal, QC, Canada) and linear PEIs were from Polysciences (Warrington, PA). Fetal Bovine Serum (FBS) was obtained from Atlanta Biologicals (Lawrenceville, GA). A 4.7 kb plasmid incorporating an enhanced green fluorescent protein (pEGFP-N2) and a kanamycin resistance gene was obtained from BD Biosciences (Mountain View, CA), and replicated in kanamycin resistant DH5-α *Ecoli* strain grown in Luria-Bertani medium [11]. The purified plasmid was dissolved in ddH_2O at 0.4 mg/mL. CRL human skin fibroblasts were obtained from a cell bank maintained at the Alberta Cross Cancer Institute (Edmonton, Alberta).

Atomic Force Microscopy (AFM). The MultiMode scanning probe microscope (Digital Instruments Inc., Santa Barbara, CA) was used for all AFM studies. A large-area scanner (J type) with a maximum *xy* scan range of 125 x 125 μm and a *z* vertical range of 5 μm was used, except for imaging naked plasmid DNA, where a small-area scanner (A type) with a maximum *xy* scan range of 0.4 x 0.4 μm and a *z* vertical range of 0.4 μm was used for higher resolution. Single

crystal silicon cantilevers were cleaned by exposure to high intensity UV light for 3 minutes before use. The oscillation amplitude of the scanning tip was registered at 0.5 V and the frequency of the oscillation was in the range of 200-400 kHz. All AFM imaging was conventional ambient tapping mode AFM. The scan rate was typically 1.0-2.0 Hz and the data collection was at 512 x 512 pixels. Images were processed and analyzed using the Nanoscope III software (V5.12).

To visualize pEGFP-N2/polymer complexes, 2 μL of pEGFP-N2 solution (0.02 mg/mL in ddH_2O), 2 μL of polymer solution (0.02 mg/mL in ddH_2O) and 2 μL of 9 mM NaCl solution were incubated for 30 minutes, and 3 μL of this solution was transferred to a freshly cleaved mica surface. After drying at room temperature for 30 minutes, the surface was blow-dried with N_2 (if necessary). Naked plasmid was visualized as above except without addition to any polymer to the sample. The chosen pEGFP-N2:polymer ratios were based on agarose gel-electrophoresis analysis of the complexes, which corresponded to ratios for complete plasmid complexation. The samples were then imaged under tapping mode as described above.

Cellular Uptake of Polymers. The PEI (25 kDa) and PLL (25 kDa) were labeled with 1 mM fluorescein isothiocyanide (FITC) according to the manufacturer's directions (PIERCE; Rockford, IL), dialyzed against 0.1 M phosphate buffer (MW cut-off: 12-14 kDa), and then against ddH_2O to remove the unreacted FITC. TNBS assay was then used to determine the polymer concentrations in the dialyzed samples [11]. FITC-labeled PLL and PEI (1-9 μg/mL) were incubated with fibroblasts grown in 6-well plates (in 2 mL basic medium/well) for ~24 h. After removing the polymer-containing media, the cells were washed with HBSS, trypsinized, centrifuged, and suspended in HBSS with 3.7% formalin for flow cytometric analysis. The

instrument threshold for the negative control sample (i.e., cells incubated with no polymers) was set-up at ~1% level. The percentage of cells exhibiting FITC-fluorescence beyond this threshold value was determined as a function of polymer concentration in the medium. The average level of fluorescence in this GFP-positive population was used as a relative measure of polymer uptake.

Cellular Uptake of pEGFP-N2. For assessment of pEGFP-N2 uptake, 20 μg of pEGFP-N2 in 300 μL ddH_2O was incubated with 100 μL solution of a succinimide ester of Cy5.5-NHS (1 mg dissolved in 300 μL DMSO; AMERSHAM, St. Laurence, QC), and allowed to react for 2 h at room temperature. The reaction was stopped by extensive dialysis against TBE buffer. 5 μL of the labeled plasmid solution was mixed with 10 μL of 1 mg/mL polymer solution (PEI, PLL, PLL-PA, and linear PEI) or 6 μL of Lipofecatmine-2000^{TM} or FuGene^{TM} 6. The solution also contained 150 mM NaCl, and incubated for 30 min at 37 ^{o}C before addition to the cells in 6-well plates (2 mL basic medium/well) for 20 h. After removing the pEGFP-N2-containing media, the cells were washed with HBSS, trypsinized, centrifuged, and suspended in HBSS with 3.7% formalin for flow cytometric analysis (λ_{ex}=690 nm, λ_{em}=705 nm). The instrument was calibrated so that the negative control sample (i.e., pEGFP-N2 without any polymeric carrier) gave ~1% cell uptake. The percentage of cells exhibiting Cy5.5-fluorescence beyond this threshold value was determined.

Transfection with pEGFP-N2. The cells used for transfections were grown in 6-well plates or on glass coverslips to assess transfections by using flow cytometry and epifluorescent microscopy, respectively. The concentrations of all reagents and incubation volumes/times used

in this study were optimized based on previously reported studies [10,11]. The polymer/pEGFP-N2 polyplexes used for transfections were prepared by mixing 0.4 mg/mL pEGFP-N2 (in ddH_2O) with 1 mg/mL polymer solutions (in ddH_2O), and bringing the volume to 50 μL with 150 mM NaCl. The polyplexes for each transfection contained 3 μg of pEGFP-N2, and 18 μg of polymer (either PLL or PEI) and added to cells grown in 2 mL medium. After 30 minute of complex formation, the polyplexes were added to the cells grown on 6-well plates. A similar procedure was used with Lipofectamine^{TM} 2000, where the volume of the lipid used was 18 μL. The source/methods for adenoviral transfections were reported previously [11]. The cells were incubated for 24 h with the transfection reagents, after which the cells were either trypsinized for assessment of EGFP expression, or the medium was replaced with fresh medium for longer time cultures. Flow cytometry was performed on a BD FACscan where the cell fluorescence was detected by λ_{ex}= 485 nm and λ_{em} = 527 nm for EGFP expression. The instrument settings were calibrated for each run so as to obtain a background level of EGFP expression of ~1% for control samples (i.e., cells incubated with pEGFP-N2 alone without any carrier). An aliquot of the cell suspension used for flow cytometry was manually counted with a hemocytometer to obtain total number of cells recovered from the wells. The cells grown on coverslips were also transfected in a similar manner, but they were fixed at desired time points (with HBSS + 3.7% formalin), the nucleus stained with Hoechst 33258 (15 min at 1 μg/mL), and the coverslips were analyzed under an epifluorescent microscope. The numbers of GFP-positive cells (based on green cytoplasmic fluorescence) were quantified as a percentage of total number of cells (based on blue nuclear fluorescence) on a coverslip.

RESULTS & DISCUSSION

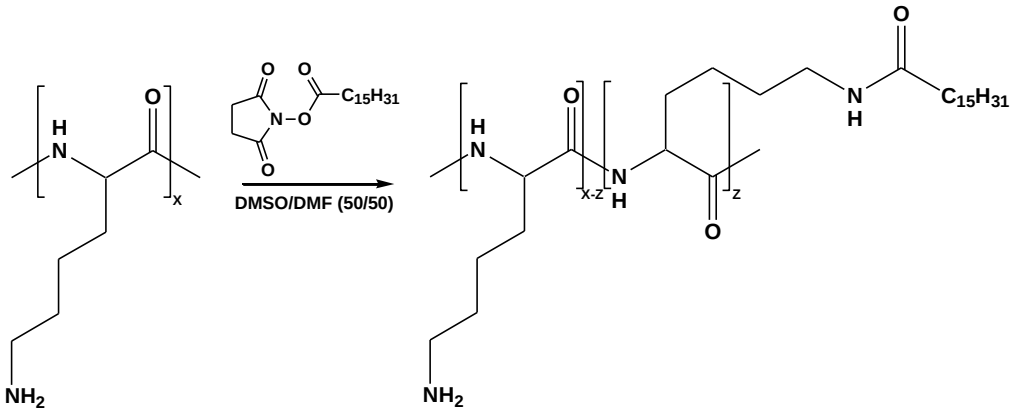

Scheme 1. Grafting of PA to PLL

To determine cellular uptake of polymers, human skin fibroblasts were cultured in DMEM containing 10% FBS, 100 U/mL penicillin, and 100 μg/mL streptomycin. The PLL and PLL-PA were labeled with fluorescein isothiocyanide (FITC) according to the manufacturer's instructions (PIERCE), along with another cationic polymer, polyethyleneimine (PEI). PEI, a relatively effective but toxic carrier, was used for comparison to PLL-based polymers. The fibroblasts were incubated with 2-18 μg/mL of the FITC-labeled polymers, and the percentage of cells displaying polymer uptake were quantified by flow cytometry. Flow cytometry was calibrated so that the cells not exposed to polymers displayed ~1% uptake as a background. Almost all cells in the population (>90%) displayed significant polymer-associated fluorescence at all polymer concentrations (**Figure 3-1A**). This was indicative of the homogeneity of the fibroblast population with respect to polymer binding. As expected, the extent of polymer binding, given by the average fluorescence for the FITC-positive cells, was proportional to the polymer concentration in medium (**Figure 3-1B**). Although polymers appeared to display differential propensity for binding (given by levels of intracellular fluorescence, **Figure 3-1B**),

this data cannot be used as a relative measure of uptake efficiency due to differences in FITC-labeling efficiency of individual polymers. It was important to note that the uptake study was conducted in the presence of a protein-rich medium (10% serum), and the proteins did not appear to impede the polymer binding/uptake even at low polymer concentration (2 μg/mL).

A critical requirement for cationic polymers for effective gene delivery is their ability to condense string-like DNA molecules into compact nano-size particles suitable for cellular uptake. Atomic Force Microscopy (AFM) was used to investigate complexation between the polymers and the plasmid DNA. A 4.7 kb plasmid (pEGFP-N2) incorporating an EGFP and a kanamycin resistance gene was replicated in DH5-α *Ecoli* strain for this purpose [14]. Freshly cleaved mica surfaces were used to deposit polymer/DNA complexes, which were prepared by complexing equal amounts of plasmid and polymer for 30 minutes. Particles smaller than ~20 nm were ignored in this analysis, since these were also visualized with 3 mM NaCl solution alone, and were likely to represent NaCl crystals formed under analysis conditions. An equivalent diameter for the larger particles was measured assuming a spherical geometry. The particles were in the size range of 55 to 312 nm (mean ± SD: 126 ± 50.7 nm) for PLL, and 50 to 200 nm (mean ± SD: 112 ± 34 nm) for PLL-PA (**Figure 3-2**; $p<0.01$, Student's *t*-test), suggesting that PA modification led to more compact particles. The distribution of the particles was uniform, with no preferential size range. A greater degree of heterogeneity was reported by Chan *et al.* [15] for PLL/plasmid particles, ranging from ~20 nm to as large as 800 nm (depending on N:P ratio). Miyata *et al.* [16], on the other hand, reported PLL/DNA particles in the 80-300 nm range similar to our results. Unlike tursoid-like particles reported in some studies, our particles were all spherical and compact. Under similar conditions, PEI gave particles ranging in size from 94 to 499 nm (mean ± SD: 270 ± 64 nm), and naked plasmid without any

polymer displayed the expected string-like structure (>1000 nm in length) with no visible particle formation (not shown). These particle sizes were consistent with the sizes found suitable for cellular uptake [17-19].

The capability of the polymers to deliver a plasmid cargo into the cells was then evaluated. After labeling pEGFP-N2 with Cy5.5 according to the manufacturer's directions (AMERSHAM), the plasmid was formulated with the carriers in 150 mM NaCl, incubated with the cells for 24 h, and the percentage of cells positive for the labeled plasmid was determined by flow cytometry. The flow cytometry was calibrated so that only ~1% of the cells displayed pEGFP-N2 association in the absence of any carrier (equivalent to cells incubated with no plasmid). pEGFP-N2 alone was not expected to penetrate into the cells due its non-compact nature, and the anionic charge of both the cell-surface and the plasmid DNA. Among the carriers tested, PEI and PLL-PA were most effective in delivering the plasmid cargo to the cells (**Figure 3-3A**). This was followed by PLL (25 kDa) and Lipofectamine^{TM} 2000, a cationic lipid formulation that is one of the most widely used commercial transfection agents. Other carriers tested, including short-branched PEI (1.8 kDa), PLL (4 kDa), and FuGene^{TM} 6 (a cationic lipid formulation) were relatively ineffective as carriers. The most effective carriers PEI and PLL-PA were able to modify >90% of the cells, again indicating a relatively uniform delivery of the plasmid cargo to the cells. In this respect, PEI and PLL-PA displayed good agreement between the polymer delivery and the DNA delivery results. However, this was not the case for PLL, since the extent of plasmid delivery seemed to be less than the polymer delivery. To determine if cell associated fluorescence actually represented internalized pEGFP-N2, Cy5.5-labeled pEGFP-N2 was complexed with PLL and PLL-PA, and incubated with the cells in the presence of Brefeldin A, a known inhibitor of cellular endocytosis at the trans-Golgi network [20-21]. After

8 h of incubation, a significant reduction in cell-associated pEGFP-N2 was observed with both carriers as a result of Brefeldin A treatment (**Figure 3-3B**), suggesting internalization of the complexes to be a significant reason for cell-associated fluorescence from flow cytometry. Confocal microscopy was additionally used to investigate the presence of pEGFP-N2 in the fibroblasts. Using AlexaFluor 546-labeled pEGFP-N2, there was no cell-associated pEGFP-N2 after 0.5 h (not shown) and 5 h incubation (**Figure 3-3C**) of the plasmid in the absence of any carriers. pEGFP-N2 complexes with the PLL-PA were visualized as red-fluorescent particles associated with the cells at both 0.5 and 5 h time points (**Figure 3-3C**). Whereas the pEGFP-N2/PLL-PA particles were present at the cell periphery at the initial 0.5 h time point, internalized particles adjacent to the cellular nuclei was clearly evident after 5 h of incubation. Unlike the initially observed distinct particles, a significant fraction of the polyplexes inside the cell was aggregated after 5 h of incubation. Taken together, these observations indicated a significant internalization of the polyplexes formed by the PLL-PA in skin fibroblasts.

The capability of PLL-PA for EGFP expression in fibroblasts was evaluated next. The pEGFP-N2/PLL-PA formulation was compared to Lipofectamine^{TM} 2000, PEI and an adenoviral system expressing GFP. Two complementary methods, one based on flow cytometry (cells grown in 6-well plates) and another based on epifluorescent microscopy (cells grown on glass coverslips), were utilized for detection of EGFP-positive cells. The gene expression was followed during a 10-day period, and cell growth was quantified during this period based on either direct cell counts with a hemocytometer (for cells used in flow cytometry) or the number of cells visualized in the microscopic field of coverslips (for cells used for microscopy). Control cells exposed to pEGFP-N2 alone exhibited ~20-fold increase in cell numbers under the experimental conditions (**Figure 3-4A**), indicating robust cell proliferation without any adverse

effect of the plasmid DNA. The growth of the cells exposed to pEGFP-N2/PLL-PA was not altered as compared to pEGFP-N2 only treated cells. Fibroblasts treated with PEI, Lipofectamine^{TM} 2000, and the adenovirus, all displayed a lack of growth during the study period (**Figure 3-4A**). The PEI was most effective in inducing EGFP expression based on the percentage of cells being positive for EGFP, while other carriers induced a similar level of gene expression (**Figure 3-4B**). The total number of GFP-positive cells was calculated based on total cell numbers counted (**Figure 3-4A**), and the % expression levels (**Figure 4B**). Based on this analysis, the PLL-PA was the most effective carrier among all carriers (**Figure 4C**); although PEI was promising in having the highest percentage of GFP-positive cells, its toxic effect in long term culture was detrimental. This high toxicity of the PEI was consistent with experiences of others, who attempted to modify PEI to improve its cell compatibility [22-24]. Finally, PLL was not effective giving an equivalent level of gene expression to that of pEGFP-N2 alone (not shown).

Similar observations were obtained when EGFP expression was followed by the epifluorescent microscopy. Cell growth, based on the number of cells counted in a standard microscopic field, was unaltered in PLL-PA exposed cells (**Figure 3-4D**), and gene expression was most effective with Lipofectamine^{TM} 2000 and PLL-PA during the 10-day study period (**Figure 3-4E**). PEI gave relatively low transfection efficiencies at early time points, which increased gradually during the study period (similar to flow cytometry results). Analysis based on the total number of cells positive for EGFP (= % GFP-positive cells x no of cells/field) also indicated PLL-PA to be the most effective carrier (**Figure 3-4F**), consistent with the flow cytometry results. Note that assessment of EGFP-positive cells by the microscopy indicated some differences from the flow cytometric assessment; for example, Lipofectamine^{TM} 2000 and

PEI gave higher and lower % EGFP-positive cells under epifluorescent microscopy as compared to flow cytometry, respectively). Several reasons might have been the reason for such a discrepancy; (i) differences in the sensitivity of each assessment technique, (ii) the need to utilize trypsinization for flow cytometry, unlike epifluorescent microscopy retaining the cells in their native state, (iii) the need to grow the cells on glass cover slips for microscopy, but not flow cytometry, where substrate-dependent changes might influence the extent of transgene expression. Irrespective of quantitative differences between the two techniques, both techniques indicated the PLL-PA to be a superior carrier as compared to other vectors, ultimately yielding 3-8 fold higher numbers of EGFP-positive cells at the end of the 10-day cell growth (see **Figure 3-4C** and **3-4F**).

CONCLUSIONS

Our collective results indicated palmitylation of the cationic polymer PLL to be a promising lead for designing improved gene carriers; under conditions that allowed robust cell growth, PLL-PA provided the highest number of cells with exogenous gene expression. The level of transgene expression, based on percentage of cells positive for EGFP, was generally comparable to the efficiencies of adenoviral (30-50%, [25]) and retroviral carriers (~60%, [26]), both of which were utilized for expression of GFP in human fibroblasts. The non-viral vectors typically yield transient gene expression and the maximal duration of expression with PA-modified PLL remains to be explored at this stage. A 10-day expression period, as observed in this study, might be sufficient for applications that require transient expression, for example, when one needs to express proteins that initiate tissue repair [27]. Other genetic disorders might require constitutive gene expression, such as systemic Factor VIII deficiency [28], and more

studies will be needed to determine the maximal duration of gene expression with palmitylated polymeric vectors. We pursued palmitylation *a priori* for improved gene delivery, since palmitic acid has the appropriate fatty acid chain length (C16) to interact with lipid membranes in a 'metastable' fashion, enabling transient associations with lipid bilayers during entry and discharge from a bilayer. Other lipids, such as saturated myristic acid (C14), unsaturated geranylgeranyl moiety (C20) and polycyclic cholesterol, are also utilized by cells for intracellular trafficking of proteins [29]. Attempts to incorporate the latter lipid into PEI have yielded a promising PEI-based carrier by an independent group [30], and future studies to identify the optimal lipid-polymer combination will be indispensable for design of more effective non-viral carriers.

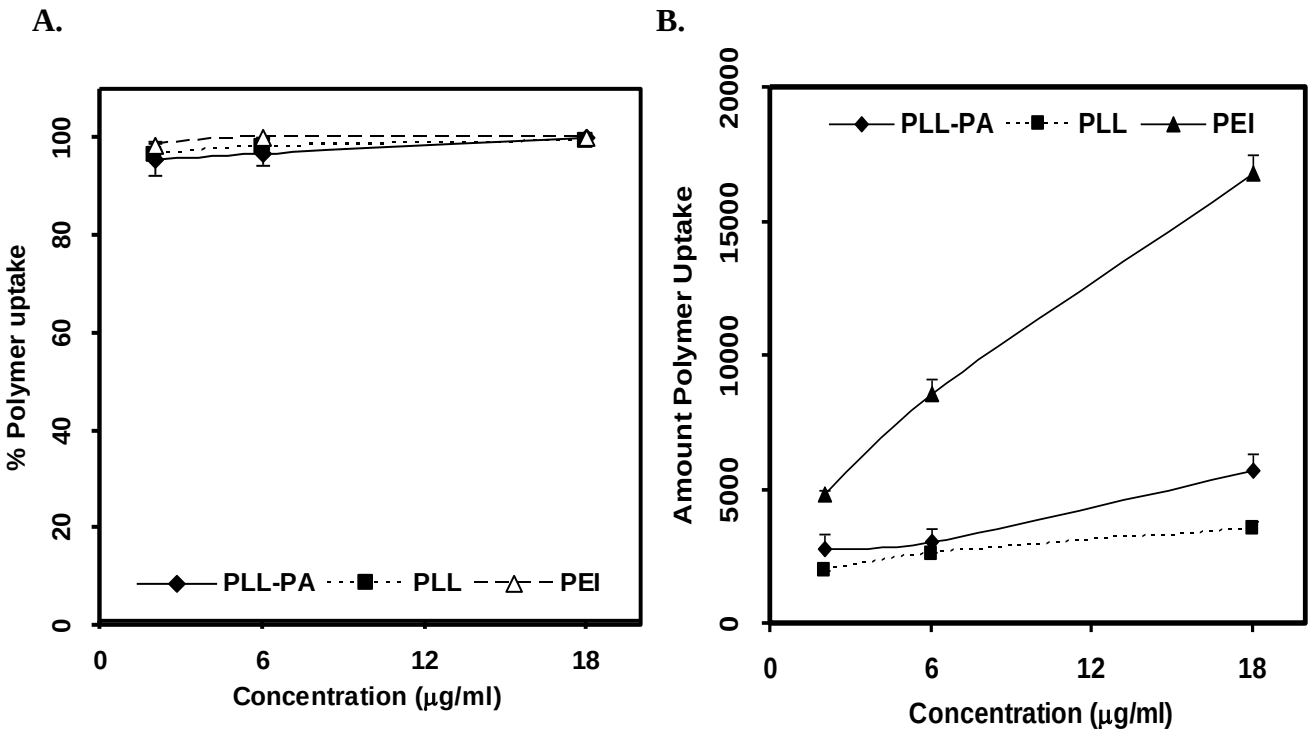

Figure 3-1. A. Cellular association of FITC-labeled polymers (mean ± SD; n=3). All polymers gave >95% FITC-positive cells irrespective of the concentration tested. **B**. The absolute polymer (in arbitrary fluorescence units) associated with FITC-positive cells. A direct relationship between the cell-associated polymer amount and the polymer concentration incubated with the cells was evident.

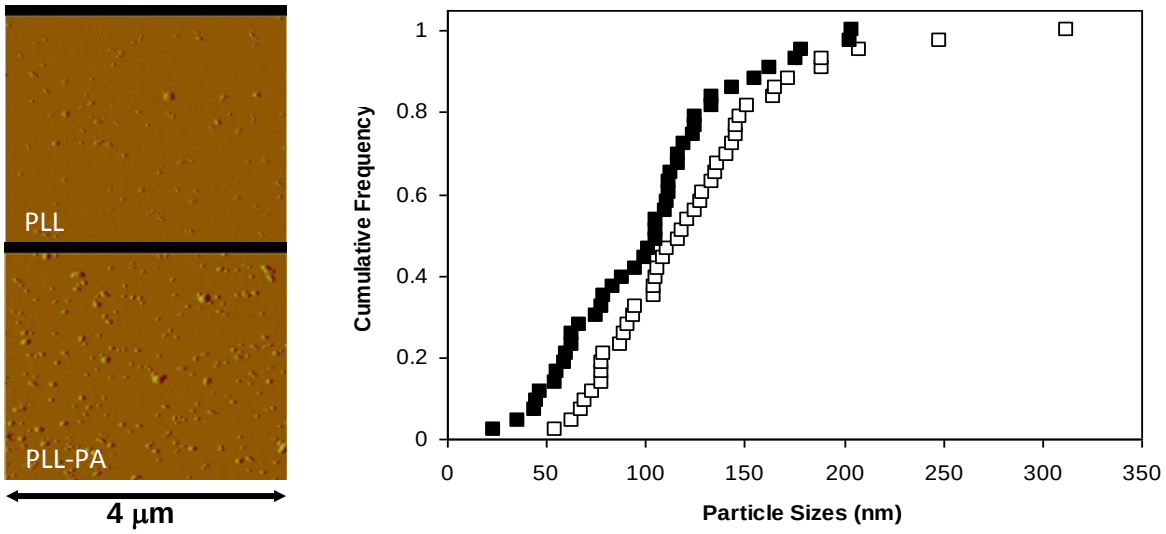

Figure 3-2. The size of particles formed by the condensation of pEGFP-N2 with PLL and PLL-PA. Representative pictures for PLL and PLL-PA complexed pEGFP-N2 particles were shown on the left, along with the cumulative distribution of particle sizes formed by these polymers. The sample preparations were performed in triplicate.

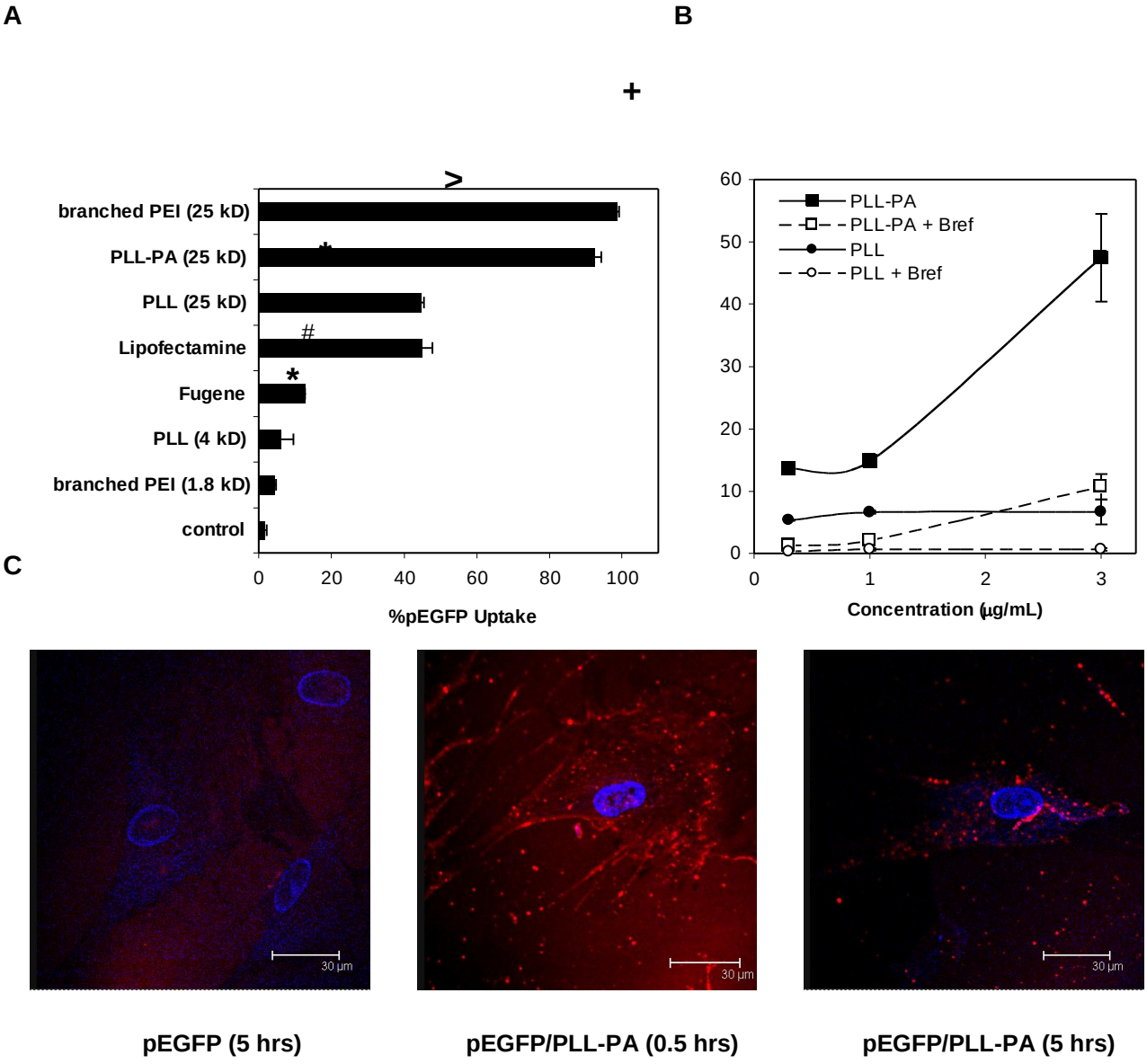

Figure 3-3. A. Cellular delivery of Cy5.5-labeled pEGFP-N2 by non-viral carriers (mean ± SD). Significant variations among the chosen carriers were evident, with PEI and PLL-PA giving the most cell-associated plasmid. #: not significantly different from control. *: significantly different from the control. >: no significant difference between PLL (25 kDa) and Lipofectamine^{TM} 2000. +: PEI significantly ($p<0.05$) higher than PLL-PA. **B**. Effect of Brefeldin A on cell associated pEGFP-N2, as investigated by the flow cytometry. Note that for both PLL and PLL-PA, the endocytosis inhibitor Brefeldin A (3.7 µM) reduced the percentage of cells positive for pEGFP-N2 after 8 h of incubation. **C**. Confocal microscopy images of fibroblasts exhibiting pEGFP-N2 uptake (cell nuclei: blue, polyplexes: red). Left. Fibroblasts incubated with pEGFP-N2 (5 h)

without any carriers. Middle. Fibroblasts incubated with pEGFP-N2/PLL-PA complexes for 0.5 h. Right. Fibroblasts incubated with pEGFP-N2/PLL-PA complexes for 5 h.

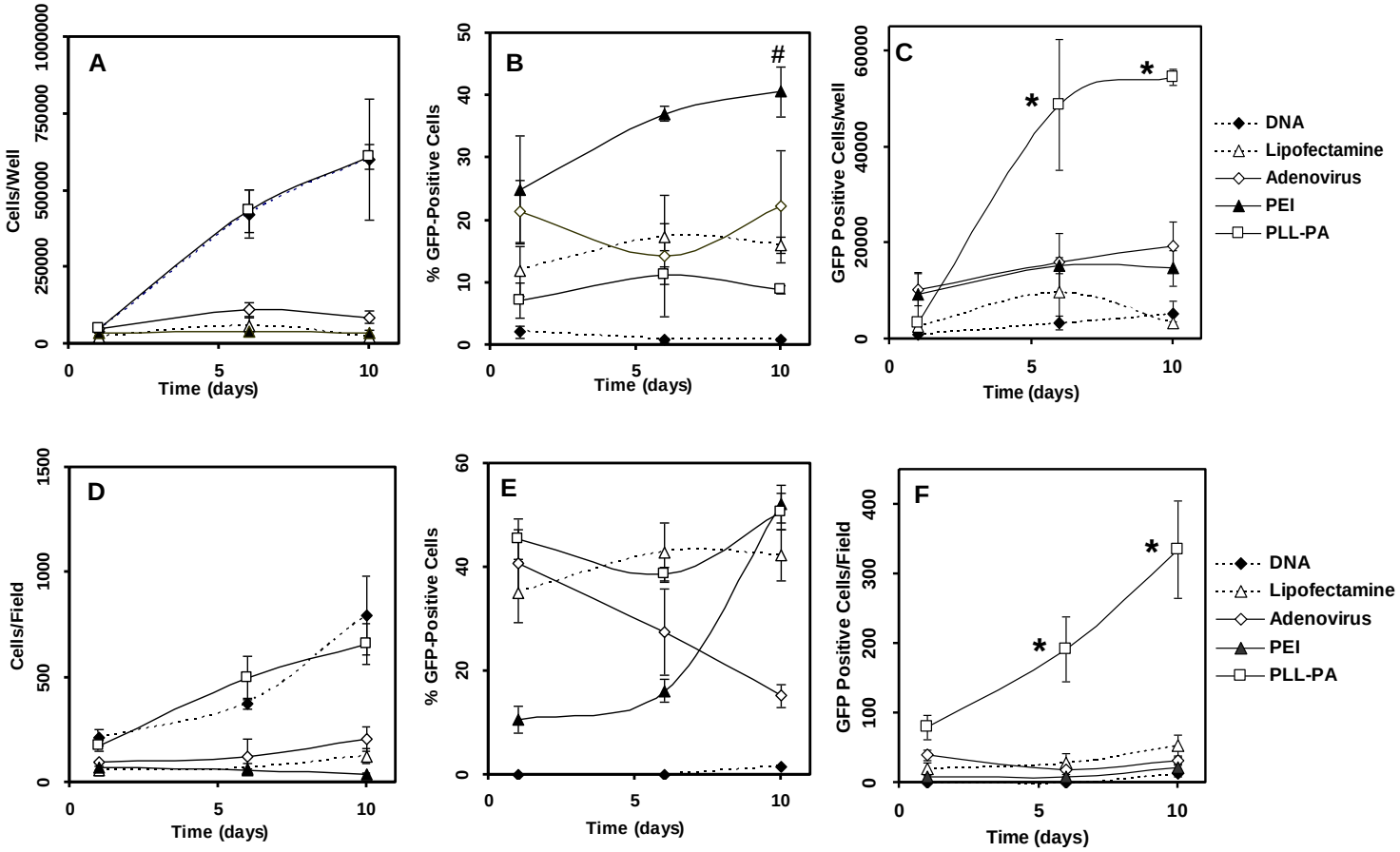

Figure 3-4. Transfection of fibroblasts with pEGFP-N2/polymer complexes, as assessed by flow cytometry (**A**, **B** and **C**) and epifluorescent microscopy (**D, E** and **F**). Note that cells exposed to pEGFP-N2 alone and pEGFP-N2/PLL-PA complex exhibited robust growth with no significant difference between the two groups (**A** and **D**). The number of cells recovered from these two groups was significantly higher than the other groups. The percentage of EGFP-positive cells was variable among the carriers (**B** and **E**), but the total number of cells positive for EGFP (based on direct cell numbers per well or number of cells in a standard microscopic field) was highest for the PLL-PA carrier (**C** and **F**). #: significantly higher than the remaining carriers on day 10 (**B**). *: significantly higher than the remaining groups on day 6 and day 10 (**C**).

REFERENCES

1. Anderson WF. Hum gene ther. Science. 1992, 256, 808-13.

2. Mastrobattista E, Van Der Aa MA, Hennink WE, Crommelin DJ. Artificial viruses: a nanotechnological approach to gene delivery. Nat Rev Drug Discov. 2006, 5, 115-21.

3. Kohn DB, Sadelain M, Glorioso JC. Occurrence of leukaemia following gene therapy of X-linked SCID. Nat Rev Cancer. 2003, 3, 477-88.

4. Zaiss AK, Muruve DA. Immune responses to adeno-associated virus vectors. Curr Gene Ther. 2005, 5, 323-31.

5. Bessis N, GarciaCozar FJ, Boissier MC. Immune responses to gene therapy vectors: influence on vector function and effector mechanisms. Gene Ther. 2004, 11, 10-17.

6. Wagner E. Strategies to improve DNA polyplexes for in vivo gene transfer: will "artificial viruses" be the answer? Pharm Res. 2004, 21, 8-14.

7. Putnam D. Polymers for gene delivery across length scales. Nat Mater. 2006, 5, 439-51.

8. Martin B, Sainlos M, Aissaoui A, Oudrhiri N, Hauchecorne M, Vigneron JP, Lehn JM, Lehn P. The design of cationic lipids for gene delivery. Curr Pharm Des. 2005, 11, 375-94.

9. Linder ME, Deschenes RJ. New insights into the mechanisms of protein palmitoylation. Biochem. 2003, 42, 4311-20.

10. Marchetto MC, Muotri AR, Burns DK, Friedberg EC, Menck CF. Gene transduction in skin cells: preventing cancer in xeroderma pigmentosum mice. Proc Natl Acad Sci. 2004, 101, 17759-64.

11. Gache Y, Baldeschi C, Del Rio M, Gagnoux-Palacios L, Larcher F, Lacour JP, Meneguzzi G. Construction of skin equivalents for gene therapy of recessive dystrophic epidermolysis bullosa. Gene Ther. 2004, 15, 921-33.

12. Brill-Almon E. Ex vivo transduction of human dermal tissue structures for autologous implantation production and delivery of therapeutic proteins. Mol Ther. 2005, 12, 274-82.

13. Incani V, Tunis E, Clements BA, Olson C, Kucharski C, Lavasanifar A, Uludag H. Palmitic acid substitution on cationic polymers for effective delivery of plasmid DNA to bone marrow stromal cells. J Biomed Mat Res. 2007, 81, 493-504.

14. Clements BA, Bai J, Kucharski C, Farrell LL, Lavasanifar A, Ritchie B, Ghahary A, Uludag H. RGD-conjugation to polyethyleneimine does not improve DNA delivery to bone marrow stromal cells. Biomacromols. 2006, 7, 1481-88.

15. Chan CK, Senden T, Jans DA. Supramolecular structure and nuclear targeting efficiency determine the enhancement of transfection by NLS-containing polylysine. Gene Ther. 2000, 7, 1690-97.

16. Miyata K, Kakizawa Y, Nishiyama N, Harada A, Yamasaki Y, Koyama H, Kataoka K. Block Catiomer Polyplexes with Regulated Densities of Charge and Disulfide Cross-Linking Directed To Enhance Gene Expression. Am Chem Soc. 2004, 126, 2355-61.

17. Oishi M, Kataoka K, Nagasaki Y. pH-Responsive PEGylated nanogels as targetable and low invasive endosomolytic agents to induce the enhanced transfection efficiency of nonviral gene vectors. Bioconjug Chem. 2006, 17, 677-88.

18. Rejman J, Oberle V, Zuhorn IS, Hoekstra D. Size-dependent internalization of particles via the pathways of clathrin- and caveolae-mediated endocytosis. Biochem J. 2004 , 377, 159-69.

19. Ogris M, Steinlein P, Kursa M, Mechtler K, Kircheis R, Wagner E. The size of DNA/transferrin-PEI complexes is an important factor for gene expression in cultured cells. Gene Ther. 1998, 5, 1425-33.

20. Fischer R, Kohler K, Fotin-Mleczek M, Brock R. A Stepwise Dissection of the Intracellular Fate of Cationic Cell-penetrating Peptides. J Biol Chem. 2004, 279,12625-35.

21. Hunziker W, Whitney JA, Mellman I. Brefeldin A and the endocytic pathway Possible implications for membrane traffic and sorting. FEBS Lett. 1992, 307, 93.

22. Moghimi SM, Symonds P, Murray JC, Hunter AC, Debska G, Szewczyk A. A two-stage poly(ethylenimine)-mediated cytotoxicity: implications for gene transfer/therapy. Mol Ther. 2005, 11, 990-5.

23. Thomas M, Klibanov AM. Enhancing polyethylenimine's delivery of plasmid DNA into mammalian cells. Proc Natl Acad Sci. 2002, 99, 14640-5.

24. Ghahary A, Li Y, Tredget EE, Kilani RT, Iwashina T, Karami A, Lin X. Expression of indoleamine 2,3-dioxygenase in dermal fibroblasts functions as a local immunosuppressive factor. J Invest Dermatol. 2004, 122, 953-64.

25. Chen Y, Miller WM, Aiyar A. Transduction efficiency of pantropic retroviral vectors is controlled by the envelope plasmid to vector plasmid ratio. Biotech Prog. 2005, 21, 274.

26. Varkey M, Gittens S, Uludag H. Growth factor delivery for bone tissue repair: an update. Expert Opinion onDrug Delivery. Exp Op Drug Del. 2004, 1, 19-36.

27. Krebsbach PH, Zhang K, Malik AK, Kurachi K. Bone marrow stromal cells as a genetic platform for systemic delivery of therapeutic proteins in vivo: human factor IX model. J Gene Med. 2003, 5, 11-7.

28. Ferri N, Paoletti R, Corsini A. Lipid-modified proteins as biomarkers for cardiovascular disease: a review Biomarkers 2005, 10, 219-37.

29. Wang DA, Narang AS, Kotb M, Gaber AO, Miller DD, Kim SW, Mahato RI. Novel branched poly(ethylenimine)-cholesterol water soluble lipopolymers for gene delivery. Biomacromols. 2002, 3, 1197-1207.

30. Furgeson DY, Chan WS, Yockman JW, Kim SW. Bioconjug Chem. Modified linear polyethylenimine-cholesterol conjugates for DNA complexation 2003, 14, 840-7.

CHAPTER IV

Further Investigation of Lipid-Substituted Poly(*L*-Lysine) Polymers for Transfection of Human Skin Fibroblasts[1]

[1]The Contents of this chapter have been previously published in: Abbasi M, Uludağ H, Incani V, Hsu CYM, Jeffery A. Further Investigation of Lipid-Substituted Poly(*L*-Lysine) Polymers for Transfection of Human Skin Fibroblasts. Biomacromolecules. 2008, 9, 1618-1630.

INTRODUCTION

Gene therapy aims to reconstitute a missing or defective gene with a correct copy in a host genome [1]. This is possible when one utilizes biocompatible gene carriers to transport the desired genes into target cells [2]. Non-viral vectors have received increased attention for gene therapy because of the concerns over the safety issues of viral vectors, among which immunogenicity, oncogenicity, and potential virus recombination have been highlighted [3]. The use of viral vectors cannot be justified in some clinical situations based on potential therapeutic benefit to be gained from the intervention [4]. New alternatives to viral carriers are accordingly sought that would transfer therapeutic genes intracellularly with high efficiency. Polycation-based synthetic gene carriers with low toxicity and high transfection efficiency are attractive non-viral substitutes in this respect [5]. Such carriers can be used directly *in vivo* to transfect cells *in situ*. *Ex vivo* modification of cells, however, is more attractive since cellular manipulations are better controlled under cell culture conditions. Bodily exposure to non-viral carriers is also minimized in this way, ultimately reducing their undesirable effects in a host.

Successful modification of human cells *ex vivo* is a multistep process where endocytosis constitutes the main route of entry for foreign DNA into cells [9]. The non-viral carriers are expected to package the exogenous DNA appropriately (i.e., bind and condense the DNA molecules into compact particles), so that it can be effectively internalized by the cells. The exogenous DNA must then survive the endosomal/lysosomal system, which aims to hydrolyze foreign macromolecules, and be released in intact form into the cytosol to be targeted to nucleus [10]. The existence of nucleases in many cellular compartments threatens the integrity of foreign DNA during this process. Deoxyribonuclease I (DNase I) or DNase I-like enzymes exist in extracellular space [11] and cellular cytoplasm [12] and has been implicated to play a role in

DNA degradation. DNase II, an acidic enzyme found in endosomes [13,28], also plays a role in destruction of foreign DNA [10]. The ability of non-viral carriers to protect against nuclease attack is paramount in enhancing the success of gene expression.

We recently reported on the design of a lipid-substituted polymer, palmitic acid-poly(*L*-lysine) (PLL-PA) conjugate, that combines the critical properties of a cationic polymer (i.e., DNA condensing ability) with that of a fatty acid (i.e., lipid membrane compatibility). The designed polymer condensed plasmid DNA into 100-200 nm particles, while enhancing the permeability of the particles through the plasma membrane. Although such a condensed particle is expected to protect exogenous DNA from DNase-mediated degradation, direct demonstration of this has not been shown in previous studies with PLL-PA. It was also not known if the nature of lipid substituent influenced the protection ability against DNases and if the transfection capacity of the designed amphiphilic polymers was dependent on the choice of the lipid substituent. In this communication, we report the use of different lipid substitutions on PLL, and explore the nature of lipid substitution on the plasmid delivery efficiency. Endogenous lipids were chosen for the purpose of polymeric substitutions since they could be conveniently metabolized by mechanisms inherent in mammalian cells. As in our previous studies [16], we utilized human skin fibroblasts to evaluate the potential of the new carriers. These cells were used since cells from skin can be readily harvested, and they can be grafted into a host after the desired modifications with minimal patient discomfort [6-8]. By using this clinically relevant cell phenotype, the clinical translation of the present results is expected to be facilitated.

MATERIALS & METHODS

Materials

PLL·Br (25,500 Da), anhydrous dimethylsulfoxide (DMSO) and N,N-dimethylformamide (DMF), caprylic acid (C8), myristic acid (C14), palmitic acid N-hydroxy-succinimide ester (NHS-C16), stearic acid (C18), oleic acid (C18:1 9Z), linoleic acid (C18:2 9Z,12Z), N-hydroxy-succinimide (NHS), and dicyclohexylurea (DCC) were purchased from Aldrich (Milwaukee, WI). Hanks' Balanced Salt Solution (HBSS with phenol red), trypsin/EDTA, and protease inhibitor cocktail were obtained from SIGMA (St. Louis, MO). Clear HBSS (phenol red free) was prepared in house. Dulbecco's Modified Eagle Medium (DMEM; high glucose with L-glutamine), Penicillin (10,000 U/mL), and Streptomycin (10 mg/mL) were from GIBCO (Grand Island, NY). Fetal Bovine Serum (FBS) was from Atlanta Biologicals (Lawrenceville, GA). Fluorescein isothiocyanate (FITC) was purchased from PIERCE (Rockford, IL). AlexaFluor 546 (AF546), dithiothreitol (DTT), Trizol, RNA out RNase inhibitor, MMLRV RT enzyme, 5x first strand buffer, and dNTP mix were from Invitrogen (Eugene, Oregon). pdN6 primers were purchased from Fermentas (Burlington, Ontario). A 4.7 kb plasmid incorporating an enhanced green fluorescent protein and a kanamycin resistance gene (pEGFP-N2) was obtained from BD Biosciences. The plasmids gWIZ (blank plasmid with CMV promoter), and gWIZ-GFP (GFP expressing plasmid with CMV promoter) used in transfection studies were purchased from Aldevron (Fargo, ND). SYBR green II RNA gel stain was purchased from Cambrex BioScience (Rockland, ME). RNeasy Mini Kit and RDD buffer were purchased from QIAGEN (Mississauga, ON). Taq DNA polymerase and ThermoPol Buffer were purchased from New England Biolabs (Ipswich, MA). The primers used in PCR reaction was

synthesized by IDT Technologies (Ottawa, Ontario). DNA-free DNase Treatment and Removal Kit were purchased from Ambion Inc. (Austin, TX).

Synthesis and Characterization of Lipid-Substituted Polymers

The lipid-substituted polymers were synthesized by N-acylation of PLL with activated fatty acid NHS-esters. The synthesis of NHS esters of fatty acids (NHS-X, were X= C8, C14, C16, C18, C18:1, C8:2) were carried out by mixing equal molar amounts of fatty acid, NHS, and DCC in dry ethyl acetate (12 mL). The reaction mixture was left stirring overnight at room temperature under argon atmosphere. Solid dicyclohexylurea by-product formed was removed by filtration and the filtrate was concentrated under reduced pressure. The crude NHS-X was re-crystallized in ethanol at 4^0C and its purity was assessed by thin layer chromatography [14]. The identity of NHS-X products was confirmed by ^{1}H-NMR. Lipid substitutions of PLL were performed by adopting a method previously described for preparation of palmitic acid substitution of PLL [15]. Briefly, NHS-X was dissolved in 1 mL of DMF and added dropwise to 15 mg of PLL in 1 mL of DMSO. The fatty acid:PLL amine ratio was either 1:1.5 or 1:6. The mixture was allowed to react for 24 h at room temperature under argon. Excess ethyl ether was added to precipitate and wash (x3) the polymers, then the polymers were dried under vacuum at ambient temperature overnight.

Polymers were analyzed by ^{1}H-NMR (Bruker 300 MHz; Billerica, MA) in D_2O. The characteristic proton shift of lipids (δ ~0.8 ppm; -CH_3) and PLL (δ ~4.3 ppm; –NH-CH-CO) were integrated, normalized for the number of protons in each peak, and used to obtain the extent of lipid substitutions on polymers **(Table 4-1)**.

Preparation of pEGFP Plasmid

pEGFP-N2 was replicated in the kanamycin resistant DH5-R *Escherichia coli* strain grown in Luria-Bertani medium. The plasmid DNA was purified using a Qiagen Plasmid Giga Kit according to the manufacturer's protocol. The concentration and purity of the plasmid were determined by UV spectroscopy as recommended by the manufacturer. The plasmid preparation was dissolved in distilled/deionized DNase free water at a concentration of 0.4 mg/mL.

Agarose Gel Electrophoresis

Gel electrophoresis was performed for assessment of (i) pEGFP binding efficiency of polymers, (ii) pEGFP/polymer dissociation upon incubation with heparin, and (iii) pEGFP/polymer degradation by DNases. For binding studies, 0.25 mg/mL pEGFP was incubated with 0.15 and 0.5 mg/mL polymer in 20 μL of NaCl (150 mM) for 1 h to form polyplexes. The N:P ratio of the polyplexes (see Results) was calculated by assuming 1 μg PLL to be equivalent to 40 nM amine nitrogen, and 1 μg of DNA to contain 3 nM phosphate. 4 μL of 6x diluted loading buffer was added to samples and they were run on a 2.5% agarose gel containing 1 μg/mL ethidium bromide (120 V for 45 min). The gels were visualized under UV illumination and bands corresponding to free pEGFP were quantified by spot densitometer using non-treated pEGFP as the control. Percent binding was calculated as: 100% x [(control pEGFP - free pEGFP)/control pEGFP].

For the dissociation study, same concentrations as above were used for polyplex formation and samples were then exposed to heparin (at 0.625% final concentration). Loading buffer was added to the samples and they were run on a gel with similar conditions as above. Gels were visualized under UV illumination and detection of free pEGFP and quantitation of free pEGFP were performed by spot densitometer using non-treated pEGFP as control. Percent dissociation was calculated as: 100% x [free pEGFP/control pEGFP].

In the degradation study, polyplexes were formed with the polymer:pEGFP concentration ratios of 0.05:0.25, 0.15:0.25, and 0.5:0.25 mg/mL respectively. Optimal DNase concentrations and digestion times for full degradation of pEGFP were determined by the preliminary studies, and these conditions (1 U/µL DNase I, 0.5 U/µL DNase II, 30 min) were used for subsequent studies. After 30 min of incubation with DNase, EDTA (0.06 mM; to stop DNase action) and heparin (0.625%; to dissociate complexes) were added and samples were incubated for 15 min. Samples were run on a gel with similar conditions as above. Detection of pEGFP and analysis was performed as previously explained and % degradation was calculated by 100 x [control pEGFP-free pEGFP/control pEGFP].

Cellular Uptake of pEGFP by Fluorescent Microscopy

To investigate cellular uptake of pEGFP, human CRL fibroblasts were grown on coverslips in 6-well plates in 1 mL of DMEM with FBS (10%) and Penicillin/Streptomycin (1%). FITC-labeled pEGFP was used to detect the plasmid uptake. For plasmid labeling, 100 µg pEGFP was reacted with 1 mM FITC (diluted from 100 mM in DMSO; reacts with $–NH_2$ groups randomly on DNA bases) in 0.3 mL H_2O, which was then placed on an orbital shaker for 3 h.

The labeled DNA was precipitated by adding 0.03 mL of 3 M sodium acetate (pH 5.2) and 0.825 mL of 95% ethanol. The solution was incubated at -20ºC for 15 min, centrifuged at 13800 rpm for 10 min, and washed with 70% ethanol (x2). The labeled/precipitated plasmid was dissolved in ddH_2O at 2 μg/mL, mixed with 10 μg/mL of polymer solutions (in 150 mM NaCl), incubated for 30 min and then added to the fibroblasts grown in triplicate. After 24 h, cells were washed using HBSS solution and fixed with 3.7% formaldehyde in HBSS. The nucleus was stained with Hoechst 33258 (20 min at 300 ng/mL) and the cells were analyzed under an epifluorescent microscope.

Cellular Uptake of pEGFP by Flow Cytometry

Cells were grown in 12-well plates in basic medium to quantitate pEGFP uptake by using AF546-labeled pEGFP**.** To obtain labeled plasmid, 500 μg AF546 was reacted with 200 μg pEGFP in 120 μL borate buffer (pH= 8.5; reacts with $–NH_2$ groups randomly on DNA bases), the mixture was then placed on an orbital shaker overnight. The labeled DNA was purified as in FITC-labeled pEGFP. 2 μg/ml of the AF546 labeled pEGFP solution was mixed with 10 μg/mL of polymer solutions in 150 mM NaCl. After incubation for 30 min, the complexes were added to the cells in 12-well plates (1 mL basic medium/well) in triplicate for 24 h. After removing the pEGFP-containing media, the cells were washed with clear HBSS, trypsinized and suspended in HBSS with 3.7% formalin DNA uptake was quantified by Becton Dickinson FACSCanto Analytic Flow Cytometer using the 635 nm laser through the FL-4 detection channel to count the AF546-positive cells (5000 events/sample). The instrument was calibrated so that the negative control sample (i.e., pEGFP without any polymeric carrier) gave 1-2% cell uptake. The

percentage of cells exhibiting AF546-fluorescence and the mean fluorescence in the total cell population were determined.

Recovery of Intact pEGFP from Cells

Cells were grown in 12-well plates in basic medium to assess the recovery of intact pEGFP as a function of time. 0.25 mg/mL AF546 labeled pEGFP-N2 was incubated with 0.5 mg/mL polymer for 1 h to form polyplexes. The polyplexes were then exposed to the cells in 12-well plates. Cells were incubated for 24 h with the polyplexes, after which the medium was replaced with fresh medium and the cells were recovered right away (day 1), and after day 3 and day 7. Supernatant of cell pellet was removed and 40 µL lysis buffer and 10 µL of 10x diluted protease inhibitor were added to the cells to lyse the cell membranes and to arrest any proteolytic activity. Cells were then placed on a shaker for 30 min and the solutions obtained after cell lysis were frozen at -80ºC until analysis. EDTA (0.06 mM) and heparin (0.625%) were incubated with 30 µL of cell lysis solution. 4 µL of 6x diluted loading buffer was added to the samples, and the samples were run on a 2.5% agarose gel (120 V for 45 min). As a reference standard, an equivalent amount of AF546 labeled pEGFP (i.e., amount equal to the total amount exposed to the cells) was run on the gel. The AF546 labeled pEGFP was detected by a Fuji FLA-5000 flat-bed scanner using the LD red laser (635nm) and results were analyzed by spot densitometer using the AF546 labeled pEGFP reference standard (i.e., amount corresponding to 100% theoretical recovery).

Analysis of GFP Expression

i. Flow Cytometry. Cells were grown in 12-well plates in basic medium to assess GFP expression by flow cytometry. The concentration of all reagents and incubation volumes/times were optimized based on previous studies.[16] The polymers were complexed with gWIZ or gWIZ-GFP plasmids by mixing 0.4 mg/mL plasmid (in ddH_2O) with 1 mg/mL polymers (in ddH_2O), and increasing the volume to 150 µL with 150 mM NaCl (50 µL/well in triplicate; 2/10 µg of pEGFP/polymer per well). Cells were incubated for 24 h with the transfection reagents, after which the medium was replaced with fresh medium. The cells were trypsinized after 1, 6 and 12 days and fixed using 3.5% formaldehyde in clear HBSS (300 µL). GFP expression was quantified by flow cytometry using a Becton Dickinson FACScanto Analytic Flow Cytometer with a fixed 488 nm argon laser through the FL-1 detection channel to count the GFP-positive cells (5000 events/sample). The instrument settings were calibrated for each run so as to obtain a background level of GFP expression of 1-2% for control samples (i.e., cells incubated with pEGFP alone without any carrier). An aliquot of the cell suspension used for flow cytometry was manually counted with a hemocytometer to obtain the total number of cells recovered from the wells. Transfection percentage was multiplied by the number of cells/well to determine the number of the transfected cells/well for each polymer at each time point. The mean fluorescence/cell for the whole population was also determined from the flow cytometry.

ii. RT-PCR. A complementary set of studies was conducted to investigate GFP expression at the mRNA level by using cells grown in 6-well plates. After 24 h of transfection of cells with complexes as above, the cells were treated with Trizol™, and the solutions were frozen at -20ºC until further processing. Harvested cells were thawed on ice and 450 µL of

chloroform:isoamyl alcohol (24:1) was added to the samples. Samples were vortexed and centrifuged at 12,000 g for 15 min to separate the aqueous phase. Samples were then treated with 250 μL of ethanol (70%) and the solutions were vortexed. The total RNA was subsequently isolated by using the RNeasy Mini Kit as directed by the manufacturer. Since initial studies indicated the possibility of plasmid contamination in isolated total RNA samples, the samples were treated with the DNA-free DNase Treatment and Removal Kit according to manufacturer's protocol, quantified the obtained RNA yield by using SYBR green reagent and frozen at -20ºC until reverse transcriptase reaction.

To synthesize the cDNA, 0.55 μg total RNA was reverse transcribed by using random hexamer primer (PdN_6**;** 4 μg/ mL) and dNTP mix (5 mM), and heated at 65ºC for 5 min. 5x synthesis buffer, DTT (0.1 M) and RNAout RNase inhibitor (1.8 U/μL) were added and the solutions were incubated at 37ºC for 2 min. MMLV RT enzyme was added to the solutions and incubated at 25ºC for 10 min, 37ºC for 50 min and 70ºC for 15 min for cDNA synthesis. For amplification, 50 ng of the synthesized cDNA was mixed with 10x ThermPol Buffer, dNTP mix (5 mM), forward sGFP or GAPDH primers (3 μM), reverse sGFP or GAPDH primers (3 μM), and Taq polymerase (5 U/μL). A housekeeping gene, glyceraldehyde-3-phosphate dehydrogenase (GAPDH), was also amplified as a control. The PCR conditions and the sequences of sGFP/GAPDH primers are shown in **Table 4-2**.

Statistical Analysis

Where shown, the results are summarized as mean ± standard deviation (SD) of the indicated number of replicates. Variations between the group means were analyzed by the

Student's *t*-test. The significance ($p<0.05$) of correlations between the variables was tested by calculating the Pearson Product-Moment Correlation Coefficient (**r**) for sample size N, and relating the correlation coefficient **r** to *t* distribution by $t = \mathbf{r} / [(1 - \mathbf{r}^2)/(N - 2)]^{1/2}$.

RESULTS

Polyplex Formation and pEGFP Protection Against Nucleases

The initial studies evaluated polyplex formation between the polymers and pEGFP. All polymers shown in **Table 4-1** were used for this purpose and it was our intent to explore whether lipid grafting affected the DNA complexation ability of the PLL. Two polymer:pEGFP ratios of 0.6:1 (N:P=8:1) and 2:1 (N:P=26.7:1) were tested, since these represented the typical ratios used in our previous studies. Complete complexation was obtained at both ratios with no free pEGFP after gel electrophoresis (not shown). pEGFP dissociation from the formed polyplexes by application of excess heparin was investigated next. The polymer:pEGFP ratio used for these studies were 0.6:1 and 2:1, respectively. The pEGFP dissociation from the polyplexes formed at the 0.6:1 ratio was almost complete, where 60-100% of the polyplexes dissociated depending on the polymer **(Figure 4-1A)**. The higher polymer:pEGFP ratio (2:1) showed higher resistance against pEGFP dissociation and dissociation obtained at this ratio was in the range of 20-70% **(Figure 4-1B)**. Significant differences among the polymers were evident in their propensity for dissociation. To investigate a correlation between the dissociation and the extent of modification, the extent of substituted $–CH_2–$ groups in polymers was determined by multiplying the degree of lipid substitution (i.e., no of lipids/PLL) by the number of $–CH_2–$ groups of each lipid. The extent of $–CH_2–$ groups substituted was plotted against the extent of polyplex dissociation; a

significant correlation (r^2=0.566; p<0.003) between these two parameters was evident **(Figure 4-1C)**. This suggests that polymers with higher substitution (i.e., hydrophobicity) were less prone to dissociation.

To investigate DNA protection ability of polyplexes, polyplexes were formed at the 0.2:1, 0.6:1 and 2:1 polymer:pEGFP ratios, and were treated with DNase I and DNase II. At the polymer:pEGFP ratio of 0.2:1, all of the pEGFP was degraded (not shown) indicating no protection ability by the polymers. At the polymer:pEGFP ratio of 0.6:1, significant degradation of the plasmid by both DNase I and DNase II was observed **(Figure 4-2A),** where 50-70% of pEGFP degradation was evident by both DNases. At the polymer:pEGFP ratio of 2:1, the complexes were protected against degradation, with PLL-CA1, PLL-CA2, PLL-MA1, PLL-MA2, and PLL-StA2 showing the highest protection **(Figure 4-2B)**. Under the experimental condition, lipid substitution did not show any additional benefit for protection against DNase since PLL was equally effective in this respect as compared to lipid-substituted PLLs. Additionally, there was no significant difference in the protection ability against DNase I or II (i.e., both enzymes appeared to degrade the polyplexes to the same extent), suggesting that polymers are equally effective against each enzyme. The results from the two polymers that gave the highest degradation, PLL-PA2 and PLL-StA1, might be misleading. These are the polymers that displayed the lowest dissociation, so that the reduced quantity of intact pEGFP band for these polymers might be reflective of the difficulties in fully dissociating the polyplexes, rather than plasmid disappearance due to degradation.

Cellular Uptake of pEGFP

A FITC-labeled pEGFP was utilized to detect pEGFP delivery into cells by microscopy. As expected, no FITC-fluorescence was evident in control cells incubated with FITC-pEGFP alone in the absence of any carriers (**Figure 4-3A**). Cells incubated with FITC-pEGFP/PLL complexes gave low levels of plasmid uptake where a relatively low fraction of cells displayed internalized FITC-pEGFP **(Figure 4-3B).** Cells incubated with the polyplexes prepared with PLL-PA2, PLL-MA2, PLL-StA1 and PLL-LA2 gave significantly high levels of intracellular FITC-pEGFP, which was visible as distinct bright particles typically outside the Hoechst-stained nuclei **(Figure 4-3C, D, E** and **F)**. The bright FITC-particles were associated with the cells and no fluorescence was evident in the extra-cellular space.

The quantitative uptake of plasmid was investigated by using flow cytometry and polyplexes formed with AF546-labeled pEGFP. Polymer:pEGFP concentrations in these studies were 10 μg/mL:2 μg/mL, since lesser amount of polymer was found less effective, and higher amount led to unacceptable toxicity in preliminary studies. At the chosen 5:1 ratio, unsubtituted PLL, PLL-CA1, and PLL-CA2 did not give significant plasmid uptake (<5% of cells positive for pEGFP), PLL-LA1 and PLL-LA2 gave intermediate uptake (45-70% of cells positive for pEGFP) and the remaining polymers showed high uptake of pEGFP (>75% of cells positive for pEGFP) **(Figure 4-4A)**. The amount of pEGFP uptake showed the same pattern as above, with polymers yielding high cellular uptake percentage also yielding high uptake amount in the cells **(Figure 4-4B)**. Note that the percentage and amount of uptake for cells exposed to PLL polyplexes is low compared to the lipid modified polymers, showing the beneficial effect of lipid substitution. The extent of substituted $–CH_2–$ groups was then correlated with the ability of polymers to deliver pEGFP into cells. A linear relationship (r^2=0.749; $p<0.0001$) between the

substituted $-CH_2-$ groups and the pEGFP delivery ability was evident **(Figure 4-4C)**. Another relationship explored was the correlation between the extent of pEGFP uptake (given by %pEGFP-positive cells) and polyplex dissociation (given by %dissociation from **Figure 4-1**). An inverse relationship (r^2=0.622; $p<0.0007$) was detected between these two variables **(Figure 4-4D)**.

Integrity of Internalized Plasmid

To gain further insight into plasmid delivery, the plasmid internalized by the cells was recovered after cell lysis, and quantitated by gel electrophoresis. AF546-labeled pEGFP was used in these studies since quantitating the integrity/amount of the delivered plasmid was considered more feasible in this way. An analysis similar to pEGFP degradation was initially conducted with AF546-labeled pEGFP, since it was important to determine the degradation profile of the labeled plasmid to ensure that it behaved in a manner similar to unlabeled plasmid. The polyplexes were formed at 2:1 polymer:plasmid ratio and their ability to protect AF546-labeled pEGFP against DNase I and DNase II degradation was evaluated. The obtained results **(Figure 4-5)** indicated that percent degradation values obtained were all <20%, relatively similar to the unlabeled pEGFP degradation study. PLL-CA1, PLL-CA2, PLL-MA2, PLL-OA1, and PLL-LA1 showed the highest protection with both AF546-labeled and unlabeled pEGFP, and PLL-OA2, PLL, PLL-LA2 and PLL-PA1 showed the lowest protection in both studies.

The recovery of AF546-labeled pEGFP over a 7-day period is summarized in **Figure 4-6** for a representative set of polymers. Based on electrophoretic mobility measurements, intact plasmid was readily recovered from the cells for some of the study groups (**Figure 4-6A**). After

4 h, a 35-50% recovery (compared to initial incubation amount) was obtained for these lipid-substituted PLLs (**Figure 4-6B**). The recovery from cells treated with PLL complexes was low and equivalent to the cells exposed to pEGFP alone without any carrier. After 1 day, a higher recovery of 60-70% was detected with PLL-PA2, PLL-MA2 and PLL-StA1, medium recovery was seen for PLL-LA2 (~40%), and low recovery for PLL (~15%). All polymers gave a decrease in pEGFP recovery after 3 days, with PLL-PA2 showing the best recovery, PLL-MA2 and PLL-StA1 showing medium recovery, PLL-LA2 showing low recovery and PLL showing no recovery at this time point. After 7 days, pEGFP recovery levels remained similar to the recovery levels obtained on day 3. The only notable change was a small decrease in plasmid recovery for PLL-PA2.

Assessment of GFP Expression by RT-PCR

The GFP expression was assessed by RT-PCR after the removal of complexes from cells on day 1. The transfections were conducted at polymer:plasmid concentrations of 10 µg/mL:2 µg/mL with polymers PLL-MA2, PLL-STA1, PLL-LA2 and PLL, based on the range of pEGFP delivery efficiency. The plasmids used were gWIZ (a blank plasmid serving as a control) and gWIZ-GFP (a GFP-incorporating plasmid). The PCR was first performed on total RNA samples without an RT step. This was intended to detect contamination, if any, of the samples with plasmid DNA (amplification with sGFP primers) or genomic DNA (amplification with GAPDH primers). No visible band was detected on gel electrophoresis with both sets of primers (**Figure 4-7A**), indicating a lack of DNA contamination in the prepared samples. The synthesized cDNA from the RNA samples was then amplified by using sGFP and GAPDH primers. Strong bands

were present for all samples amplified with the GAPDH primers (**Figure 4-7A**), indicating the presence of the house-keeping GAPDH mRNA in all samples. Amplification of the cDNA by sGFP primers resulted bands for all polyplexes prepared with gWIZ-GFP (i.e., PLL-MA2/gWIZ-GFP, PLL-StA1/gWIZ-GFP, PLL-LA2/gWIZ-GFP, and PLL/gWIZ-GFP), but not for the polyplexes prepared with the gWIZ. This was indicative of the successful GFP expression only for the cells transfected with the functional GFP-expressing plasmid. Note that PLL appeared to be as effective as the other polymers in this assay. Densitometric analysis of the obtained bands at the expected GFP location also indicated the presence of the GFP transcript for the complexes formed with gWIZ-GFP, but not gWIZ **(Figure 4-7B)**. Due to large standard deviations between duplicate samples in Densitometric analysis, the efficacy of different polymers could not be compared.

A similar study was subsequently conducted on days 1, 6, and 10 after transfection, and similar to the above results, GFP expression was detected on day 1 after transfection **(Figure 4-8A)** by the lipid-modified polymers. GFP expression levels decreased on days 6 and 10 after transfection but were evident. PLL-StA2 appeared to be the best transfectant in this time period study.

Assessment of GFP Expression by Flow Cytometry

Using the same complexes described in RT-PCR assessment, GFP expression was additionally analyzed by flow cytometry. The use of 'blank' complexes (i.e., with gWIZ) was especially important in this assessment, since our initial studies indicated that fibroblasts treated with polymers and/or blank complexes gave some autofluorescence in flow cytometry. This

would have obviously complicated GFP analysis, possibly leading to erroneously higher GFP assessment in flow cytometry. Changes in number of cells recovered after treatment were used as a measure of treatment toxicity. Cells treated with gWIZ in the absence of polymers served as control, since no toxicity was associated with plasmid treatment alone in our hands (not shown). A similar cell growth pattern was detected whether the polyplexes was prepared with gWIZ or gWIZ-GFP. Polyplexes formed with PLL-MA2 and PLL-LA2 showed higher toxicity over the 10-day study period. PLL-StA1 showed no toxicity in the first two time points (days 1 and 6), but some toxicity was detected on day 10. PLL showed no toxicity over the 10 day time period, and cell numbers were comparable with the gWIZ control **(Figure 4-9A)**.

Transfection efficiency (10-12% GFP-positive cells) remained relatively constant over the 10-day time period for complexes prepared with PLL-StA1 and PLL-MA2 (**Figure 4-9B**). Delivery of gWIZ by these polymers resulted in 2-6% GFP-positive cells, indicating the level of autofluorescence induced by virtue of incubating cells with the complexes. The unsubstituted PLL did not yield any transfection, since no difference was noted in the percentage of GFP-positive cells between gWIZ and gWIZ-GFP delivery (**Figure 4-9B**). PLL-LA2 gave variable transfection percentages at different time points, its peak being at day 6 (**Figure 4-9B**). The amount of fluorescence/cell was also analyzed by measuring the mean fluorescence of the cell population (**Figure 4-9C**). Based on these results, PLL-StA1 and PLL-MA2 was again most effective among the polymers tested. The polymers showed the same pattern of transfection efficiency based on the total number of transfected cells obtained by multiplying the percentage of transfection (**Figure 4-9B**) by the number of cells recovered/well (**Figure 4-9A**). Based on this analysis, PLL-StA1 proved to be the most efficient polymer in this study, showing ~4 fold increase in the number of transfected cells/well compared to the unmodified PLL **(Figure 4-9D)**.

DISCUSSION

Sevral experiments were conducted to obtain successful non-viral transfection with amphiphilic polymeric carriers. We first investigated the complexation of plasmid DNA with the carriers. Previous studies showed that palmitic acid-substitution on PLL led to a reduced tendency of PLL to condense plasmid DNA [16] but, once condensation occurred at sufficient polymer:DNA ratios, the lipid substitution gave more condensed complexes, based on reduced complex sizes as measured (25-200 vs. 50-300 nm for PLL-PA vs. PLL, respectively). This study showed that, in addition to palmitic acid, other endogenous lipids can be used for PLL substitution to achieve effective DNA condensation. Based on plasmid DNA binding studies at three polymer:DNA ratios, no obvious differences were evident in the ability of lipid-substituted polymers for complexation. The stability of the complexes, based on dissociation upon heparin exposure, was also similar at low polymer:DNA ratios but, at higher ratios, the extent of lipid substitution, rather than the nature of the lipid, determined the complex stability. The total number of $–CH_2–$ groups was used as a measure of lipid substitution, since we could not precisely control the number of lipids attached per PLL. We, therefore, cannot reach to a definitive conclusion whether a certain degree of substitution or a lipid chain length was critical for complex stability. An inverse correlation between the number of substituted $–CH_2–$ groups and the extent of dissociation suggested that 'hydrophobic' content of polymers, rather than a particular lipid, was critical for the complex dissociation.

Sensitivity of naked DNA to nucleases is one of the critical barriers that lower transfection efficiency [17]. As observed with permeabilized cells, cytoplasmic nuclease activity has an inhibitory effect on intracellular transport of DNA [21]. In addition to apoptotic nucleases [25,29] and caspase-3 activated DNase, DNase I and DNase II [22-28] are the main enzymes

responsible for chromosomal DNA degradation. As a result of complex formation, plasmid DNA was shown to be protected by all amphiphilic polymers in this study as long as the polymer:DNA ratio (w:w) was at least 2:1. Complexation was successful at lower ratios (as assessed by electrophoretic mobility measurements), but this did not lead to nuclease protection. DNase I and DNase II were equally effective in degrading DNA complexes, highlighting the importance of both types of nucleases in delivery via non-viral vectors. Since DNase I is found in serum and extracellular space as well as in the cytoplasm of cells and DNase II is typically endosomal, the complexes are likely to experience the nuclease threat throughout their path to the cell nucleus. No correlation was evident between the DNase protection ability of the polymers and the extent of substitution, unlike the heparin-induced dissociation. It must be noted that the polymers that appeared to protect the plasmid DNA the least were also the complexes that gave most stable complexes (i.e., PLL-PA2 and PLL-StA1; **Figure 4-1** and **4-2**). Therefore, lower recovery of intact DNA observed for these polymers in the degradation study was more likely due to lack of complete dissociation by the heparin (i.e., the step necessary for electrophoretic analysis of degradation), rather than degradation *per se*. Since the least-substituted polymers PLL-CA1 and PLL-CA2, allowed complete dissociation and gave no obvious degradation, we conclude that all polymers protected the plasmid DNA to an equivalent extent at the high polymer:DNA ratio (2:1).

High internalization of plasmid DNA into cells was the clear benefit of the previously prepared PLL-palmitic acid carrier.[16] Palmitic acid is the main fatty acid esterified to free thiol of protein cysteines for cellular trafficking and membrane crossing of the proteins. Other saturated (myristic and stearic) and unsaturated (oleic and arachidonic) endogenous fatty acids, however, are also employed for this purpose [20] and some of these fatty acids were explored for DNA

delivery in this study. It is evident that all lipid-substitution on PLL beneficially impacted intracellular plasmid DNA delivery, except the polymers with caprylic acid substitutions. It can be inferred from the latter polymers that the plasmid delivery efficiency was due to the lipids added onto the PLL, and not simply chemical modification of PLL's ε-NH_2 groups *per se*. Otherwise, the caprylic acid-substituted PLLs would have been also effective. It can be inferred that a lipid chain length longer than C8 was needed for successful plasmid delivery. To firmly confirm this observation, PLLs with higher caprylic acid substitutions (i.e., substitutions that match the –CH_2– content of longer lipid substituted PLL) are needed, which could not be prepared in our lab at this time. Considering all polymers tested, the intracellular delivery was strongly correlated with the extent of –CH_2– substitution on PLL. In agreement with this conclusion, other groups also reported an increase in cellular uptake or transfection efficiency with increasing hydrophobic character of carriers. Sato *et al.* [18], using lipoglutamate with different alkyl chains, noted an increased cellular uptake and transfection efficiency with increasing chain length of the carrier. Kurisawa *et al.* [19], using hydrophobic butylmethacrylate-substituted poly(*N*-isopropylacrylamide), showed increased transfection efficiency with increasing butylmethacrylate substitution of the carriers.

Effective complexation is an absolute necessity for internalization, but this was not the critical property influencing cellular delivery by our polymers. Rather, the polymers' ability to resist heparin-induced dissociation (a measure of complex stability) might have been more critical. Efficient cellular uptake requires the complex stability during membrane passage, as the extracellular matrix of cells contains heparin and heparin-like molecules, and this can inhibit DNA internalization due to complex dissociation [34-36]. Rapid complex dissociation in cytoplasm might also cause DNA degradation by nucleases, reducing any chances of successful

transfection [37]. Once delivered intracellularly by the more-effective polymers (i.e., PLL-MA, PLL-PA, PLL-StA), a significant fraction of the plasmid remained intact up to 7 days after a significant decrease (~30%) from day 1 to day 7. These results confirmed the previous reports [30,31], which showed the DNA-condensing agents, such as PLL or PEI, to enhance the transfection efficiency by prolonging the half-life of intact plasmid DNA in the cytosol. This is bound to lead to a higher nuclear localization of exogenous DNA due to its persistence around the nuclear membrane, which might increase its chance of random nuclear uptake at the time of cell division and/or specific transport through nuclear pores. Our methodology to detect the integrity of the plasmid required heparin-induced dissociation of the cell extracts before gel analysis. Without heparin dissociation, it was not possible to have plasmid migration into the electrophoresis gel, indicating that the plasmid was bound to other molecules. It is not known whether the polymeric carriers are still bound to the plasmid, or if they have been replaced with other endogenous molecules. This is a critical issue that will require additional studies for clarification.

The polymers that gave high cellular DNA uptake, PLL-StA1 and PLL-MA2, also gave higher transfection efficiency based on flow cytometry assessment. In addition to flow cytometry methodology used in previous studies [15,16], successful GFP expression was demonstrated by using RT-PCR in this study. The RT-PCR better revealed the differences between GFP and blank (i.e., gWIZ-GFP vs. gWIZ) transfected cells. Cells exposed to gWIZ alone did provide a false auto-fluorescence in flow cytometry studies, which is concerning for any studies that rely on flow cytometry solely to assess GFP expression. The RT-PCR indicated a more transient GFP expression, since the polymers did not give any detectable GFP transcript with gWIZ-GFP after day 6 (not shown). PLL-MA2 showed an unexpected lack of cellular growth while other carriers

did not affect cellular growth as compared to gWIZ treated controls. Although GFP expression gradually increased in fibroblasts treated with both PLL-MA2 and PLL-StA1, PLL-StA1 gave the highest numbers of transfected cells/well due to its better compatibility with the fibroblasts.

Other viral and non-viral carriers were reported in the literature for transfection of skin fibroblasts. Lattanzi *et al*. [38] have used an adenoviral vector expressing Myo cDNA for myogenic transformation of murine fibroblasts. The adenoviral delivery was more efficient than transfection with calcium phosphate, Lipofectamine™ 2000, and electroporation: 83% vs. 1-15%, respectively. Elmadbouh *et al*. [39] compared transfection efficiencies of Fugene™ 6 (non-liposomal cationic lipid), ExGen™500 (linear polyethyleneimine), and a histidylated PLL in fibroblasts from different species such as rats, rabbits and humans. The reporter gene used in these studies was secreted alkaline phosphatase, so that it was not possible to determine the percentage of cells successfully modified (as in this study). Nevertheless, (i) transfection efficiency of the carriers was found to depend on the origin of fibroblasts (human fibroblasts being more difficult to modify as compared to rabbit-derived fibroblasts), and (ii) Fugene™ 6 was more efficient than the other carriers. No 'blank' complexes were used in these studies, so these results need to be interpreted with caution since our studies did show an elevated autofluorescence in some transfections with the blank plasmid. Hellgren *et al*.[40] assessed the transfection efficiency of FuGene™ 6, Tfx™-50 and LipoTaxi™ reagents. Their target cells were human and rabbit fibroblasts isolated from skin, and they utilized VEGF or ß-galactosidase-coding plasmids. They also reported that human fibroblasts proved to be more difficult to transfect than rabbit fibroblasts and FuGene™ 6 was the most efficient carrier in their studies as 50% of rabbit fibroblasts and ~10% of human fibroblasts were modified with this carrier, and expression was undetectable with LipoTaxi™ and low with Tfx™-50. The transfection

efficiency with our most successful polymer (PLL-StA1) was comparable to the studies of Hellgren *et al.* with FuGene^{TM} 6. Hellgren *et al*., however did use carriers alone as controls for their studies and did not obtain apparent positive results by the carriers alone [40]. The major limitation of non-viral carriers is insufficient transfection rates for therapeutic applications, and it is not clear if the 10-12% transfection obtained with the most successful carrier in our hands, PLL-StA1, will be sufficient for this purpose. This may depend on clinically required delivery rate for individual proteins, but, alternatively, PLL-StA1 could be further engineered in order to obtain higher transfection rates.

In conclusion, we evaluated a library of amphiphilic polymers to explore structure-function relationships based on complex formation and dissociation, nuclease protection, and cellular delivery and transgene expression. The extent of lipid substitution was critical in reducing complex dissociation in response to a heparin-challenge and, in parallel, correlated positively with intracellular delivery of a plasmid DNA. Complexes with ≥2:1 (w/w) DNA:polymer ratio displayed effective DNA protection against DNase I and DNase II, which were equipotent in degradation of plasmid DNA. PLL was not able to deliver the plasmid DNA into cells, but PLL substituted with lipids longer than caprylic acid transformed the polymer into an efficient DNA carrier. The amount of intracellular plasmid peaked after 24 h of complex incubation, after which intracellular levels of intact plasmid was gradually decreased. It will be important to determine the reason for this decrease. The transfection of skin fibroblasts was most effective with carriers substituted with myristic and stearic acids. These studies are collectively providing important evidence for critical properties of lipid-substituted amphiphilic polymers for effective gene delivery.

Table 4-1. List of polymers synthesized and tested in this study. The polymer abbreviations used in the text and in some Figures are indicated. The extent of lipid and lipid methylene (-CH_2-) substitution are shown for each polymer.

Polymer Name	Abbreviation in text (Figures)	Lipids/PLL	-CH_2-/PLL
Poly-l-Lysine Caprylic Acid 1	PLL-CA1 (CA1)	6.9	55.2
Poly-l-Lysine Caprylic Acid 2	PLL-CA2 (CA2)	3.9	31.2
Poly-l-Lysine Myristic Acid 1	PLL-MA1 (MA1)	9.9	138.6
Poly-l-Lysine Myristic Acid 2	PLL-MA2 (MA2)	8.7	121.8
Poly-l-Lysine Palmitic Acid 1	PLL-PA1 (PA1)	9.8	156.8
Poly-l-Lysine Palmitic Acid 2	PLL-PA2 (PA2)	7.4	118.4
Poly-l-Lysine Stearic Acid 1	PLL-StA1 (StA1)	10	180
Poly-l-Lysine Stearic Acid 2	PLL-StA2 (StA2)	4.9	88.2
Poly-l-Lysine Oleic Acid 1	PLL-OA1 (OA1)	6.2	111.6
Poly-l-Lysine Oleic Acid 2	PLL-OA2 (OA2)	6.7	120.6
Poly-l-Lysine Linoleic Acid 1	PLL-LA1 (LA1)	4.5	81.0
Poly-l-Lysine Linoleic Acid 2	PLL-LA2 (LA2)	2.3	41.4

Table 4-2. Primer sequences and conditions for the PCR reaction. The primers for GFP were designed in house, whereas the primers for GAPDH were adopted form Low *et al.* (2005).

Gene	Sequence	Expected Product	PCR Conditions
GFP	sGFP-F3: AACGGCCACAAGTTCTCTGTC sGFP-R3: GTGTCCCAGAATGTTGCCATCT	329 bp	94ºC 30 sec 59ºC 30 sec 72ºC 2.5 min
GAPDH	GAPDH-F1: ACCACAGTCCATGCCATCAC GAPDH-R1: TCCACCACCCTGTTGCTGTA	454 bp	94ºC 30 sec 62ºC 30 sec 72ºC 45 sec

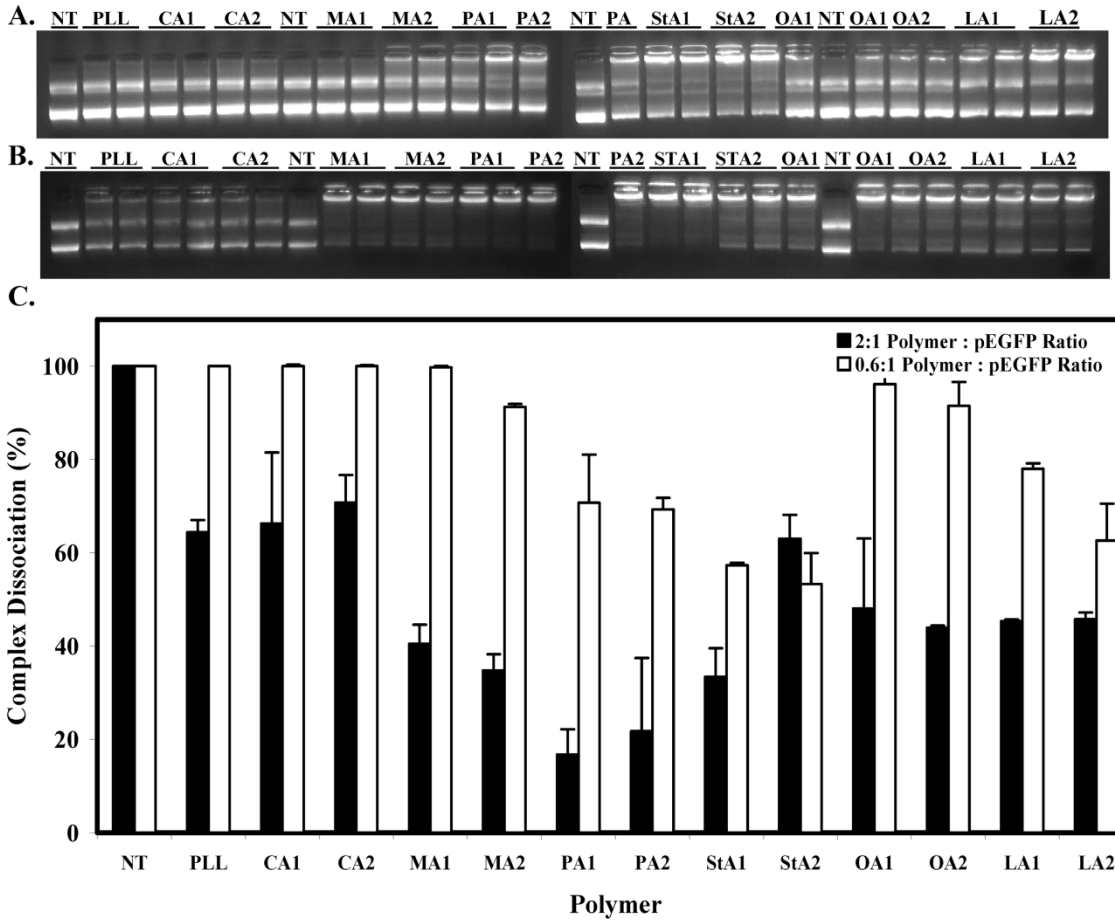
A.
NT PLL CA1 CA2 NT MA1 MA2 PA1 PA2 NT PA StA1 StA2 OA1 NT OA1 OA2 LA1 LA2
B.
NT PLL CA1 CA2 NT MA1 MA2 PA1 PA2 NT PA2 STA1 STA2 OA1 NT OA1 OA2 LA1 LA2
C.
2:1 Polymer : pEGFP Ratio
0.6:1 Polymer : pEGFP Ratio
Complex Dissociation (%)
0
20
40
60
80
100
NT PLL CA1 CA2 MA1 MA2 PA1 PA2 StA1 StA2 OA1 OA2 LA1 LA2
Polymer

D.

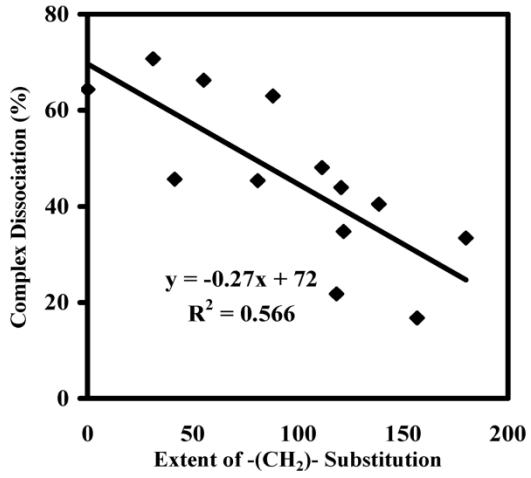
Complex Dissociation (%)
0
20
40
60
80
y = -0.27x + 72
R2 = 0.566
0
50
100
150
200
Extent of -(CH2)- Substitution

Figure 4-1. **A**. Heparin-induced dissociation of pEGFP from the polyplexes (in duplicate) formed at the polymer:pEGFP ratios of 0.6:1. **B**. Heparin-induced dissociation of pEGFP from the polyplexes (in duplicate) formed at the polymer:pEGFP ratios of 2:1. **C**. Percent (%) dissociation obtained after densitometric analysis of free pEGFP bands from the dissociated complexes. The results (mean ± SD of duplicate measurements) indicated almost complete dissociation of polyplexes formed at the 0.6:1 ratio, and dissociation to a lesser extent at the 2:1 ratio, consistent with the higher amount of polymer used for polyplex formation in the latter case. **D.** A correlation between the extent of methylene ($-CH_2-$) substitution and %dissociation of polyplexes (at 2:1 ratio) among the individual polymers indicated a significant ($p<0.003$) inverse relationship.

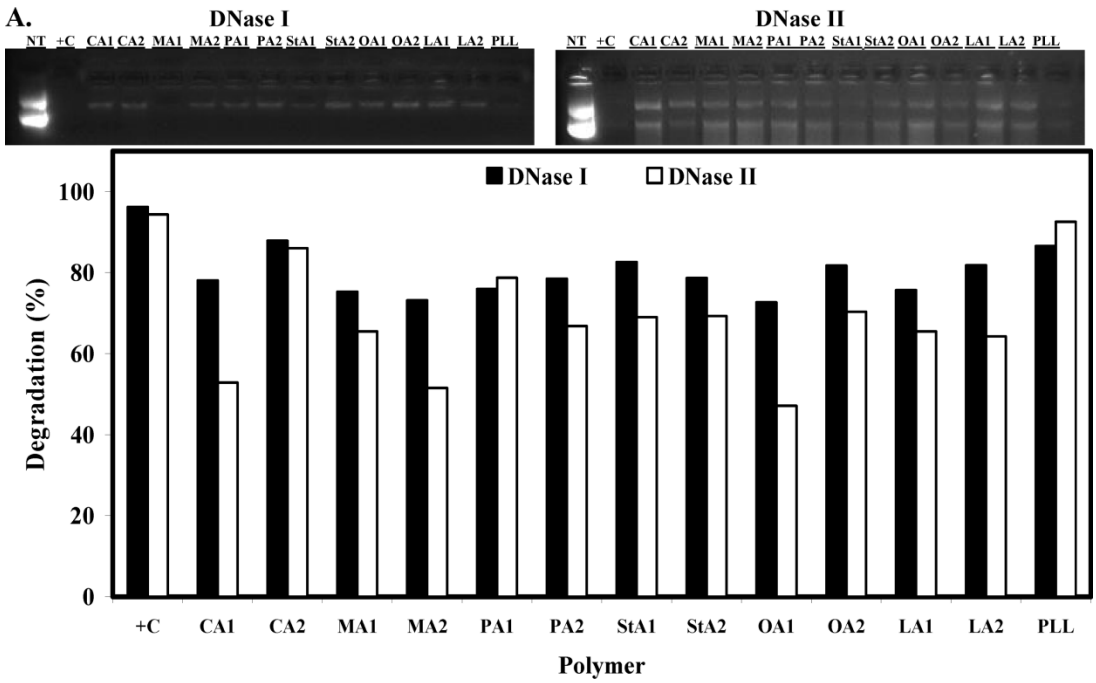
A.
DNase I
DNase II
NT +C CA1 CA2 MA1 MA2 PA1 PA2 StA1 StA2 OA1 OA2 LA1 LA2 PLL
DNase I
DNase II
Degradation (%)
0
20
40
60
80
100
+C CA1 CA2 MA1 MA2 PA1 PA2 StA1 StA2 OA1 OA2 LA1 LA2 PLL
Polymer

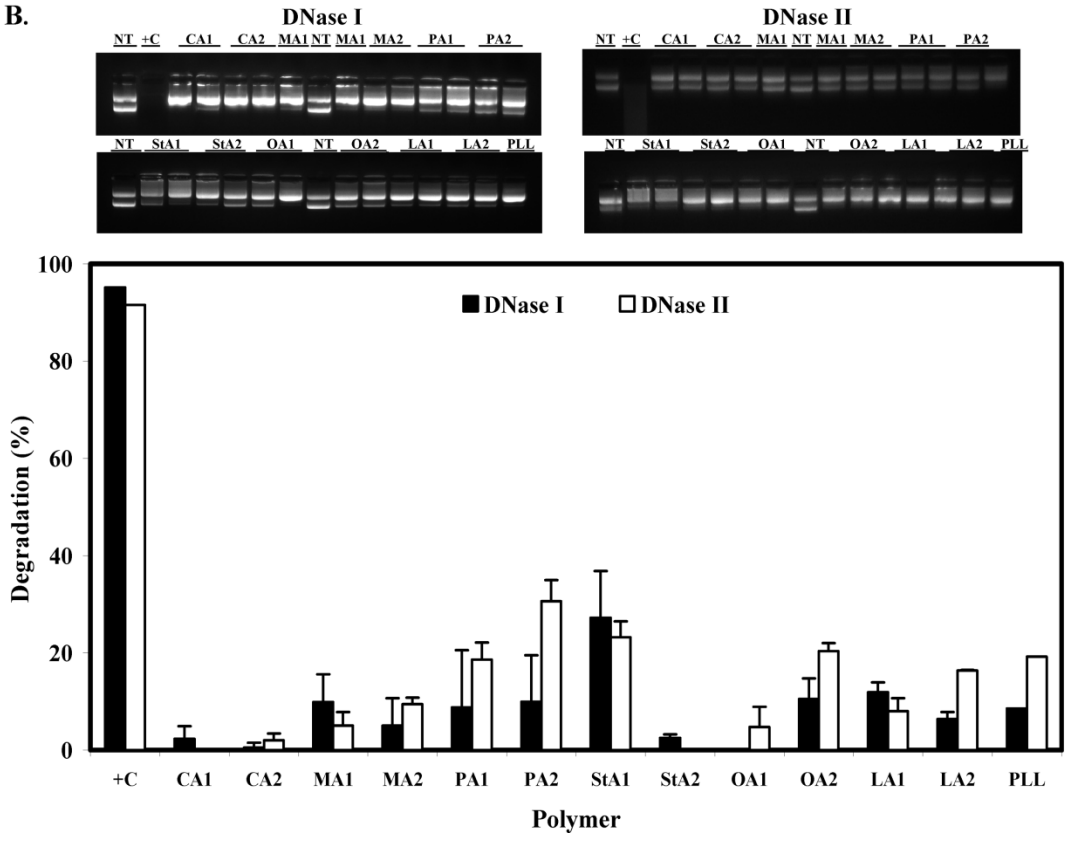
B.
DNase I
DNase II
NT +C CA1 CA2 MA1 NT MA1 MA2 PA1 PA2
NT StA1 StA2 OA1 NT OA2 LA1 LA2 PLL
DNase I
DNase II
Degradation (%)
0
20
40
60
80
100
+C CA1 CA2 MA1 MA2 PA1 PA2 StA1 StA2 OA1 OA2 LA1 LA2 PLL
Polymer

Figure 4-2. **A.** Protection of pEGFP in polyplexes (polymer:pEGFP ratio = 0.6:1) against DNAse I and DNAse II. Based on densitometry, the polymers were not able to protect the pEGFP in polyplexes (>50% degradation for all polymers), with no clear differences in protection against the two nucleases. **B.** Protection of pEGFP in polyplexes (polymer:pEGFP ratio = 2:1) against DNAse I and DNAse II. No significant degradation was evident for pEGFP in these polyplexes, except for polymers that displayed high binding affinity to pEGFP (see **Figure 1**). The latter was likely to be an artifact due to inability of polyplexes to dissociate (i.e., inability to recover all pEGFP on gels).

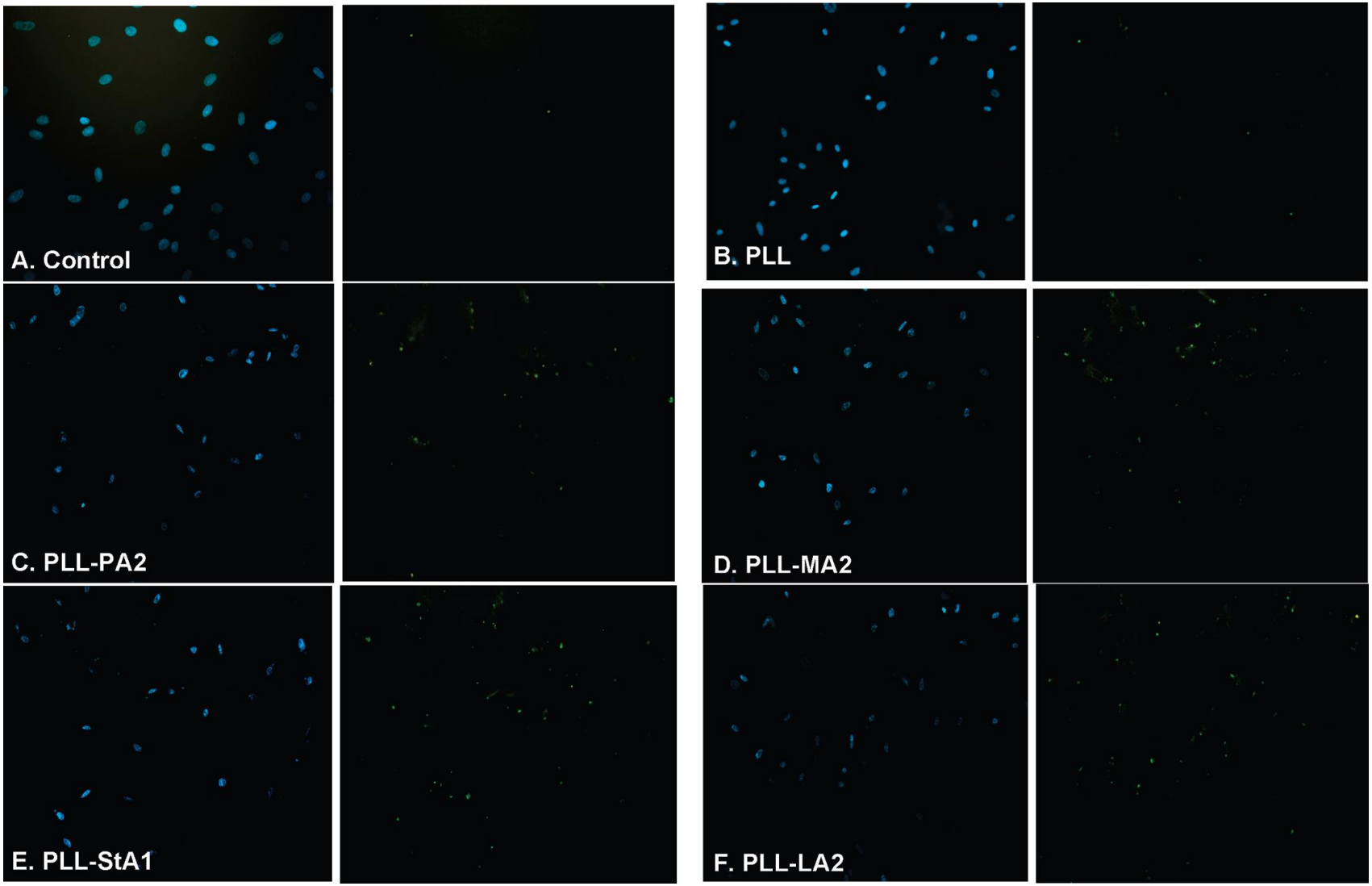

Figure 4-3. Cellular uptake of pEGFP complexes with no carrier (**A**), PLL (**B**), PLL-PA2 (**C**), PLL-MA2 (**D**), PLL-STA1 (**E**) and PLL-LA2 (**F**). The complexes were formed with FITC-labeled pEGFP and cells were counter-stained with Hoechst 33258 for nuclear visualization (left micrographs in each series). No plasmid uptake was evident for co-carrier samples, and relatively less pEGFP uptake was seen with PLL as compared to the lipid-substituted polymers. The bright green fluorescence of pEGFP polyplexes was typically associated with the cells, and found free distinct from the cells.

A.

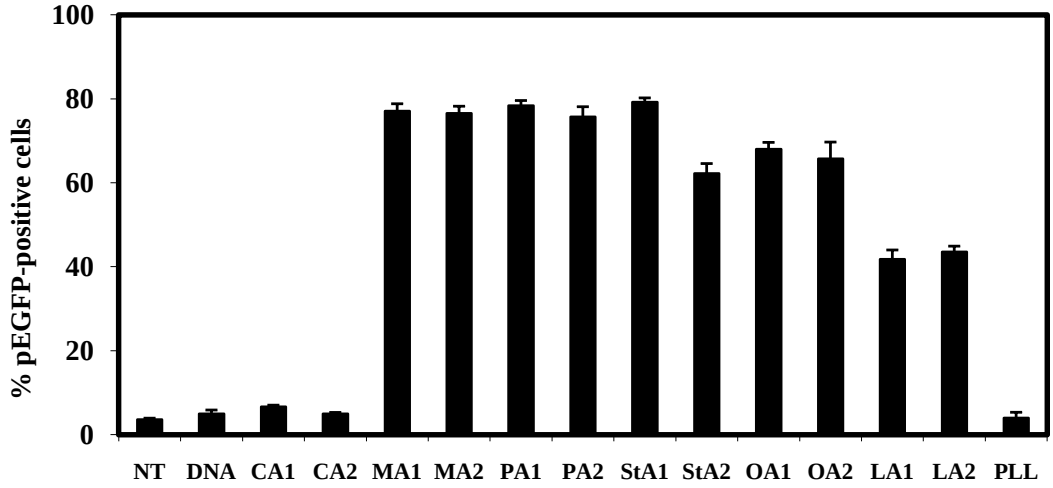
% pEGFP-positive cells
100
80
60
40
20
0
NT DNA CA1 CA2 MA1 MA2 PA1 PA2 StA1 StA2 OA1 OA2 LA1 LA2 PLL

B.

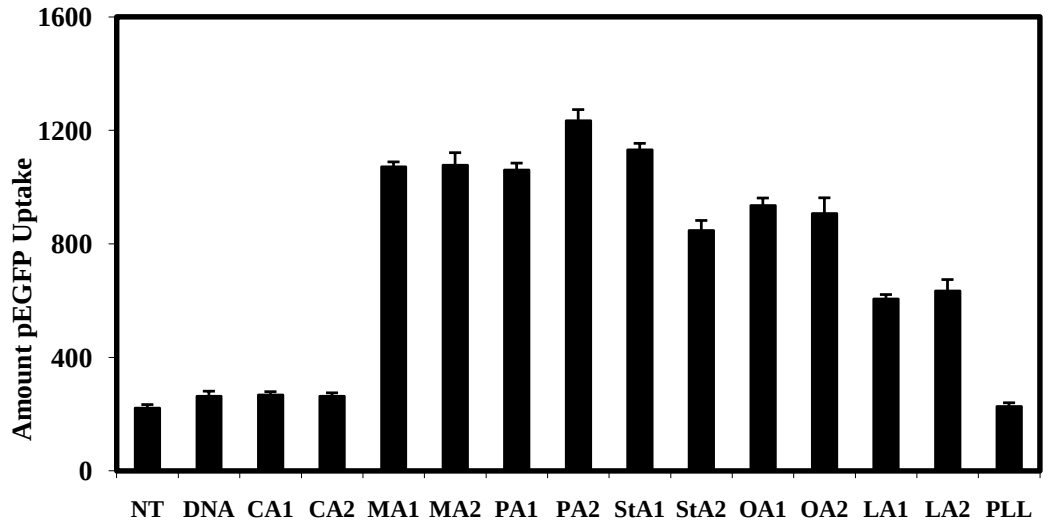
Amount pEGFP Uptake
1600
1200
800
400
0
NT DNA CA1 CA2 MA1 MA2 PA1 PA2 StA1 StA2 OA1 OA2 LA1 LA2 PLL

C.

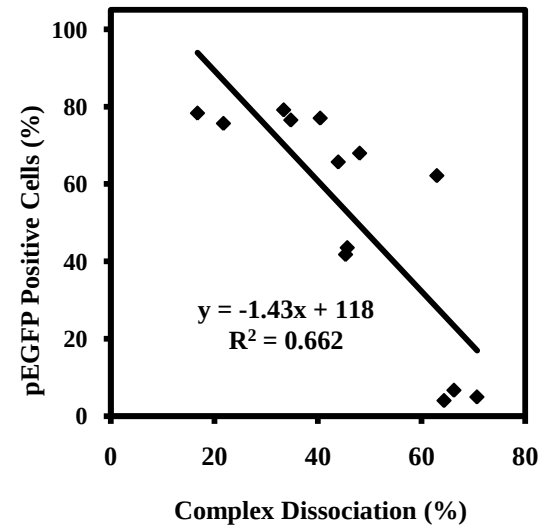
pEGFP Positive Cells (%)
100
80
60
40
20
0
y = -1.43x + 118
R2 = 0.662
0 20 40 60 80
Complex Dissociation (%)

D.

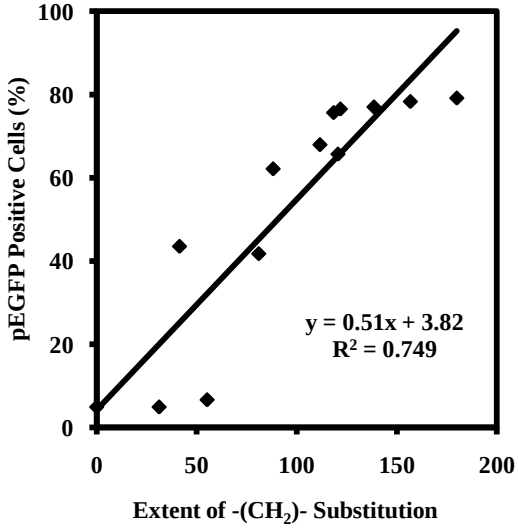
pEGFP Positive Cells (%)
100
80
60
40
20
0
y = 0.51x + 3.82
R2 = 0.749
0 50 100 150 200
Extent of -(CH2)- Substitution

Figure 4-4. A. Cellular uptake of pEGFP complexes based on flow cytometric determination of percentage of cells positive for pEGFP. The complexes were formed with AF546-labeled pEGFP, and no treatment (NT) and plasmid alone (DNA) served as controls. Unsubstituted PLL, PLL-CA1 and PLL-CA2 yielded insignificant delivery, PLL-LA1 and PLL-LA2 showed intermediate delivery, and the remaining polymers provided high delivery of pEGFP to the cells. **B**. Amount of pEGFP uptake by the cells, as given by mean fluorescence of the population (in arbitrary units). The amount of uptake paralleled the results based on the %pEGFP-positive cells in **A**. **C.** A significant ($p<0.001$) positive correlation was obtained between the %pEGFP-positive cells and the extent of $-CH_2-$ substitution. **D.** A significant ($p<0.001$) negative correlation was obtained between the %pEGFP-positive cells and the extent of complex dissociation.

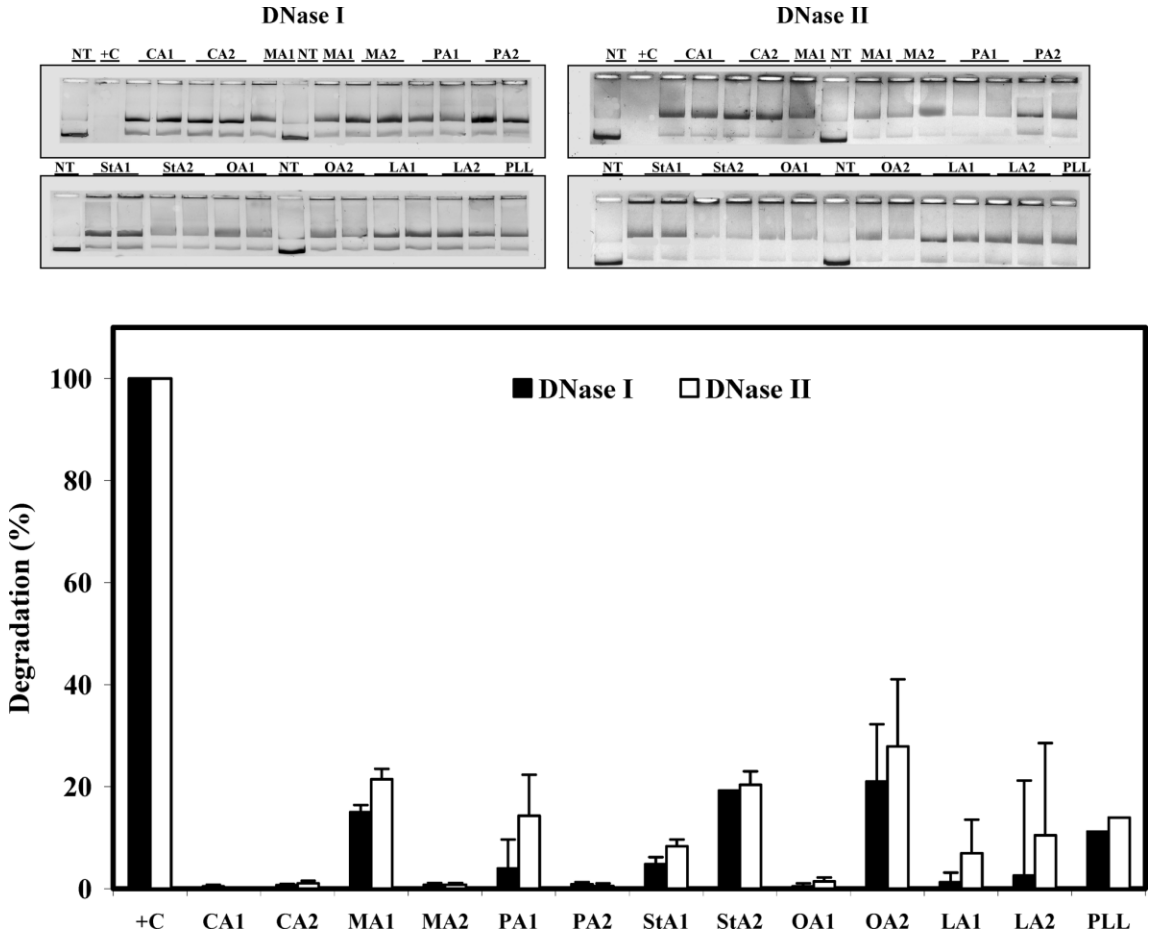

Figure 4-5. Degradation of AF546-labeled pEGFP complexed with different polymers. NT refers to the pEGFP exposed to no enzymes, and +C refers to the pEGFP exposed to the enzyme in the absence of polymers. The latter sample indicated no apparent effect of the labeling on DNAse-mediated degradation. The polyplexes were formed at polymer:pEGFp ratio of 2:1. As in **Figure 1**, (i) polyplex formation by most polymers protected the pEGFP against degradation (degradation less than ~20% in all cases), and (ii) no apparent difference was evident between the two DNAses.

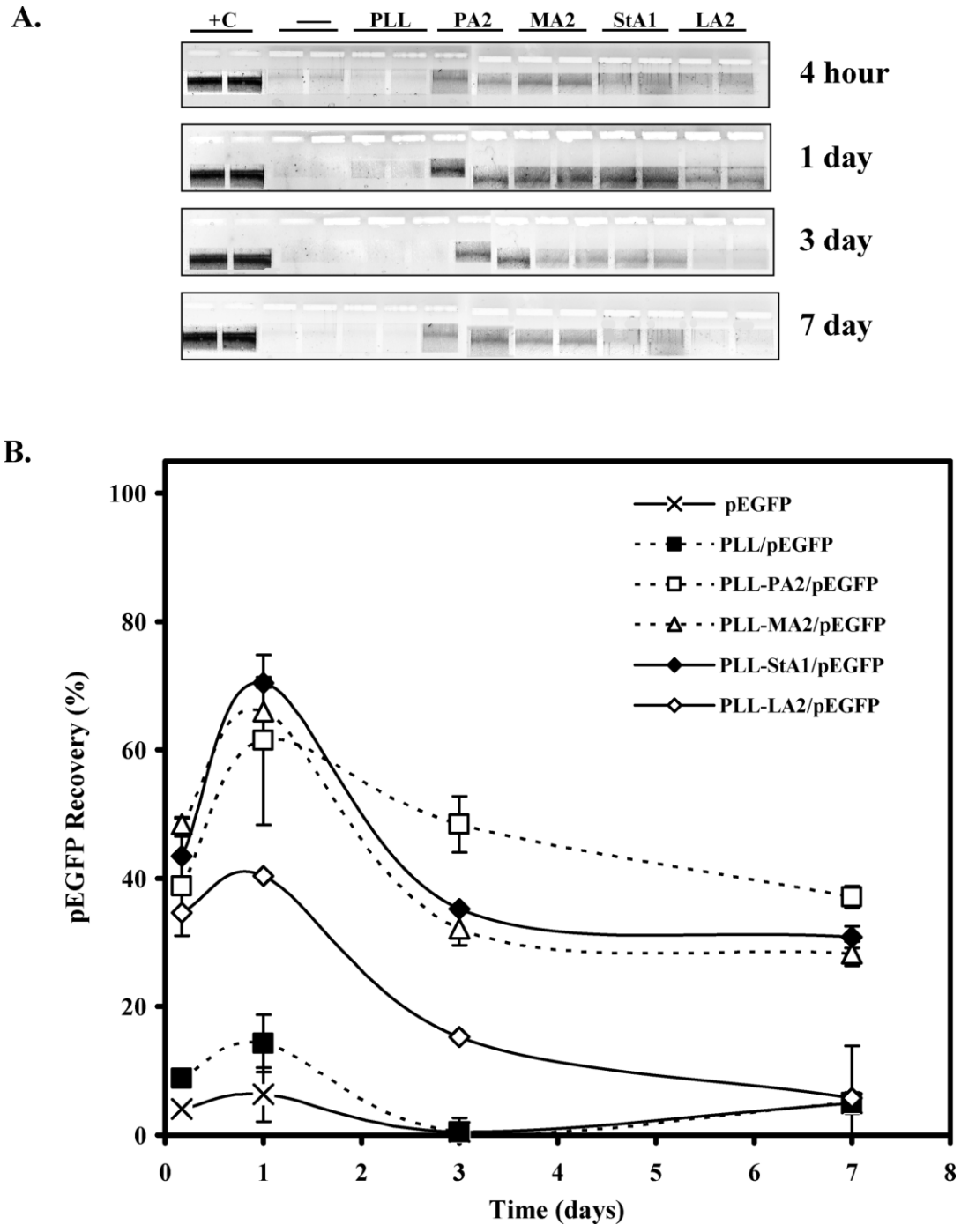

Figure 4-6. Time course of pEGFP recovery after polyplex exposure to the cells. The uptake of pEGFP was followed by using AF546-labeled pEGFP, which was extracted from the cells after 4 h, 1 day, 3 days and 7 days. **A** shows the pEGFP bands obtained on agarose gels (for duplicate wells of cells grown in 6-well plates), and **B** shows the quantitative pEGFP recovery based on densitometric analysis of the gels. Note the difference in pEGFP recovery for the lipid-substituted PLLs and the native PLL throughout the time period. The peak recovery was obtained on day 1, the time at which the polyplexes were removed from the cells. PLL-PA2, PLL-MA2 and PLL-STA1 gave the highest pEGFP recovery.

A.

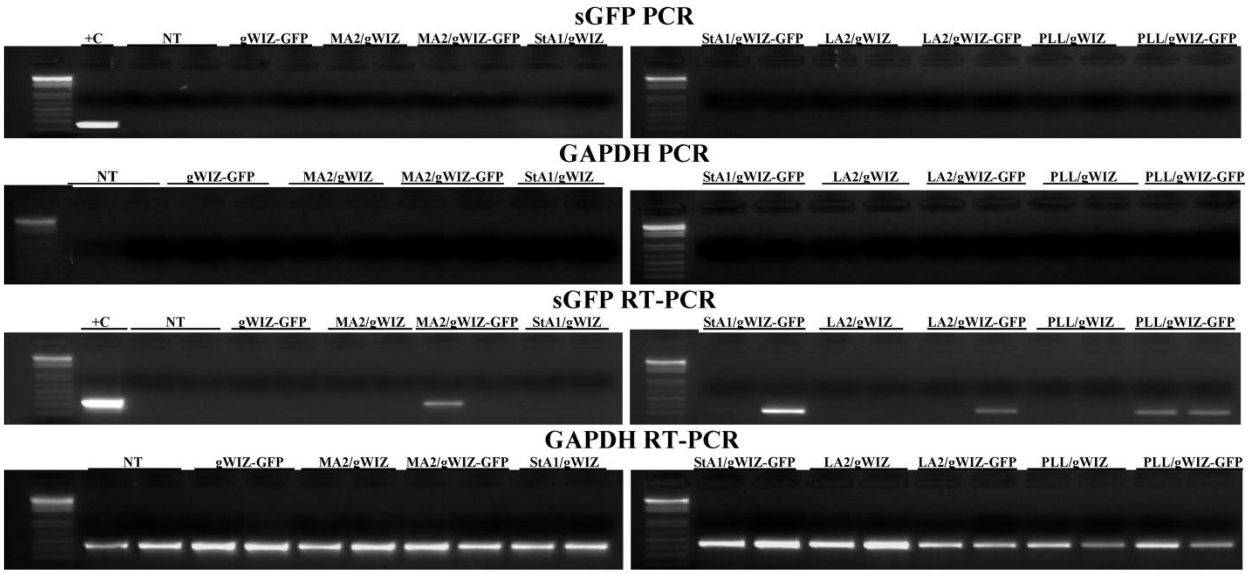

B.

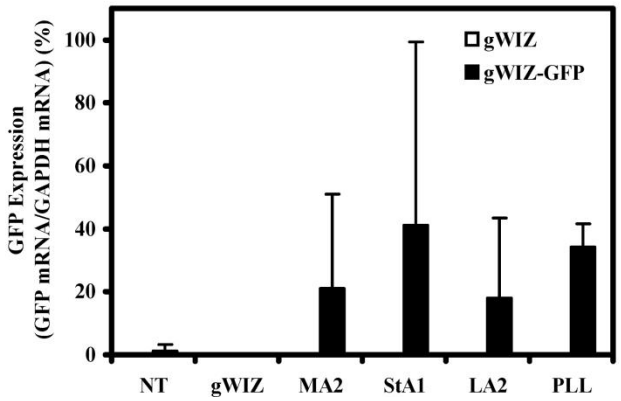

Figure 4-7. A. PCR and RT-PCR analysis of GFP and GAPDH expression by the cells on day 1. The amplification was conducted by using sGFP and GAPDH primers. PCR without RT was used to detect DNA contamination. No bands were evident in these samples (**A1** and **A2**), indicating insignificant levels of contamination, if any. RT-PCR with GAPDH primers indicated the corresponding transcript in all samples (**A3**). RT-PCR with sGFP primers indicated the corresponding transcript in samples transfected with gWIZ-GFP plasmid, but not the control gWIZ plasmid (**A4**). **B.** Quantitative assessment of GFP expression (as GFP/GAPDHG mRNA ratio) as determined by densitometer.

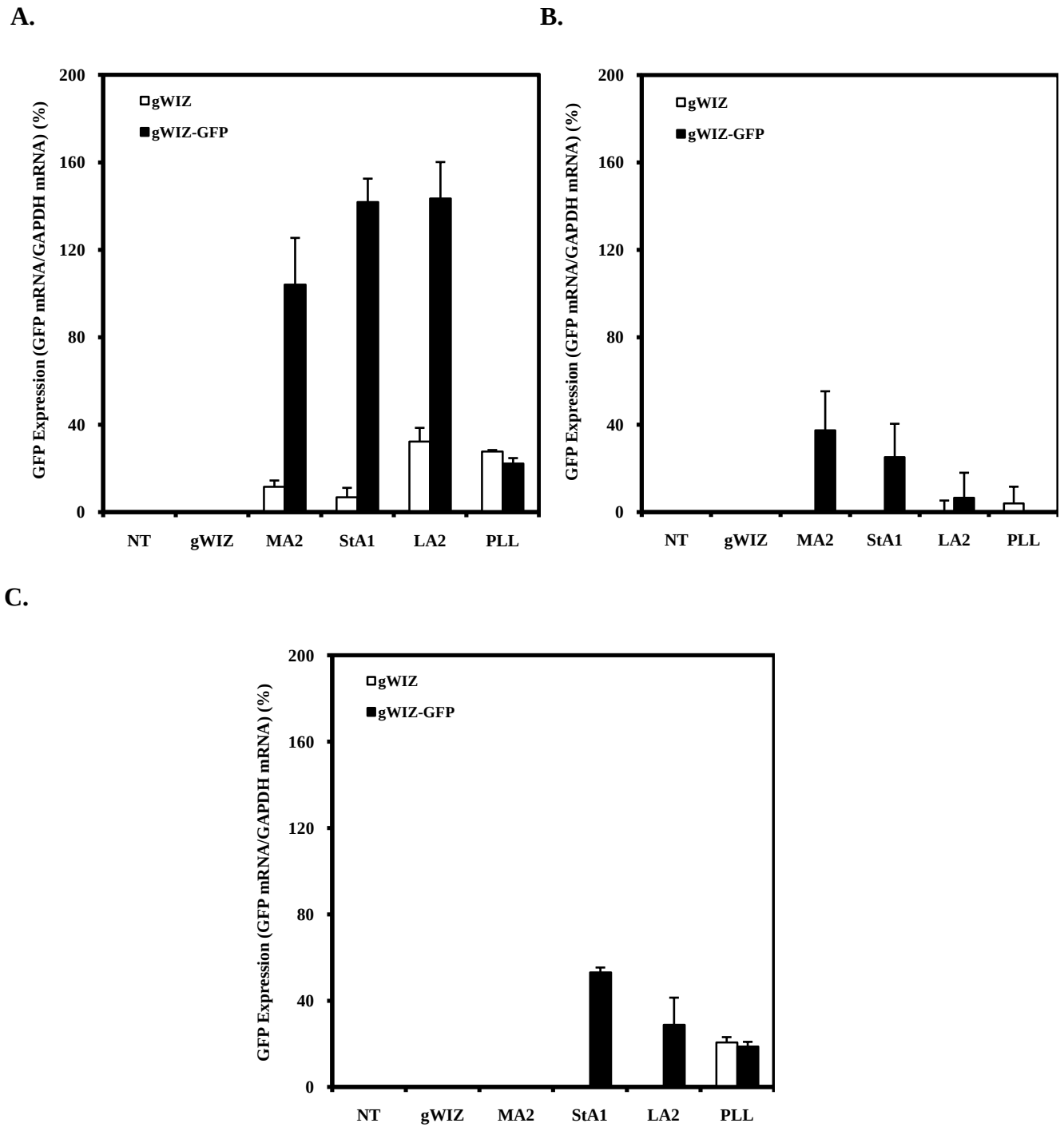

Figure 4-8. PCR and RT-PCR analysis of GFP and GAPDH expression by the cells on day 1 (A), day 6 (B), and day 10 (C). Amplification was conducted by using sGFP and GAPDH primers. PCR without RT was used to detect DNA contamination. High level of GFP expression was detected at day 1 after transfection by the lipid-modified polymers. Decreased levels of GFP expression were detected on days 6 and 10 after transfection.

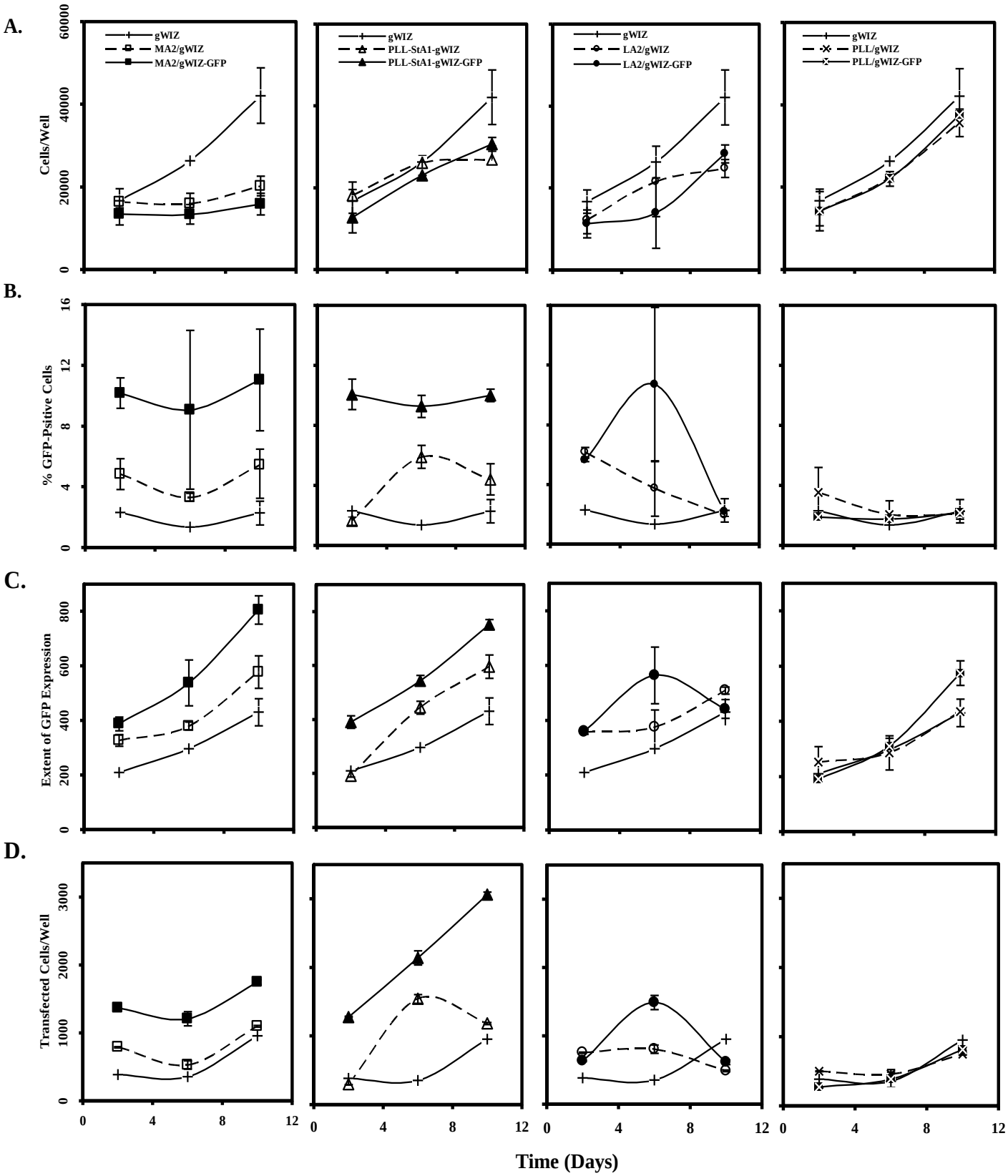
A.
B.
C.
D.
gWIZ
MA2/gWIZ
MA2/gWIZ-GFP
PLL-StA1-gWIZ
PLL-StA1-gWIZ-GFP
LA2/gWIZ
LA2/gWIZ-GFP
PLL/gWIZ
PLL/gWIZ-GFP
Cells/Well
% GFP-Psitive Cells
Extent of GFP Expression
Transfected Cells/Well
Time (Days)

Figure 4-9. Transfection of cells with polyplexes, as assessed by the flow cytometry. The cells were treated with gWIZ alone without any carrier, or with polyplexed formed with gWIZ and gWIZ-GFP complexed with the polymers PLL-MA2, PLL-STA1, PLL-LA2 and PLL. **A.** The number of cells recovered from the wells as a function of assessment time. All polymers, except PLL, showed some amount of toxicity especially at day 10. **B**. The extent of GFP expression given by the percentage of cells positive for GFP. PLL-STA1 and PLL-MA2 showed the highest transfection percentage at all time points, and control plasmid gWIZ gave autofluorescence above the background in some cases. **C**. The extent of GFP expression given by the total fluorescence of the cell population. The results were similar to the results based on %GFP-positive cells. **D**. The total number of cells positive for pEGFP (calculated by multiplying the number of cells per well with %GFP-positive cells) was highest for the PLL-STA1 at the end of day 10.

REFERENCES

1. Anderson WF. Hum gene ther. Science. 1992, 256, 808-13.
2. Mastrobattista E, van der Aa MA, Hennink WE, Crommelin DJ. Artificial viruses: a nanotechnological approach to gene delivery. Nat Rev Drug Discov. 2006, 5, 115-21.
3. Yang Y, Su Q, Grewal IS, Schilz R, Flavell RA, Wilson JM. Transient subversion of CD40 ligand function diminishes immune responses to adenovirus vectors in mouse liver and lung tissues. J Virol. 1996, 70, 6370-7.
4. Cavazzana-Calvo M, Thrasher A, Mavilio F. The future of gene therapy. Nature. 2004, 427, 779-81.
5. Schmidt-Wolf GD, Schmidt-Wolf IGH. Non-viral and hybrid vectors in human gene therapy: an update. Trend Mol Med. 2003, 9, 67-72.
6. Yu WH, Kashani-Sabet M, Liggitt D, Moore D, Heath TD, Debs RJ. Topical gene delivery to murine skin. J Invest Dermat. 1999, 112, 370-5.
7. Gache Y, Baldeschi C, Del Rio M, Gagnoux-Palacios L, Larcher F, Lacour JP, Meneguzzi G. Construction of skin equivalents for gene therapy of recessive dystrophic epidermolysis bullosa. Hum Gene Ther. 2004, 15, 921-33.
8. Brill-Almon E, Stern B, Afik D, Kaye J, Langer N, Bellomo S, Shavit M, Pearlman A, Lippin Y, Panet A, Shani N. Ex vivo transduction of human dermal tissue structures for autologous implantation production and delivery of therapeutic proteins. Mol Ther. 2005, 12, 274-82.
9. Pampinella F, Lechardeur D, Zanetti E, MacLachlan I, Benharouga M, Lukacs GL, Vitiello L. Analysis of differential lipofection efficiency in primary and established myoblasts. Mol Ther. 2002, 5, 161–9.

10. Pinto-González D, Krieser RJ, Eastman A, Barry MA. Deoxyribonuclease II is a Lysosomal Barrier to Transfection. Mol Ther. 2003, 8, 957-63.

11. Barry ME, Pinto-Gonza´lez D, Orson FM, McKenzie G J, Petry, GR, Barry, MA. Role of endogenous endonucleases and tissue site in transfection and CpG-mediated immune activation after naked DNA injection. Hum Gene Ther. 1999, 10, 2461-80.

12. Pollard H, Toumaniantz G, Amos J-L, Avet-Loiseau H, Guihard G, Behr J-P, Escande D. Ca2+-sensitive cytosolic nucleases prevent efficient delivery to the nucleus of injected plasmids. J Gene Med. 2001, 3, 153-64.

13. Shiokawa D, Tanuma S. DLAD, a novel mammalian divalent cation-independent endonuclease with homology to DNase II. Nucleic Acids Res. 1999, 27, 4083-9.

14. Lapidot Y, Rappoport S, Wolman, YJ. Use of esters of *N*-hydroxysuccinimide in the synthesis of *N*-acylamino acids. J Lip Res. 1967, 8, 142-5.

15. Incani V, Tunis E, Clements BA, Olson C, Kucharski C, Lavasanifar A, Uludag H. Palmitic acid substitution on cationic polymers for effective delivery of plasmid DNA to bone marrow stromal cells. J Biomed Mat Res. 2007, 81, 493-504.

16. Abbasi M, Uludag H, Incani V, Olson C, Lin X, Clements B, Rutkowski D, Ghahary A, Palmitic Acid-Modified Poly-L-Lysine for Non-Viral Delivery of Plasmid DNA to Skin Fibroblasts Weinfeld. Biomacromols. 2007, 8, 1059-63.

17. Smedt SCD, Demeester J, Hennink WE. Cationic polymer based gene delivery systems. Pharm Res. 2000, 17, 113-26.

18. Sato T, Kawakami T, Shirakawa N, Okahata Y. Chem Soc Jpn. 1995, 68, 2709-15.

19. Kurisawa M, Yokoyama M, Okano T. Transfection efficiency increases by incorporating hydrophobic monomer units into polymeric gene carriers. J Control Rel. 2000, 68, 1-8.
20. Hallak H, Brass LF, Manning DR. Failure to myristoylate the alpha subunit of Gz is correlated with an inhibition of palmitoylation and membrane attachment, but has no affect on phosphorylation by protein kinase C. J Biol Chem. 1994, 269, 4571-6.
21. Hagstrom JE, Ludtke JJ, Bassik MC, Sebestyen MG, Adam SA, Wolff JA. Nuclear import of DNA in digitonin-permeabilized cells. J Cell Sci. 1997, 110, 2323-31.
22. Wyllie AH. Glucocorticoid-induced thymocyte apoptosis is associated with endogenous endonuclease activation. Nature. 1980, 284, 555-6.
23. Polzar B, Peitsch MC, Loos R, Tschopp J, Mannherz HG. Overexpression of deoxyribonuclease I (DNase I) transfected into COS-cells: its distribution during apoptotic cell death. Eur J Cell Biol. 1993, 62, 397-405.
24. Polzar B, Zanotti S, Stephan H, Rauch F, Peitsch MC, Irmler M, Tschopp J, Mannherz HG. Distribution of deoxyribonuclease I in rat tissues and its correlation to cellular turnover and apoptosis (programmed cell death). Eur J Cell Biol. 1994, 64, 200-10.
25. Peitsch MC, Mannherz HG, Tschopp J. The apoptosis endonucleases: cleaning up after cell death? Trends Cell Biol. 1994, 4, 37-41.
26. Torriglia A, Chaudun E, Chany-Fournier F, Jeanny JC, Courtois Y, Counis MF. Involvement of DNase II in nuclear degeneration during lens cell differentiation. J Biol Chem. 1995, 270, 28579-85.
27. Rauch F, Polzar B, Stephan H, Zanotti S, Paddenberg R, Mannherz HG. Androgen ablation leads to an upregulation and intranuclear accumulation of deoxyribonuclease I in rat prostate epithelial cells paralleling their apoptotic elimination. J Cell Biol. 1997, 137, 909-23.

28. Barry MA, Eastman A. Identification of deoxyribonuclease II as an endonuclease involved in apoptosis. Arch Biochem Biophys. 1993, 300, 440-50.
29. Montague JW, Hughes FM, Cidlowski JA. Native recombinant cyclophilins A, B, and C degrade DNA independently of peptidylprolyl cis-trans-isomerase activity. Potential roles of cyclophilins in apoptosis. J Cell Biol. 1997, 272, 6677-84.
30. Chiou HC, Tangco MV, Levine SM, Robertson D, Kormis K, Wu CH, Wu GY. Enhanced resistance to nuclease degradation of nucleic acids complexed to asialoglycoprotein-polylysine carriers. Nucl Acids Res. 1994, 22, 5439-46.
31. Pollard H, Remy JS, Loussouarn G, Demolombe S, Behr JP, Escande D. Polyethylenimine but not cationic lipids promotes transgene delivery to the nucleus in mammalian cells. J Biol Chem. 1998, 273, 7507-11.
32. Meilander-Lin NJ, Cheung PJ, Wilson DL, Bellamkonda RV. Sustained in vivo gene delivery from agarose hydrogel prolongs nonviral gene expression in skin. Tiss Eng. 2005, 11, 546-55.
33. Varkey M, Gittens S, Uludag H. Growth factor delivery for bone tissue repair: an update. Drug Del. 2004, 1, 19-36.
34. Hawley P, Gibson I. Interaction of oligodeoxynucleotides with mammalian cells. Antisense Nuc. Acid Drug Del. 1996, 6, 185-96.
35. Ruponen M, Ronkko S, Honkakoski P, Pelkonen J, Tammi M, Urtti A. Extracellular glycosaminoglycans modify cellular traf- ficking of lipoplexes and polyplexes. J Biol Chem. 2001, 276, 33875-80.
36. Mislick KA, Baldeschwieler JD Proc. Extracellular glycosaminoglycans modify cellular trafficking of lipoplexes and polyplexes. Natl Acad Sci USA. 1996, 93, 12349-54.

37. Arigita C, Jan Zuidam N, Crommelin DJA, Hennink WE. Association and dissociation characteristics of polymer/DNA complexes used for gene delivery. Pharm Res. 1999, 16, 1534-41.

38. Lattanzi L, Salvatori G, Coletta M, Sonnino C, Cusella De Angelis MG, Gioglio L, Murry CE, Kelly R, Ferrari G, Molinaro M, Crescenzi M, Mavilio F, Cossu G. High efficiency myogenic conversion of human fibroblasts by adenoviral vector-mediated MyoD gene transfer. An alternative strategy for ex vivo gene therapy of primary myopathies. J Clin Invest. 1998, 101, 2119-28.

39. Elmadbouh I, Rossignol P, Meilhac O, Vranckx R, Pichon, C, Pouzet B, Midoux P, Michel J-BJ. Gene Med. 2004, 6, 1112-24.

40. Hellgren I, Drvota V, Pieper R, Enoksson S, Blomberg P, Islam KB, Sylvén C. Highly efficient cell-mediated gene transfer using non-viral vectors and Fugene™ 6: in vitro and in vivo studies. Cell Mol Life Sci. 2000, 57, 1326-1333.

CHAPTER V

A Review on siRNA-Mediated P-glycoprotein (P-gp)

Down-Regulation for Cancer Therapy

5.1 Background on Drug Resistance

Resistance to drugs is among the major causes of failure of cancer chemotherapy [1]. Major mechanisms of drug resistance include: (i) decreased intracellular uptake of drugs soluble in the physiological medium, (ii) genetic and phenotypic changes in cells that change the capacity of drugs to cause the desired cell damage, and (iii) increased efflux of especially hydrophobic drugs by cell-surface transporters, leading to the multidrug resistance (MDR) phenomena [2]. As most chemotherapeutic drugs are hydrophobic, MDR is consistently detected in tissues undergoing chemotherapy [3,4]. The induction of MDR can cause simultaneous resistance to different drugs with different targets and chemical structures [5]. This phenomenon can be either intrinsic or acquired as a result of exposure to chemotherapeutic agents. Acquired MDR is a common occurrence in breast and ovarian cancers where 50-70% of patients typically display MDR [6]. One reason for acquired resistance is the insufficient drug concentration exposed to tumor cells, so that the cells adapt to low concentrations of drugs without undergoing drug-induced cell death. A relatively short circulation time of chemotherapeutic agents limiting their access to tumor mass, as well as limited drug diffusion into the interstitial spaces of the tumors could lead to such a low drug concentration *in situ*. Phenotypic alterations in the tumor cells could also cause the acquired MDR as tumor cells change their membrane surface composition at different stages of neoplasmic growth [7].

5.2 P-glycoprotein (P-gp): Biology and Pharmacological Modulation

5.2.1 Introduction to P-gp (ABCB1, MDR1)

Three ATP binding cassette (ABC) family members including P-gp, multidrug resistance protein 1 (MRP1), and breast cancer resistance protein (BCRP), are believed to be the main efflux pumps involved in MDR. Among these transporters, P-gp is the most common protein involved in ATP-dependent efflux of drugs in various cancerous tissues [8,9]. P-gp is normally present at the apical surface of epithelium lining the colon, small intestine, bile ductules and kidney proximal tubules, where it secretes xenobiotics and various metabolites into bile, urine and the lumen of gastrointestinal tracks. In adrenal glands, P-gp is responsible for the transportation of hormones from these glands. It is also present in endothelial cells of the blood-brain barrier, blood-testis barrier and the blood-ear barrier, where it protects these susceptible organs from toxic xenobiotics. Its structure consists of two membrane-bound domains, each made of six transmembrane helices, and two cytoplasmic nucleotide binding sites that bind and hydrolyze ATP [10]. The nucleotide binding domains form a dimeric structure with a 5 nm pore, which closes at the cytoplasmic side and enables P-gp to efficiently efflux intracellular substrates out of the cell.

The P-gp has a broad substrate family ranging from drugs to biological compounds [11]. Several classes of chemotherapy drugs including vinca alkaloids, anthracyclines, epipodophyllo-toxin, and taxanes are effective substrates of P-gp [12,13]. Transport of drugs through P-gp is a multi-step process. Initially, the substrate enters the binding pocket in the cytoplasmic section. This causes P-gp to undergo an ATP-dependant conformational change and drive the substrate

across the membrane to the extracellular space. The P-gp returns to its original conformation after drug release into the extracellular space.

5.2.2 Chemical Inhibitors of P-gp

The abundance of P-gp and its ability to recognize a wide range of drugs as a substrate make it extremely difficult to modulate this transporter protein and impede its transport function. Chemical P-gp inhibitors have been the choice for this purpose for more than 30 years. Based on their affinity and specificity for P-gp, the chemical inhibitors have been divided into three generations. First generation inhibitors are calcium channel blockers (e.g., verapamil) and immunosuppressants (e.g., cyclosporine A). Their drawback is that they are highly toxic at effective doses due to off-target activities [14,15]. The second generation inhibitors have higher specificity and affinity to P-gp and thus are more effective than the first generation. They consist of analogues of dexverapamil, dexniguldipine, valspodar (PSC 833), and biricodar (VX-710). Although they show limited off target activity, they are substrates for cytochrome p450 and block this enzyme, which is required for the metabolism of xenobiotics and especially drugs. This causes a dramatic increase in toxicity by the co-administered drugs [16]. The third generation P-gp inhibitors show enhanced selectivity, limited toxicity and minimal pharmacokinetic interactions. These include the anthranilamide derivative tariquidar (XR9576), diketopiperazine derivative XR9051, the cyclopropyldibenzosuberane zosuquidar (LY335979) and the substituted diarylimidazole ONT- 093. The only drawback of their application is that they block other ABC transporter proteins as well as P-gp. This results in toxicity as ABC

transporters have other critical physiological roles and they protect the brain, kidney, testis, ovary and hematopoetic stem cells from unwanted chemicals [16]. Several reviews have focused on clinical significance of P-gp inhibition by chemical regulators, and discussed various commercially-available and novel P-gp modulators [5,17,18]. I will not repeat this literature here and the reader is referred to these reviews for an in-depth discussion on this topic.

5.2.3 Specific Down-Regulation of P-gp

Unlike chemical regulators, RNAi technology may provide a more effective approach for down-regulation of specific protein targets. The clinical potential of RNAi is actively explored in cancer therapy based on synthetic analogues of RNAi, namely short interfering RNAs (siRNAs). The siRNA based approach has been first shown to be effective in mammalian cells by Elbashir *et al*. (2001). The siRNAs are usually double-stranded, 21-25 nucleotide-long molecules, generated through the breakdown of long dsRNAs by enzymes known as dicers. siRNA is then activated through binding to RNA induced silencing complex (RISC) [19], which unwinds the siRNA duplex and produces an oligonucleotide that binds to a specific sequence on the target mRNA, leading to cleavage and disposal of the resulting dsRNA [20,21]. Among the potential advantages of using siRNA are its reduced toxicity on non-target tissues as compared to the conventional P-gp inhibitors (which exhibits broad range of activities in various tissues) and high degree of specificity on desired gene targets [22,23]. The G/C content of siRNA has been reported to be significant in siRNA efficiency for P-gp down-regulation. It has been reported that efficient siRNA sequences contain 30-52% G/C content. The presence of A/U at the 5’ end of

the antisense strand was suggested to increase efficiency [24,25], where 3 to 5 A/Us at the antisense strand were beneficial. Low internal stability of the siRNA at the 5'-end of the antisense strand was also considered important for duplex unwinding and efficient entry into RISC sequences [26].

Other molecules that may be useful in sequence-specific down-regulation of P-glycoprotein are micro-RNAs (miRNAs) [27], hammerhead ribozymes [28], and antisense oligonucleotides (ASO) [29]. miRNAs are single stranded 19-25 nucleotides produced from hairpin RNAs by dicer activity. They are partially complimentary to mRNA and inhibit translation by binding to various mRNA sequences. Similar to siRNA, miRNA function is also associated with the RISC multiprotein complex [30]. Using miRNA for P-gp down-regulation and Oligofectamine^{TM} for delivery, Zhu *et al.* were able to suppress P-gp levels by 40% in the human ovarian cancer cell line A2780, and its multidrug resistant counterpart, A2780DX5. They further showed that P-gp down-regulation by the chosen miRNA increased sensitivity to chemotherapeutic drug vinblastine by ~50% [27].

Hammerhead ribozymes are 30-40 nucleotide long, catalytic RNAs that are able to control the expression of genes by eliminating specific RNAs. They are functional after expressing ribozymes within the target cell or by delivering the ribozymes to the cell as a preformed entity [31]. The structure of hammerhead ribozymes contains three base-paired stems and a highly conserved core of residues required for RNA cleavage. Nagata *et al.* used hammerhead ribozymes, designed to cleave MDR1 mRNA (anti-MDR1) in HCT-8DDP a human colon cancer cell line with multidrug resistance. The anti-MRP ribozyme treated cells were more sensitive to doxorubicin (DOX) and etoposide (VP-16) by 2.5- and 4.1-fold, respectively, as

compared with the un-treated HCT-8DDP cells. Similarly, the anti-MDR1 ribozyme treated HCT-8DDP ells were more sensitive to DOX and VP-16 by 2.3- and 3.8-fold, respectively. While the anti-MRP ribozymes and anti-MDR1 ribozymes significantly reduced resistance to DOX and VP-16, these ribozymes did not affect the resistance to cisplatin, methotrexate and 5-fluorouracil [28].

ASOs are nucleotide sequences complementary to a target mRNA, which bind and prevent mRNA expression. ASOs have to recruit RNase to cleave the target mRNA, ultimately blocking mRNA translation. Refika *et al.* investigated the effect of simultaneous down-regulation of MDR-1 and BCL-2 for increased accumulation of the chemotherapeutic drug DOX in drug-resistant MCF-7 cells. They used a liposome for simultaneous delivery of ASOs and DOX and were able to decrease P-gp in MCF-7 cells by 3-fold [29]. A high concentrations of ASOs was needed for effective down-regulation, which have been reported to have off target toxicities. Motomura *et al.* used Lypolymine, a cationic liposome (Transfectam; Biospra, Marlbourough, MA), to deliver different concentrations of ASOs the human myelogenous leukemia cells K562 and the adriamycin-resistant phenotype K562/ADM[16]. An ASO concentration-dependant down-regulation of P-gp was observed; 25-75% P-gp down-regulation was achieved at 2.5-20 μM ASO concentrations [32].

A review on siRNA-mediated down-regulation of P-gp has been previously published, where RNAi inhibition of P-gp in 9 different studies has been assessed [33], but this review was limited in scope and the full extent of P-gp down-regulation in the literature and the carriers used for siRNA delivery have not reviewed. In this report, a detailed review of the siRNA-based approaches for P-gp down-regulation is provided.

5.3 Previous Approaches for siRNA Down-Regulation of P-gp

5.3.1 Mechanism of siRNA Function

The double stranded siRNA functions in the cytoplasm and acts as a suppressant against the expression of undesired genes. For an efficient RNA interference and protein knockdown, several successive steps have to be successfully completed. Initially, extracellular siRNA has to cross the lipid bilayer comprising the plasma membrane. For this purpose, a carrier is required with high affinity to siRNA as siRNA can not cross the cellular membrane on its own due to its anionic nature. This carrier should act to protect siRNA against extracellular and intracellular enzymes that hydrolyze free nucleic acids in physiological milieu. It is believed that the siRNA-carrier complex adsorbs and enters the cell through non-receptor-mediated endocytosis [34]. The complex will most likely be transported in endosomes where siRNA has to be protected from degradation by the endosomal/lysosomal system and somehow escape this entrapment. After endosomal escape, the siRNA has to be separated from its carrier and function in the cytoplasm through the RISC multiprotein complex. The optimal outcome of this event is the specific binding of siRNA to target mRNA and ultimately the target mRNA cleavage and degradation. Ineffective siRNA knockdown could be due to failure in any of these steps. In the case of the MDR1 gene, successful siRNA delivery is expected to lead to decreased MDR1 expression, reduced population of P-gp molecules on cell surface, reduced efflux of chemotherapeutic drugs from cells, and increased concentration of drugs in treated cells, resulting in increased cellular necrosis and/or apoptosis.

Another barrier to effective down-regulation of P-gp is the long half-life of P-gp protein. A half-life of a protein is the time taken for half of the protein population to be metabolized in a cell. siRNA down-regulation of P-gp limits the production of new P-gp, but a therapeutic effect is observed only when the overall P-gp population is reduced. Naked siRNA is rapidly degraded in physiological milieu and has a very short half-life (minutes to hours) [34,35]. Thus, siRNA persistence in cells is critical for its gene silencing activity, especially in the case of proteins with long half lifes (P-gp has a half-life of 14-17 h) [16-18]. The combined effects of short duration of down-regulation from the introduced synthetic siRNAs, and a long half-life of endogenous proteins results in only a partial reduction of P-gp activity. Stable expression of MDR1 shRNAs targeting different regions of the coding sequence has been shown to be more effective against long-lived proteins [36]. Proteins with half lives of minutes to 2 h have been considered to be short-lived proteins and proteins with >16 h half lives have been considered to be long-lived proteins [37]. In order to increase the half-life and bioavailability of synthetic siRNAs, various groups have made efforts to chemically modify siRNA while sustaining gene silencing activity. A study by Chiu *et al.* has shown that the 2'-OH of siRNA is not required for the siRNA function through the RISC complex. They have further showed that 2'-Fluoro and 2'-OMe modification of siRNA increased siRNA half-life when exposed to cytoplasmic extracts, without limiting its silencing ability. Furthermore, by strengthening the U-A linkage and modifying the P-S backbone linkages, this group has shown that siRNA stability in serum can be increased with no effect on the siRNA silencing ability [38]. Layzer *et al.* compared the half-life of 2'-Fluoro modified siRNA to unmodified 2'-OH-siRNA and evaluated the kinetics of gene silencing in HeLa cells. Their modification increased siRNA half-life in serum from 24 h to >72 h, however,

it did not affect gene silencing after siRNA treatment [39]. This suggests that siRNA half-life may not have been the limiting factor in their study and rapidly dividing of HeLa cells might have diluted the siRNA excessively. They did not test the modified siRNA on other cells and the results may have been different had they further investigated silencing in less rapidly dividing cells. These modification methods might be especially significant when siRNA silencing is performed *in vivo*, as RNases are at high concentrations in the lymph, blood, and extracellular matrix [40].

Even though siRNA action is sequence specific, limitations of siRNA mediated silencing have been recognized due to off-target down-regulation of mammalian genes. The reason behind this phenomenon is not exactly clear, however it is thought to be associated with similarities in mRNA sequences between the target sequence and other un-related sequences [41]. This off-target activity can be reduced by the use of low siRNA concentrations for silencing [42]. Most siRNA concentrations reported to be efficient in MDR reversal have been >100 nM [Figure 1]. Although the efficiency of siRNA down-regulation can be significantly increased by using higher concentrations, this has been repeatedly reported to affect mammalian gene expression. Persengiev *et al.* reported an increase as well as a decrease in the expression of various mammalian genes in response to a luciferase siRNA treatment (where no natural target is expected to exist). They observed a concentration-dependent effect of siRNA in various genes with siRNA concentrations >25 nM [42]. Semizarov *et al.* also tested this issue and observed off-target effects of siRNA at 100 nM concentration, but not at the 20 nM concentration [41]. Therefore, the reported data strongly favor the use <20 nM siRNA concentrations for MDR1 down-regulation to minimize off-target effects. Another reason behind the off-target activity

might be the fact that double stranded RNA can activate several protein kinases, such as p38, JNK2, IKK and PKR [43-46]. Induction of these signaling pathways can alter gene expression in an unpredictable way by regulating the activity of transcription factors such as NF-κB, IRF-3, and ATF-1 [45].

5.3.2 Delivery Vehicles for siRNA

As stated before, a carrier is an absolute necessity for siRNA delivery into cells and several types of carriers have been used for this purpose. Lipid-based carriers are among the most commonly used carriers for siRNA delivery for the purpose of P-gp down-regulation **(Table 1)**. The ease of synthesis and versatility makes them an appropriate choice for siRNA delivery and they have shown high efficiency in *in vitro* studies. However, a few drawbacks are associated with the use of these carriers such as toxicity, immunogenicity and lack of stability. Lipofectamine^{TM} 2000 and Oligofectamine^{TM} are the most common lipid-based carriers used for siRNA down-regulation and many groups have reported success in P-gp down-regulation by applying these carriers *in vitro* **(Table 1)**. Stierle *et al.* used Oligofectamine^{TM} to deliver P-gp siRNA to inhibit P-gp and obtain 60-80% P-gp down-regulation in MCF7 cells by using a combination of two siRNA sequences [47,48]. They used western blots to detect P-gp down-regulation, but its consequences on intracellular drug accumulation and cytotoxicity were not investigated. This study used a relatively low concentration of siRNA (20 nM). As described previously, siRNA concentrations >100 nM have been shown to affect gene expression in mammalian cells. They tested a combination of two siRNA sequences for efficient down regulation of MDR1, but no beneficial effect was noted using this approach; i.e., the P-gp down-regulation with the combined siRNAs did not surpass the P-gp down-regulation observed with

the single siRNA. Nieth *et al.* detected P-gp down-regulation in the MDR human gastric carcinoma cell line EPG85-257RDB and the human pancreatic carcinoma cell line EPP85-181RDB (established by *in vitro* exposure to daunorubicin). Oligofectamine™ was used for siRNA delivery and P-gp was down-regulated by as much as ~58% in the MDR gastric cancer cells, and ~89% in the pancreatic carcinoma MDR cells by using flow cytometry. This group did not perform drug accumulation and toxicity assays in this study, so that functional consequences of P-gp down-regulation were unknown [49].

Li *et al.* used esiMDR1, produced by endoribonuclease digestion of long double-stranded MDR1 RNA, to silence MDR1–EGFP fusion protein expression at very low concentrations of 1-30 nM. Their maximal P-gp down-regulation (~80%, based on mRNA analysis by PCR) was at ~30 nM RNAi in MCF7/R cells using Lipofectamine™ 2000 for delivery. Toxicity to chemotherapeutic drug daunorubicin was also assessed after down-regulation of P-gp. A 20% increase in toxicity of esiRNA was seen for daunorubicin-treated cells, as compared to no esiRNA treated cells [50].

Wu *et al.* investigated siRNA delivery to MDR human breast cancer cell lines, MCF-7/AdrR and MCF-7/BC-19, and their parental drug sensitive MCF-7 cells. Oligofectamine™ was used for siRNA delivery, which resulted in a maximum of ~65% P-gp down-regulation at 200 nM siRNA, as determined by western blot. They further investigated drug accumulation in these cells and detected ~2 fold increase in the accumulation of chemotherapeutic drugs (paclitaxel and doxorubicin) in the P-gp siRNA-treated cells compared to the Oligofectamine™ treated cells. Several reasons were suggested for not obtaining 100% P-gp inhibition: (i) high content of P-gp requiring excessive siRNA for delivery, (ii) long half-life of P-gp (14-17 h), requiring prolonged

presence of siRNA in the cells, and (iii) low delivery efficiency, requiring more effective delivery systems [51]. None of these issues were investigated in their study, but they are expected to be critical in this thesis work as well. P-gp levels will inevitably vary in different cell lines and a P-gp staining assay would determine the content of P-gp in each cell line. This will determine the extent of efficiency of the delivery system in each cell line. A survey of the efficiency of various carriers for siRNA delivery would also determine the extent of success of Oligofectamine^{TM} in comparison to other carriers for siRNA delivery. The duration of siRNA inhibition obtained by this group was ~24 h and the silencing effect of siRNA was lost after 72 h, consistent with the results obtained by the author's group [52].

Liu *et al.* designed a novel carrier combination by using advantages of both lipids (compatibility with cell membranes) and polymers (nucleic acid condensation) for siRNA delivery. They designed a carrier from 1:16 mixture of polyethyleneimine (PEI linear 1.2 kDa) with crosslinked diacrylate and used this carrier to deliver P-gp siRNA to the drug resistant human colon cancer CD133+ cells. They reported decreased toxicity, enhanced stability, and improved delivery of this delivery vehicle compared to the polymeric carrier PEI. ~70% P-gp mRNA knockdown was shown based on PCR assessment. They also detected reduction in the P-gp protein based on assessment by western blot (extent of reduction not quantitated). The siRNA concentration used in this study was 2.25 μg/mL (~200 nM), a concentration considered too high for non-specific effects. Paclitaxel treatment of cells after siRNA delivery showed a 10-30% increase in the cytotoxicity [53].

A common polymeric carrier used for siRNA delivery is PEI. This polymer is experimental at this stage and has not been used for clinical applications due to the fact that the

concentration needed for high efficiency leads to unacceptable toxicity and immune responses in the body [54]. The PEI provides stronger siRNA protection compared to lipid-based carriers, and increase siRNA half-life in cytoplasm [55,56]. PEI polyplexes with siRNA use adsorptive endocytosis or fluid-phase endocytosis for internalization into cells. Fluid-phase endocytosis is a nonspecific process that involves the bulk uptake of solutes proportional to their extracellular concentration, while in adsorptive endocytosis molecules are bound to the cell surface and concentrated before internalization [57]. Cytoplasmic movements of polyplexes are dependent on physiochemical properties of polyplexes like particle size and surface charge. The PEI toxicity is associated with perturbation of the cellular membrane of the modified cells. This induces necrotic changes and ultimately leads to activation of mitochondria associated apoptosis after 24 h of PEI exposure [58]. In order to improve siRNA delivery efficiency and reduce the toxicity caused by cationic polymer-mediated siRNA delivery, several modifications have been investigated. The modifications attempted with branched PEI include ethyl acrylate substitution [59], addition of hydrophobic moieties [60], and incorporation of reducible crosslinkers [53]. In a study by our group, lipid (stearic acid and oleic acid) modification of PEI has lead to an increase in siRNA delivery in the B16.F10 melanoma cells compared to the unmodified PEI [60].

Poly(l-lysine) (PLL) is another commercially available gene carrier that show limited transfection efficiency in plasmid DNA delivery. It has not been used for siRNA delivery after lipid (stearic acid) substitution on the polymer; a significant increase in siRNA delivery was seen with the MDA435/LCC6 MDR cells, as compared to unmodified PLL (~10 fold-increase). Furthermore, lipid-modified PLL protected siRNA better than the unmodified PLL against serum degradation and ultimately increased the siRNA half-life in cells. P-gp expression was reduced

by 50-60% using this carrier when the cells were treated with a low concentration of siRNA (20 nM). This led to a 3-fold increase in DOX accumulation in these cells and a ~30% increase in cytotoxicity. Lipofectamine^{TM} 2000 showed variable results in our hands for P-gp down-regulation (suppression was obtained at times but not consistently) and did not lead to a significant increase in drug uptake. Lipid modification of PEI by oleic acid (PEI-OA) did not result in improvements in the down-regulation of P-gp down-regulation in this study [52]. In a previous report, we obtained effective siRNA delivery against integrin α_v in B16 melanoma cells with PEI-OA [60]. Possible differences in cell types and the target gene could explain the differences between these two studies. In another study by our group, Xiong *et al.* used a novel family of biodegradable poly(ethyleneoxide)-block-poly(3-caprolactone) (PEO-b-PCL) based copolymers with polyamine side chains tetraethylenepentamine (TP), spermine (SP), and N,N-dimethyldipropylenetriamine (DP) on the PCL block to produce micelles for siRNA delivery. These polymeric micelles could be useful for the purpose of systemic delivery to tumors, as their parent polymer (i.e., PEI-b-PCL) is ideally suited for systemic delivery, while the polyamine side chains provide a high density of amines for siRNA binding. The polymers were able to effectively bind to siRNA, protect it from degradation by nuclease and release the complexed siRNA efficiently upon interaction with anionic macromolecules (e.g., heparin). Based on flow cytometry and confocal microscopy, siRNA formulated in PEO-b-PCL micelles showed efficient cellular uptake into the MDA435/LCC6 MDR-1 cells and exhibited a maximum of ~60% P-gp down-regulation using a range of siRNA concentrations from 100 to 300 nM [61]. These are relatively high concentrations and may reflect the fact that this delivery system was micellar in nature and was designed to remain soluble in physiological fluids. To improve this delivery

vehicle further, a peptide decorated PEO-b-PCL micelle mimicking viral particles was synthesized for siRNA encapsulation and delivery. The peptides used for micellar decoration were integrin $\alpha_v\beta_3$-binding peptide RGD4C and the cell-penetrating peptide TAT, the same peptide motifs used by some viruses for cell attachment and entry [62]. The RGD motif in the penton base of adenovirus is used for cellular internalization of viruses through binding to the $\alpha_v\beta_3$ integrins [63]. HIV-1 TAT peptide is also used for binding of viruses to cells via interaction with cellular glycosaminoglycans [64]. This induces their aggregation and activates the mechanism for cell membrane translocation. As some transformed cells overexpress $\alpha_v\beta_3$ integrin [65], this approach could be useful for targeting cancer cells to increase delivery efficiency and gene silencing, ultimately lowering the siRNA concentration needed. Compared to non-peptide conjugated micelle/siRNA complexes, RGD-, TAT-, and RGD/TAT-micelles resulted in approximately 2-fold increase in the percentage of siRNA-positive cells (65, 60 and 75% siRNA-positive cells by peptide-micelle/siRNA complexes vs. 37% siRNA positive cells by the non-peptide micelle/siRNA complex). P-gp down-regulation at the mRNA and protein level was also performed using the peptide decorated micelles. A ~70% down-regulation in P-gp mRNA and ~55% reduction in P-gp protein levels were observed with 100 nM siRNA. Drug accumulation was also increased following peptide-micellar treatment; ~2-fold increase in DOX uptake was observed, leading to a 3-fold increase in cytotoxicity [62].

While many groups have successfully showed the reversal of MDR by down-regulation of P-gp *in vitro* (as reviewed above), to our knowledge, Xiao *et al.* are among the only groups that have taken the next step and pursued *in vivo* P-gp down-regulation for MDR reversal and tumor suppression. This group used a Stealth^{TM} RNAi delivery system (Invitrogen) for siRNA

interference in the human lung carcinoma cells NCI-H460. Stealth™ RNAi shares the same interfering properties of siRNA but shows less off-target activities due to chemical inactivation of the sense strand. Lipofectamine™ 2000 was used in their *in vitro* approach, and they were able to down-regulate P-gp mRNA by ~60% (determined by PCR) and decrease P-gp levels by ~60% (determined by western blot) at the dose of 100 nM RNAi. Nude mice were used in their *in vivo* studies and 80 μM of the Stealth™ RNAi was delivered by electroporation directly into tumors (without a carrier). Their maximal P-gp down-regulation in the tumor cells was ~80%, and after P-gp down-regulation and chemotherapeutic treatment by Navelbine (Vinorelbine Tartrate), the maximal reduction of tumor size was by ~60% after 13 days [66]. It should be noted that a high degree of variation was seen in the size of drug-treated, no siRNA receiving tumors in this study (0.4 to 1 cm^3). An *in vivo* drug uptake and toxicity assay would have been beneficial to further compare changes in drug kinetics in siRNA-treated and no siRNA treated tumor cells.

Figure 1 shows the outcome of P-gp down-regulation attempted by various groups based on siRNA delivery. The solid diamonds denote P-gp down-regulation at the mRNA level (as detected by RT-PCR), while the white squares show P-gp protein down-regulation (as detected by flow cytometry or western blot). While most studies employ a range of siRNA concentrations to detect the best concentration for P-gp down-regulation at the mRNA and/or protein level, the concentration used for maximal down-regulation of P-gp is shown in the figure. It can be seen that the lower concentrations of siRNA were as effective as the higher concentrations for MDR1 down-regulation. It should be noted that there are significant variations in cell lines and delivery methods used to compile the Figure 1, and this will be explored in the next section.

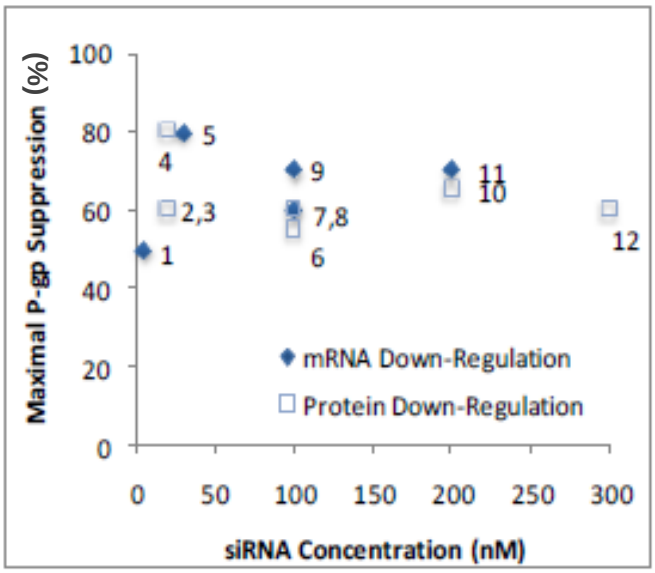

Figure 5-1. The siRNA concentrations used for maximal down-regulation of the P-gp at the mRNA and protein levels in various cell lines. A similar siRNA concentration has effective for P-gp down-regulation at both mRNA and protein levels. Also, relatively lower concentrations of siRNA were as effective as the high concentrations for P-gp down-regulation. The numbers in the figure corresponds to the following references; 1 = 51, 2 = 50, 3 = 56, 4 = 51, 5 = 54, 6 = 68, 7 = 52, 8 = 52, 9 = 68, 10 = 55, 11 = 57, 12 = 65.

5.3.3 Expression of Silencer Molecules (shRNA) Against P-gp In Situ

For long-term stable RNAi, expression vectors have been developed for *in situ* expression of silencer molecules. Expression vectors in the form of plasmid or viruses are intended to produce RNA transcripts that function similarly to siRNA. This may include vectors for small hairpin RNA (shRNAs, a small single stranded RNA sequence with a tight hairpin

turn), or expression cassettes producing sense and antisense strands which hybridize inside the cell to form functional siRNA [67-69]. As with siRNA, carriers are needed to deliver the expression vector into target cells. Yague *et al.* used the expression vector pSUPER to express shRNA in the leukemia cell line KD30 cells. Using this method, they were able to suppress P-gp mRNA by ~95% as detected by PCR. This led to a 90% decrease in the P-gp protein levels as detected by flow cytometry. They were able to completely restore cellular sensitivity against DOX, PTX, and colchicin as a result of *in situ* shRNA expression. This cell line was derived from the K562 leukemic cells, generated by a single-step selection after exposure to low DOX concentrations equivalent to that found in the plasma of leukaemia patients [70]. These authors discussed the reason behind incomplete knockdown of P-gp by other groups; with engineered cell lines that have a much higher surface concentration of P-gp, it will be more difficult to silence complete P-gp down-regulation. While native-like cells used in this study will be less challenging in this respect, whether all of the population can be effectively transfected remains to be seen as no selection method was used in their study.

Zhang *et al.* used Oligofectamine^{TM} to deliver the expression vector pSilencer MDR-1 plasmid siRNA (Ambion) and transfected ovarian MDR cells COC1/DDP and SKOV3/DDP. The cells were developed by stepwise selection in increasing concentration of cisplatin (DDP) from the parent cell lines COC1 and SKOV. They were able to suppress P-gp mRNA in these cells by a maximum of 50-60% [71]. Xing *et al.* used an oligo/Lipofectamine complex to transfect shRNA in the human ovarian cancer cell lines, A2780, CAOV3, SKOV3 and SW626 by using a shRNA-expressing linearized vector. PCR and western blot were used to show P-gp down-regulation at the mRNA and protein levels, however, an exact, quantitative level of down-

regulation was not given by this group. They were able to increase Taxol-induced apoptosis in these cells by 2-3 folds, based on propidium iodide staining and flow cytometry [72].

Viral vectors are also suitable for RNAi induction due to their ability to produce effective transfection in target cells. Adeno-associated viruses (AAV) have many advantages among the viral vectors available for transfection. They are able to transduce both dividing and non-dividing cells with immunogenic or pathogenic host response, and they lead to long-term expression [73]. The limitation of the use of AAV is that it has a single strand DNA sequence and it requires a complimentary strand before gene expression can take place. Efforts have been made to overcome this limitation and the new AAVs have shown higher transfection efficiency [74]. The self-complementary recombinant AAV (scAAV) vector is ideal for the short Pol III-based cassettes used for hairpin siRNA expression and can be used as a vector for siRNA transfection of a cancer-associated gene. Xu *et al.* used ScAAV to transfect anti-MDR1 hairpin siRNA vectors and were able to reduce P-gp levels after 2 days in the NCI/ADR-RES human breast cancer cells. Knockdown of the P-gp mRNA was complete (by real time PCR) within 3 days, and a ~70% reduction in P-gp protein level (by western blots) was detected after 3 days. Further studies by flow cytometry showed 90% P-gp protein reduction after 6 days and 80% after 7 days based on mean fluorescence of cells. This lead to an 8-fold increase in Rhodamine (a non-pharmacological substrate of P-gp) uptake in the transfected cells after 1 h Rhodamine exposure. A 2-fold increase in the DOX toxicity of the transfected cells was detected compared to the control cells, but the extent of intracellular drug accumulation was not assessed [75].

While most attempts have been successful for only transient P-gp down-regulation, using a self-inactivating retroviral expression vector, Hua *et al.* have been able to gain stable P-gp

down-regulation in drug-resistant cell line MES-SA/DX5 (established from the human sarcoma cell line MES-SA) in the presence of increasing DOX concentrations. The hygromycin-resistant selecting marker was used to select transfected cells in the hygromycine resistant MES-SA/DX5 cells. A ~90% P-gp down-regulation was obtained using western blot after 2 month transfection in the selected cell lines. The reason for the lack of suppression of the remaining 10% of P-gp was suggested to be due to insufficient siRNA induction in those cells and a further reduction in P-gp expression may be achieved by additional rounds of transfection [76]. Selection of the transfected cells by specific markers is a good approach for obtaining high transfection efficiency *in vitro*, however *in vivo* approaches using this technique would introduce unacceptable systemic toxicities and are not likely to be a clinical reality.

5.4 Synopsis

This chapter can be divided into three sections. In the first section of this chapter, a broad introduction to drug resistance, MDR, P-gp and the chemical inhibitors of P-gp is provided. In the second section, sequence specific down-regulation of P-gp using molecular level therapeutics is assessed and the approaches for P-gp down-regulation using miRNA, hammerhead ribozymes, and antisense oligonucleotides are reviewed. In the third and final section of this chapter, the siRNA delivery/expression methods using viral and non-viral carriers for the purpose of P-gp down-regulation for the potential therapy of various types of cancer are reviewed. Furthermore, the siRNA concentration, cell line, and the effectiveness of each approach are evaluated.

In the next 2 chapters of this thesis, I aim to use a novel approach for siRNA down-regulation of P-gp by using cationic polymers. In the first chapter, I will use an *in vitro* approach

using a low siRNA concentration (20 nM) and will detect P-gp down-regulation and the increase in chemotherapeutic drug uptake of cells after P-gp suppression. In the second chapter I will aim to detect an *in vivo* approach for siRNA down-regulation of P-gp by: (1) establishing a tumor in SCID mice; (2) detecting siRNA uptake in tumor cells, and; (3) evaluating P-gp down-regulation and chemotherapeutic drug uptake in tumor cells. To our knowledge, only one group has used an *in vivo* approach for the siRNA down-regulation of P-gp (reviewed above) and translation of *in vitro* success of P-gp down-regulation to *in vivo* studies is vital for the future of MDR reversal in cancer therapy.

Reference	Cell Line	Carrier	siRNA	siRNA Concentration	MDR1 Suppression
Xiao *et al*.	nude mice NCI-H460 tumor xenografts	Lipofectamine™ 2000	StealthTM RNAi 3 (5'-AACUUGAGCAGCAUCAUUGGCGAGC-3')	100 nM	50-79% P-gp mRNA Inhibition by PCR
Xing *et al*.	Human ovarian cancer cell lines, A2780, CAOV3, SKOV3 and SW626	Oligofectamine™/ Lipofectamine™ 2000 complex	Plasmid shRNA 5'GATCCCATTCGCTATGGCCGTGAATTCAAGAGA TTCACGGCCATAGCGAATGTTTTTTG-3' and 5'-GCTTTTCCAAAAAACATTCGCTATGGCCGTGA ATCTCTTGAATTCACGGCCATAGCGACTTAA-3'	200 nM	70-80% reduction of P-gp mRNA by PCR
Stierle *et al*.	MCF7 Cells	Oligofectamine™ Transfection	S1: 5'-GAAACCAACUGUCAGUGUA	20 nM	~55% P-gp Down-Regulation (48), 45% at 72h
			S2: 5'-CUUUGGCUGCCAUCAUCCA		~35% P-gp Down Regulation (48h) , No Diff at 72h
			S1+S2		~60% P-gp Down-Regulation (48) No Diff at 72h
Li L. *et al*.	MCF-7/R cells	Lipofectamine™ 2000	endonuclease-prepared small interfering RNA (EsiRNA)	0.7 nM	~80% P-gp suppression
Stierle *et al*.	MCF7-R (doxorubicin-resistant line)	Oligofectamine™	Si_1 5'-UACACUGACAGUUGGUUUCdTdTdTdTAUGUGAC UGU CAACCAAAG-5' Si_2 5'-UGGAUGAUGGCAGCCAAAGdTdTdTdTACCUACU ACC GUCGGUUC-5' Si_3 5'-UACGGUGCAAUUCGUAUCdTdTdTdTdTAUGCCAC AG UUAAGCAUAG	5 nM siRNA	Up to 50% P-gp mRNA reduction by PCR
Zhang *et al*.	MDR human ovarian cancer cells, COC1/DDP	Oligofectamine™	MDR-1: 5V-AAGGAAAAGAAACCAACTGTC-3V;	150 nM	Exact extent not given

Wu *et al*.	MCF-7/AdrR and MCF-7/BC-19	Oligofectamine™	5’-GGAAAAGAAACCAACUGUCdTdT(sense) dTdTCCUUUUCUUUGGUUGACAG-5’(antisense)	200nM siRNA	Maximum: 65% P-gp mRNA down-regulation
Stierle *et al*.	NIH-3T3 cells NIH-MDRG185 Cells MCF7-S MCF7-R	Oligofectamine™	(antisense, 5’-UACACUGACAGUUGGUUUCdTdT; sense, 5’-GAAACCAACUGUCAGUGUAdTdT). (antisense, 59-UGGAUGAUGGCAGCCAAAGdTdT; sense, 59-CUUUGGCUGCCAUCAUCCAdTdT). (antisense 59UACGGUGUCAAUUCGUAUCdTdT; sense, 59 GAUACGAAUUGACACCGU-AdTdT)	20nM	Up to 80% P-gp suppression by flow cytometry in MCF7 cells
Jun Huaa *et al*.	Multiple drug-resistant cell line MES-SA/DX5 (ATCC CRL-1977	Lipofectamine™ 2000	sense: 5VAGGCCAACATACATGCCTTC 3V, anti-sense: 5VGCTCCTTGACTCTGCCATTC 3V, sense: 5VAACTGGGACGACATGGAQGAA 3V, anti-sense: 5VAGAGGCGTACAGGGATAGCA 3V.	300 nM	~90% P-gp suppression after 2 month transfection

Table 5-1. A summary of published literature that employed lipid mediated siRNA delivery for P-gp down-regulation.

REFERENCES

1. Gillet JP, Efferth T, Remacle J. Chemotherapy-induced resistance by ATP-binding cassette transporter genes. Biochim Biophys Acta. 2007, 1775, 237-62.
2. Kerbel RS. Molecular and physiologic mechanisms of drug resistance in cancer: an overview. Cancer & Metastasis Reviews. 2001, 20, 1-2.
3. Eckford PDW, Sharom FJ. ABC efflux pump-based resistance to chemotherapy drugs. Chem Rev. 2009, 109, 2989–3011.
4. Higgins CF, Gottesman MM. Is the multidrug transporter a flippase? Trends Biochem Sci. 1992, 17, 18–21.
5. Renata Lehn Linardi, Cláudio Corrêa Natalini. Multi-drug resistance (MDR1) gene and P-glycoprotein influence on pharmacokinetic and pharmacodymanic of therapeutic drugs. Ciência Rural. 2006, 36, 336-41.
8. Loo TW, Clarke DM. Recent progress in understanding the mechanism of P-glycoprotein-mediated drug efflux. J Membr Biol. 2005, 206, 173-85.
9. Chen Y, Simon SM. *In Situ* biochemical demonstration that P-glycoprotein is a drug efflux pump with broad specificity. JCB. 2000, 148, 5863-70.
10. Aller SG, Yu J, Ward A, Weng Y, Chittaboina S, Zhuo R, Harrell P, Trinh YT, Zhang Q, Urbatsch IL, Chang G. Structure of P-glycoprotein reveals a molecular basis for poly-specific drug binding. Science. 2009, 323, 1718-22.

11. Scala S, Akhmed N, Rao US, Paul K, Lan L, Dickstein B, Lee J-S, Elgemeie GH, Stein GH, Bates SE. P-glycoprotein substrates and antagonists cluster into two distinct groups. Mol Pharmacol. 1997, 51, 1024–33.
12. Schinkel AH, Wagenaar E, Mol CA, van Deemter L. P-glycoprotein in the blood-brain barrier of mice influences the brain penetration and pharmacological activity of many drugs. J Clin Invest. 1996, 97, 2517–24.
13. Edith A. Perez, MD. Modulating drug resistance in metastatic breast cancer. Com Oncol. 2008, 5, 2-9.
14. Hegewisch-Becker S. MDR1 reversal: criteria for clinical trials designed to overcome the multidrug resistance phenotype. Leukemia. 1996, 10, S32-S38.
15. Van Zuylen L, Nooter K, Sparreboom A, Verweij J. Development of multidrug-resistance convertors: sense or nonsense? Invest New Drugs. 2000, 18, 205-20.
16. Thomas H, Coley HM. Overcoming multidrug resistance in cancer: P-gp modulators. Cancer Cont. 2003, 10, 159-65.
17. Liscovitch M, Lavie Y. Cancer multidrug resistance: A review of recent drug discovery research. I Drugs. 2002, 5, 349-55.
18. Varma MSV, Ashokraj Y, Dey CS, Panchagnula R. P-glycoprotein inhibitors and their screening: a perspective from bioavailability enhancement. Pharmacol Res. 2003, 48, 347-59.
19. Kawasaki H, Taira K, Morris KV. siRNA induced transcriptional gene silencing in mammalian cells. Cell Cyc. 2005, 4, 442-8.
20. Tang G. siRNA and miRNA: an insight into RISCs. Trends Biochem Sci. 2005, 30, 106-14.
21. Schutze N. siRNA technology. Mol Cell Endocrinol. 2004, 213, 115-9.

22. Luo Q, Kang Q, Song WX, Luu HH, Luo X, An N, Luo J, Deng, Jiang W, Yin H, Chen J, Sharff KA, Tang N, Bennett E, Haydon RC, He TC. Selection and validation of optimal siRNA target sites for RNAi-mediated gene silencing. Gene. 2007, 395, 160-9.
23. Fuchs U, Borkhardt A. The application of siRNA technology to cancer biology discovery. Adv Cancer Res. 2007, 96, 75-102.
24. Boese Q, Leake D, Reynolds A, Read S, Scaringe SA, Marshall WS, Khvorova A. Mechanistic insights aid computational short interfering RNA design, Methods Enzymol. 2005, 392, 73-96.
25. Reynolds A, Leake D, Boese Q, Scaringe S, Marshall WS, Khvorova A. Rational siRNA design for RNA interference. Nat Biotechnol. 2004, 22, 326-30.
26. Khvorova A, Reynolds A, Jayasena SD. Functional siRNAs and miRNAs exhibit strand bias. Cell. 2003, 115, 209-16.
27. Zhu H, Wu H, Liu X, Evans BR, Medina DJ, Liu CG, Yang JM. Role of MicroRNA miR-27a and miR-451 in the regulation of MDR1/P-glycoprotein expression in human cancer cells. Biochem Pharmacol. 2008, 76, 582–8.
28. Nagata J, Kijima H Hatanaka H, Asai S, Miyachi H, Abe Y, Yamazaki H, Nakamura M, Watanabe N, Mine T, Kondo T, Scanlon KJ, Ueyama Y. Reversal of drug resistance using hammerhead ribozymes against multidrug resistance-associated protein and multidrug resistance 1 gene. Int J Oncol. 2002, 21, 1021-6.
29. Pakunlu RI, Wang Y Saad M, Khandare JJ, Starovoytov V, Minko T. *In vitro* and *in vivo* intracellular liposomal delivery of antisense oligonucleotides and anticancer drug. J Cont Rel. 2006, 114, 153-62.

30. Pillai RS. MicroRNA function: Multiple mechanisms for a tiny RNA? RNA. 2005, 11, 1753-61.

31. Amarzguioui M. Prydz H. Hammerhead ribozyme design and application. Cell Mol Life Sci. 1998, 54, 1175–1202.

32. Motomura S. Motoji T, Takanashi M, Wang YH, Shiozaki H, Sugawara I, Aikawa E, Tomida A, Tsuruo T, Kanda N, Mizoguchi H. Inhibition of P-glycoprotein and recovery of drug sensitivity of human acute leukemic blast cells by multidrug resistance gene (mdr1) antisense oligonucleotides. Blood. 1998, 91, 3163-71.

33. Lage H. Reversal of MDR1/P-glycoprotein-mediated multidrug resistance by RNA interference. Int Cong Series. 2005, 1277, 144–5.

34. Akhtar S, Benter IF. Nonviral delivery of synthetic siRNAs *in vivo*. J of Clin Inves. 2007, 117, 3623-32.

35. Dykxhoornn DM, Lieberman J. Knocking down disease with siRNAs. Cell. 2006, 126, 231-35.

36. Yague E, Higgins CF, Raguz S. Complete reversal of multidrug resistance by stable expression of small interfering RNAs targeting MDR1. Gene Ther. 2004, 11, 1170–4.

37. Ahlberg J, Berkenstam A, Henell F, Glaumann H. Degradation of short and long lived proteins in isolated rat river lysosomes. J Biol Chem. 1985, 260, 5847-54.

38. Chiu Y-L, Rana TM. siRNA function in RNAi: A chemical modification analysis. RNA. 2003. 9, 1034-48.

39. Layzer JM, Mccaffrey AP, Tanner AK, Huang Z, Kay M.A, Sullenger BA. *In vivo* activity of nuclease-resistant siRNAs. RNA. 2004, 10, 766–71.

40. Lechner MC, Magalhães MCD. RNase activities in blood serum of several vertebrates. Cell Mol Life Sci. 1973, 29, 1479-80.

41. Bartz JAL, Schelter SR Schelter J, Kobayashi SV, Burchard J, Mao M, Li B, Cavet G, Linsley PS. Expression profiling reveals off-target gene regulation by RNAi. Nature Biotechnol. 2003, 21, 635-7.

41. Semizarov D, Frost L, Sarthy A, Kroeger P, Halbert DN, Fesik SW. Specificity of short interfering RNA determined through gene expression signatures. Proc Natl Acad Sci USA. 2003, 100, 6347–52.

42. Persengiev SP, Zhu X, Green MR. Nonspecific, concentration-dependent stimulation and repression of mammalian gene expression by small interfering RNAs (siRNAs). RNA. 2004, 10, 12–8.

43. Kumar A, Haque J, Lacoste J, Hiscott J, Williams BR. Double-stranded RNA-dependent protein kinase activates transcription factor NF-αB by phosphorylating I _B. Proc Natl Acad Sci. 1994, 91, 6288–92.

44. Chu WM, Ostertag D, Li Z-W, Chang L, Chen Y, Hu Y, Williams B, Perrault L, Karin M. JNK2 and IKKβ are required for activating the innate response to viral infection. Immunity. 1992, 11, 721–31.

45. Williams BR. PKR: A sentinel kinase for cellular stress. Oncogene. 1999, 18, 6112–20.

46. Yang YL, Reis LF, Pavlovic J, Aguzzi A, Schäfer R, Kumar A, Williams BR, Aguet M, Weissmann C. Deficient signaling in mice devoid of double-stranded RNA-dependent protein kinase. EMBO J. 1995, 14, 6095-106.

47. Stierle´ V, Laigle A, Jolle`s B. Modulation of the efficiency of a siRNA directed against MDR1 expression in MCF7-R cells when combined with a second siRNA. Biochimie. 2007, 89, 1033-6.

48. Stierle´ V, Laigle A, Jolle`s B. Modulation of MDR1 gene expression in multidrug resistant MCF7 cells by low concentrations of small interfering RNAs. Biochemical Pharmacol. 2005, 70, 1424–30.

49. Nieth C, Priebsch A, Stege A, Lage H. Modulation of the classical multidrug resistance (MDR) phenotype by RNA interference (RNAi). FEBS Lett. 2003, 545, 144-50.

50. Li L, Xu J, Min T, Huang W. Reversal of MDR1 gene-dependent multidrug resistance using low concentration of endonuclease-prepared small interference RNA. Eur J Pharmacol. 2006, 536, 93-7.

51. Wu H, Hait WN, Yang JM. Small interfering RNA-induced suppression of *MDR1* (P-glycoprotein) restores sensitivity to multidrug-resistant cancer cells. Cancer Res. 2003, 63, 1515–9.

52. Abbasi M, Lavasanifar A, Berthiaume LC, Weinfeld M, Uludağ H. Cationic polymer mediated siRNA delivery for P-glycoprotein (P-gp) down-regulation in tumor cells. Cancer. 2010, In Press.

53. Liu C, Zhao G, Liu J, Ma N, Chivukula P, Perelman L, Okada K, Chen Z, Gough D, Yu L. Novel biodegradable lipid nano complex for siRNA delivery significantly improving the chemosensitivity of human colon cancer stem cells to paclitaxel. J Con Rel. 2009, 140, 277–83.

54. Urban-Klein B, Werth S, Abuharbeid S, Czubayko F, Aigner A. RNAi-mediated gene-targeting through systemic application of polyethyleneimine (PEI)-complexed siRNA *in vivo.* Gene Ther. 2005, 12, 461–6.

55. Akhtar S, Benter IF. Nonviral delivery of synthetic siRNAs *in vivo*. J Clin Invest. 2007, 117, 3623–32.

56. Dykxhoorn DM, Palliser D, Lieberman J. The silent treatment: siRNAs as small molecule drugs. Gene Ther. 2006, 13, 541–52.

57. Khalil IA, Kogure K, Akita H, Harashima H. 2006. Uptake pathways and subsequent intracellular trafficking in nonviral gene delivery. Pharmacol Rev. 2006, 58, 32-45.

58. Moghimi SM, Symonds P, Murray JC, Hunter AC, Debska G, Szewczyk A. A two-stage poly(ethylenimine)-mediated cytotoxicity: implications for gene transfer/therapy. Mol Ther. 2005, 11, 990–5.

59. Zintchenko A, Philipp A, Dehshahri A, Wagner E. Simple modifications of branched PEI lead to highly efficient siRNA carriers with low toxicity. Bioconjugate Chem. 2008, 19, 1448-55.

60. Alshamsan A, Haddadi A, Incani V, Samuel J, Lavasanifar A, Uludağ H. Formulation and Delivery of siRNA by Oleic Acid and Stearic Acid Modified Polyethyleneimine. Mol Pharma. 2009, 6, 121–33.

61. Xiong XB, Uludağ H, Lavasanifar A. Biodegradable amphiphilic poly(ethylene oxide)-block-polyesters with grafted polyamines as supramolecular nanocarriers for efficient siRNA delivery. Biomat. 2009, 30, 242–53.

62. Xiong XB, Uludağ H, Lavasanifar A. Virus-mimetic polymeric micelles for targeted siRNA delivery. Biomat. 2010, in press.

63. Medina-Kauwe LK. Endocytosis of adenovirus and adenovirus capsid proteins. Adv Drug Deliv Rev. 2003, 55, 1485-96.

64. Bayer P, Kraft M, Ejchart A, Westendorp M, Frank R, Rosch P. Structural studiesof HIV-1 Tat protein. J Mol Biol. 1995, 247, 529-35.

65. Pecheur I, Peyruchaud O, Serre C-M, Guglielmi J, Voland C, Bourre F, Margue C, Cohen-Solal M, Buffet A, Kieffer N, Clézardin P. Integrin αvβ3 expression confers on tumor cells a greater propensity to metastasize to bone. The FASEB Journal. 2002, 16, 1266-8.

66. Xiao H, Wu Z, Shen H, Luo A-L, Yang Y-F, Li X-B, Zhu D-Y. *In vivo* Reversal of P-Glycoprotein-Mediated Multidrug Resistance by Efficient Delivery of Stealth^{TM} RNAi. Basic & Clin Pharmacol & Toxicol. 103, 342–8.

67. McIntyre G, Fanning G. Design and cloning strategies for constructing shRNA expression vectors. BMC Biotechnol. 2006, 6:1.

68. Tran N, Cairns MJ, Dawes IW, Arndt GM. Expressing functional siRNAs in mammalian cells using convergent transcription. BMC Biotechnol. 2003, 3, 21-28.

69. Lee NS, Kim DH, Alluin J, Robbins M, Gu S, Li H, Kim J, Salvaterra PM, Rossi JJ. Functional and intracellular localization properties of U6 promoter-expressed siRNAs, shRNAs, and chimeric VA1 shRNAs in mammalian cells. RNA. 2008, 14, 1823-33.

70. E Yague, CF Higgins and S Raguz. Complete reversal of multidrug resistance by stable expression of small interfering RNAs targeting MDR1. Gene Ther. 2004, 11, 1170–4.

71. Zhang T, Guan M, Jin HY, Lu Y. Reversal of multidrug resistance by small interfering double-stranded RNAs in ovarian cancer cells. Gynecol Oncol. 2005, 97, 501–7.

72. Xing H, Wang S. Knock-down of P-glycoprotein reverses taxol resistance in ovarian cancer multicellular spheroids. Oncol Reports. 2007, 17, 117-22.

73. Vorburger SA, Hunt KK. Adenoviral Gene Therapy. The Oncologist. 2002, 7, 46-59.

74. Hillgenberg M, Hofmann C, Stadler H, Löser P. High-Efficiency System for the Construction of Adenovirus Vectors and Its Application to the Generation of Representative Adenovirus-Based cDNA Expression Libraries. J Virol. 2006, 80, 5435-50.

75. Xu D, McCarty D, Fernandes A, Fisher M, Samulski RJ, Juliano RL. Delivery of MDR1 Small Interfering RNA by Self-Complementary Recombinant Adeno-Associated Virus Vector. Mol Ther. 2005, 11, 523-30.

76. Huaa J, Mutcha DJ, Herzog TJ. Stable suppression of MDR-1 gene using siRNA expression vector to reverse drug resistance in a human uterine sarcoma cell line. Gynecol Oncol. 2005, 98, 31-8.

CHAPTER VI

Cationic Polymer Mediated siRNA Delivery for P-glycoprotein (P-gp) Down-Regulation in Tumor Cells

[1]The Contents of this chapter have been previously published in: Abbasi M, Lavasanifar A, Berthiaume LG, Weinfeld M, Uluda**ğ** H. Cationic Polymer Mediated siRNA Delivery for P-glycoprotein (P-gp) Down-Regulation in Tumor Cells. Cancer. 2010, In Press.

INTRODUCTION

Breast cancer is among the main causes of mortality among cancer patients. An estimated 22,400 women in Canada were diagnosed with breast cancer in 2008 and ~ 5,300 women died of it [1]. Chemotherapy is still among the main treatment option for breast cancer patients, although its effectiveness can be limited by multidrug resistance (MDR) [2,3]. MDR is caused by overexpression of cell-membrane transporters, of which P-glycoprotein (P-gp) has been identified as the most common form [4]. P-gp is a member of the ABC-transporter family known for multidrug resistance in breast [5-7] and ovarian cancer cells [8-10]. P-gp acts as an ATP dependant efflux pump that excludes the therapeutic drugs out of the cellular system. Thus, in order to increase drug uptake in tumor cells with high P-gp contents, one can suppress this transporter protein to gain increased efficiency in chemotherapy. P-gp activity can be prevented by (i) blocking the binding site for the chemotherapeutic agents (i.e., chemical inhibitors), (ii) interfering with the ATP hydrolysis needed to undertake the efflux [11], and (iii) changing the of the lipid bilayer integrity [12]. Based on these avenues, several types of inhibitors and modulators of P-gp activity have been explored. First generation inhibitors were pharmacological compounds, such as calcium channel blockers (verapamil) and immunosuppressants (cyclosporine A, CyA). These drugs do not have high P-gp affinity and show high toxicity at their effective dosage. The second generation of P-gp inhibitors, such as dexverapamil and non-immunosuppressive analogues of CyA, lack obvious pharmacological activity and display higher P-gp affinities. The third generation of inhibitors, such as LY335979 and OC144093, show even higher P-gp affinities and display less toxicity [13].

Down-regulation of gene expression by RNA interference (RNAi) has been gaining momentum since its discovery in 1998 [14]. The therapeutic potential of RNAi has been quickly recognized and synthetic analogues of RNAi, namely short interfering RNAs (siRNAs), are beginning to be employed in clinical therapy. siRNA is usually a short, 21-23 nucleotide molecule which acts by binding to the RNA induced silencing complex (RISC) [15]. RISC unwinds the siRNA duplex and produces an oligonucleotide that binds to a specific sequence on target mRNA and cleaves it. The resulting dsRNA is then disposed by the cellular system [16-18]. Among the advantages of using siRNA is its reduced toxicity on non-specific tissues as compared to conventional drugs (such as P-gp inhibitors) and high degree of specificity on desired targets. It has been considered as a viable therapeutic option in cancer treatment [19-21]. The main obstacle for therapeutic use of siRNA is the lack of transport through cellular plasma membrane as well as the degrading enzymes in the cytosol and endosomal/lysosomal system. siRNA cannot cross the lipid bilayer of cells on its own and needs a carrier to deliver it across the cellular membrane. It also needs to be protected against degrading enzymes in the cytosol, and released from the cell's endosomal/lysosomal system. Successful attempts have been made by various research groups using siRNA to suppress the MDR1 gene responsible for overexpression of P-gp. Different carriers for siRNA delivery have been used for this purpose. Some success has been showed for the application of viral carriers in P-gp suppression [22], but there is concern in the application of viral carriers due to chances of uncontrolled cell proliferation of cells (oncogenicity) [23], inflammation of the target tissues [24], and cellular immune responses mounted against viruses [25].

We have shown previously that lipid-modified polymers are efficient carriers, which are able to condense nucleotides (plasmid DNA), deliver them across cellular membranes and protect them against degradation [26,27]. In this study, we explored the feasibility of this type of carriers on siRNA delivery for P-gp down-regulation by using a P-gp specific siRNA [28-31]. Our ultimate goal is to suppress transporter activity responsible for chemoresistance and to increase drug concentrations in tumor cells. The drugs that will be used in this study are breast cancer chemotherapeutic drugs doxorubicin (DOX) and paclitaxel (PTX), as they have shown to be the most potent drugs for breast cancer treatment [32-34]. The uptake of these drugs into P-gp expressing MDA435/LCC6 cells were measured and compared to the drug uptake by the control (wild type) phenotype. The drug uptake was assessed with or without siRNA inhibition and its consequences on drug toxicity were evaluated.

MATERIALS & METHODS

Materials

Poly(*L*-lysine) bromine (PLL.Br; 25,500 Da), polyethyleneimine (PEI) and anhydrous dimethylsulfoxide (DMSO) were purchased from Aldrich (Milwaukee, WI). Hanks' Balanced Salt Solution (HBSS with phenol red), trypsin/EDTA, 3-(4,5-Dimethyl-2-thiazolyl)-2,5-diphenyl-2H-tetrazolium bromide (MTT), Rhodamine, CyA and protease inhibitor cocktail were obtained from SIGMA (St. Louis, MO). Clear HBSS (phenol red free) was prepared in house. RPMI Medium 1640, penicillin (10000 U/mL), and streptomycin (10 mg/mL) were from GIBCO (Grand Island, NY). Fetal bovine serum (FBS) was from PAA Laboratories Inc (Etobicoke, ON).

The FAM-labeled Negative Control siRNA was purchased from Ambion (Austin, TX). The FITC-labeled Mouse Anti-Human P-gp was purchased from BD Biosciences Pharmingen TM (San Diego, CA). The HS-ABCB1-4-HP siRNA and the negative control siRNA were purchased from QIAGEN (Mississauga, Ontario). Doxorubicin hydrochloride was from Fluka Analytical (India). Lipofectamine^{TM} 2000 was purchased from Invitrogen (Carlsbad, CA). Wild-type MDA-435/LCC6 cells (referred as WT cells) and their MDR1 transfected phenotype (referred as MDR1 cells) were kindly provided by Dr. R Clarke from Georgetown University Medical School (Washington, DC).

Carriers Used for siRNA Delivery

The carriers used for siRNA delivery were PLL, stearic acid-substituted PLL-StA (PLL-StA), PEI, oleic acid-substituted PEI (PEI-OA) and Lipofectamine^{TM} 2000. The synthesis and characterization of stearic acid-modified PLL with the degree of substation of 10 stearic acids per PLL has been described previously by Abbasi *et al.* (27). The synthesis and characterization of oleic acid modified PEI with the degree of substitution of 4.6 oleic acids per PEI has been described by Alshamsan *et al.* [35].

P-gp Labeling and Detection

The MDR1 and WT cells were seeded in 24-well plates in 0.5 mL RPMI medium, and allowed to attach overnight. The medium was then aspirated and 0.25 mL of fresh medium

(RPMI with 10% FBS and 1% penicillin/streptomycin) was added to the cells. To label P-gp, cells were treated with 10 μL of the FITC-labeled anti-human P-gp for 30 min prior to analysis. Cells were then washed using clear HBSS, trypsinized and suspended in HBSS with 3.7% formalin. Flow cytometry was performed on a Beckman Coulter (Cell Lab Quanta) flow cytometer using the FL1 channel for P-gp detection. The instrument was calibrated so that the negative control sample (i.e., non-treated cells) gave 1-2% cells positive. The percentage of cells exhibiting P-gp and the mean fluorescence in the total cell population were determined.

MTT Assay on DOX and PTX Treated Cells

The MDR1 and WT cells were seeded in 24-well plates in 0.5 mL RPMI medium, and allowed to attach overnight. The medium was then aspirated and 0.25 mL of fresh medium (RPMI with 10% FBS and 1% penicillin/streptomycin) was added to the cells. Multiple concentrations of DOX and PTX ranging from 0.003 to19 μg/mL were incubated with the cells (in triplicate) for a period of 24 h. At the end of the incubation period, 20 μL of MTT stock solution in PBS (5 mg/mL) was added to each well. After 3 h, medium was aspirated and the precipitated formazan was dissolved in 200 μL of DMSO. Cell viability was determined by measuring the optical absorbance differences between 570 and 650 nm using an ELX 800 universal microplate reader (BIO-TEK Instruments, Inc. VT, USA). The cell viability as a percentage of control (untreated) cells was calculated by [A]test/[A]control × 100%.

DOX Uptake by Flow Cytometry

The MDR1 and WT cells were seeded in 24-well plates in 0.5 mL RPMI medium, and allowed to attach overnight. The medium was then aspirated and 0.25 mL of fresh medium (RPMI with 10% FBS and 1% penicillin/streptomycin) was added to the cells. Multiple concentrations of DOX ranging from 0.003 to19 μg/mL were incubated with the cells for a period of 24 h. After removing the DOX containing media, the cells were washed with clear HBSS, trypsinized and suspended in HBSS and 3.7% formalin. DOX uptake was quantified by a Beckman-Coulter flow cytometer (Cell Lab Quanta) using the FL-2 detection channel to assess the DOX-positive cells (~3000 events/sample). The instrument was calibrated so that the negative control sample (i.e., non-treated cells) gave 1-2% cells positive for DOX. The percentage of cells exhibiting DOX and the mean fluorescence in the total cell population were determined.

CyA Inhibition of P-gp

The MDR1 cells were grown in 24-well plates in 0.5 mL RPMI medium. The medium was then aspirated after 24 h and 0.25 mL of fresh medium (RPMI with 10% FBS and 1% penicillin/streptomycin) was added to the cells. Cells were exposed to 5 μg/mL CyA and variable DOX concentrations (0.2, 0.6 and 2 μg/mL) to detect DOX accumulation after P-gp inhibition. The cells were prepared for flow cytometry as described before, and DOX assessment was performed using the FL-2 channel to detect the percentage of cells exhibiting DOX uptake and the mean fluorescence in the total cell population.

Agarose Gel Electrophoresis

Gel electrophoresis was performed to assess (i) siRNA binding efficiency of carriers, (ii) siRNA/carrier dissociation upon incubation with heparin, and (iii) siRNA/carrier degradation by 25% serum. For binding studies, 0.05 mg/mL siRNA was incubated 0.5 mg/mL carrier in 20 μL volume for 30 min to form complexes. 4 μL of 6x diluted loading buffer was added to samples and they were run on a 1.5% agarose gel containing 1 μg/mL ethidium bromide (120 V for 30 min). The gels were visualized under UV illumination and bands corresponding to free siRNA were quantified by spot densitometer using nontreated siRNA as a control (data not shown). Percent binding was calculated as 100 × [(control siRNA – free siRNA)/control siRNA]. For the dissociation study, same concentrations as above were used for complex formation and samples were then exposed to heparin (at 0.625% final concentration). Loading buffer was added to the samples and they were run on a gel with similar conditions as above. Gels were visualized under UV illumination and detection and quantitation of free siRNA were performed by spot densitometer using nontreated siRNA as control. Percent dissociation was calculated as 100 × [free siRNA/control siRNA] (data not shown).

In the degradation study, complexes were formed with the carrier/siRNA concentration ratios of 0.05:0.5, 0.05:0.25, and 0.5:0.25 mg/mL respectively. Optimal serum concentrations and digestion times for full degradation of siRNA were determined by the preliminary studies (not shown), and these conditions (25% serum for 4 and 24 h) were used for subsequent studies. After 4 and 24 h of incubation with siRNA, EDTA (to final concentration of 0.06 mM; to stop serum action) and heparin (to final concentration of 0.625%; to dissociate complexes) were added and samples were incubated for 15 min. Samples were run on a gel with similar conditions

as above. Detection of siRNA and analysis were performed as previously explained and % siRNA recovery was calculated as 100 × [free siRNA/control siRNA].

Cellular Uptake of siRNA by Flow Cytometry

The MDR1 and WT cells were seeded in 24-well plates in 0.5 mL RPMI medium, and allowed to attach overnight. The medium was then aspirated and 0.25 mL of fresh medium (RPMI with 10% FBS and 1% penicillin/streptomycin) was added to the cells to quantitate siRNA uptake by the cells. A FAM-labeled scrambled siRNA was used for detection of siRNA by the flow cytometry. A final concentration of 0.35 μg/mL of FAM-labeled siRNA was incubated with 3.5 μg/mL of carrier in 150 mM NaCl for 30 min. The complexes were then exposed to the cells in 24-well plates (in triplicates). After 24 h, the media containing the complexes were removed, the cells were washed with clear HBSS, trypsinized and suspended in HBSS with 3.7% formalin. siRNA uptake was quantified by the Beckman-Coulter flow cytometer (Cell Lab Quanta) using FL-1 detection channel to assess the FAM-positive cells (~3000 events/sample). The instrument was calibrated so that the negative control sample (i.e., no treatment) gave 1-2% cells positive for FAM-labeled siRNA. The percentage of cells exhibiting FAM-labeled siRNA uptake and the mean fluorescence in the total cell population were determined.

Recovery of Intact siRNA from Cells

The MDR1 and WT cells were grown in 12-well plates in 0.5 mL RPMI medium to assess the recovery of intact siRNA as a function of time. The medium was then aspirated and 0.5 mL of fresh medium (RPMI with 10% FBS and 1% penicillin/streptomycin) was added to the cells. 0.35 μg/mL FAM labeled siRNA was incubated with 3.5 μg/mL carrier and 150 mM NaCl for 30 m to form complexes. The complexes were then exposed to the cells for 24 h, after which the medium was replaced with fresh medium and the cells were recovered after 4 to 72 h. At indicated time points, cells were washed using clear HBSS, trypsinized, and diluted in 40 μL lysis buffer and 10 μL of 10× diluted protease inhibitor to lyse the cell membranes and arrest any proteolytic activity. Cells were then placed on a shaker for 30 min and the solutions obtained after cell lysis were treated with heparin (0.625%) for 20 min and EDTA (0.06 mM) for 5 minutes. A total of 4 μL of 6× diluted loading buffer was added to the samples, and the samples were run on a 1.5% agarose gel (120 V for 35 min). As a reference standard, an equivalent amount of the FAM-labeled siRNA (i.e., amount equal to the total amount exposed to the cells) was run on the gel. The FAM-labeled siRNA was detected by a Fuji FLA-5000 flat-bed scanner using the LD blue laser (485 nm) and results were analyzed by spot densitometer using the non-recovered FAM-labeled siRNA as the reference standard (i.e., amount corresponding to 100% theoretical recovery).

P-gp Suppression with siRNA

The MDR1 and WT cells were seeded in 24-well plates in 0.5 mL RPMI medium, and allowed to attach overnight. The medium was then aspirated and 0.25 mL of fresh medium (RPMI with 10% FBS and 1% penicillin/streptomycin) was added to the cells to explore the effect of siRNA-mediated down-regulation. An ABCB1 siRNA specific for P-gp suppression was used for this experiment. Initially, 3.5 μg/mL PLL-StA, PEI, PEI-OA, or Lipofectamine^{TM} 2000 was incubated with 0.35, 0.7, and 1.75 μg/mL ABCB1 siRNA and 150 mM NaCl for 30 min to form complexes. The complexes were then exposed to cells for 24 and 72 h to give final concentrations of 20, 40 and 100 nM siRNA in medium. After these time points, 10 μL of the FITC-labeled anti human P-gp antibody was added to the cells and cells were incubated in room temperature for 30 min. The cells were then washed with clear HBSS, trypsinized and suspended in HBSS with 3.7% formalin. The amount of P-gp in cells was quantified by Beckman-Coulter flow cytometer (Cell Lab Quanta) using the FL-1 detection channel to count the FITC-positive cells (~3000 events/sample). The instrument was calibrated so that the negative control sample (i.e., no treatment with antibody) gave 1-2% cells positive for FITC. The percentage of cells exhibiting FITC-fluorescence and the mean fluorescence in total cell population were determined.

In a follow-up study where the effect of siRNA treatment period on P-gp down-regulation was explored, 3.5 μg/mL PLL-StA, PEI, PEI-OA, or Lipofectamine^{TM} 2000 was incubated with 0.35 μg/mL ABCB1 siRNA for 30 min to form complexes. Complexes were then added to cells either once (after 24 h), twice (after 24 and 48 h) or three times (after 24, 48 and 72 h) at a concentration of 20 nM. At indicated time points, 10 μL of the FITC labeled anti

human P-gp antibody was added to the cells, and the cells were prepared for flow cytometry for assessment of P-gp levels as described above.

DOX Uptake after siRNA Treatment

The MDR1 cells were grown in 24-well plates in 0.5 mL RPMI medium. The medium was then aspirated after 24 h and 0.25 mL of fresh medium (RPMI with 10% FBS and 1% penicillin/streptomycin) was added to the cells. The complexes were prepared with 0.35 μg/mL siRNA and 3.5 μg/mL PLL-StA, PEI, PEI-OA, and Lipofectamine™ 2000 and added to the cells for 24 or 48 h (fresh complexes prepared and added to cells after 24 h in the latter case). Cells were also treated with 0.2, 0.6 and 2 μg/mL DOX at day 2 to detect DOX uptake of cells after P-gp suppression. Analysis was performed at day 3. The flow cytometry was performed using the FL-2 channel as described previously to detect DOX uptake.

An MTT assay was also performed on the siRNA/carrier-treated, drug exposed cells. Similar to the previous experiment, cells were treated with double exposure of siRNA-carrier complexes on days 1 and 2. DOX or PTX at 0.2, 0.6 and 2 μg/mL was exposed to the cells at day 2 and the MTT assay was performed at day 3 as previously described.

Statistical Analysis

Where shown, the results are summarized as mean ± standard deviation (SD) of the indicated number of replicates. Variations between the group means were analyzed by the

Student's t-test. The significance ($p < 0.05$) of correlations between the variables was tested by calculating the Pearson product-moment correlation coefficient (r) for sample size N and relating the correlation coefficient r to t distribution by t) r/[(1 - r2)/(N - 2)]1/2.

RESULTS

Characterization of MDA435/LCC6 MDR1 and WT cells

The P-gp levels in MDR1 and WT cells were assessed after staining the cells for P-gp protein. Approximately 90% of MDR1 cells stained positive for the P-gp as compared to only ~1% WT cells **(Figure 6-1A).** A significant difference between the two cell phenotypes was also evident when the total fluorescence of the cell population was assessed, indicating a higher level of P-gp protein in MDR1 cells **(Figure 6-1B).** The sensitivity of the cells to DOX and PTX were shown in Figure 2B. After 24 h of DOX treatment, the MDR1 cells showed higher viability as compared to the WT cells. A precipitous drop in cell viability was observed at 0.3 μg/mL DOX for the WT cells, unlike the MDR1 phenotype **(Figure 6-2A).** Similar results were obtained after 72 h of DOX treatment (Figure 2B). With PTX treatment, MDR1 phenotype again showed higher viability as compared to the WT cells after 24 h of treatment, with a precipitous drop in viability at ~3 μg/mL **(Figure 6-2C)**. After 72 h of PTX treatment, WT cells displayed more cytotoxicity as compared to MDR1 cells with a precipitous drop in viability at ~3 μg/mL **(Figure 6-2D)**.

The DOX uptake by the cells was assessed as a function of DOX concentration **(Figure 6-3)**. No uptake was detected at <0.03 μg/mL DOX, after which a DOX concentration-dependent

uptake was seen in both cell types. At 0.3 μg/mL, ~20% of MDR1 cells showed uptake whereas ~80% of WT cells displayed DOX uptake. Almost all cells for both cell types displayed uptake at >0.6 μg/mL DOX **(Figure 6-3A)**. The mean fluorescence of the cell population, a representative of the amount of DOX in cells, showed a clear difference between the MDR1 and WT cells, the latter giving higher uptake at all concentrations tested **(Figure 6-3B)**. The PTX uptake could not be assessed by flow cytometry since the drug displayed no autofluorescence. The effect of classical P-gp inhibitor CyA on DOX uptake in MDA435/LCC6/MDR1 cells was also evaluated. Between 0.2 and 2 mM DOX, a drastic increase in DOX uptake was evident with the CyA treatment of the cells, based on both the percentage of cells positive for DOX **(Figure 6-3C)** or mean DOX levels in the cell population **(Figure 6-3D)**. CyA yielded almost 100% DOX positive cells where increasing DOX uptake by X-fold at the highest DOX concentration tested (2 μg/mL). The PTX uptake was not assessed by flow cytometry since the drug displayed no autofluorscence.

siRNA Complexation and Delivery

Incubating the control (scrambled) siRNA with the carriers PLL, PLL-StA, PEI, PEI-OA, and Lipofectamine^{TM} 2000 at 1:10 siRNA:carrier ratio resulted in complete siRNA complexation with no free siRNA detectable with gel electrophoresis (not shown). Incubating the complexes with excess heparin, however, resulted in complete recovery of the siRNA (not shown). The stability of the siRNA complexes in serum (25%) was analyzed by forming complexes at siRNA:carrier ratios of 1:1, 1:3, and 1:10. After 4 h incubation with serum, all carriers showed

complete protection of siRNA, except Lipofectamine^{TM} 2000 at the lowest (1:1) ratio, which showed ~70% protection **(Figure 6-4A)**. After 24 h incubation, PLL and Lipofectamine^{TM} 2000 at the lowest (1:1) ratio afforded no siRNA protection. PLL yielded complete protection at higher ratios, but Lipofectamine^{TM} 2000 afforded only 60-70% protection. All other carriers provided complete siRNA protection at all ratios **(Figure 6-4B)**.

The siRNA uptake with the PLL-StA, PEI, PEI-OA, and Lipofectamine^{TM} 2000 was investigated by flow cytometry. The siRNA uptake was evident with all carriers with no differences between WT and MDR1 cells. In both cases, the siRNA uptake reached a maximal value of 80- 100% of cells in 8 h, and remained high after 24 h. After 48 h, PEI and PEI-OA displayed maximal values while PLL-StA and Lipofectamine^{TM} 2000 showed significant decrease (~45%). The uptake after 72 h displayed a similar pattern with a slight decrease in values **(Figure 6-5A)**. The accumulation of siRNA in MDR1 and WT cells was investigated by recovering the internalized siRNA at different time points and assessing it quantitatively by gel electrophoresis. The WT and MDR1 cells showed no significant difference in siRNA recovery and the maximum amount of siRNA was recovered at 8-24 h. At these time points, PEI and PEI-OA showed the highest amount of siRNA recovery (40-45%), PLL-StA showed 30- 35% and Lipofectamine^{TM} 2000 showed 15-20% siRNA recovery. The siRNA amount was reduced significantly at 48 and 72 h, although PEI and PEI-OA showed ~20% siRNA recovery at these time points (**Figure 6-5B)**.

P-gp Suppression by siRNA

A siRNA specific for P-gp was delivered to MDR1 cells by the carriers and P-gp levels were assessed with flow cytometry. After 24 h exposure, 20 nM siRNA (1:10 siRNA:carrier ratio) delivered by Lipofectamine^{TM} 2000 showed the highest P-gp suppression (~80%). The delivery with PLL-StA (~55%), PEI (~40%) and PEI-OA (~40%) resulted in lower P-gp suppression. The 40 nM siRNA (1:5 siRNA:carrier ratio) delivery by PLL-StA, PEI, and Lipofectamine^{TM} 2000 showed 35, 25, and 20% P-gp suppression, respectively. The 100 nM siRNA (1:2 siRNA:carrier ratio) showed ~30% P-gp suppression when delivered by Lipofectamine^{TM} 2000, ~15% P-gp suppression when delivered by PLL-StA, and no reduction when delivered by PEI **(Figure 6-6A)**. After 72 h treatment, the extent of P-gp suppression was generally lower (~30% with PLL-StA, 20-35% with PEI, ~20% with Lipofectamine^{TM} 2000). PEI-OA was not effective for P-gp suppression at 40 and 100 nM siRNA (1:5 and 1:2 siRNA:carrier ratio) **(Figure 6-6B)**.

To investigate time course of P-gp suppression, the cells were treated with siRNA for 3 days with daily changes of complexes. The siRNA delivered by PLL-StA showed ~40% P-gp suppression at all times. The PEI and PEI-OA delivered siRNA showed no P-gp suppression at day 1, ~35% suppression at day 2 and 20% suppression at day 3. With

Lipofectamine^{TM} 2000, ~40% P-gp suppression was detected at days 2 and 3, but no suppression was detected at day 1 **(Figure 6-7)**.

DOX Uptake and Cytotoxicity after siRNA Delivery to Cells

The DOX uptake after P-gp suppression was assessed by flow cytometry. There was an increase in DOX uptake of the ABCB1 siRNA-treated cells as compared to the scrambled siRNA treated cells **(Figure 6-8)**. When ABCB1 siRNA was delivered by PLL-StA, 1.3 to 2.5-fold increased DOX levels were obtained when MDR1 cells were incubated with 0.2-2.0 μg/mL DOX ($p < 0.02$). No significant increase in DOX uptake was detected when the ABCB1 siRNA was delivered with PEI and PEI-OA. The Lipofectamine^{TM} 2000 delivered siRNA also effectively increased DOX uptake by ~2-fold at 0.6 and 2.0 μg/mL DOX **(Figure 6-8)**.

The cytotoxicity of DOX and PTX was subsequently assessed upon P-gp suppression. After siRNA delivery by PLL-StA, a 30% differential decrease in cell viability was detected between the ABCB1 and scrambled siRNA ($p<0.01$). The siRNA delivery with PEI was not effective in enhancing the DOX cytotoxicity. There was a ~30% decrease in cell viability when ABCB1 siRNA was delivered by Lipofectamine^{TM} 2000 and cells were exposed to 0.2 μg/mL DOX ($p<0.02$). Exposure to 0.6 μg/mL DOX concentration showed ~15% decrease in cell viability ($p<0.05$) and exposure to 2 μg/mL DOX did not show difference is cell viability for Lipofectamine^{TM} 2000 delivered siRNA **(Figure 6-9A)**. Analogous results were obtained when cells were treated with PTX; (i) PLL-StA delivered siRNA gave ~20% decrease in cell viability at the tested PTX concentrations ($p<0.04$), (ii) The PEI and PEI-OA were not effective in increasing the cytotoxicity of PTX, and (iii) Lipofectamine^{TM} 2000 displayed ~20% decrease in cell viability analogous to the PLL-StA carrier ($p<0.05$; **Figure 6-9B)**.

DISCUSSION

We have previously shown that palmitic, myristic, and stearic acid-substituted PLL are efficient carriers for plasmid DNA delivery into mammalian cells [26,27]. Biodegradability, relative compatibility with cells yielding low toxicity, and lack of genome integration (and the associated possibility of oncogenicity) makes these polymers a favorable option for therapeutic applications. The fact that a similarly high efficiency was obtained when our polymers were used for siRNA delivery opens a new possibility to use of the lipid-substituted polymeric carriers for therapeutic applications. The ever growing population of people diagnosed with breast cancer is well documented and the need for new therapeutic approaches for breast cancer is essential. Limitations of chemotherapy due to MDR are emphasized in the literature [28-31] and siRNA knockdown of P-gp is a promising option in this respect. There are other proteins involved in MDR, such as MDR-associated proteins 1 and 2 (MRP1, MRP2) [36-38], lung resistance-related protein (LRP) [39,40], and breast cancer resistance protein (BCRP) [41], but P-gp is most consistently linked to MDR in breast cancer cells [42-44], hence our focus on this therapeutic target for silencing.

Our approach towards reversing MDR was to confirm the presence of P-gp and drug resistance in the chosen cell model. Increased multidrug resistance in human tumor cells is developed through expression of MDR1 and MDR2 genes [45-47]. The MDR1 gene is overexpressed in response to drug treatment [45,48,49], but the mechanism of MDR2 expression is independent of drug treatment [46,50]. This MDR1 over-expression was clearly detected in MDA435/LCC6 cells as the flow cytometry showed >90% of the transformed cells were positive for P-gp and the level of P-gp was 7-fold increased in the MDR1 phenotype. The higher

cytotoxicity experienced with the WT cells was also another indication of the higher uptake of DOX and PTX in these cells and, conversely, the presence of multidrug resistance in the MDA435/LCC6 MDR1 cells. To further prove the presence of multidrug resistance in the MDR1 cells, DOX uptake into these cells was compared to the DOX uptake in the WT cells. A ~4-fold increase in the percentage of DOX-positive cells was detected in the WT cells compared to the MDR1 cells. Eventually, as the DOX concentration was increased, all of the MDR1 cells showed DOX uptake but the amount of uptake was ~4-fold higher in the WT cells, providing further evidence for multidrug resistance in the MDR1 cells.

All carriers were able to protect siRNA against serum degradation at 1:10 siRNA:carrier ratios, but only polymeric carriers protected the siRNA against degradation at reduced siRNA:carrier ratios (1:3 and 1:1; not shown). The weak protection afforded by the Lipofectamine^{TM} 2000 was consistent with other reports that showed superior ability of polymers to protect siRNA against serum nucleases [27,39]. The lipid modification of PLL led to higher delivery of siRNA into the cells. The PLL-StA enabled siRNA delivery to almost all cells (~90% by flow cytometry), but displayed a significant drop in siRNA levels after 48 h. This delivery pattern was similar to the delivery with Lipofectamine^{TM} 2000. The gradual decrease in siRNA levels perhaps reflects the release of siRNA in the cytosol, leading to a gradual degradation of the molecule with intracellular nucleases. Whereas up to 30% of the siRNA incubated with the cells was recovered after 8-24 h, almost no siRNA was recovered from the cells after 48 h, which provided an indication of the time frame for complete siRNA degradation in the cytosol with the PLL-StA and Lipofectamine^{TM} 2000 **(Figure 6-5)**. The PEI and PEI-OA showed a strong ability for siRNA delivery into the cells providing delivery to almost all (80-95%) cells after 48-72 h.

The fact that siRNA uptake and intracellular kinetics was similar in WT and MDR1 cells was indicative of P-gp over-expression not affecting siRNA uptake and/or efflux.

Our results showed that higher carrier:siRNA ratios were more effective in P-gp knockdown in cells. This can be due to a better intracellular delivery of siRNA (since the ς-potential of complexes will be higher) or better encapsulation of siRNA increasing its half-life inside the cytosol. This finding was consistent with the literature where higher target gene knockdown was usually observed with the application of higher carrier:siRNA ratios [51, 52]. Using lower siRNA concentrations (and higher carrier:siRNA ratios) is desired to minimize off-target and/or non-specific siRNA activity [53,54]. By delivering 20 nM siRNA 60-80% and ~60% suppression of P-gp levels was obtained with Lipofectamine^{TM} 2000 and PLL-StA, respectively, in MDR1 cells. Our long term siRNA exposure in cells did not seem to be as efficient, as only ~30% P-gp suppression was gained in the best case **(Figure 6-6B)**. This was in line with the siRNA recovery data that indicated complete intracellular degradation of siRNA after 48 h. To overcome this issue and to extend P-gp suppression for a longer period, multiple siRNA treatment of cells was used but the final outcome was not hugely improved (~40% P-gp suppression after 72 h; see **Figure 6-7**).

The ultimate goal of P-gp knockdown is to impede drug efflux and increase intracellular levels of drugs that are P-gp substrates. However, treatment of cells with siRNA complexes alone was shown to lead to autofluorescence, complicating DOX uptake assessment. This phenomenon was dependent on the carrier as well as carrier concentration, and particularly manifested by the PEI complexes. Cell treatment with complexes prepared with non-specific siRNA was necessary to account for this apparent artifact. It was evident that higher

concentrations of PEI (>1.75 µg/mL) lead to cytotoxicity and auto-fluorescence that gave false indications of DOX uptake in flow cytometry. The PLL-StA resulted in up to 2.5-fold increase in DOX-positive MDR1 cells, while siRNA delivery by PEI did not result in considerable increase in DOX-positive cells. The siRNA delivery with Lipofectamine^{TM} 2000 yielded desirable increase in DOX uptake only at the highest concentration tested **(Figure 6-8)**. The complementary cytotoxicity studies with the MTT assay showed ~35% and ~25% increase in the cytotoxicity of DOX and PTX treated cells, respectively, after siRNA delivery by PLL-StA. There was a good consistency between the carrier efficiency to suppress P-gp and drug cytotoxicities obtained. To eliminate any complication from cytotoxic drugs (which could potentially eliminate a sub-population of cells displaying high uptake), the cellular uptake of P-gp substrate Rhodamine was also explored after P-gp down-regulation, which yielded results similar to the DOX uptake studies (not shown). The CyA treated cells **(Figure 6-3D)** showed much higher elevation in DOX uptake (>10-fold) in both the percentage of cells displaying DOX uptake and absolute DOX levels as compared to the siRNA-treated cells, indicating that siRNA meditated silencing could be further enhanced. However, the non-specific toxicity associated with CyA [55] prevents its clinical application as P-gp suppressor.

Other groups have also attempted P-gp suppression for MDR reversal **(Table 5-1)**. Stierlé *et al.* showed up to 60% P-gp suppression after 48 h in MCF-7 cells using siRNA delivery by Oligofectamine^{TM}. This lead to ~20% increase in drug uptake in these cells [56]. Wu *et al.* also used siRNA delivery by Oligofectamine^{TM} in MCF-7 cells and showed up to 65% P-gp suppression after 24 h [57]. Xu *et al.* used a self-complementary recombinant Adeno-Associated Virus (scAAV) for siRNA transfection to the NCI/ADR-RES human breast cancer cells and

detected up to 100% P-gp suppression [58]. Li *et al.* showed 60- 80% P-gp suppression by using Lipofectamine^{TM} 2000 on MCF7/R cells [59]. Using co-block polymers for siRNA delivery, our previous studies yielded 50-60% P-gp suppression in the same MDA435/LCC6/MDR1 cells [60]. Finally, Zhang *et al.* showed 30-55% P-gp suppression with Oligofectamine^{TM} /siRNA delivery to various ovarian cancer cell lines [61]. Our P-gp suppression results using lipid modified polymers are comparable with the data in the literature as we were able to suppress P-gp by ~60% using PLL-StA for siRNA delivery. Lipofectamine^{TM} 2000 (a carrier similar to Oligofectamine^{TM}) showed variable results in our hands (40-80% P-gp suppression) and did not to a significant increase in drug uptake. Other research groups have also shown improvements in siRNA delivery using lipid modification of polymers. Using cholesterol modification of PEI, Kim *et al.* showed higher efficiency in siRNA delivery in PC3 cells to inhibit VEGF expression [70]. It needs to be noted that siRNA delivery by oleic acid modified PEI did not result in improvements in P-gp suppression in this study. In a previous report, we obtained effective siRNA delivery with PEI-OA [35]. Possible differences in cell types and the target gene could explain the differences between these two studies.

The inhibition of P-gp has been also attempted with conventional pharmacological agents in order to overcome MDR. Important conclusions were reached on this path; Krishna *et al.* proposed two factors for overcoming MDR: selective localization of drugs and effective blockade of P-gp in tumor cells [62]. Schinkel *et al.* stated that P-gp inhibition at tumor sites will lead to altered P-gp function in normal tissues, resulting in pharmacokinetic interactions that could cause toxicity [63,64]. Lima *et al.* have shown that flurazepam inhibited P-gp transport activity by 60%, leading to daunorubicin efflux in 80% of the cells [65]. Zhu *et al.* introduced E6

as a novel MDR inhibitor that effectively reversed MDR in rat brain microvessel endothelial cells [66]. Jiang *et al.* have shown that CyA exhibits greater MDR modulating activity than other MDR modulators in leukaemia cells *in vitro* [67]. Shin *et al.* showed that trifluoperazine (TFP) may have utility as an adjuvant in the therapy of leukemia for MDR reversal in the cancer patients [68]. Finally, Gao *et al.* showed that down-regulating transcription of MDR1 by blocking transcription activating sites can reduce the expression of MDR1 mRNA and P-gp, and thus reversing MDR of carcinoma cells [69]. The main drawback that has been reported in this approach is the lack of selective localization of anticancer drugs in tumor tissue and, consequently, unintended effects of these drugs in other cells. P-gp suppression using our cationic polymers may reduce the chances of non-specific activities if they are designed for tumor-targeting. Lipid-based carriers such as Oligofectamine^{TM} and Lipofectamine^{TM} 2000 have also shown promising results for siRNA delivery, but they are not as effective as polymers in siRNA encapsulation (as detected by our serum degradation assay), possibly reducing the half-life of siRNA in circulation due to degradation. Complete encapsulation of siRNA by polymers should increases the siRNA stability and prolong its activity. Lipid carriers also tend to show toxicity at their effective dosage. Viral carriers for siRNA are probably the most effective tools for siRNA transfection but, as previously stated, there are serious limitations for their repeated use (limited loading capacity, immunogenicity, oncogenicity, inflammation, etc.).

Our future work will focus on designing more specific siRNA sequences for P-gp suppression and applying carriers with better efficiency for more complete shutdown of P-gp expression. The use of lipid-modified PLL for delivery of gene-specific siRNAs is a novel approach for treatment of breast cancer. This will be a new contribution to the literature and as

concern increases over the use of viral carriers in gene therapy, the use of our safe polymers could just be the key to the use of gene therapy for cancer treatment.

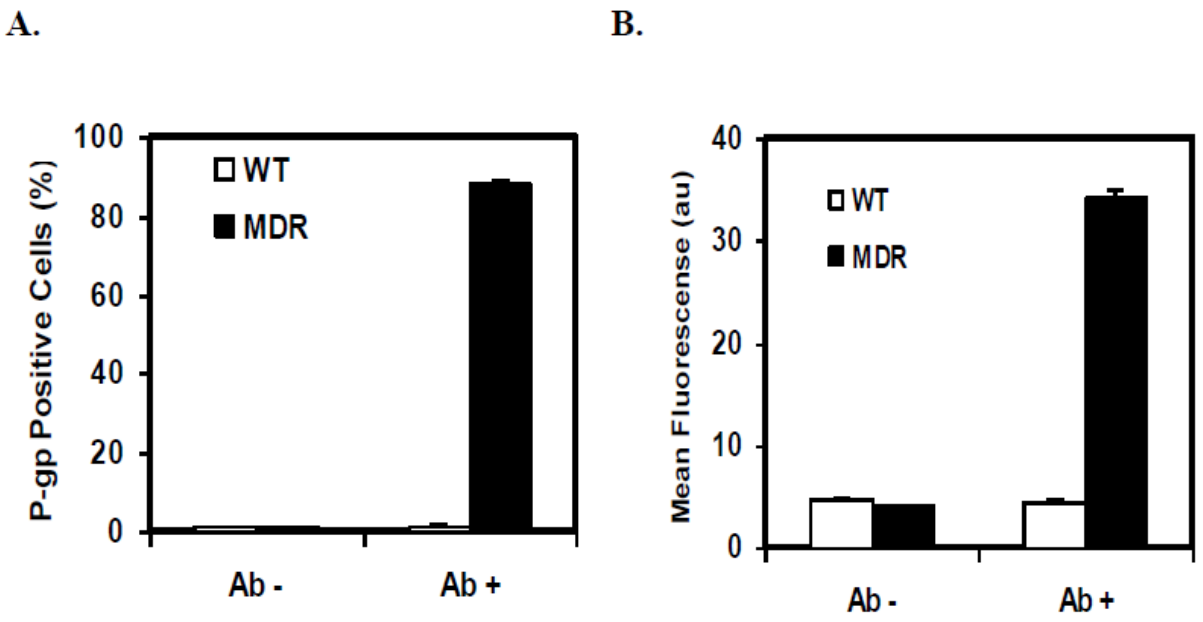

Figure 6-1. Demonstration of the presence of P-gp in the MDR cells by antibody staining of P-gp and flow cytometry. The cells treated with Ab are defined as (Ab+) and the control cells are defined as (Ab-) **(A)** ~90% of the MDA435/LCC6 MDR cells are shown to contain P-gp, compared to 1% of the control WT cells. **(B)** Mean fluorescence of the cells, an indication of P-gp population, confirmed the high population of P-gp in the MDR cells.

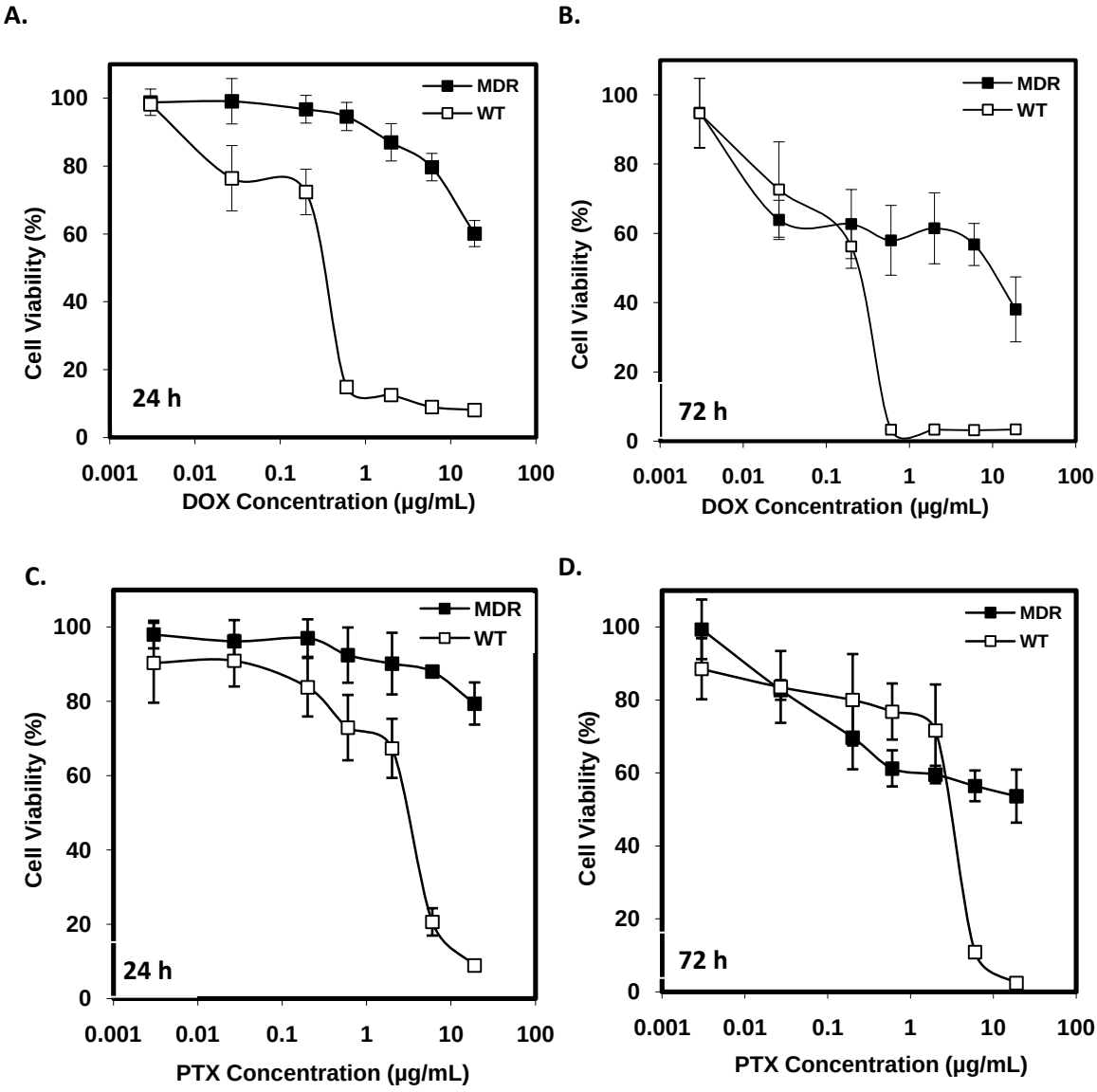

Figure 6-2. Sensitivity of MDA435/LCC6 cells to DOX and PTX. **(A)** After 24 h DOX exposure, the viability of MDR1 cells gradually decreased as DOX concentration was increased, giving ~60% cell viability with 30 µg/mL DOX, whereas the WT cells show only ~10% viability at DOX concentrations >0.3 µg/mL. **(B)** After 72 h DOX exposure, the sensitivity of the MDR1 cells to DOX was increased. Only 40% viability was detected at 30 µg/mL DOX whereas the WT cells showed the same trend as the 24 h DOX treatment. **(C)** 24 h PTX exposure did not affect viability of the MDR1 cells unlike the WT cells which displayed 10-20% viability at >3 µg/mL PTX. (D) 72 h PTX exposure gave a gradual decrease in viability of the MDR1 cells, reaching ~60% viability after at 30 µg/mL PTX. The WT cells displayed the same trend as the 24 h PTX exposure.

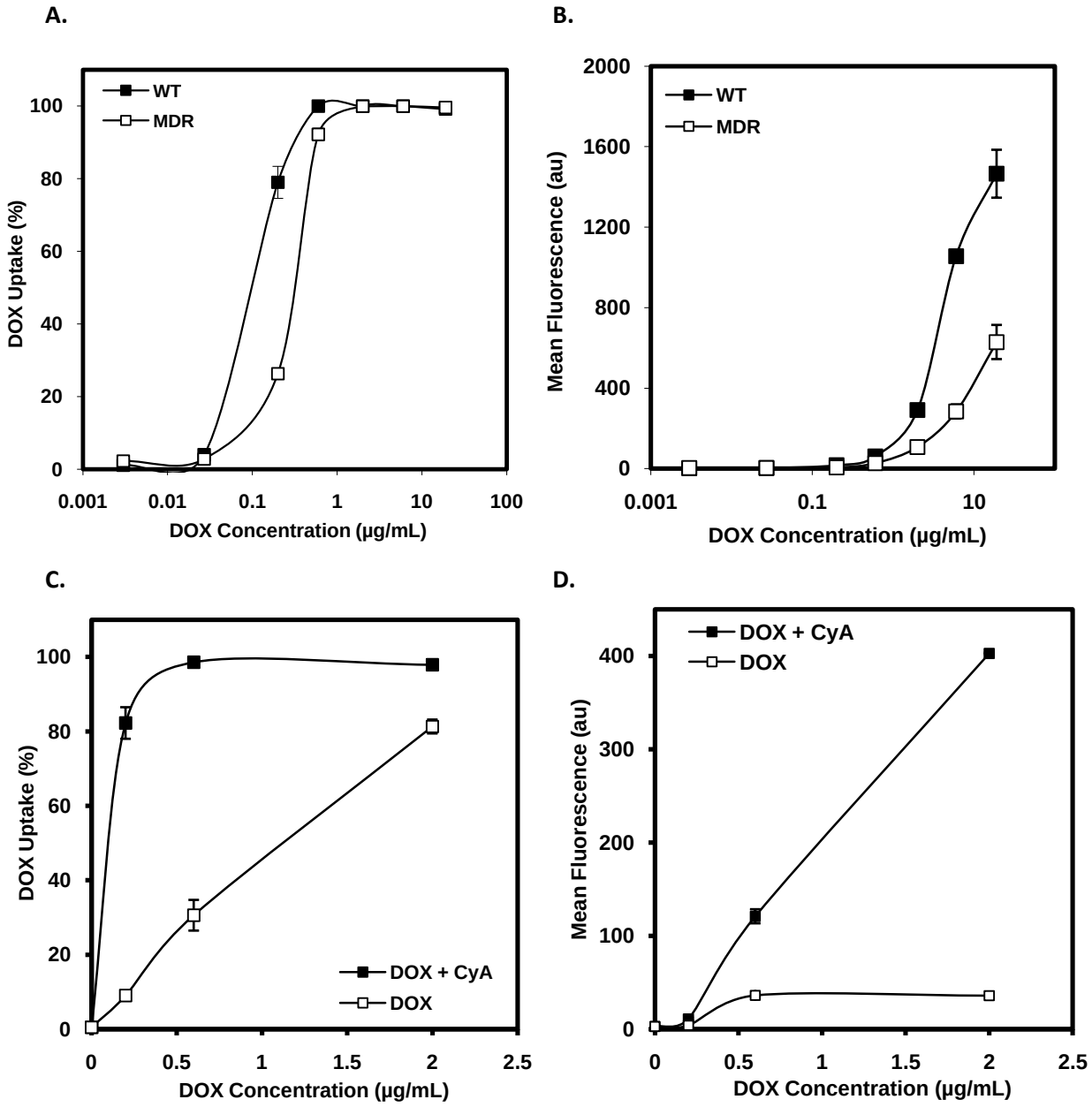

Figure 6-3. DOX uptake by MDA435/LCC6 cells. Note the significantly higher proportion of DOX-positive WT cells between 0.03 and 0.3 µg/mL DOX **(A),** and the increased mean DOX levels in WT cells in the same concentration range (**B)**. Pretreatment of the MDR1 cells with CyA increased the percentage of the DOX-positive cells **(C)** as well as the amount of DOX internalized by the cells **(D)**.

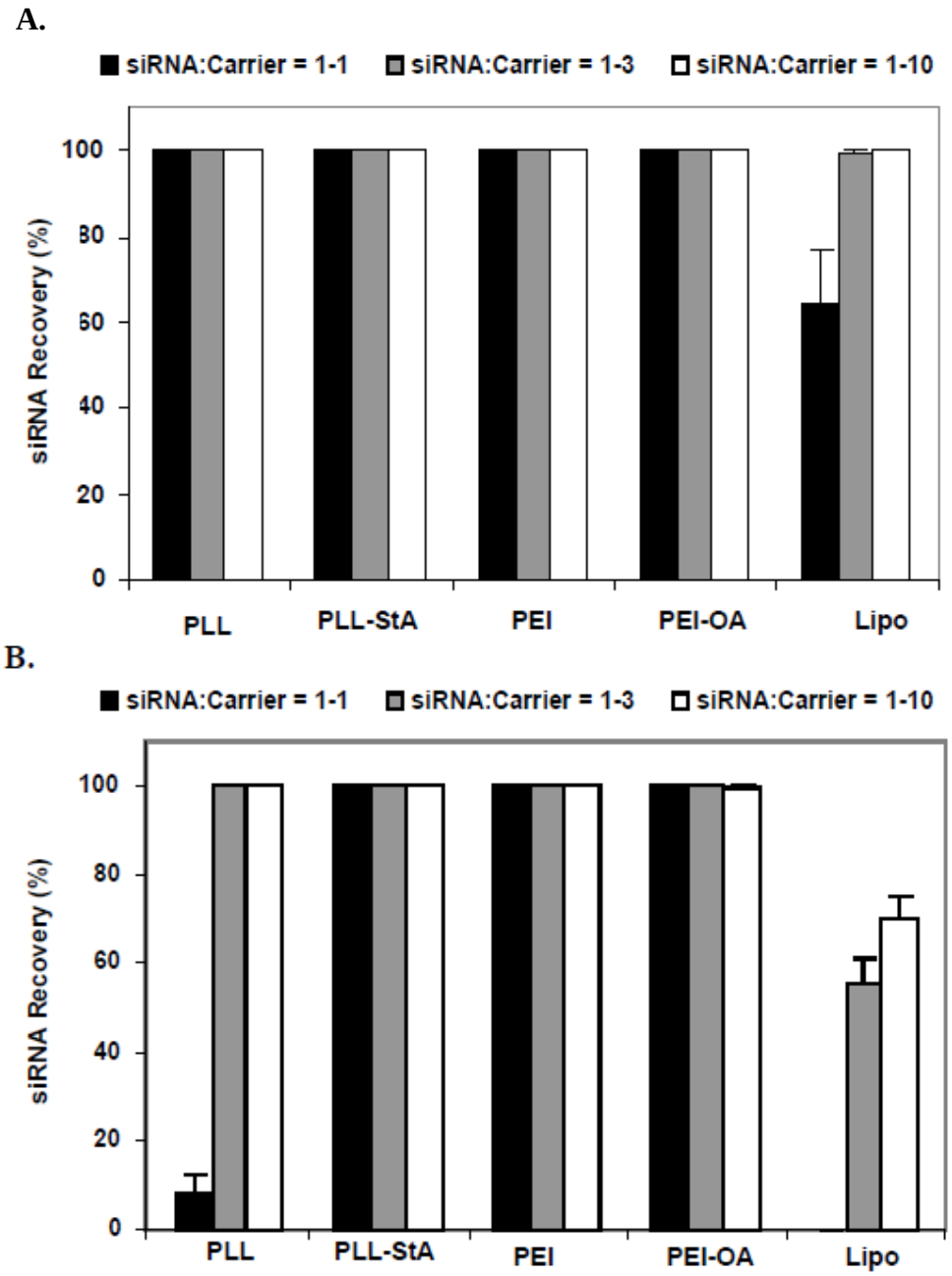

Figure 6-4. siRNA encapsulation by carriers and protection against degradation by rat serum. The tested polymers at all three concentrations showed complete protection after 4 h incubation. Lipofectamine™ 2000 showed partial siRNA protection at the 1:1 siRNA: Lipofectamine™ 2000 ratio and complete protection at the 1:3 and 1:10 ratios **(A)**. after 24 h incubation all polymers at all ratios showed complete siRNA protection, accept for PLL which shoed ~10 siRNA recovery at the 1:1 siRNA:carrier ratio. Lipofectamine™ 2000 showed no protection at the 1:1 ratio and partial protection at the 1:3 and 1:10 ratios **(B)**.

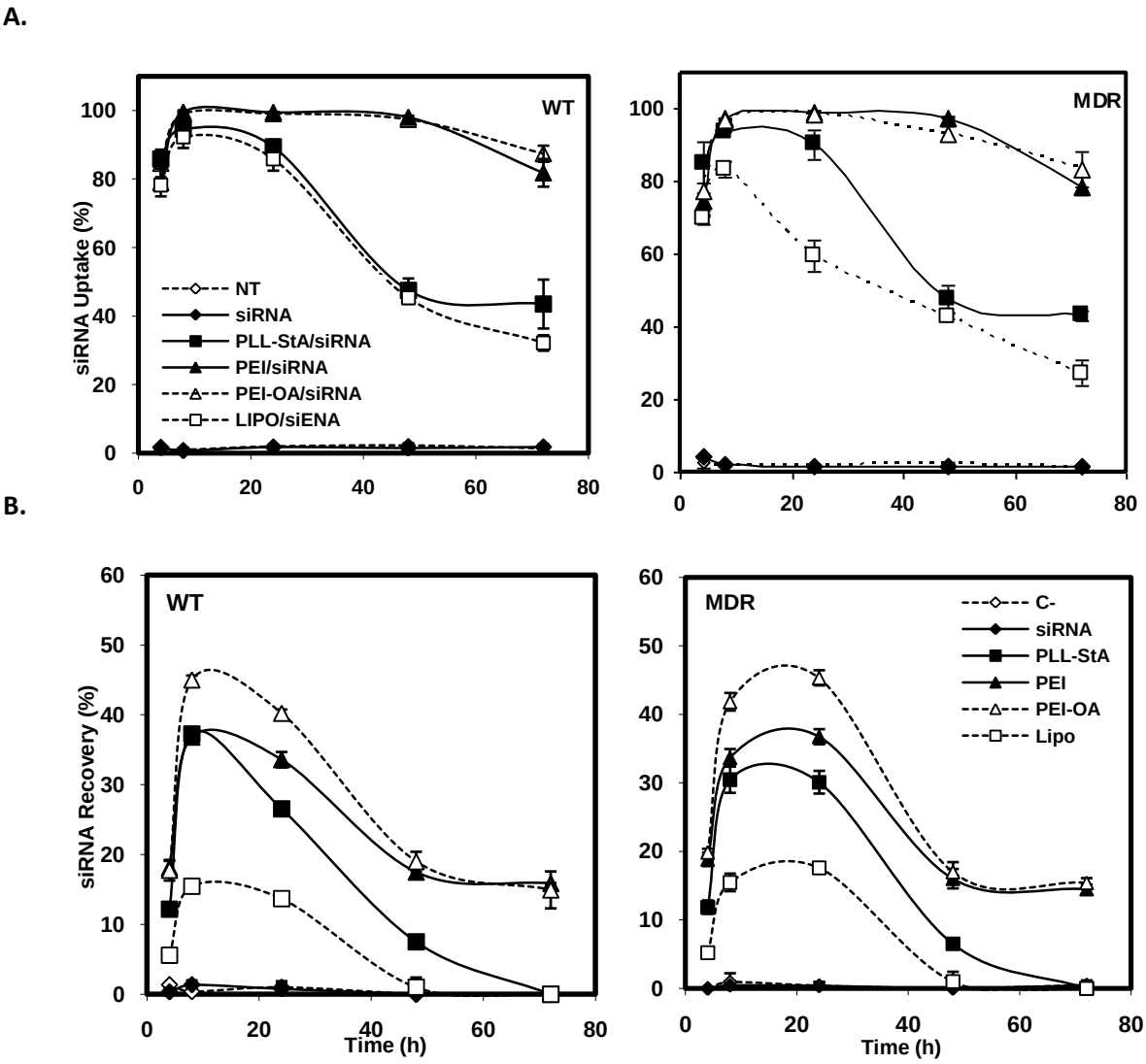

Figure 6-5. **(A)** siRNA uptake of the wild type (WT) and multidrug resistant (MDR) cells over a 72 h time course, determined by flow cytometry. No difference was detected in siRNA uptake of the WT and MDR cells. PEI and PEI-OA proved the most efficient with 80-100% uptake, whereas PLL-StA and Lipofectamine™ 2000 showed maximum efficiency at 8-24 h, after which the uptake was reduced to 40-50% at 48 and 72 h. (**B**) The siRNA recovery from WT and MDR1 cells after extracting the siRNA from the cells. Some siRNA could be recovered from the cells after 4 h, and maximal uptake was typically observed at 8-24 h. As with flow cytometry analysis, the PEI and PEI-OA gave the highest siRNA internalization (40-45% at 24 h). The cells treated with PLL-StA and Lipofectamine™ 2000 complexes showed 30-35% and ~15% siRNA recovery at the same time point. At 48 and 72 h, ~20% siRNA could be recovered from the cells treated with PEI and PEI-OA complexes.

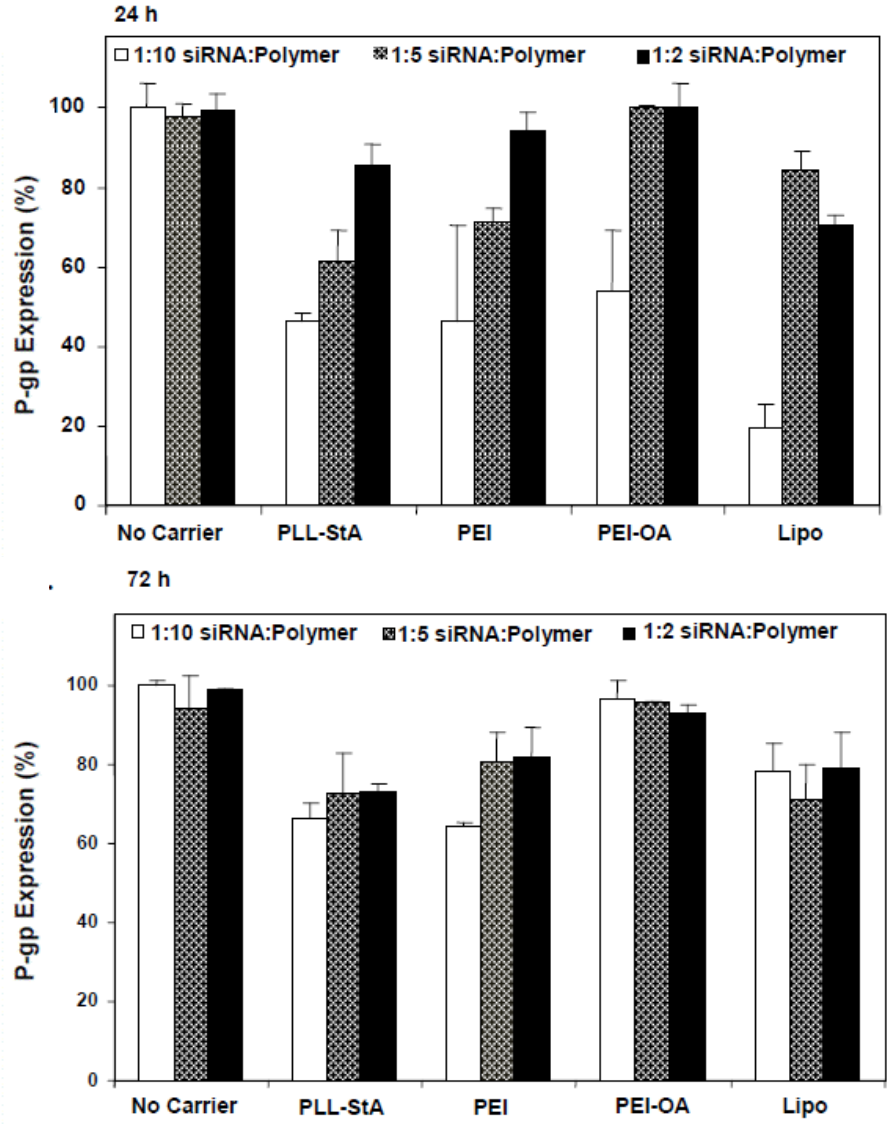

Figure 6-6. P-gp down-regulation in MDR1 cells after ABCB1-siRNA treatment. The level of P-gp was detected by flow cytometry after 24, and72 h treatment of siRNA:carrier ratios of 1:10, 1:5, and 1:10 and normalized with respect to the untreated cells. At the 24 h time point, the 1:10 ratio was shown to be the most effective ratio, down-regulating P-gp by 55% using PLL-StA, ~40-50% by PEI and PEI-OA, and 75% by Lipofectamine^{TM} 2000. The other ratios were not beneficiary fo P-gp down-regulation **(A)**. At the 72 h time point, PLL-StA was the most effective carrier, down-regulating P-gp by ~30% at all ratios. PEI was only effective at the 1:10 siRNA:carrier ratio (35%), PEI did not show any effect, and Lipofectamine^{TM} 2000 showed ~20% efficiency at all ratios **(B)**.

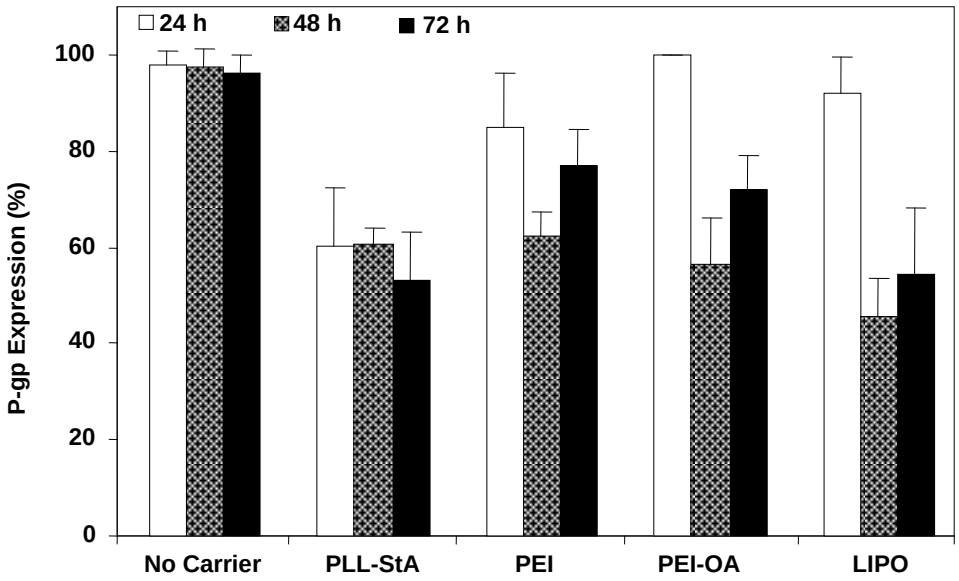

Figure 6-7. P-gp down-regulation in MDR1 cells after ABCB1-siRNA treatment. The level of P-gp was detected by flow cytometry after 24, 48 and 72 h treatment of siRNA and normalized with respect to the untreated cells. The PLL-StA/siRNA treated cells gave 40-50% P-gp down-regulation during the 72 h study period. The PEI/siRNA and PEI-OA/siRNA treated cells showed almost no Pgp down-regulation after 24 h, but displayed ~40% down-regulation after 48 h and ~20% down-regulation after 72 h. The siRNA delivered with the Lipofecatmine™ 2000 showed no P-gp down-regulation at 24 h, but ~50% and ~40% P-gp down-regulation at 48 and 72 h, respectively.

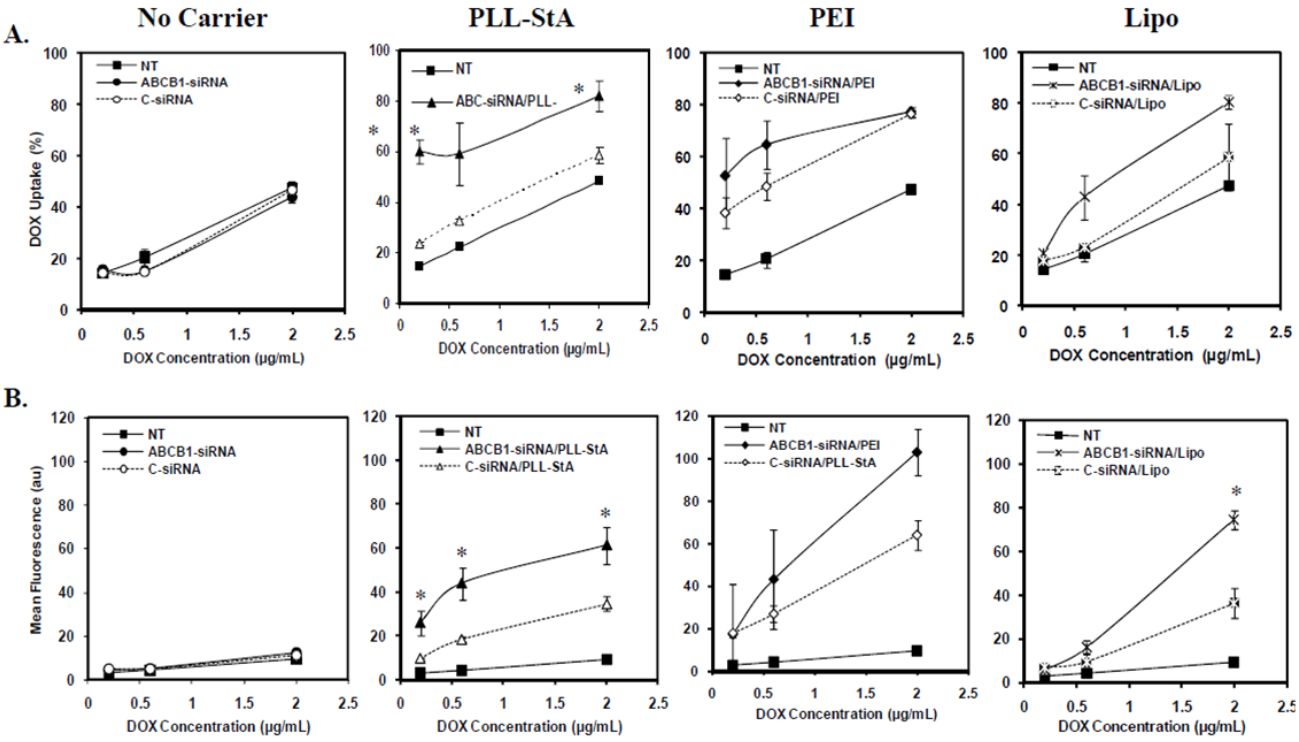

Figure 6-8. Flow cytometric analysis of DOX uptake in MDR cells treated with ABCB1 and control siRNA complexes. The results are summarized as the %DOX-positive cells (**A**) or mean DOX fluorescence per cell (**B**). In the absence of any carrier, incubating siRNA with the cells did not change the DOX uptake pattern. A clear difference between the control and ABCB1-siRNA treated cells were evident in the case of PLL-StA and Lipofectamine™ 2000, where pretreatment of cells with ABCB1 siRNA lead to a 2-3 fold increase in DOX uptake of cells. Little difference in the DOX uptake of ABCB1 vs. control siRNA treated cells in the case of PEI was detected.

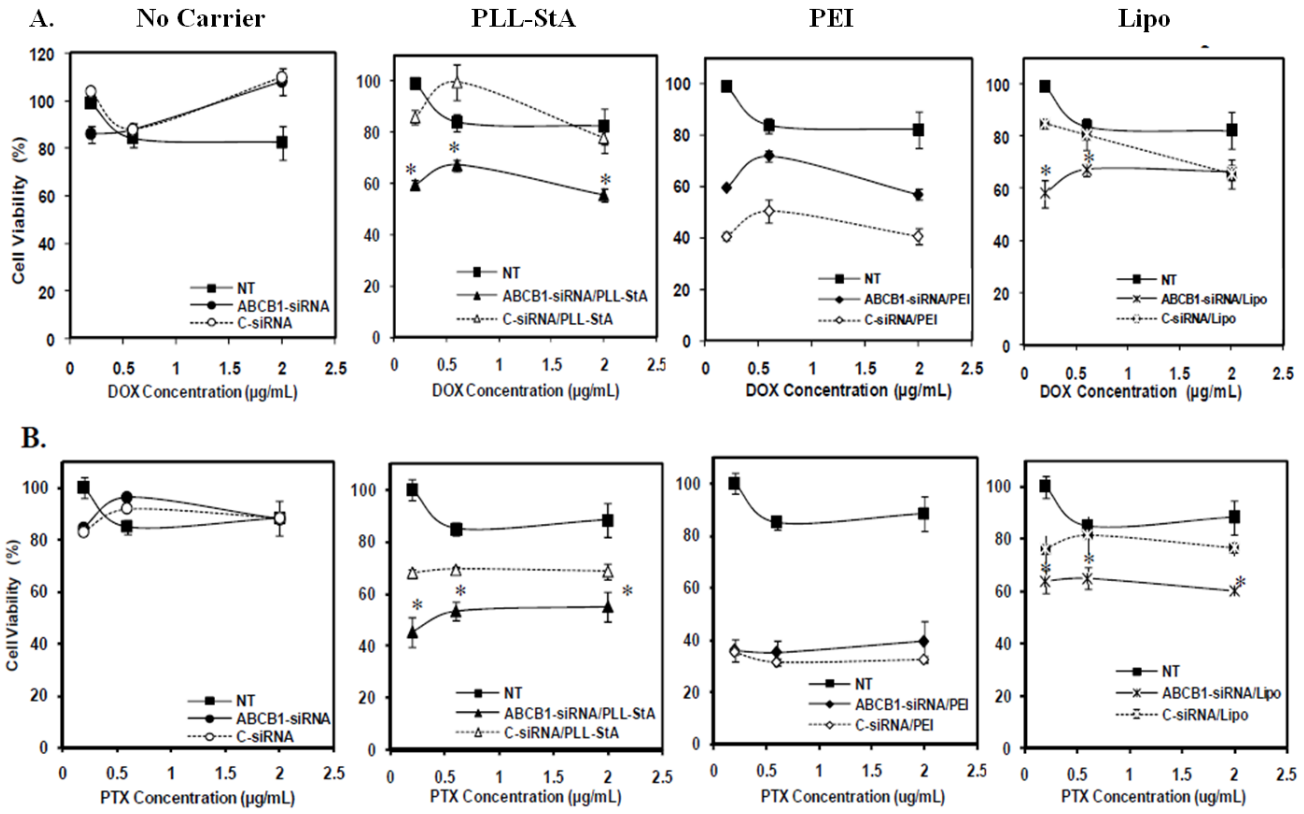

Figure 6-9. DOX and PTX cytotoxicity on MDR1 cells treated with ABCB1 siRNA-carrier complexes, scrambled siRNA (C-siRNA)-carrier complexes or no treatment (NT) as determined by the MTT assay. **(A)** For cells treated with DOX, PLL-StA showed the highest efficiency leading up to ~30% increase in cytotoxicity of the ABCB1 treated cells. PEI lead to nonspecific cytotoxicity in cells and Lipofectamine^{TM} 2000 led to 20% increase in cytotoxicity at the lowest DOX concentration. (**B**) For cells treated with PTX, PLL-StA and Lipofectamine^{TM} 2000 showed the highest efficiency leading up to ~20% increase in cytotoxicity after ABCB1-siRNA treatment. As in DOX treated cells, PEI lead to nonspecific cytotoxicity in the cells. * denotes signifince of $P<0.05$.

REFERENCES

1. Canadian Breast Cancer Foundation (http://www.cbcf.org/breastcancer).

2. American Cancer Society (http://www.cancer.org).

3. Gillet JP, Efferth T, Remacle J. Chemotherapy-induced resistance by ATP-binding cassette transporter genes. Biochim Biophys Acta. 2007, 1775, 237-62.

4. Loo TW, Clarke DM. Recent progress in understanding the mechanism of P-glycoprotein-mediated drug efflux. J Membr Biol. 2005, 206,173-85.

5. Wu H, Hait WN, Yang J-M. Small interfering RNA-induced suppression of MDR1 (P-glycoprotein) restores sensitivity to multidrug-resistant cancer cells. Cancer Res. 2003, 63, 1515–9.

6. Stierle´ V, Laigle A, Jolle`s B. Modulation of MDR1 gene expression in multidrug resistant MCF7 cells by low concentrations of small interfering RNAs. Biochem Pharmacol. 2005, 70, 1424–30.

7. Li L, Xu J, Min T, Huang W. Reversal of MDR1 gene-dependent multidrug resistance using low concentration of endonuclease-prepared small interference RNA. Eur J Pharmacol. 2006, 536, 93–7.

8. Zhang T, Guan M, Jin HY, Lu Y. Reversal of multidrug resistance by small interfering double-stranded RNAs in ovarian cancer cells. Gynecol Oncol. 2005, 97, 501–7.

9. Duan Z, Brakora KA, Seiden MV. Inhibition of ABCB1 (MDR1) and ABCB4 (MDR3) expression by small interfering RNA and reversal of paclitaxel resistance in human ovarian cancer cells. Mol Cancer Ther. 2004, 3, 833-8.

10. Xing H, Wang S, Weng D, Chen G, Yang X, Zhou J, Xu G, Lu Y, Ma D. Knock-down of P-glycoprotein reverses taxol resistance in ovarian cancer multicellular spheroids. Onc Rep. 2007, 17, 117-22.

11. Shapiro AB, Ling V. Effect of quercetin on Hoechst 33342 transport by purified and reconstituted P-glycoprotein. Biochem Pharmacol. 1997, 53, 587–96.

12. Drori S, Eytan GD, Assaraf YG. Potentiation of anticancer drug cytotoxicity by multidrug-resistance chemosensitizers involves alterations in membrane fluidity leading to increased membrane permeability. Eur J Biochem. 1995, 228, 1020–9.

13. Varma MVS, Ashokraj Y, Dey CS, Panchagnula R. P-glycoprotein inhibitors and their screening: a perspective from bioavailability enhancement. Pharmacol Res. 2003, 48, 347–59.

14. Fire A, Xu S, Montgomery MK, Kostas SA, Driver SE, Mello CC. Potent and specific genetic interference by double-stranded RNA in Caenorhabditis elegans. Nature. 1998, 391, 744-5.

15. Kawasaki H, Taira K, Morris KV. siRNA induced transcriptional gene silencing in mammalian cells. Cell Cycle. 2005, 4, 442–8.

16. Tang G. siRNA and miRNA: an insight into RISCs. Trends Biochem Sci. 2005, 106, 23-34.

17. Caplen NJ, Mousses S. Short interfering RNA (siRNA)-mediated RNA interference (RNAi) in human cells. Ann. N.Y. Acad. Sci. 2003, 1002, 56–62.

18. Schutze, N. siRNA technology. Mol. Cell. Endocrinol. 2004, 213, 115–9.

19. Sachses C, Echeverri CJ. Oncology studies using siRNA libraries: the dawn of RNAi-based genomics. Oncogene. 2004, 23, 8384–91.

20. Luo Q, Kang Q, Song WX, Luu HH, Luo X, An N, Luo J, Deng ZL, Jiang W, Yin H, Chen J, Sharff KA, Tang N, Bennett E, Haydon RC, He TC. Selection and validation of optimal siRNA target sites for RNAi-mediated gene silencing. Gene. 2007, 395, 160–9.

21. Fuchs U, Borkhardt A. The application of siRNA technology to cancer biology discovery. Adv Cancer Res. 2007, 96, 75–102.

22. Dong Xu, McCarty D, Fernandes A, Fisher M, Samulski RJ, Juliano RL. Delivery of MDR1 small interfering RNA by self-complementary recombinant adeno-associated virus vector. Mol Ther. 2005, 11, 523–30.

23. Kohn DB, Sadelain M, Glorioso JC. Occurrence of leukaemia following gene therapy of X-linked, SCID. Nat. ReV. Cancer. 2003, 3, 477–88.

24. Muruve DA. The innate immune response to adenovirus vectors. Hum Gene Ther. 2004, 15, 1157–66.

25. Zaiss AK, Muruve DA. Immune responses to adeno-associated virus vectors. Curr Gene Ther. 2005, 5, 323–31.

26. Abbasi M, Uludağ H, Incani V, Olson C, Lin X, Clements BA, Rutkowski D, Ghahary A, Weinfeld M. Palmitic acid-modified poly(*l*-lysine) for non-viral delivery of plasmid DNA to skin fibroblasts. Biomacromols. 2007, 8, 1059–63.

27. Abbasi M, Uludağ H, Incani V, Hsu CYM, Jeffery A. Further investigation of lipid-substituted poly(*l*-lysine) polymers for transfection of human skin fibroblasts. Biomacromols. 2008, 9, 1618–30.

28. Xing H, Wang S, Weng D, Chen G, Yang X, Zhou J, Xu G, Lu Y, Ma D. Knock-down of P-glycoprotein reverses taxol resistance in ovarian cancer multicellular spheroids. Oncol Rep. 2007, 17, 117-22.

29. Li L, Xu J, Min T, Huang W. Reversal of MDR1 gene-dependent multidrug resistance using low concentration of endonuclease-prepared small interference RNA. Eur J Pharmacol. 2006, 536, 93-7.

30. Stierle V, Laigle A, Jolles B. Modulation of MDR1 gene expression in multidrug resistant MCF7 cells by low concentrations of small interfering RNAs. Biochem Pharmacol. 2005, 70, 1424-30.

31. Westermarck J, Kahari VM. FASEB J. Regulation of matrix metalloproteinase expression in tumor invasion. 1999, 13, 781-92.

32. Biganzoli L, Cufer T, Bruning P, Coleman RE, Duchateau L, Rapoport B, Nooij M, Delhaye F, Miles D, Sulkes A, Hamilton A, Piccart M. Doxorubicin-paclitaxel: A safe regimen in

terms of cardiac toxicity in metastatic breast carcinoma patients. Results from a European organization for reasearch and treatment of cancer multicenter trial. Cancer. 2003, 97, 40-5.

33. Gehl J, Boesgaard M, Paaske T, Vittrup Jensen B, Dombernowsky P. Combined doxorubicin and paclitaxel in advanced breast cancer: effective and cardiotoxic. Annals Oncol. 1996, 7, 687-93.

34. Ludwig H. Doxorubicin and paclitaxel improve survival compared with fluorouracil, doxorubicin and cyclophosphamide for women with metastatic breast cancer. 2001, 2, 202-4.

35. Alshamsan A, Haddadi A, Incani V, Samuel J, Lavasanifar A, Uludag H. Formulation and delivery of siRNA by oleic acid and stearic acid modified polyethyleneimine. Mol Pharmaceutics. 2009, 6, 121-33.

36. Burger H, Foekens JA, Look MP, Meijer-van Gelder ME, Klijn JG, Wiemer EA, Stoter G, Nooter K. RNA Expression of Breast Cancer Resistance Protein, Lung Resistance-related Protein, Multidrug Resistance-associated Proteins 1 and 2, and Multidrug Resistance Gene 1 in Breast Cancer: Correlation with Chemotherapeutic Response. Clin Cancer Res. 2003, 9, 827–36.

37. Borst P, Evers R, Kool M, Wijnholds J. A family of drug transporters: the mutidrug-resistance-associated proteins. J Natl Cancer Inst. 2000, 92, 1295–302.

38. Cole SP, Bhardwaj G, Gerlach JH, Mackie JE, Grant CE, Almquist KC, Stewart AJ, Kurz EU, Duncan AM, Deeley RG. Overexpression of a transporter gene in a multidrug-resistant human lung cancer cell line. Science. 1992, 258, 1650–54.

39. Dalton WS, Scheper RJ. Lung resistance-related protein: determining its role in multidrug resistance. J Natl Cancer Inst. 1999, 91, 1604–5.

40. Scheffer GL, Schroeijers AB, Izquierdo MA, Wiemer EA, Scheper RJ. Lung resistance-related protein/major vault protein and vaults in multidrug-resistant cancer. Curr Opin Oncol. 2000, 12, 550–556.

41. Doyle LA, Yang W, Abruzzo LV, Krogmann T, Gao Y, Rishi AK, Ross DD. A multidrug resistance transporter from human MCF-7 breast cancer cells. Proc Natl Acad Sci USA. 1998, 95, 15665–70.

42. Gottesman MM. Mechanisms of cancer drug resistance. Annu Rev Med. 2002, 53, 615–27.

43. Bradley G, Ling VP. P-glycoprotein, multidrug resistance and tumor progression. Cancer Metast Rev. 1994, 13, 223–33.

44. Gottesman MM, Fojo T, Bates SE. Multidrug resistance in cancer: role of ATP-dependent transporters. Nat Rev Cancer. 2001, 2, 48–58.

45. Devault A, Gros P. Two members of the mouse mdr gene family confer multidrug resistance with overlapping hut distinct drug specificities. Mol Cell Biol. 1990, 10, 1652-63.

46. Gros P, Raymond M, Bell J, Housman D. Cloning and characterization of a second member of the mouse mdr gene family. Mol Cell Biol. 1988, 8, 2770-78.

47. Hsu SI, Cohen D, Kirschner LS, Lothstein L, Hanstein M, Horwitz SB. Structural analysis of the mouse marla (P-glycoprotein) promoter reveals the basis for differential transcript heterogeneity in multidrug-resistant J774.2 cells. Mol Cell Biol. 1990, 10, 3596-606.

48. Gros P, Ben Neriah. Y, Croop JM, Housman. DE. Isolation and expression of a complementary DNA that confers multidrug resistance. Nature. 1986, 323, 728-31.

49. Ueda K, Cardarelli C, Gottesman MM, Pastan I. Expression of a full-length cDNA clone for the human MDR1 gene confers resistance to colchicines, doxorubicin and vinblastine. Proc Nail Acad Sci. USA. 1987, 84, 3004-8.

50. Schinkel AH, Roelofs MEM, Borst P. Characterization of the human MDR3 P-glycoprotein and its recognition by P-glycoprotein specific monoclonal antibodies. Cancer Res. 1991, SI, 2628-35.

51. Leng Q, Scaria P, Zhu J, Ambulos N, Campbell PA, Mixson J. Highly branched HK peptides are effective carriers of siRNA. J Gene Med. 2005, 7, 977–86.

52. Duan Y, Guan X, Ge J, Quan D, Zhuo Y, Ye H, Shao T. Cationic nano-copolymers mediated IKKβ targeting siRNA inhibit the proliferation of human Tenon's capsule fibroblasts *in vitro*. Mol Vis. 2008, 14, 2616-28.

53. Persengiev SP, Zhu X, Green M. Nonspecific, concentration-dependent stimulation and repression of mammalian gene expression by small interfering RNAs (siRNAs). RNA. 2004, 10, 12-18.

54. Scacheri PC, Rozenblatt-Rosen O, Caplen NJ, Wolfsberg TG, Umayam L, Lee JC, Hughes CM, Shanmugam KS, Bhattacharjee A, Meyerson M, Collins FS. Short interfering RNAs can induce unexpected and divergent changes in the levels of untargeted proteins in mammalian cells. Proc Natl Acad Sci. 2004, 101,1892–97.

55. Kabasakal L, Halaĉ M, Nisli C, Oguz O, Onsel C, Civi G, Uslu I. The effect of P-glycoprotein function inhibition with cyclosporine A on the biodistribution of Tc-99m sestamibi. Clin Nucl Med. 2000, 25, 20-3.

56. Stierlé V, Laigle A, Jollès B. Modulation of MDR1 gene expression in multidrug resistant MCF7 cells by low concentrations of small interfering RNAs. Biochem Pharmacol. 2005, 70, 1424–30.

57. Wu H, Hait WN, Yang J-M. Small interfering RNA-induced suppression of MDR1 (P-glycoprotein) restores sensitivity to multidrug-resistant cancer cells. Cancer Res. 2003, 63, 1515–19.

58. Xu D, McCarty D, Fernandes A, Fisher M, Samulski RJ, Juliano RL. Delivery of MDR1 small interfering RNA by self complementary recombinant adeno-associated virus vector. Mol Ther. 2005, 11, 2005.

59. Li L, Xu J, Min T, Huang W. Reversal of MDR1 gene-dependent multidrug resistance using low concentration of endonuclease-prepared small interference RNA. Euro J of Pharm. 2006, 536, 93-97.

60. Xiong XB, Uludağ H, Lavasanifar A. Biodegradable amphiphilic poly(ethylene oxide)-block-polyesters with grafted polyamines as supramolecular nanocarriers for efficient siRNA delivery. Biomat. 2009, 2, 242-53.

61. Zhang T, Guan M, Yan Jin H, Lu Y. Reversal of multidrug resistance by small interfering double-stranded RNAs in ovarian cancer cells. Gynecol Oncol. 2005, 97, 501-7.

62. Krishna R, Mayer LD. The use of liposomal anticancer agents to determine the roles of drug pharmacodistribution and P-glycoprotein (PGP) blockade in overcoming multidrug resistance (MDR). Anticancer Res. 1999, 19, 2885-91.

63. Schinkel AH, Mol CA, Wagenaar E, van Deemter L, Smit JJ, Borst P. Multidrug resistance and the role of P-glycoprotein knockout mice. Eur J Cancer. 1995, 31, 1295-8.

64. Schinkel AH. Pharmacological insights from P-glycoprotein knockout mice. Int J Clin Pharmacol & Ther. 1998, 36, 9-13.

65. Lima, SAC, Tavares J, Gameiro P, de Castro B, Cordeiro-da-Silva A. Euro J of Pharmacol. 2008, 581, 30-6.

66. Zhu, H-J, Wang JS, Guo, Q-L, Jiang Y, Liu G-Q. Reversal of P-glycoprotein mediated multidrug resistance in K562 cell line by a novel calmodulin inhibitor, E6. Bio & Pharma Bulletin. 2005, 28, 1974-8.

67. Jiang XR, Kelsey SM, Wu YL, Newland AC. Circumvention of P-glycoprotein-mediated drug resistance in human leukaemic cells by non-immunosuppressive cyclosporin D analogue, SDZ PSC 833. Brit J Haematol. 1995, 90, 375-83.

68. Shin S Y, Choi BH, Kim JR, Kim J-H, Lee YH. Reversal of multidrug resistance by synthetic and natural compounds in drug-resistant MCF-7 cell lines. Euro J Pharma Sci. 2006, 28, 300-6.

69. Gao, P, Zhou G-y, Yin G, Wang Z-f, Liu W-j, Lin X-y. Reversal of multidrug resistance property of carcinoma cells by down-regulating transcription of mdr-1. Chinese J Pathol. 2003, 32, 563-6.

70. Kim WJ, Chang C-W, Lee M, Kim SW. Efficient siRNA delivery using water soluble lipopolymer for anti-angiogenic gene therapy. J Con Rel. 2007, 118, 357–63.

CHAPTER VII

Cationic Polymer Mediated siRNA Delivery for P-glycoprotein (P-gp) Down-Regulation in NOD-SCID Mice Tumor Models

INTRODUCTION

Multidrug resistance (MDR) of tumor cells to hydrophobic drugs is among the major factors limiting the efficiency of chemotherapy in various types of cancers [1]. MDR is defined as simultaneous resistance to different drugs with different targets and chemical structures [2]. MDR is consistently detected in tissues undergoing chemotherapy [3,4]. The MDR arises from elevated presence of ATP cassette transporter (ABC) proteins on cell surfaces that act as an ATP dependent efflux pump. The expression of the efflux pumps is up-regulated in tumor cells undergoing chemotherapy [5], resulting in increased efflux of hydrophobic chemotherapeutic drugs out of the cells. Among these transporters, P-gp is believed to be the most common protein causing MDR [6,7]. P-gp is normally present at the apical surface of epithelium lining the colon, small intestine, bile ductules and kidney peroximal tubules where it secretes xenobiotics and metabolites into bile, urine and the lumen of gastrointestinal tracks. It is also present in the endothelial cells of the blood-brain barrier, blood-testis barrier and the blood-ear barrier, where it protects these sensitive organs from toxic xenobiotics [8]. The abundance of P-gp and its ability to recognize a wide range of drugs as a substrate make it extremely difficult to modulate this transporter protein and impede its transport function. Chemical P-gp inhibitors have been the choice for this purpose for more than 30 years; however they produce undesirable off target activities, leading to unacceptable toxicities [9,10].

Small interfering RNAs (siRNAs) have the potential to suppress the expression of any specific gene at the RNA level, and prevent expression of proteins that lead to mortal diseases such as cancer [11], severe immunodeficiency (SID) [12], and multiple sclerosis [13]. To efficiently serve this purpose in cancer therapy, specific siRNA sequences need to be delivered

against 'aberrant' mRNA molecules of tumor cells, facilitate the degradation of the targeted mRNA, and result in sustained suppression of undesired gene(s). *In vitro* suppression of P-gp using various siRNA delivery and siRNA expression systems have been relatively successful [14-19] and, in some cases (i.e., under selection pressures), complete knockdown of target genes have been feasible [20,21]. However translation of these results to clinical studies has been challenging, as certain additional limitations exist in *in vivo* siRNA delivery. Systemic delivery of siRNA can lead to undesired side effects, caused by non-specific siRNA activity on mRNA sequences with partial complementary sequences [22]. Intratumural injection, on the other hand, could limit the diffusion of the injected siRNA into non-specific sites and is therefore beneficial for apical tumors [23]. Another limitation of *in vivo* siRNA delivery includes rapid siRNA degradation in the physiological milieu [24]. Chemical modification of siRNA has been used by research groups to increase siRNA half-life *in vivo* [25]. Encapsulation of siRNA by liposomes and polymeric micelles provides protection for the siRNA against rapid degradation and increases the circulation life of siRNA *in vivo*.

Viral carriers including retrovirus, adenovirus, and adeno-associated virus (AAV) have been previously used for siRNA expression and P-gp down-regulation [19-21]. These studies, however, have been limited to *in vitro* cell systems as certain drawbacks are associated with the *in vivo* application of viruses. They are difficult to produce and can carry limited amounts of DNA, and have the potential to give rise to uncontrolled proliferation of modified cells [26]. Adenoviruses can trigger inflammatory and/or immunological reaction against modified cells [27,28], and retroviruses can potentially activate oncogenes leading to cancer [29]. Non-viral delivery systems that have been previously used for P-gp down-regulation consist of lipid-based

carriers such as Lipofectamine™ 2000, Oligofectamine™, and liposomes [14-18]. Despite the partial success of their application *in vitro,* the *in vivo* use of lipid-based carriers has been questioned due to considerable side effects. Acute inflammatory reactions have been reported in animals treated with intravenous injection of lipoplexes [30]. Significant toxicity has also been associated with lipid mediated gene delivery [31,32]. Therefore, these carriers have been limited to *in vitro* studies thus far.

An alternative non-viral carrier for siRNA delivery is polymeric carriers. These carriers posses a strong positive charge and thus are able to form tight complexes with the negatively charged siRNAs via electrostatic interactions. This interaction can effectively formulate siRNA molecules into nanosize particles, which facilitate the intracellular uptake of siRNA. A major benefit of using polymers is that they can be engineered to increase biocompatibility and to minimize host immune reactions. A drawback of these carriers is their low effectiveness, which will hamper their utility in a clinical setting. In a previous report, we described an efficient siRNA carrier, engineered by grafting stearic acids on poly-*L*-lysine (PLL-StA), for effective siRNA encapsulation, protection, and delivery into the drug resistance MDA435/LCC6 MDR1 melanoma cells [33]. We showed that ~55% P-gp down-regulation was feasible by using this carrier and that effective drug concentrations could be increased intracellularly as a result of P-gp down-regulation, resulting in better efficacy in drug action. However similar to other P-gp knockdown approaches, this study was limited to *in vitro* observations and it was not known whether the proposed approach could be applied to a tumor model *in vivo*. In the current study, we investigated the intracellular fate of siRNA and used the developed PLL-StA to deliver a combination of three siRNAs specific for P-gp knockdown. A commonly used cationic carrier,

namely branched 25 kDa PEI, was additionally utilized as a reference carrier, since this polymer was previously employed for siRNA delivery in studies by Liu *et al*. [34] and Alshamsan *et al*. [35]. An *in vivo* tumor model derived from P-gp over-expressing cells was employed to assess P-gp down-regulation in NOD-SCID mice.

METHODS

Materials

Poly-*L*-lysine (PLL; 25,500 Da), polyethyleneimine (PEI; branched, 25,000 Da) and anhydrous dimethylsulfoxide (DMSO) were purchased from Aldrich (Milwaukee, WI). Hanks' Balanced Salt Solution (HBSS) and trypsin/EDTA, and Heparin Sulfate were obtained from Sigma (St. Louis, MO). Clear HBSS (phenol red free) was prepared in house. RPMI 1640 medium, penicillin (10000 U/mL), and streptomycin (10 mg/mL) were from Gibco Invitrogen (Burlington, ON). Fetal bovine serum (FBS) was from VWR International (Mississauga, ON). The FAM-labeled negative control siRNA was purchased from Gene Pharma Co. LTD (Shanghai, China). The FITC-labeled mouse anti-human P-gp antibody was purchased from BD Biosciences Pharmingen™ (San Diego, CA). An ABCB1-siRNA against P-gp (designated as siRNA 1; Cat No: SI00018732) and a nonspecific (control) siRNA were purchased from QIAGEN (Mississauga, Ontario). The ABCB1-siRNAs, siRNA 2 and siRNA 3 were custom synthesized by Integrated DNA Technologies Canada (Toronto, ON). The Pegylated liposomal doxorubicin (DOX) hydrochloride (Doxil®) was from Schering-Plough Canada Inc. Wild-type MDA-435/LCC6 cells (referred to as WT cells) and their MDR1 transfected phenotype (referred

as MDR1 cells) were kindly provided by Dr. R. Clarke (Georgetown University Medical School, Washington, DC). A lysis buffer was prepared by mixing 0.1% Tween in 50 mM Tris-Cl and 150 mM NaCl. The Shandon Cryomatrix™ used for histological embedding was purchased from Thermo Scientific (Pittsburgh, PA).

Cells Culture and Tumor Model

MDA-435/LCC6 MDR1 melanoma cells were grown and propagated in RPMI medium supplemented with 10% FBS and 1% penicillin-streptomycin at 37 ºC. Cells were grown and expanded in 75 mL flasks. To harvest cells, cells were washed with HBSS, and trypsinization was performed with 2 mL of trypsin per flask. Cells counts were performed by hemocytometer. Female SCID mice were purchased from the Jackson Laboratory (Bar Harbor, ME, USA). All experiments were performed in accordance with the University of Alberta guidelines for the care and use of laboratory animals. All experiments were performed using 4–6 week old female mice. For tumor formation, ~2 million MDA-435/LCC6 WT or MDR1 cells were injected into the right flank of the mice. After 3 weeks, at tumor size of ~150 mm^3, intratumoral injection of siRNA and/or tail vein injection of Doxil® was performed (see below for details).

siRNA Carrier Sequences and Carriers

Three siRNA sequences specific for P-gp down-regulation were used in this study:

siRNA 1; sense: 5'-CAGAAAGCUUAGUACCAAAdTdT,

antisense: UUUGGUACUAAGCUUUCUGTC-3'.

siRNA 2; sense: 5'-GUAUUGACAGCUAUUCGAAGAGUG,
antisense: CCACUCUUCGAAUAGCUGUCAAUAC-3'.

siRNA 3; sense: 5' GAAACCAACUGUCAGUGUA,
antisense: UACACUGACAGUUGGUUUC-3'.

The carriers used for siRNA delivery were PLL, PLL-StA and PEI. The synthesis and characterization of the PLL-StA (degree of substitution: ~10 stearic acids per PLL) have been described previously by Abbasi *et al.* [36].

Cellular Uptake of Complexes by Confocal Microscopy

The MDA-435/LCC6 MDR1 cells were seeded on glass cover glasses in 12-well plates. Twenty four hours later, the cells were treated with FAM-labeled or non-labeled siRNA, combined PLL-StA and PEI. After 1, 4, 8, 24, 72 and 144 hours, the cells were fixed, and the cell nuclei were stained with 300 ng/mL Hoechst 33258 for 30 min. A Leica TCS-SP2 multiphoton confocal laser scanning microscope (TCS-MP) was used to detect cell-associated FAM-siRNA.

***In Vitro* P-gp Down-Regulation with siRNA**

MDA-435/LCC6 MDR1 cells in 24-well plates (with 0.25 mL of medium) were incubated with the chosen siRNAs specific for P-gp down-regulation either alone or in combination (see **Legends**). A final concentration of 0.35 μg/mL of siRNA was incubated with 3.5 μg/mL of carrier in 150 mM NaCl to form complexes for 30 min. Complexes were then added to cells in triplicates either once (after 24 h), twice (after 24 and 48 h) or three times (after

24, 48 and 72 h) at a concentration of 20 nM siRNA (0.35 mg/ml). At indicated time points, 10 μL of the FITC-labeled anti human P-gp antibody was added to the cells. The cells were then washed with clear HBSS, trypsinized and suspended in HBSS with 3.7% formalin. The amount of P-gp in cells was quantified by Beckman-Coulter flow cytometer (Cell Lab Quanta) using the FL-1 detection channel to detect the mean fluorescence of the cells (~5000 events/sample). The mean fluoresence of the FL1 population (an indicative of the amount of P-gp in all cells) was normalized against the mean fluorescence of the no siRNA treated cells and used as % P-gp expression.

In Vivo Tumor Cell Uptake of siRNA

Upon tumor formation in SCID mice, intratumor injections of siRNA with and without polymers was performed. 6.5 μg of FAM-labeled siRNA with or without 32 μg of polymer was injected intratumorly at a final volume of 40 μL into the tumors formed at the right flank of SCID mice. As a control, unlabeled scrambled siRNA (C-siRNA) and its polymeric complexes were injected in order to account for any autofluorescence that might be induced as a result of injection *per se*. After 24 h, the mice were euthanized by CO_2 aphyxsiation, and the tumors were surgically excised. Half of the tumor was initially used to assess the siRNA uptake of tumor cells by using fluorescence microscopy. Briefly, tumors were extracted, cut in half and one-half is preserved in Shandon Cryomatrix^{TM} and frozen. Sectioning of the tumor was performed by a Leica CM-3050-S Cryostat and stained by DAPI for nuclear staining. The FAM-siRNA uptake of cells was assessed using a FSX 100 Olympus fluorescent microscope.

The other half of the tumor was used to assess quantitative siRNA uptake by flow cytometry and gel electrophoresis. For flow cytometry, approximately one-quarter of the extracted tumors were homogenized by a Pyrex$^{(R)}$ Tissue Grinder, filtered through a 35-µm mesh and suspended in 3.7% formalin in HBSS. The cells displaying FAM-labeled siRNA uptake was determined by a Beckman-Coulter flow cytometer (Cell Lab Quanta) using the FL-1 detection channel to assess the FAM-siRNA-positive cells (~10000 events/sample). The instrument was calibrated so that the negative control sample (i.e., non-treated cells) gave 1-2% cells positive for FAM-siRNA.

Finally, the siRNA uptake was determined by recovering the siRNA from MDA-435/LCC6 MDR1 tumors and assessing its integrity by gel electrophoresis. For this, the cells extracted from one quarter of the tumors were washed with HBSS, centrifuged and the cell pellets were lyzed with 40 µL lysis buffer. Cells were then placed on a shaker for 30 min and the solutions obtained after cell lysis were treated with heparin (0.625%) for 20 min. Four µL of 6× diluted loading buffer was added to the samples, and the samples were run on a 1.5% agarose gel (120 V for 35 min). As a reference standard, an equivalent amount of the FAM-labeled siRNA (i.e., amount equal to the total amount injected to the tumors) was run on the gel. The FAM-labeled siRNA was detected by a Fuji FLA-5000 flat-bed scanner using the LD blue laser (485 nm) and percent recovery was calculated based on the spot densitometry as follows: 100% × [recovered siRNA amount/injected siRNA amount].

In Vivo Tumor Cell Uptake of DOX

After establishing MDR1 and WT tumors in SCID mice, 100 µL of 51 µg of Doxil® diluted in saline (equivalent to 3 mg/kg) was injected via the tail vain of mice. After 24 hours, the mice were euthanized, tumors were extracted, the extracted tumors were homogenized by a Pyrex(R) Tissue Grinder, filtered through a 35-µm mesh, and suspended in 3.7% formalin in HBSS. DOX uptake of cells was quantified by a Beckman-Coulter flow cytometer (Cell Lab Quanta) using the FL-2 detection channel to determine percentage of DOX-positive cells and the mean DOX fluorescence (~10000 events/sample). The instrument was calibrated so that the negative control sample (i.e., non-treated cells) gave1-2% cells positive for DOX.

In Vivo P-gp Suppression and DOX Uptake

The complexes of PLL-StA/ABCB1-siRNA and PEI/ABCB1-siRNA were injected intratumorally by using the combination of three siRNA sequences (siRNA 1+2+3) and, after 24 h, 51 µg of Doxil® (3 mg/Kg) was injected intravenously into the tail vein of the mice. After a further 24 h, mice were euthanized and the tumors were recovered, processed, filtered and suspended in 3.7% formalin in HBSS. 10 µL of FITC P-gp antibody was added to the cells and the cells were analyzed by flow cytometry using a Beckman-Coulter flow cytometer (Cell Lab Quanta) using the FL-1 detection channel to assess the FAM-siRNA-positive cells (~10000 events/sample) and FL2 channel to assess the DOX-positive cells. The flow cytometry was previously optimized for similtanous detection of DOX and P-gp using *in vitro* cultured cells.

RESULTS

In Vitro siRNA Uptake

An initial study was conducted to investigate the fate of siRNA delivered by the cationic polymers, with the purpose of determinig siRNA persistence in MDA-435/LCC6 MDR1 cells. The cells were exposed to a single dose of siRNA complexes for 24 h for this purpose, after which the siRNAs were removed. Confocal microscopy images of the cells exposed to free FAM-siRNA or FAM-siRNA/polymer shown in **Figure 7-1** over a period of 7 days. In cells treated with free FAM-siRNA, no siRNA was detected at any of the time points **(Figure 7-1A)**, indicating lack of cellular uptake in the absence of a polymeric carrier. The PEI/FAM-siRNA treated cells showed limited,if any, uptake of siRNA after 1 h, but the PLL-StA/FAM-siRNA treated cells gave cell-associated FAM-siRNA particles at this time point. At the subsequent time points, the uptake of PLL-StA/FAM-siRNA and PEI/FAM-siRNA complexes was qualitatively similar. The cell-associated FAM-siRNA particles increased significantly after 6 h of siRNA exposure in cells treated with both polymer complexes. After 1 day, a uniform distribution of particles in the cytoplasm was detected. After 3 days, the particles are concentrated around the nuclear membrane (**Figure 7-1B**) and the particles completely disappeared after 7 days (**Figure 7-1C**).

In Vitro P-gp Down-Regulation

The suppression of P-gp by the 3 different siRNAs at days 1, 2 and 3 are shown in **Figure 7-2**. The treatment of cells with siRNA in the absence of a carrier did not lead to P-gp

suppression at any of the time points, consitent with the lack of siRNA uptake by the MDR1 cells. The siRNA delivery with PLL-StA and PEI showed similar efficiency in P-gp suppression at all time points. The siRNA-2, siRNA-3, and their combination (siRNA-2/-3) were the least effective in P-gp suppression, leading to ~23% P-gp suppression at day 1, and ~41% P-gp suppression at days 2 and 3. The siRNA-1 delivery with the polymers gave ~52% P-gp suppression at day 1, and ~47% P-gp suppression at days 2 and 3. The efficiency of siRNA-1/-2 and siRNA-1/-3 combinations for P-gp suppression was similar to the efficiency of siRNA 1 at the investigated time points. The siRNA-1/-2/-3 was the most effective siRNA combination in P-gp suppression, leading to ~65% P-gp suppression at day 1, ~59% P-gp suppression at day 2, and ~73% P-gp suppression at day 3.

In Vivo siRNA Uptake in Tumors

For tumor formation, ~2 x 10^6 MDA-435/LCC6 WT or MDR1 cells were injected into the right flank of the mice. After 3 weeks, an average tumor size of ~150 mm^3 was reached, at which point intratumoral injections of siRNA and siRNA complexes were performed. The siRNA uptake on extracted tumors was initially analyzed by epifluorescent microscopy one day after siRNA injection. The FAM-siRNA treated cells (i.e., without a carrier) gave limited siRNA localization at the tumors **(Figure 7-3A)**. The injection of PLL-StA/FAM-siRNA complexes showed a relatively high amount of siRNA dispersed evenly throughout the tumor **(Figure 7-3B)**. The PEI/FAM-siRNA treated cells also showed a high amount of siRNA uptake, but the

siRNA was more concentrated in certain areas of the tumors and appeared to be less dispersed and/or aggregated **(Figure 7-3C)**.

The siRNA uptake in tumor cells was quantitated by flow cytometry. The PEI/FAM-siRNA and PLL-StA/FAM-siRNA treated cells showed a similarly high percentage of siRNA-positive cells (70-75%) after 24 h of injection. The PEI/C-siRNA and PLL-StA/C-siRNA treated cells showed 18±5% and 9±2% siRNA-positive cells, indicating some level of autofluorescence as a result of siRNA delivery by PEI and PLL-StA. The naked FAM-siRNA treated cells showed 7±1% siRNA-positive cells at 24 h post-injection. At 96 h, the percentage of siRNA positive cells was reduced significantly, yielding 39±3% for the PEI/FAM-siRNA treated tumors and 22±6% for the PLL-StA/FAM-siRNA treated tumors **(Figure 7-4A)**. The amount of siRNA uptake (as determined by the mean fluorescence) was higher in the PEI/FAM-siRNA treated tumors compared to the PLL-StA/FAM-siRNA treated tumors at the 24 and 96 h time points **(Figure 7-4B**; 1.6-fold and 2.5-fold, respectively).

The siRNA recovery from tumor cells after intratumoral injection was also assessed by gel electrophoresis after extracting the siRNA from the tissue mass. Since this approach is based on intact siRNA quantitation after gel migration, it provides a measure of intact siRNA in the tumor tissue. The PEI/FAM-siRNA treated tumor cells showed the highest siRNA recovery after 24 h (42±1%). The PLL-StA/FAM-siRNA treated cells showed 31±7% recovery ($p<0.004$ vs. PEI/FAM-siRNA treated tumors), and the naked FAM-siRNA treated cells showed 12±2% siRNA recovery **(Figure 7-5)**.

DOX Uptake after Doxil® Injection

Systemic injection of tumor-bearing mice with Doxil® was performed to assess tumor localization of the drug. The Doxil® injection in mice bearing the WT tumors resulted in 22±1% DOX-positive tumor cells, but Doxil® injection in MDR1 tumor bearing mice resulted no measurable uptake of the drug (**Figure 7-6A**), consistent with the phenotypic features of the tumor reconstituting cells. The mean fluorescence of the WT and MDR1 tumor cells showed a similar trend as well, wherr the WT tumor cells gave the highest amount of DOX uptake and MDR1 tumor cells displayed no apparent uptake (**Figure 7-6B**).

***In Vivo* P-gp Down-Regulation**

Intratumoral injection of P-gp specific siRNAs was performed to assess P-gp down-regulation in the established MDR1 tumors. The siRNA used for this purpose was the combination of the three siRNAs (siRNA 1+2+3) as this was the most efficient siRNA tested *in vitro*. As the base line, untreated tumors yielded 88±2% P-gp positive cells from the tumors. The tumors treated with free P-gp specific siRNA (i.e., without any polymeric carrier) and C-siRNA/polymer complexes showed no significant down-regulation of P-gp, based on lack of changes in either the extent of %P-gp positive tumor cells (**Figure 7-7A**) or the mean P-gp level in tumor cells (**Figure 7-7B**). The tumors treated with ABCB1-siRNA/PEI and ABCB1-siRNA/PLL-StA had 66±1% and 42±2% P-gp respectively. The changes in mean fluorescence of the cell population (indicating the relative levels of P-gp) confirmed the above results, as the

cells treated with P-gp specific siRNA complex of PLL-StA showed the highest amount of P-gp down-regulation.

Systemic Doxil® injection in the tumor bearing mice pre-treated with C-siRNA/polymer or ABCB1-siRNA/polymer was also performed. Results were normalized and compared to the no Doxil® treated controls. To our surprise, no Doxil® uptake was detected in the extracted tumor cells pre-treated with ABCB1-siRNA/polymer **[Figure 8]**.

DISCUSSION

The role of MDR in chemotherapy deficiency has been well established in various types of cancers [1], and the resistance of tumor cells to toxic chemotherapeutics is a major drawback of chemotherapy in the treatment of breast cancer [14], ovarian cancer [17,18], gastric cancer [37], and pancreatic cancer [38]. Attempts to reverse the MDR phenomenon has mainly focused on P-gp, the most consistent protein linked to efflux of chemotherapeutic drugs [6,7]. Therefore P-gp suppression has been the proposed solution for the reversal of P-gp mediated MDR. *In vitro* approaches for P-gp down-regulation using various siRNA sequences and various siRNA delivery methods in different tumor cells have been attempted. Lipid based siRNA carriers such as Lipofectamine™ 2000 and Oligofectamine™ have been beneficial in P-gp down-regulation at the mRNA and protein level [14-18]. siRNA transfection in tumor cells using viral vectors has also been shown to knockdown P-gp [19-21]. Additionally, uptake and efficiency of chemotherapeutic drugs after siRNA down-regulation has been shown to increase in *in vitro* studies. However translation of this success to in *vivo* has been a challenge as the limitations of

viral and lipid-based carriers (as previously discussed) has significantly hampered their *in vivo* use. We previously showed that Lipofectamine^{TM} 2000 offers poor protection against serum nucleases after siRNA complexation, as compared to polymeric carriers, such as PEI and PLL-StA, whose complexation with siRNA offers improved protection against nuclease attack [36]. This is presumably a significant shortcoming of the lipid-based carriers in animal models as reports have shown that this carrier is unstable in the physiological milieu, and additionally it could lead to inflammatory and toxic responses. In this study, we have used a novel carrier PLL-StA and attempted a parallel approach of *in vitro* and *in vivo* siRNA delivery for P-gp down-regulation.

Confocal microscopy studies was initially conducted to determine the intracellular fate of siRNA after uptake into MDA 435/LCC6 MDR1 cells. This study was conducted to determine (i) the time required for siRNA uptake (ii) the time required for siRNA dissociation from complex (iii) *in situ* residence time of siRNA. As expected, cells treated with free FAM-siRNA did not show siRNA uptake in any of the designated time points. Using PLL-StA and PEI for siRNA delivery, uptake into cells was detected within 1 h of complex exposure and, by 24 h exposure, the FAM-siRNA particles was spread evenly in large frequency within the cell. Significant intracellular trafficking was evident subsequently since the siRNA was concentrated at the intracellular and nuclear membranes on day 3, after which the siRNA disappeared by day 7. It could be seen that siRNA particles detected at the 1 and 6 h time points were larger, more compact and more dispersed as compared to particles at later time points. This may suggest that the siRNA at early time points were localized in endosomes, whereas the siRNA particles detected after 24 h were released from the endosomes and were spread in the cytosol.

Our previous studies on *in vitro* P-gp down-regulation using PLL-StA had resulted in a maximum of ~55% P-gp reduction at the protein level, using a relatively low siRNA concentration (20 nM siRNA-1) [33]. The significance of using low siRNA concentrations to limit modulation of non-specific genes has been well established [39-41]. In this study, an attempt was made to improve on our previous results, more specifically to increase (i) the efficiency of knockdown, and (ii) the duration of P-gp down-regulation. To increase the efficiency of siRNA P-gp knockdown, we used a combination of three different siRNA sequences. The G/C content of siRNA molecules has been reported to be significant in siRNA efficiency for P-gp down-regulation. It has been reported that efficient siRNA sequences contain 30-52% G/C content [42]. Additionally, the presence of A/U at the 5' end of the antisense strand was shown to increase siRNA efficiency [43]. The first few sequences of the 5'-end of the antisense strand were suggested to contain 3 to 5 A/U, since low internal stability of the siRNA at the 5'-end of the antisense strand was considered important for duplex unwinding and efficient entry into RISC sequences [44]. Our siRNA 1 contained 38% G/C, siRNA 2 contained 44% G/C, and siRNA 3 contained 42% G/C. Additionally, out of the first 7 sequences of the 5'-terminal of our siRNA 1 contained 5 A/U, siRNA 2 contained 3 A/U, and siRNA 3 contained 4 A/U sequences. Based on these considerations, all 3 siRNAs were expected, and shown, to be effective at P-gp down-regulation. Using a combination of 2 or 3 specific siRNAs did lead to a significant increase in gene silencing in a study by Ji *et al.* [45], while Holen *et al.* saw no beneficial effect using this method [46]. Stierlé *et al.* observed that mixing very efficient and slightly efficient siRNA molecules resulted in gene silencing induced by only the more efficient siRNA [14]. We observed similar results to Stierlé *et al.* as the combination of our most efficient

siRNA sequence (siRNA 1) with the less efficient siRNA sequences (siRNAs 2 and 3) resulted in similar efficiency to that of siRNA 1. As expected, the combination of siRNA 2+3 did not prove beneficial, however, the combination of all three siRNA sequences (siRNA 1+2+3) resulted in a significant increase in efficiency (maximum of 75% P-gp protein down-regulation in the MDA435/LC66 MDR1 cells). It should be noted that a higher dose of siRNA is applied when a combination of multiple siRNA sequences are used. This concentration is 40 nM in the case of two siRNAs and 60 nM in the case of three siRNAs and this could contribute in increasing the efficiency of P-gp down-regulation. However as our previous studies have shown no beneficial effect in using siRNA 1 doses as high as 100 nM for P-gp down-regulation in the MDA435/LCC6 MDR1 cells [33], we conclude that the higher siRNA concentration is not the reason for the beneficial effect seen in this study. To increase the duration of P-gp knockdown, repeated exposure of siRNA/polymer complexes to cells was attempted. Our previous reports had confirmed the maximum efficiency of siRNA action at 24 h after a single treatment, and loss of the silencing effect after 72 h of siRNA/polymer exposure [34]. We therefore exposed siRNA complexes to cells every 24 h for a period of 3 days to increase the duration of P-gp knockdown and were able to prolong P-gp down-regulation for a period of 72 h.

The *in vivo* siRNA uptake studies with flow cytometry confirmed the presence of FAM-siRNA in injected tumor cells. Both polymers were able to deliver siRNA into cells, but PEI appeared to be more effective than the PLL-StA in this respect, showing a higher percentage of FAM-siRNA positive cells and a higher mean fluorescence as an indication of higher concentration of FAM-siRNA in cells. This was in line with our siRNA recovery results from gel electrophoresis, where ~42% of the injected siRNA was recovered from the PEI/FAM-siRNA

injected tumor cells as compared to ~30% by PLL-StA. It is likely that the siRNA bound to PLL-StA was dissociated faster than the PEI bound siRNA, causing faster disappearance of the former siRNA. As expected, there was a significant reduction in siRNA levels in tumors after 96 h, reducing by 56% in the PEI/FAM-siRNA treated tumors and by 68% in the PLL-StA/FAM-siRNA treated tumors. This level of reduction was in line with our previous *in vitro* results [34], where ~20% reduction was seen with PEI delivered FAM-siRNA and a ~50% reduction with PLL-StA delivered FAM-siRNA from 24 to 72 h in MDA-435/LCC6 MDR1 cells. Considering that free siRNA is degraded within 24 hours in the presence of serum (unpublished observations), the FAM-siRNA that is detected at tumor cells at the 96 h time point is expected to be in a complex with carriers. None of the other studies focusing on P-gp down-regulation in animal models explored *in situ* siRNA pharmacokinetics [14-21], and our studies provide some (albeit limited) information in this regard.

The ultimate goal of P-gp knockdown is to impede drug efflux and increase intracellular levels of drugs that are P-gp substrates. However, the treatment of cells with siRNA complexes alone led to autofluorescence, which was most evident during the quantitation of *in situ* siRNA levels. This phenomenon depended on the type of carrier in this study, particularly being manifested with the PEI complexes. This was apparently not an issue with DOX uptake studies, where no changes from the background were evident with MDR1 cells. Systemic Doxil® injection in the mice bearing the MDR1 and WT tumors showed that ~23% of the tumor cells displayed DOX uptake in the WT tumor bearing mice. The tumor cells in the MDR1 tumor bearing mice showed strong resistance to the injected Doxil®, and no uptake was detected in the

extracted MDR1 tumor cells. This result was in line with the P-gp levels in the cells constituting the tumors, and proves the presence of MDR in the MDR1 tumor cells *in vivo*.

As *in vivo* knockdown of P-gp is required for successful chemotherapy and tumor suppression, our next study focused on *in vivo* siRNA delivery for P-gp down regulation. The combination of three ABCB1-siRNAs (siRNA 1+2+3) was used for this purpose as this siRNA had proved to be the most efficient siRNA in our *in vitro* studies (75% P-gp down regulation). When the ABCB1-siRNA delivered by our novel PLL-StA and the PEI, a higher efficiency was detected for PLL-StA compared to PEI (58% vs 34% P-gp down regulation). It was unexpected that PLL-StA was more effective *in vivo*, since we had seen a similar efficiency for PLL-StA and PEI for *in vitro* P-gp down regulation and *in vivo* siRNA uptake. This difference could be due to the tighter complex formation between PEI and siRNA compared to PLL-StA and siRNA as determined from our preliminary studies by gel electrophoresis [36]. Efficient complex dissociation in the cytosol is required for siRNA binding to the RISC complex and deficiency in dissociation of siRNA and PEI may reduce siRNA bioavailability in the cytosol, leading to a lower P-gp mRNA knockdown and ultimately a lower P-gp down regulation. The in *vivo* P-gp down-regulation was expected to lead to an increase in DOX accumulation in cells after systemic Doxil® injection. However, no DOX uptake was detected in ABCB-1 siRNA treated tumor cells. From our DOX uptake results it was detected that only a 23% DOX uptake was detected in the tumor cells when a 3 mg/KG concentration of Doxil® was injected systematically into the WT non-MDR mice. This was a very low DOX uptake that is detected in the control groups and may be the reason for the fact that no DOX uptake is detected in the ABCB1-siRNA treated MDR tumors cells. Increasing the Doxil® concentration, changing the injection method, and a

prolonged injection of Doxil® may be beneficial in increasing the DOX uptake into the MDR tumor cells with a reduced P-gp population.

A limited number of research groups have also attempted *in vivo* down-regulation of P-gp and MDR reversal. Xiao *et al.* used a Stealth™ RNAi delivery system (Invitrogen) for siRNA interference in the human lung carcinoma cells NCI-H460. Stealth™ RNAi shares the same interfering properties of siRNA but shows less off-target activities due to chemical inactivation of the sense strand. Nude mice were used in their *in vivo* studies and 80 μM of the Stealth™ RNAi was delivered by electroporation directly into tumors (without a carrier). Their maximal P-gp down-regulation in the tumor cells was ~80%, and after P-gp down-regulation and chemotherapeutic treatment by Navelbine (Vinorelbine Tartrate), the maximal reduction of tumor size was by ~60% after 13 days [47]. Patil *et al.* used the nanoparticle poly(D,L-lactide-co-glycolide) for simultaneous delivery of siRNA and chemotherapeutic drug paclitaxel. They used biotin for tumor targeting and used the tail vain injection method, and a concentration of 20mg/Kg PTX was used in combination with 20 μg of the ABCB1-siRNA in their study. Breast cancer tumors developed in BALB/c mice and after a single dose injection of their nanoparticles they were able to reduce the tumor volume by 50% after 16 days [48]. In a study by Pan *et al*. HepG2/mdr cells were used for subcutaneous tumor formation in nude mice. 1 or 1.5 mg/Kg pSUPER siRNA vector was used for intraperitoneal (IP) injection of ABCB1-siRNA and after 72 h, mice were injected with a 1.5 mg/Kg dose of the chemotherapeutic drug Adriamycin twice a week for two weeks by IP injection. The tumor volume was reduced by 58% after two weeks and the P-gp expression was reduced by 29% [49]. Our in vivo P-gp down-regulation results are higher than those obtained by Pan *et al*., but lower compared to the results obtained by Xiao *et*

al. (29%<58%<80%). Differences in cell lines, tumor volume, injection method, and the differences in the sequences and the concentration of the injected siRNA are factors that significantly contribute to these differences. Our in vivo DOX accumulation studies after 24 h of systemic Doxil® injection did not result in increased accumulation of DOX in tumor cells and it remains to be seen if increasing the Doxil® concentration, changing the injection method, and a prolonged injection of Doxil® will be beneficial for this purpose.

In summary, this study investigated the intracellular fate of siRNA after uptake into the MDA 435/LCC6 MDR1 cells. We have also used two approaches to increase the efficiency and duration of siRNA knockdown of P-gp in the drug resistant MDA-435/LCC6 MDR1 cells *in vitro* and further determined that *in vivo* siRNA uptake into the tumor cells was feasible using the polymeric carriers PEI and PLL-StA. Using specific siRNAs to down-regualte P-gp, we demonstrated successful P-gp down-regulation after tumoral injection in NON-SCID mice. Although MDA-435/LCC6 WT cells displayed the expected DOX accumulation after systemic Doxil® injection, tumors derived from MDA-435/LCC6 MDR1 cells did not yield DOX accumulation with or without P-gp down-regulation.

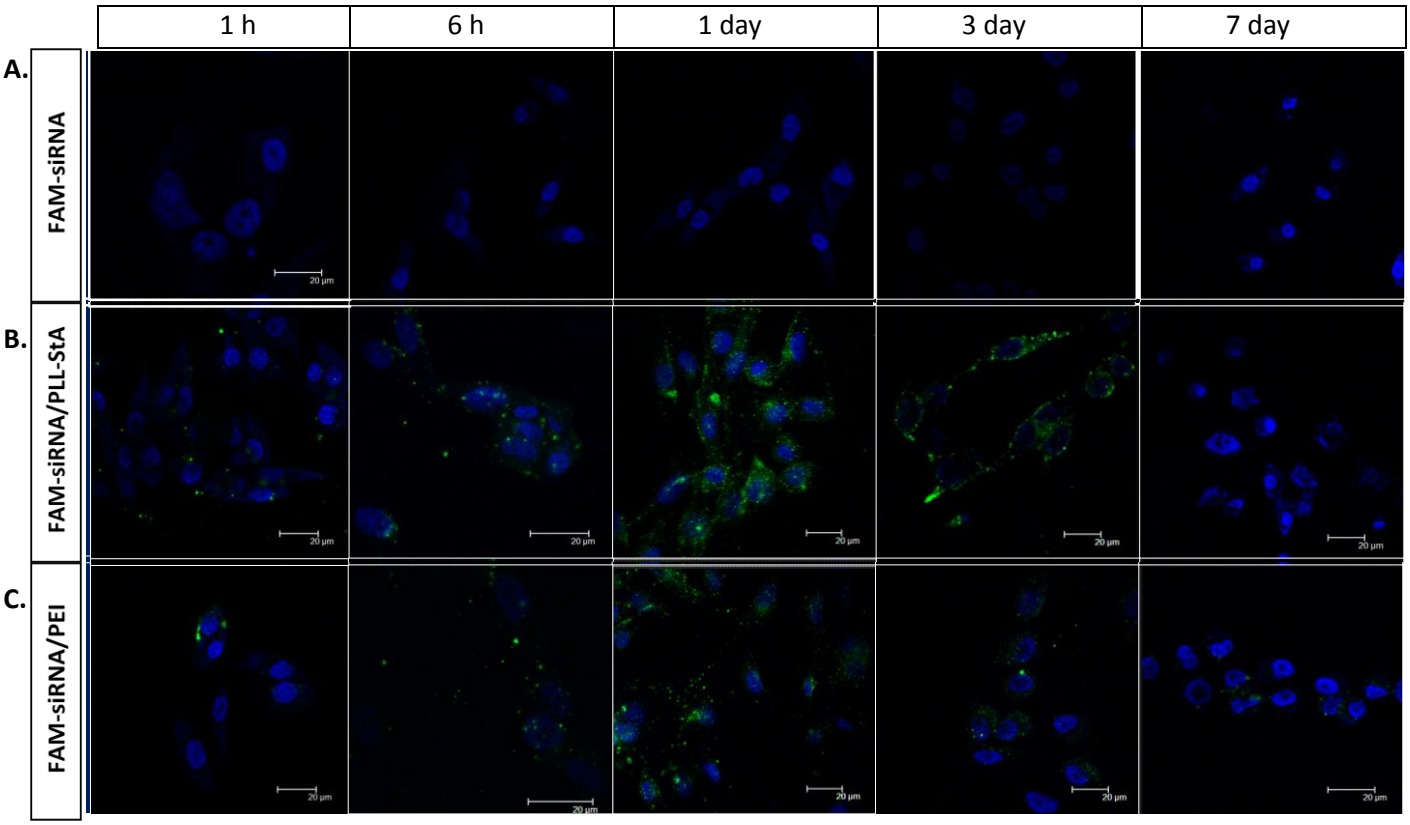

Figure 7-1. Confocal microscope assessment of siRNA uptake in the MDA-435/LCC6 MDR1 cells. The cells are exposed to free FAM-siRNA **(A)** or PLL-StA/FAM-siRNA **(B)** or PEI/FAM-siRNA **(C)** for a period of 1 h, 6 h, 1 day, 3 days, and 7 days. The Hoeschst 33258 stained cell nuclei are detected in blue and the FAM-siRNA is detected in green. Note that the siRNA particles in the 1 h and 6 h time points are larger and separated, indicating their entrapment in the endosomes.

A. Day 1

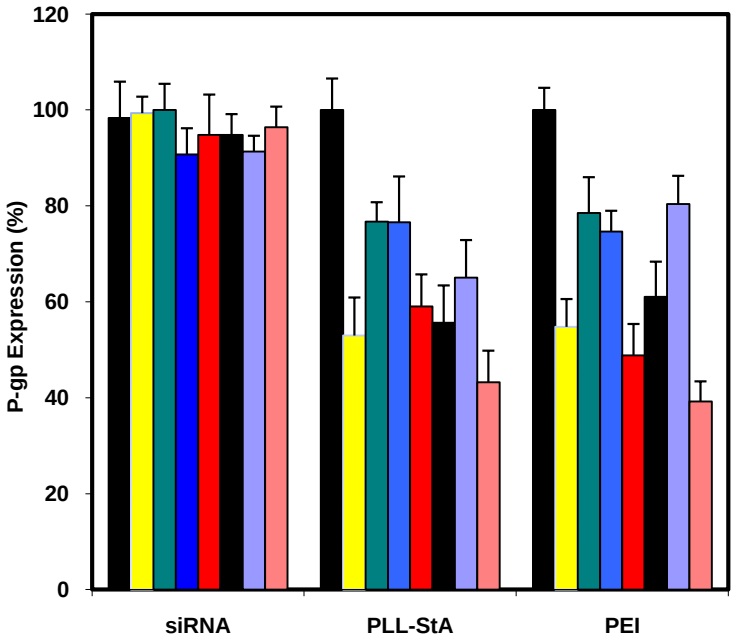

B. Day 2

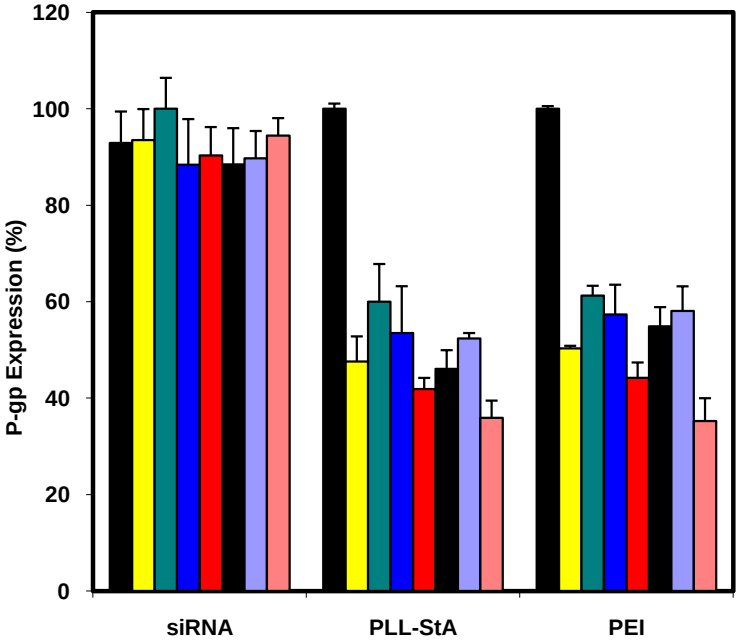

C. Day 3

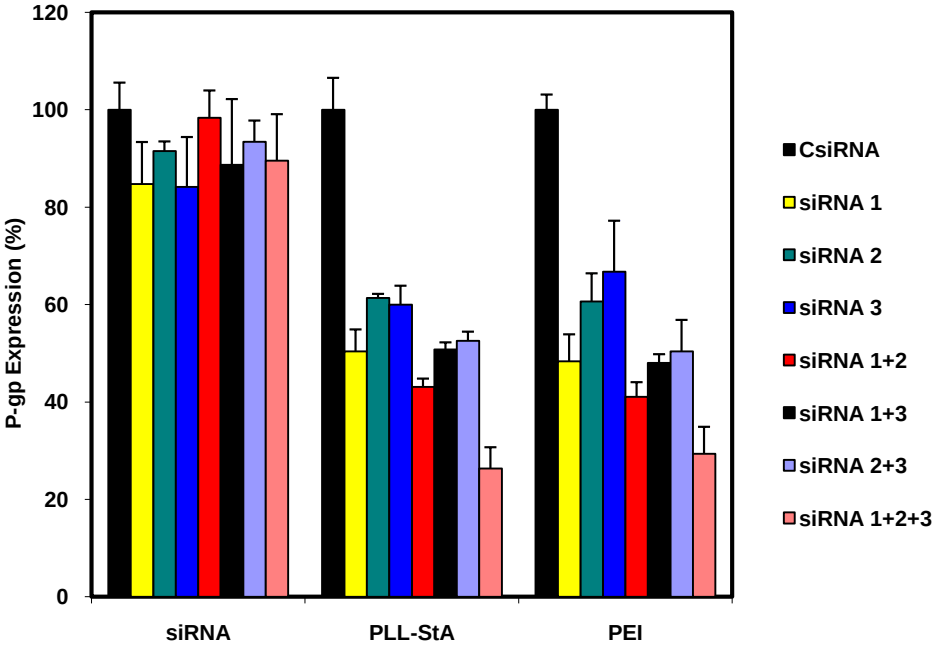

Figure 7-2. P-gp down-regulation in MDR1 cells after siRNA-1, siRNA-2, and siRNA-3 treatment. The level of P-gp was detected by flow cytometry after 24, 48 and 72 h treatment of siRNA and normalized with respect to the untreated cells. The concentration of siRNA used at each time point is either 20 nM (one siRNA), 40 nM (combination of two siRNAs), or 60 nM (combination of three siRNAs). The PLL-StA and PEI showed similar efficiency P-gp down-regulation using siRNA. siRNA-1 showed ~52% P-gp suppression at day 1, and 47% P-gp suppression at days 2 and 3. The efficiency of siRNA-1/-2 and siRNA-1/-3 for P-gp suppression was similar to the efficiency of siRNA 1 at the studied time points. siRNA-1/-2/-3 was the most effective siRNA combination in P-gp suppression leading to ~65% P-gp suppression at day 1, ~59% P-gp suppression at day 2, and ~73% P-gp suppression at day 3. The siRNA-2, siRNA-3, and their combination (siRNA-2/-3) were the least effective in P-gp suppression, leading to ~23% P-gp suppression at day 1, and ~41% P-gp suppression at days 2 and 3.

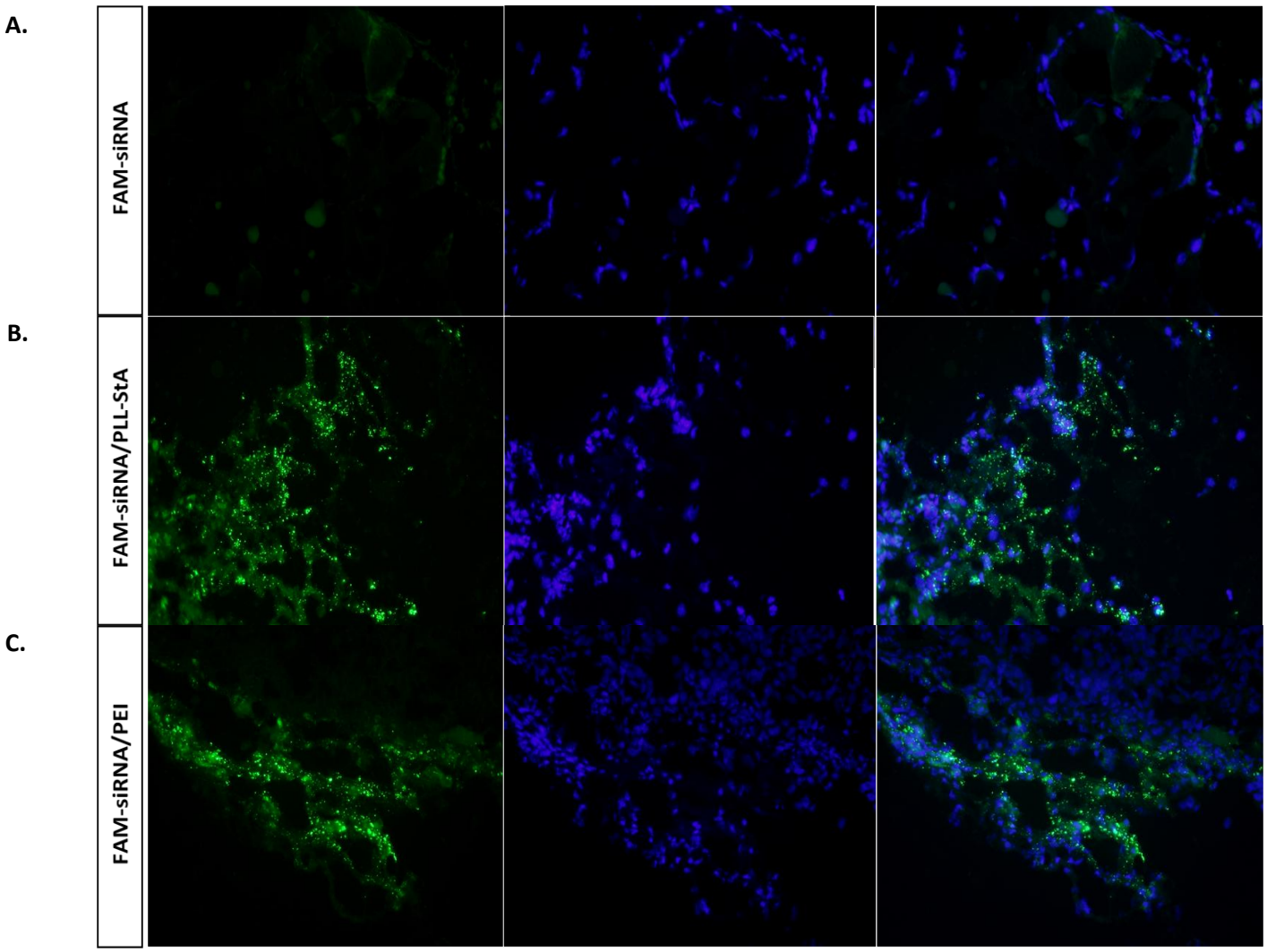

Figure 7-3. Epifluorescent microscope assessment of the histology sectioned tumor tissue treated with free FAM-siRNA **(A)** or PLL-StA/FAM-siRNA **(B)** or PEI/FAM-siRNA **(C)**. The DAPI stained cell nuclei are detected in dark blue and the FAM-siRNAs are detected in green. The free FAM-siRNA treated cells showed no siRNA uptake, whereas the PLL-StA/FAM-siRNA and the PEI/FAM-siRNA treated cells show significant siRNA uptake.

A.

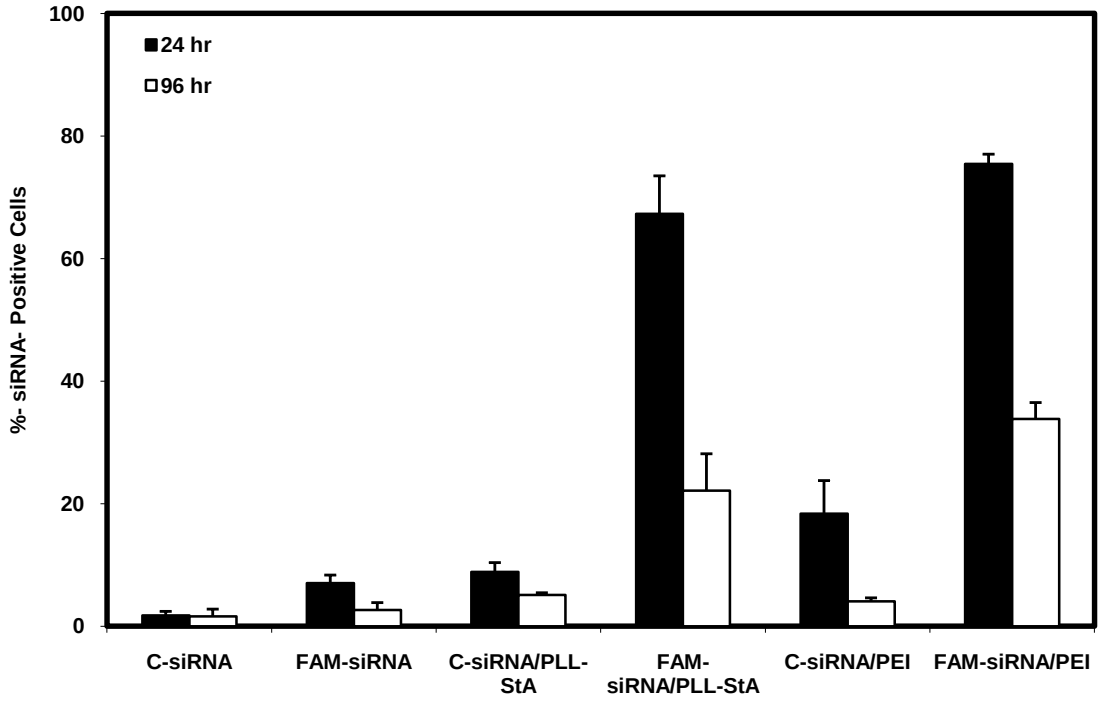
100
80
60
40
20
0
%- siRNA- Positive Cells
24 hr
96 hr
C-siRNA
FAM-siRNA
C-siRNA/PLL-StA
FAM-siRNA/PLL-StA
C-siRNA/PEI
FAM-siRNA/PEI

B.

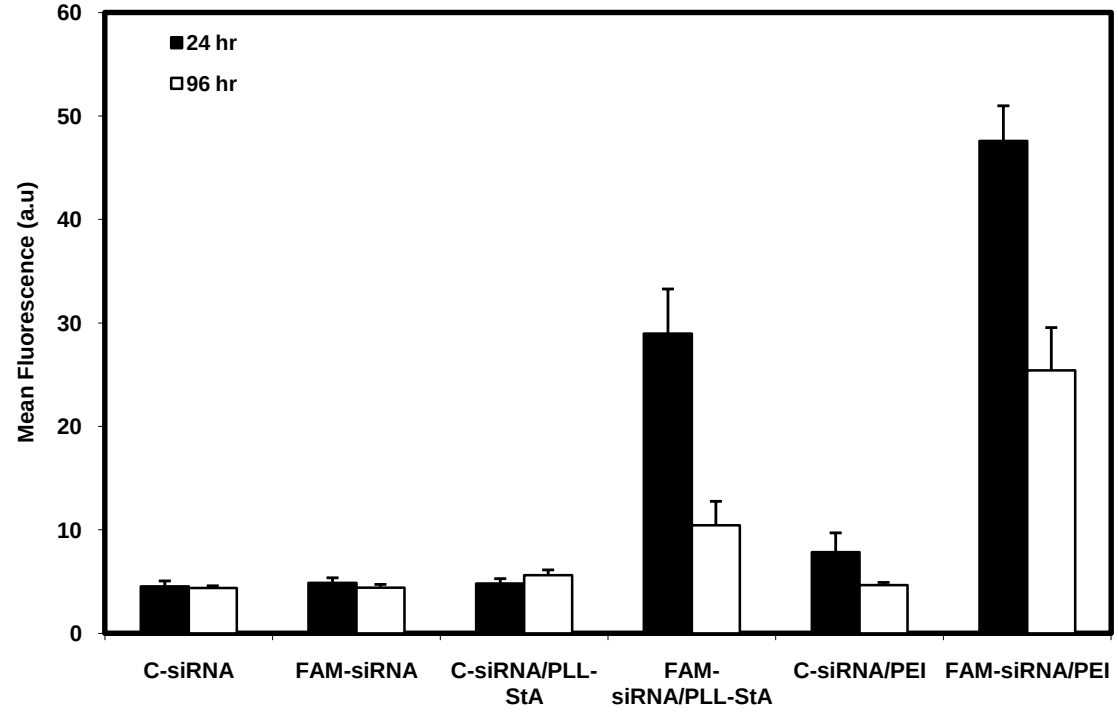
60
50
40
30
20
10
0
Mean Fluorescence (a.u)
24 hr
96 hr
C-siRNA
FAM-siRNA
C-siRNA/PLL-StA
FAM-siRNA/PLL-StA
C-siRNA/PEI
FAM-siRNA/PEI

Figure 7-4. (A) FAM-siRNA uptake of the tumors over two time points of 24 h and 96 h, determined by flow cytometry. At 24 h, PEI proved the most efficient with 75% FAM-siRNA uptake, whereas PLL-StA showed 67% FAM-siRNA uptake. At the 96 h time point, PEI showed 33% FAM-siRNA uptake and PLL-StA showed 22% FAM-siRNA uptake. **(B)** Mean fluorescence of the cells further showed that the cells treated with PEI/FAM-siRNA contained the highest concentration of FAM-siRNA at the 24 h and 96 h time point.

A.

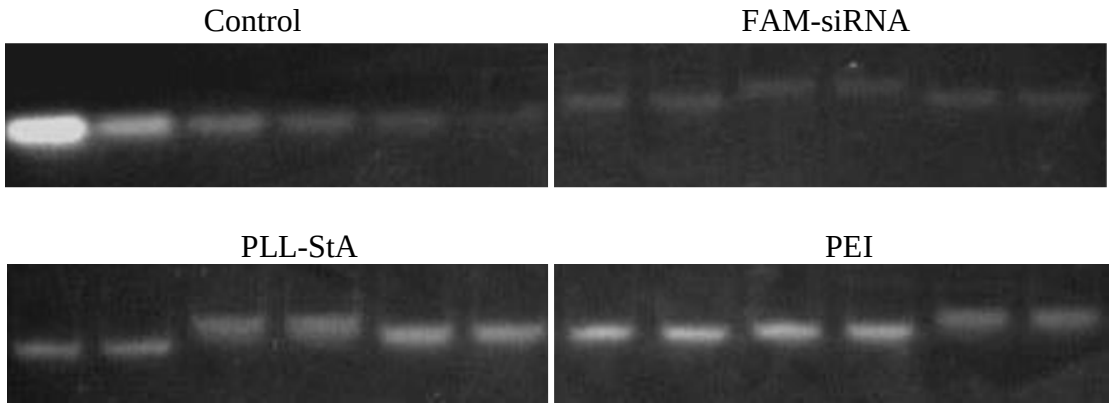

B.

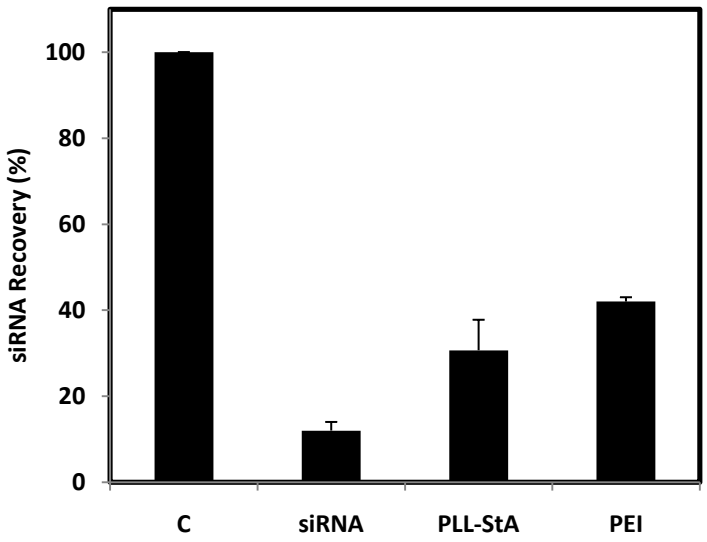

Figure 7-5. The siRNA recovery from the tumors after extracting the siRNA from the MDA-435/LCC6 MDR1 tumor cells after 24 h. As with flow cytometry analysis, the PEI gave the highest siRNA internalization with 42% FAM-siRNA recovery, while the tumors injected with PLL-StA/FAM-siRNA showed 30% FAM-siRNA recovery.

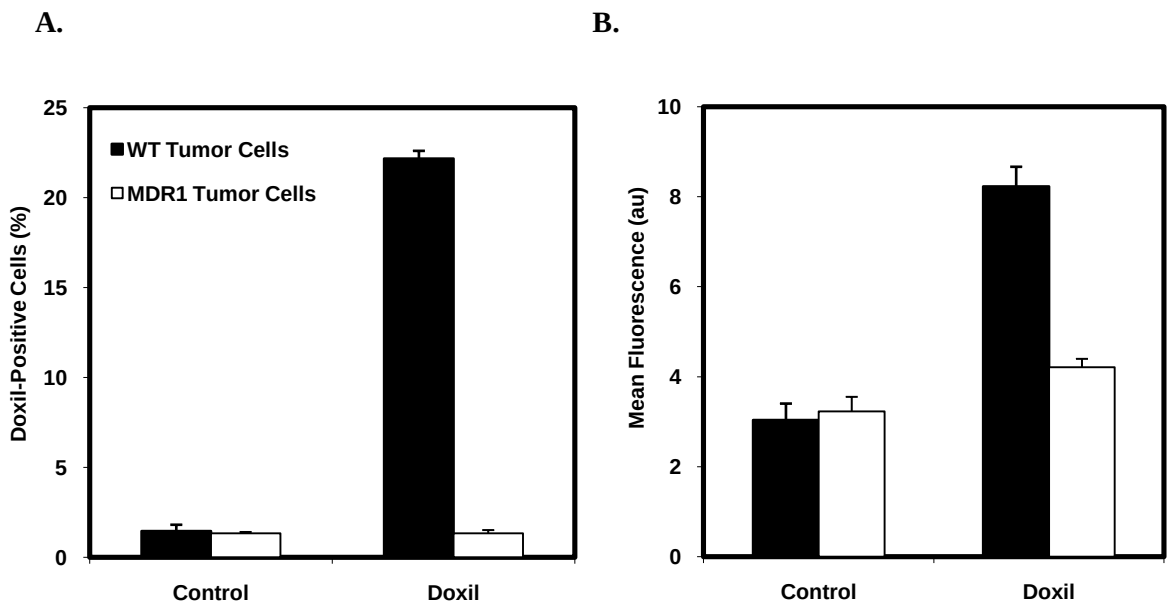

Figure 7-6. Flow cytometric analysis of Doxil uptake in the MDR1 and WT tumors 24 h after tail vein injection of Doxil. The results are summarized as the %Doxil-positive cells (**A**) or mean Doxil fluorescence per cell (**B**). A clear difference between the MDR1 and WT tumor cells was evident in the % of cells showing Doxil uptake.

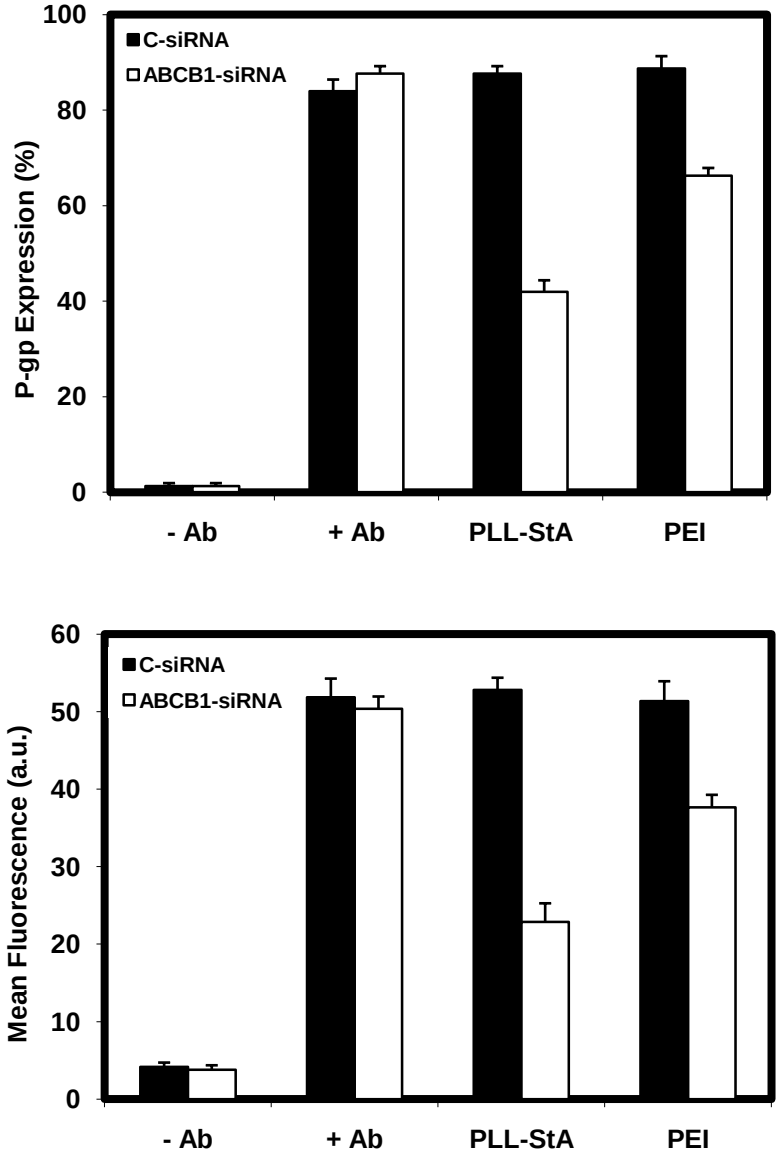

Figure 7-7. *In vivo* P-gp down regulation by ABCB1-siRNA after 24 h of intratumoral injection of siRNA determined by flow cytometry. **(A)** The tumors treated with ABCB1-siRNA/PLL-StA proved the most efficient, showing 58% P-gp down regulation in the tumor cells, while the tumors treated with ABCB1-siRNA/PEI showed 34% P-gp down regulation. It was also confirmed that the tumors treated with C-siRNA showed no P-gp down-regulation **(B)** The mean fluorescence of the population confirmed that the tumors treated with ABCB1-siRNA/PLL-StA showed the lowest concentration of P-gp.

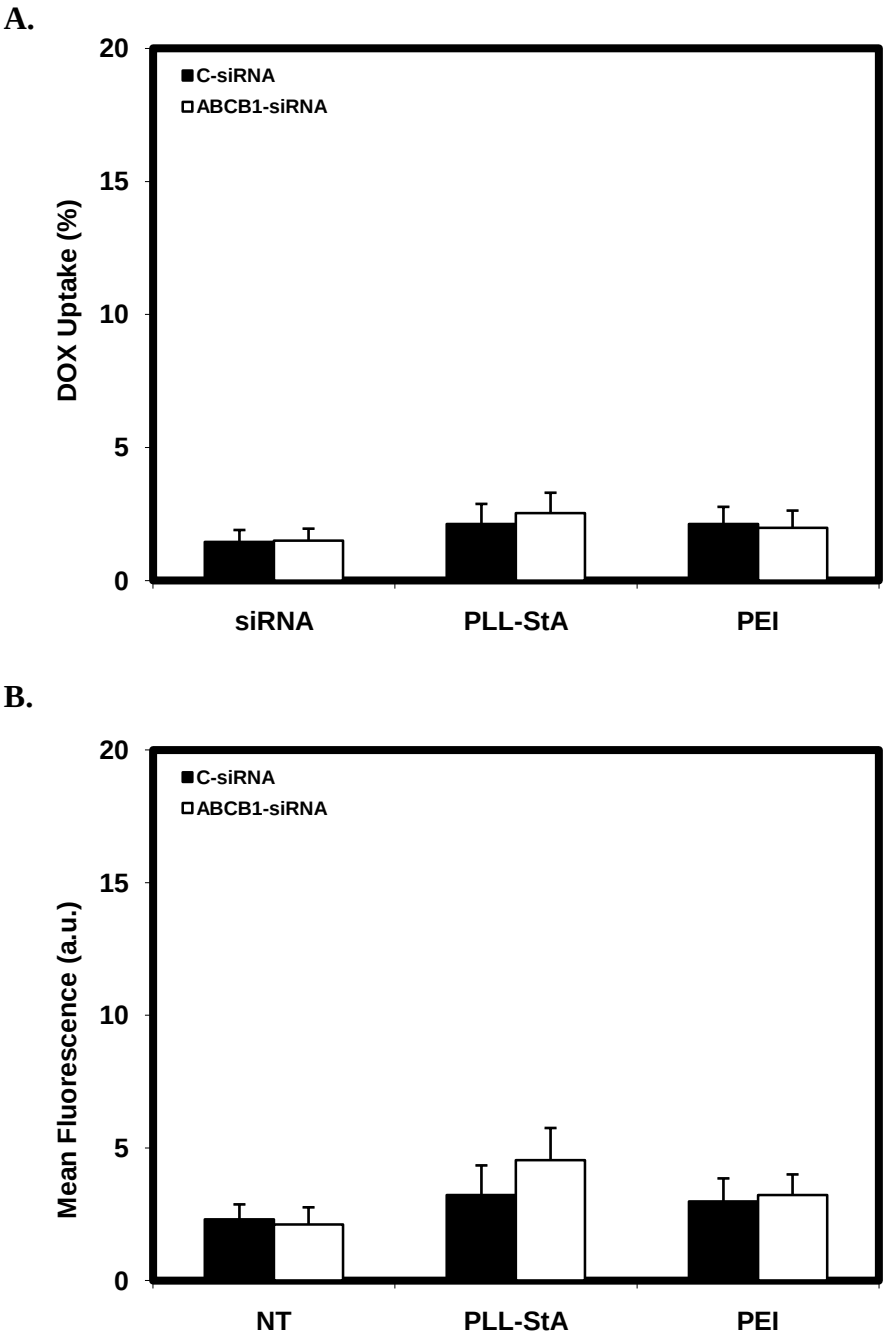

Figure 7-8. *In vivo* DOX uptake of the ABCB1-siRNA treated tumor cells after 24 h of systemic Doxil® injection by flow cytometrry. No difference is detected between the naked siRNA treated tumor cells and the polymer/siRNA treated cells. Furthermore, no difference is detected in the DOX uptake of the ABCB1-siRNA/polymer treated tumor cells and the C-siRNA/polymer treated tumor cells.

REFERENCES

1. Kerbel RS. Molecular and physiologic mechanisms of drug resistance in cancer: an overview. Cancer & Metastasis Reviews. 2001, 20, 1-2.
2. Linardi RL, Natalini CC. Multi-drug resistance (MDR1) gene and P-glycoprotein influence on pharmacokinetic and pharmacodymanic of therapeutic drugs. Ciência Rural, 2006. 36, 336-41.
3. Eckford PDW, Sharom FJ. ABC efflux pump-based resistance to chemotherapy drugs. Chem Rev. 2009, 109, 2989–3011.
4. Higgins CF, Gottesman MM. Is the multidrug transporter a flippase? *Trends Biochem Sci.* 1992, 17, 18–21.
5. Loo TW, Clarke DM. Recent progress in understanding the mechanism of P-glycoproteinmediated drug efflux. J Membr Biol. 2005, 206, 173-85.
6. Schinkel AH, Borst P. Binding properties of monoclonal antibodies recognizing external epitopes of the human MDR1 P-glycoprotein. Int J Cancer. 1993, 55, 478-84.
7. Chen Y, Simon SM. *In situ* biochemical demonstration that P-glycoprotein ss a drug efflux pump with broad specificity. JCB. 2000, 148, 5863-70.
8. Beaulieu E, Demeule M, Ghitescu L, Beliveau R. P-glycoprotein is strongly expressed in the luminal membranes of the endothelium of blood vessels in the brain. Biochem J. 1997, 326, 539-44.
9. Van Zuylen L, Nooter K, Sparreboom A, Verweij J. Development of multidrug-resistance convertors: sense or nonsense? Invest New Drugs. 2000, 18, 205-20.

10. Thomas H Coley HM. Overcoming Multidrug Resistance in Cancer: P-gp Modulators. Cancer Cont. 2003, 10, 159-65.
11. Kim SH, Jeong JH, Lee SH, Kim SW, Park TG. Local and systemic delivery of VEGF siRNA using polyelectrolyte complex micelles for effective treatment of cancer. J Cont Rel. 2008, 129, 107–16.
12. Song E, Lee S-K, Dykxhoorn DM, Novina C, Zhang D, Crawford K, Cerny J, Sharp PA, Lieberman J, Manjunath N, Shankar P. Sustained small interfering RNA-mediated human immunodeficiency virus type 1 inhibition in primary macrophages. J Virol. 2003, 77, 7174-81.
13. Kim S-S, Ye C, Kumar P, Chiu I, Subramanya S, Wu H, Shankar P, Manjunath N. Targeted delivery of siRNA to macrophages for anti-inflammatory treatment. Mol Ther. 2010, 185, 993–1001.
14. Stierle´ V, Laigle A, Jolle`s B. Modulation of MDR1 gene expression in multidrug resistant MCF7 cells by low concentrations of small interfering RNAs. Biochem Pharmacol. 2005, 70, 1424–30.
15. C. Nieth, Priebsch A, Stege A, Lage H. Modulation of the classical multidrug resistance (MDR) phenotype by RNA interference (RNAi). FEBS Lett. 2003, 545, 144– 150.
16. Akhtar S, Benter IF. Nonviral delivery of synthetic siRNAs *in vivo*. J Clin Invest. 2007, 117, 3623–32.
17. Zhang T, Guan M, Jin HY, Lu Y. Reversal of multidrug resistance by small interfering double-stranded RNAs in ovarian cancer cells. Gynecol Oncol. 2005, 97, 501–7.

18. Xing H, Wang S. Knock-down of P-glycoprotein reverses taxol resistance in ovarian cancer multicellular spheroids. Oncol Rep. 2007, 17, 117-22.
19. Xu D, McCarty D, Fernandes A, Fisher M, Samulski RJ, Juliano RL. Delivery of MDR1 small interfering RNA by self-complementary recombinant adeno-associated virus vector. Mol Ther. 2005, 11, 4, 523-30.
20. Huaa J, Mutcha DJ, Herzog TJ. Stable suppression of MDR-1 gene using siRNA expression vector to reverse drug resistance in a human uterine sarcoma cell line. Gynecol Oncol. 2005, 98, 31–38.
21. Yague E, Higgins CF, Raguz S. Complete reversal of multidrug resistance by stable expression of small interfering RNAs targeting MDR1. Gene Ther. 2004, 11, 1170–74.
22. Jackson AL, Bartz SR, Schelter J, Kobayashi SV, Burchard J, Mao M, Li B, Cavet G, Linsley PS. Expression profiling reveals off-target gene regulation by RNAi. Nat Biotech. 2003, 21, 635-7.
23. WangY, Hu JK, Krol A, Li YP, Li CY, Yuan F. Systemic dissemination of viral vectors during intratumoral injection. Mol Cancer Ther. 2003, 2, 1233-42.
24. Buyens K, Lucas B, Raemdonck K, Braeckmans K, Vercammen J, Hendrix J, Engelborghs Y, De Smedt SC, Sanders NN. A fast and sensitive method for measuring the integrity of siRNA-carrier complexes in full human serum. J Control Rel. 2008, 18, 67-76.
25. Chiu Y-L, Rana TM. siRNA function in RNAi: A chemical modification analysis. RNA. 2003, 9, 1034-48.
26. Kohn DB, Sadelain M, Glorioso JC. Occurrence of leukaemia following gene therapy of X-linked SCID. Nat Rev Cancer. 2003, 3, 477–88.

27. Zaiss AK, Vilaysane A, Cotter MJ, Clark SA, Meijndert SC, Colarusso P, Yates RM Petrilli V, Tschopp J, Muruve DA. Antiviral antibodies target adenovirus to phagolysosomes and amplify the innate immune response. J Immunol. 2009, 182, 7058-68.
28. Bessis N, GarciaCozar FJ, Boissier MC. Immune responses to gene therapy vectors: influence on vector function and effector mechanisms. Gene Ther. 2004, 11, S10-S17.
29. Hacein-Bey-Abina S, Garrigue A, Wang GP, Soulier J, Lim A, Morillon E, Clappier E, Caccavelli L, Delabesse E, Beldjord K, Asnafi V, MacIntyre E, Cortivo LD, Radford I, Brousse N, Sigaux F, Moshous D, Hauer J, Borkhardt A, Belohradsky BH, Wintergerst U, Velez MC, Leiva L, Sorensen R, Wulffraat N, Blanche S, Bushman FD, Fischer A, Cavazzana-Calvo M. Insertional oncogenesis in 4 patients after retrovirus-mediated gene therapy of SCID-X1. J Clin Inves. 2008, 118, 3132–42.
30. Song YK, Liu F, Chu S, Liu D. Characterization of cationic liposome-mediated gene transfer *in vivo* by intravenous administration. Hum Gene Ther. 1997, 8, 1585-94.
31. Ruiz FE, Clancy JP, Perricone MA, Perricone MA, Bebok Z, Hong JS, Cheng SH, Meeker DP, Young KR, Schoumacher RA, Weatherly MR, Wing L, Morris JE, Sindel L, Rosenberg M, van Ginkel FW, McGhee JR, Kelly D, Lyrene RK, Sorscher EJ. A clinical inflammatory syndrome attributable to aerosolized lipid-DNA administration in cystic fibrosis. Hum Gene Ther. 2001, 12, 751-61.
32. Scheule RK, George JA, Bagley RG, Marshall J, Kaplan JM, Akita GY, Wang KX, Lee ER, Harris DJ, Jiang C, Yew NS, Smith AE, Cheng SH. Basis of pulmonary toxicity associated with cationic lipid-mediated gene transfer to the mammalian lung. Hum Gene Ther. 1997, 8, 689-707.

33. Abbasi M, Lavasanifar A, Berthiaume LC, Weinfeld M, Uludağ H. Cationic polymer mediated siRNA delivery for P-glycoprotein (P-gp) down-regulation in tumor cells. Cancer. 2010, In Press.

34. Liu C, Zhao G, Liu J, Ma N, Chivukula P, Perelman L, Okada K, Chen Z, Gough D, Yu L. Novel biodegradable lipid nano complex for siRNA delivery significantly improving the chemosensitivity of human colon cancer stem cells to paclitaxel. J Con Rel. 2009, 140, 277–83.

35. Alshamsan A, Haddadi A, Incani V, Samuel J, Lavasanifar A, Uludağ H. Formulation and Delivery of siRNA by Oleic Acid and Stearic Acid Modified Polyethyleneimine. *Mol Pharma*. 2009, 6, 121–33.

36. Abbasi M, Uludağ H, Incani V, Hsu CYM, Jeffery A. Further investigation of lipid-substituted Poly(L-Lysine) polymers for transfection of human skin fibroblasts. Biomacromol. 2008, 9, 1618-30.

37. Shen H, Pan Y. Reversal of Multidrug Resistance of Gastric Cancer Cells by Downregulation of TSG101 with TSG101siRNA. Cancer Biol & Ther. 2004, 3, 561-565.

38. Theyer G, Schirmböck M, Thalhammer T, Sherwood ER, Baumgartner G, Hamilton G. Role of the MDR-1-encoded multiple drug resistance phenotype in prostate cancer cell lines. J Urol. 1993, 150, 1544-7.

39. Persengiev SP, Zhu X, Green MR. Nonspecific, concentration-dependentstimulation and repression of mammalian gene expression by small interfering RNAs (siRNAs). RNA 2004, 10, 12–8.

40. Semizarov D, Frost L, Sarthy A, Kroeger P, Halbert DN, Fesik SW. Specificity of short interfering RNA determined through gene expression signatures. Proc Natl Acad Sci. 2003, 100, 6347–52.

41. Kumar, A., Haque, J., Lacoste, J., Hiscott, J., and Williams, B.R. Double-stranded RNA-dependent protein kinase activates transcription factor NF-kappa B by phosphorylating I kappa B. Proc Natl Acad Sci. 1994, 91, 6288–92.

42. Boese Q, Leake D, Reynolds A, Read S, Scaringe SA, Marshall WS, Khvorova A. Mechanistic insights aid computational short interfering RNA design, Methods Enzymol. 2005, 392, 73-96.

43. A. Reynolds, D. Leake, Q. Boese, S. Scaringe, W.S. Marshall, A. Khvorova, Rational siRNA design for RNA interference. Nat Biotech. 2004, 22, 326-30.

44. A. Khvorova, A. Reynolds, S.D. Jayasena, Functional siRNAs and miRNAs exhibit strand bias. Cell. 2003, 115, 209-16.

45. Ji J, Wernli M, Klimkait T, Erb P. Enhanced gene silencing by the application of multiple specific small interfering RNAs. FEBS Lett. 2003, 552, 247-52.

46. Holen T, Amarzguioui M, Wiiger MT, Babaie E, Prydz H. Positional effects of short interfering RNAs targeting the human coagulation trigger Tissue Factor. Nucleic Acids Res. 2002, 30, 1757-66.

47. Xiao H, Wu Z, Shen H, Luo A-L, Yang Y-F, Li X-B, Zhu D-Y. *In vivo* Reversal of P-glycoprotein-mediated multidrug resistance by rfficient delivery of stealth^{TM} RNAi. Basic & Clin Pharmacol & Toxicol. 2008, 103, 342–48.

48. Patil YB, Swaminathan SK, Sadhukha T, Ma L, Panyam J. The use of nanoparticle-mediated targeted gene silencing and drug delivery to overcome tumor drug resistance. Biomaterials. 2010, 31, 358–365.
49. Pan G-D, Yang J-Q, Yan L-N, Chu J-P, Liu Q, Xiao Y, Yuan L. Reversal of multi-drug resistance by pSUPER-shRNA-mdr1 in vivo and in vitro. World J Gastroenterol. 2009, 15, 431-440.

CHAPTER VII

Conclusions and Future Recommendations

Two therapeutic approaches employing gene-based molecules were investigated in this thesis work: (i) plasmid DNA delivery to human CRL fibroblasts (*in vitro*) (**CHAPTERS II to IV**), (ii) short interfering RNA (siRNA) delivery to suppress gene expression in MDA-435/LCC6 MDR1 cells (*in vitro*) and NOD-SCID mice tumors (*in vivo*) (**CHAPTERS V to VII**). In this section of my thesis, I will provide the conclusions of my research on these two approaches separately. I will also discuss future avenues that could be taken to continue and further develop these fields.

8.1 Plasmid DNA Delivery for Modification of Skin Fibroblasts

Gene therapy using plasmid DNA delivery is a means to reconstitute an impaired or missing gene with a correct copy in a host. This is possible when a gene carrier transports the candid gene across the cellular membrane, and into the host cell's nucleus [1]. Gene carriers that have been developed for the purpose of DNA delivery are composed of viral carriers and non-viral carriers. The primary focus of my study has been non-viral gene carriers, and specifically cationic polymers. The cationic polymers possess a strong positive charge and are thus able to bind and condense the negatively charged DNA (through an electrostatic reaction) so that it can be effectively internalized by the cells. The exogenous DNA must then survive the endosomal/lysosomal system, which aims to hydrolyze foreign macromolecules, and be released in intact form into the cell's cytosol to be targeted to the nucleus.

In **CHAPTER III** of this thesis, we reported the design of a lipid-substituted polymer, palmitic acid-poly(*L*-lysine) (PLL-PA) conjugate, which combines the critical properties of a

cationic polymer (i.e., DNA condensing ability) with that of a fatty acid (i.e., lipid membrane compatibility). The efficiency of this polymer was compared to other commercially available gene carriers such as PEI, Lipofectamine^{TM} 2000, and adenovirus for the transfection of the reporter gene pEGFP in human CRL fibroblasts. PLL-PA was able to condense plasmid DNA into 100-200 nm particles, a size suitable for cellular uptake. Using the lipid-substituted polymer for plasmid DNA condensation lead to a significant increase in the permeability of the particles through the cell membrane (40% by PLL vs 92% by PLL-PA after 24 hours) (**CHAPTER III, Figure 3A)**. This clearly demonstrated the beneficial effect of lipid modification of PLL on cellular uptake of complexes. Furthermore, the PLL-PA showed no toxicity in the cells for a period of 7 days. This was another significant finding, as toxicity is a major hurdle that is detected in cells transfected with some of the popular commercially available gene carriers (PEI, Lipofectamine^{TM} 2000). The PLL-PA showed a moderate ability to transfect the human CRL fibroblast cells compared to some of the other carriers (specifically adenovirus), but due to lack of toxicity, it was proven to be the most efficient gene carrier by transfecting the highest number of viable cells.

In **CHAPTER IV** of my thesis, I studied further modified PLLs, i.e., polymers modified with C8 to C20 fatty acids, and aimed to overcome the barriers to successful transfection. Successful transfection of cells is a multistep process in which the initial step is successful internalization of DNA into the cells. We showed in our previous study that PLL-PA delivery of DNA resulted in 92% cellular uptake. After internalization, DNA must survive the endosomal/lysosomal system, which aims to hydrolyze foreign macromolecules, and be released in intact form into the cytosol to be targeted to the nucleus. We conducted a study to detect

whether our lipid modified polymers were able to protect DNA against degradation by nucleases (the enzymes present at endosomes). The ability of nonviral carriers to protect against nuclease attack is paramount in enhancing the success of gene expression. It was determined that all of the lipid modified polymers at the 2:1 polymer:plasmid DNA ratio were able to protect plasmid DNA against degradation. Next, we investigated the polymers' ability to resist heparin-induced dissociation (a measure of complex stability). Rapid complex dissociation in cytoplasm causes DNA degradation by nucleases, reducing any chances of successful transfection [2]. It was determined that once delivered intracellularly by the more-effective polymers (i.e., PLL-MA, PLL-PA, PLL-StA), a significant fraction of the plasmid remained intact up to 7 days after a significant decrease (~30%) from day 1 to day 7. These results confirmed the previous reports which showed the DNA-condensing agents to enhance the transfection efficiency by prolonging the half-life of intact plasmid DNA in the cytosol [3,4]. It was determined that the polymers with higher degree of lipid substitution were able to form tighter complexes with DNA and also protected DNA better against degradation by nucleases. It was further proven that these polymers with a higher lipid content (i.e. PLL-MA and PLL-StA) showed a higher cellular uptake and ultimately the highest level of transfection in the human CRL fibroblast cells. It can be concluded from these results that the transfection efficiency of the lipid modified polymers is dependent on the degree of lipid substitution (extent of hydrophobicity) and not due to modification by a specific fatty acid.

My studies on using lipid modified polymeric gene carriers has determined that these carriers are efficiently able to encapsulate DNA and deliver it across the cellular membrane. As the delivery method proposed for these complexes is endocytosis, these complexes end up in

endosomes. Efficient endosomal escape of DNA is essential for efficient transfection of target cells, and therefore future studies for the improvement of these gene carriers should focus on systems that could increase endosomal escape of these complexes. These systems could include using lysosomotropic agents such as chloroquine, which are able to cause endosome eruptions by lowering the endosomal pH.

Nuclear uptake of the internalized gene is another essential component for efficient transfection. In the current delivery method, nuclear localization of exogenous DNA is due to its persistence around the nuclear membrane, which might increase its chance of random nuclear uptake at the time of cell division and specific transport through nuclear pores. Processes that can facilitate nuclear uptake can be used as supplements to improve transfection efficiency. Nuclear localizing sequences (NLS) can be attached to complexes to enhance nuclear uptake of the internalized DNA to further improve transfection efficiency.

8.2 siRNA Delivery for Cancer Therapy

Small interfering RNAs (siRNAs) are able to suppress the expression of any specific gene at the mRNA level, and prevent expression of proteins that lead to diseases. Free siRNA is negatively charged and cannot cross the cellular membranes. Furthermore, free siRNA is rapidly degraded by the RNase enzymes that are present in the physiological milieu. Therefore, a carrier is required for siRNA encapsulation and delivery to target cells. Our preliminary experiments on this issue determined that our lipid modified polymers showed a high efficiency in siRNA encapsulation and delivery. Therefore, to further pursue a therapeutic approach for the application of our polymers, we investigated the efficiency of lipid modified carriers in siRNA

delivery for the knockdown of P-gp. P-gp is over-expressed in tumor cells and leads to efflux of chemotherapeutic drugs. Reversal of this process – known as multidrug resistance - could be beneficial in increasing the efficiency of chemotherapy in cancer treatment.

As previously discussed, siRNA encapsulation and protection is critical for siRNA function. Our initial studies determined that the PLL-StA efficiently encapsulated siRNA and protected it against degradation by serum. This was critical for siRNA survival and targeting of the RISC complex. In **CHAPTER VI** of this thesis we show that using PLL-StA for siRNA delivery into the drug resistant MDA-435/LCC6 MDR1 cells, 90-100% cellular uptake of siRNA was detected. Furthermore, ~60% of the delivered siRNA was recovered from the cells after 24 h. The internalized siRNA was indeed able to survive the enzymes in the endosomal/lysosomal system of the cells and only 30-40% of the internalized siRNA was lost. Finally, it was shown that by delivering PLL-StA/ABCB1-siRNA to the MDA-435/LCC6 MDR1 cells, the P-gp concentration of cells can be reduced by more than half (~55%). While most attempts for siRNA down-regulation of P-gp have been attempted with >100 nM siRNA concentrations, a key issue in our study was that a low siRNA concentration (20 nM) was used for P-gp down-regulation. The significance of using low siRNA concentrations to limit down-regulation and up-regulation of non-specific genes has been well established [5,6], and to avoid these issues, siRNA concentrations <20 nM are recommended [7]. It should also be noted that the MDA-435/LCC6 MDR1 cells are a subtype of the MDA-435/LCC6 WT cells with transfected P-gp, and the P-gp is overexpressed to a larger extent than that of the endogenous tumor cells. Therefore our P-gp down-regulation results maybe an underestimate of the actual potential of the PLL-StA/ABCB1-siRNA complexes in P-gp down-regulation of the endogenous cells. When the ABCB1-siRNA

treated cells were additionally treated with the chemotherapeutic drug DOX and PTX, a 3-fold increase in drug uptake and a 30% increase in cytotoxicity was detected compared to the C-siRNA treated cells. This clearly showed the effect of P-gp knockdown in the increase in chemotherapy efficiency. The results of this study showed that use of lipid-modified PLL for delivery of gene-specific siRNAs is an effective approach for down-regulating specific molecular targets.

In the first section of **CHAPTER VII**, an attempt was made to improve on our previous P-gp down-regulation results using the same low siRNA concentration. Approaches were used to (i) increase the efficiency of knockdown, and (ii) increase the duration of P-gp down-regulation. To increase the efficiency of siRNA P-gp knockdown, we used a combination of three siRNA sequences with specific characteristics for efficient knockdown of P-gp. This combination of siRNA sequences (siRNA 1+2+3) resulted in a significant increase in efficiency (maximum of 75% P-gp protein down-regulation in the MDA435/LC66 MDR1 cells). To increase the duration of P-gp knockdown, repeated exposure of siRNA/Polymer complex was attempted. As siRNA half-life in the cells is ~24 h. Our previous reports had confirmed the maximum efficiency of siRNA at 24 h and loss of effect at 72 h [8]. We therefore exposed cells to siRNA complexes every 24 h for a period of 3 days and increased the duration of P-gp knockdown for 3 days. In the next section of this chapter, we detected siRNA delivery for P-gp down-regulation and MDR reversal *in vivo*. Efficient *in vivo* delivery of siRNA can be potentially beneficial in the treatment of many mortal diseases including cancer, severe immunodeficiency, and multiple sclerosis. To efficiently serve this purpose, specific siRNA sequences should be delivered to the mRNA of the tumor cells, degrade the targeted mRNA, and result in sustained suppression of the undesired

gene. *In vitro* approaches for P-gp down-regulation using various siRNA sequences and various siRNA delivery methods in different tumor cells have been attempted by lipid based siRNA carriers (Lipofectamine^{TM} 2000 and Oligofectamine^{TM}) [9-12] and viral vectors [13-15]. Additionally, uptake and efficiency of chemotherapeutic drugs after siRNA down-regulation has been shown to increase in some *in vitro* studies. However, translation of this success to *in vivo* studies has rarely been attempted and to our knowledge, the only study consisting of a combination of *in vitro* and *in vivo* approaches for P-gp down-regulation and MDR reversal has been by Xiao *et al.* In their *in vitro* approach, Lipofectamine^{TM} 2000 delivery of siRNA led to ~60% down-regulation of P-gp mRNA and protein in human lung carcinoma cells NCI-H460. In their *in vivo* approach, they used intratumoral siRNA injection (i.e., without a carrier) and electroporation and suppressed P-gp levels by 80% [16]. We also attempted a parallel approach of *in vitro* and *in vivo* siRNA delivery for P-gp down-regulation using a novel approach for siRNA delivery. In this study, we have looked at the intracellular fate of siRNA after uptake into the MDA 435/LCC6 MDR1 cells. We have also used two approaches to increase the efficiency and duration of siRNA knockdown of P-gp in the drug resistant MDA-435/LCC6 MDR1 cells *in vitro* and further determined that *in vivo* siRNA uptake into the tumor cells is feasible using PLL-StA. Using an ABCB1 siRNA to detect P-gp knockdown and the increase in Doxil uptake of the MDA-435/LCC6 MDR1 cells *in vivo* will further determine the efficiency of this delivery system.

The next study in this path is to detect continuous siRNA injection for sustained P-gp knockdown and detection of the long term effect of Doxil injection on tumor suppression. This will determine if the in vivo P-gp suppression and the increase in Doxil injection of the MDA-

435/LCC6 MDR1 tumor cells will result in an increase in the efficiency of chemotherapy and tumor suppression. For this purpose, PLL-StA/ABCB1-siRNA complexes should be injected intratumorally in 24 h intervals and systemic Doxil injection should be performed. The size of the tumors should be assessed to detect tumor suppression after chemotherapy. Among the issues that could also be improved in our system is the short duration of siRNA efficiency which required repeated siRNA exposure for sustained knockdown of the P-gp. Future studies that can be used in this direction could include chemical modification of siRNA for increased half-life of siRNA in *in vivo* studies. Our *in vivo* siRNA uptake studies determined that ~66% of siRNA was lost after 96 h. This siRNA loss can be reduced by using siRNA modification to increase its stability against degradation in the physiological milieu. In order to increase the half-life and bioavailability of synthetic siRNAs, various groups have made efforts to chemically modify siRNA while sustaining gene silencing activity. Studies have showed that 2'-Fluoro and 2'-OMe modification of siRNA increased siRNA half-life when exposed to cytoplasmic extracts, without limiting its silencing ability [17]. Furthermore, by strengthening the U-A linkage and also modifying the P-S backbone linkages they have sown that siRNA stability in serum can be increased with no affect on the siRNA silencing ability [18]. Additionally 2'-F-modified siRNA modification increased siRNA half-life in serum from 24 hours to >72 hours [19]. These modification methods are especially significant when siRNA silencing is performed *in vivo*, as RNases are at high concentrations in the lymph, blood, and extracellular matrix.

Overall, the aim of Part II of this thesis work was to introduce a novel gene carrier for the purpose of siRNA delivery for cancer therapy. The main advantage of synthetic polymeric carriers is that they can be engineered in such a way to reduce immunogenic and toxicological

reactions from the hosts. The PLL-StA successfully served this purpose by efficiently encapsulating and delivering the siRNA to target cells and lead to the knockdown of the undesired gene P-gp. This study showed effective accumulation of chemotherapeutic agents in cells after P-gp knockdown as well as increased cytotoxicity of DOX and PTX, two issues not clearly shown with other non-viral approaches in siRNA delivery. We conclude that lipid-substituted polymeric carriers are safe alternatives to viral delivery systems for *in vitro* and *in vivo* siRNA delivery for cancer therapy.

REFERENCES

1. Verma IM, Somia N. Gene therapy-promises, problems and prospects. Nature. 1997, 389, 239-42.
2. Arigita C, Zuidam NJ, Crommelin DJ, Hennink WE. Association and dissociation characteristics of polymer/DNA complexes used for gene delivery. Pharma Res. 1999, 16, 1534-41.
3. Chiou HC, Tangco MV, Levine SM, Robertson D, Kormis K, Wu CH, Wu GY. Enhanced resistance to nuclease degradation of nucleic acids complexed to asialoglycoprotein-polylysine carriers. Nucl Acids Res. 1994, 22, 5439-46.
4. Pollard H, Remy JS, Loussouarn G, Demolombe S, Behr JP, Escande D. Polyethyleneimine but not the cationic lipids promotes transgene delivery to the nucleus in mammalian cells. J Biol Chem. 1998, 273, 7507-11.
5. Persengiev SP, Zhu X, Green M. Nonspecific, concentration-dependent stimulation and repression of mammalian gene expression by small interfering RNAs (siRNAs). RNA. 2004. 10, 12-8.
6. Scacheri PC, Rozenblatt-Rosen O, Caplen NJ, Wolfsberg TG, Umayam L, Lee JC, Hughes CM, Shanmugam KS, Bhattacharjee A, Meyerson M, Collins FS. Short interfering RNAs can induce unexpected and divergent changes in the levels of untargeted proteins in mammalian cells. Proc Natl Acad Sci. 2004, 101, 1892-7.
7. Semizarov D, Frost L, Sarthy A, Kroeger P, Halbert DN, Fesik SW. Specificity of short interfering RNA determined through gene expression signatures. Proc Natl Acad Sci USA. 2003, 100, 6347–52.

8. Abbasi M, Lavasanifar A, Berthiaume LC, Weinfeld M, Uludağ H. Cationic polymer mediated siRNA delivery for P-glycoprotein (P-gp) down-regulation in tumor cells. Cancer. 2010, In Press.
9. Stierle´ V, Laigle A, Jolle`s B. Modulation of MDR1 gene expression in multidrug resistant MCF7 cells by low concentrations of small interfering RNAs. Biochem Pharmacol. 2005, 70, 1424–30.
10. Nieth C, Priebsch A, Stege A, Lage H. Modulation of the classical multidrug resistance (MDR) phenotype by RNA interference (RNAi). FEBS Lett. 2003, 545, 144– 50.
11. Akhtar S, Benter IF. Nonviral delivery of synthetic siRNAs *in vivo*. J Clin Invest. 2007, 117, 12, 3623–32.
12. Zhang T, Guan M, Jin HY, Lu Y. Reversal of multidrug resistance by small interfering double-stranded RNAs in ovarian cancer cells. Gynecol Oncol. 2005, 97, 501–7.
13. Xu D, McCarty D, Fernandes A, Fisher M, Samulski RJ, Juliano RL. Delivery of MDR1 small interfering RNA by self-complementary recombinant adeno-associated virus vector. Mol Ther. 2005, 11, 4, 523-30.
14. Huaa J, Mutcha DJ, Herzog TJ. Stable suppression of MDR-1 gene using siRNA expression vector to reverse drug resistance in a human uterine sarcoma cell line. Gynecol Oncol. 2005, 98, 31–8.
15. Yague E, Higgins CF, Raguz S. Complete reversal of multidrug resistance by stable expression of small interfering RNAs targeting MDR1. Gene Ther. 2004, 11, 1170–4.

16. Xiao H, Wu Z, Shen H, Luo A-L, Yang Y-F, Li X-B, Zhu D-Y. *In vivo* Reversal of P-Glycoprotein-Mediated Multidrug Resistance by Efficient Delivery of Stealth^{TM} RNAi. Basic & Clinical Pharmacology & Toxicology. 2008, 103, 342–8.
17. Ahlberg J, Berkenstam A, Henell F, Glaumann H. Degradation of short and long lived proteins in isolated rat river lysosomes. J Biol Chem. 1985, 260, 5847-54.
18. Chiu Y-L, Rana TM. siRNA function in RNAi: A chemical modification analysis. RNA. 2003, 9, 1034-48.
19. Layzer JM, Mccaffrey AP, Tanner AK, Huang Z, Kay M.A, Sullenger BA. *In vivo* activity of nuclease-resistant siRNAs. RNA. 2004, 10, 766–71.